2023
October

Academic Studies in **ENGINEERING**

EDITOR
Prof. Dr. Çoşkun ÖZALP

gece kitaplığı

İmtiyaz Sahibi • Yaşar Hız
Genel Yayın Yönetmeni • Eda Altunel
Yayına Hazırlayan • Gece Kitaplığı
Editör • Prof. Dr. Çoşkun ÖZALP

Birinci Basım • Ekim 2023 / ANKARA

ISBN • 978-625-425-227-3

Gece Kitaplığı
Adres: Kızılay Mah. Fevzi Çakmak 1. Sokak Ümit Apt
No: 22/A Çankaya/ANKARA Tel: 0312 384 80 40

www.gecekitapligi.com
gecekitapligi@gmail.com

Baskı & Cilt
Bizim Buro
Sertifika No: 42488

Academic Studies in Engineering

October 2023

Editor

Prof. Dr. Çoşkun ÖZALP

CONTENTS

CHAPTER 1

MICROBIAL BIOREMEDIATION OF POLLUTANTS

Numan YILDIRIM[1], Gokhan Onder ERGUVEN[2]

1 Prof.Dr., Munzur University, Tunceli Vocational School, Department of Plant and Animal Production, Organic Agriculture Programme, TR62000 Tunceli, Turkey, numanyildirim44@gmail.com, ORCID: 0000-0003-1109-8106

2 Doç.Dr., Munzur Unıversity, Faculty of Economics and Administrative Sciences, Department of Urbanization and Environmental Issues, TR62000 Tunceli, Turkey, gokhanondererguven@gmail.com, ORCID: 0000-0003-1573-080X

1. Inroduction

1.1. Bioremediation

Bioremediation, a nature-inspired and sustainable approach, has emerged as a powerful tool in addressing environmental contamination and pollution. As anthropogenic activities continue to impact ecosystems and water resources, the need for effective and eco-friendly remediation strategies has become increasingly evident. Bioremediation harnesses the inherent capabilities of microorganisms to degrade, transform, or immobilize pollutants, offering a viable solution to mitigate the adverse effects of pollutants on both terrestrial and aquatic environments (Krzmarzick et al., 2018; Masindi et al., 2021).

The concept of bioremediation is rooted in the profound metabolic diversity of microorganisms, including bacteria, fungi, algae, and other microorganisms, which possess the capacity to metabolize a wide range of organic and inorganic compounds. These microorganisms play a crucial role in the Earth's natural processes of nutrient cycling and pollutant breakdown, making them invaluable allies in combating pollution caused by industrial discharges, agricultural runoff, and other sources of contamination (Kour et al., 2018).

Bioremediation strategies encompass a spectrum of approaches, from in-situ methods that leverage the microbial communities existing in the polluted environment, to ex-situ techniques where microorganisms are cultivated and introduced to target contaminants. The mechanisms driving bioremediation include biodegradation, bioaccumulation, and biosorption, each of which exploits the microbial ability to transform pollutants into harmless byproducts or to sequester them for subsequent removal (Sharma et al., 2021).

The application of bioremediation is not limited to a specific type of pollutant, as it has proven successful in addressing a diverse array of contaminants, including hydrocarbons, heavy metals, pesticides, and emerging pollutants. The versatility of bioremediation lies in its adaptability to different environmental conditions, making it a valuable tool in various settings, from terrestrial soils to aquatic ecosystems. While bioremediation offers numerous benefits, it is not without challenges. Factors such as microbial diversity, environmental conditions, nutrient availability, and interactions with native species can influence the success of bioremediation efforts. Advancements in biotechnology and molecular techniques have led to the development of genetically engineered microorganisms with enhanced pollutant degradation capabilities, raising ethical and regulatory considerations (Alaira et al., 2021).

In this context, this review aims to provide an overview of the fundamental concepts, mechanisms, applications, challenges, and future directions of bioremediation. By exploring the potential of microorganisms as agents of environmental restoration, we delve into the multidisciplinary nature of bioremediation and its role in shaping sustainable solutions for environmental contamination.

2. Bacterial Bioremediation

Bacterial bioremediation stands as a promising and innovative approach to address the escalating challenges posed by environmental pollution and contamination. As human activities continue to release an array of pollutants into the environment, ranging from hazardous chemicals to heavy metals, there is an urgent need for effective and sustainable strategies to mitigate these impacts. Bacterial bioremediation capitalizes on the remarkable metabolic diversity and adaptability of bacteria to remediate polluted sites and restore ecological balance (Egorova et al., 2013).

Bacteria, being ubiquitous and diverse microorganisms, have evolved over eons to thrive in a wide range of environments, including those tainted by pollutants. This unique capability has been harnessed in bioremediation, where bacteria play a pivotal role in breaking down, transforming, and neutralizing contaminants. By utilizing their inherent enzymatic pathways, bacteria can convert complex pollutants into less harmful compounds or incorporate them into their cellular structures, effectively reducing the concentration and toxicity of pollutants (Suyamud et al., 2018).

The versatility of bacterial bioremediation is evident in its application across different scenarios, such as contaminated soils, sediments, groundwater, and industrial effluents. In-situ bioremediation methods involve the stimulation of indigenous bacterial populations already present at the polluted site, while ex-situ approaches involve isolating and cultivating specific bacterial strains for targeted contaminant degradation. The success of these strategies hinges on understanding the unique physiological and biochemical characteristics of bacteria and tailoring the approach to suit the specific contaminant and environmental conditions (Horváthová et al. 2018; Cervantes-González et al., 2019).

In recent years, advancements in biotechnology have enabled the genetic modification of bacteria to enhance their bioremediation capabilities. Engineered bacteria can be designed to express novel enzymes or pathways that efficiently degrade specific pollutants, offering a promising solution for stubborn contaminants that are resistant to natural degradation processes. However, the deployment of genetically modified organisms also raises ethical and regulatory concerns that must be carefully navigated.

This review aims to provide an in-depth exploration of bacterial bioremediation, encompassing its underlying principles, mechanisms, applications, challenges, and future prospects. By delving into the intricate interplay between bacteria and pollutants, we seek to uncover the transformative potential of bacterial bioremediation as a sustainable tool to restore and safeguard our environment.

2.1. Bacterial Bioremediation and its Utilized Bacterial Species:

Bacterial bioremediation has emerged as a powerful tool in the arsenal of environmental management, offering an eco-friendly and efficient means to tackle various forms of pollution and contamination. Central to the success of this approach are the diverse bacterial species that possess the remarkable ability to degrade, transform, and detoxify a wide range of pollutants. These bacterial champions are selected and employed strategically based on their metabolic capabilities, affinity for specific contaminants, and adaptability to the target environment (Egorova et al., 2013).

Pseudomonas putida: This versatile bacterium is renowned for its exceptional metabolic diversity and is often employed in bioremediation efforts. Pseudomonas putida has the ability to degrade a plethora of organic compounds, including hydrocarbons, pesticides, and aromatic compounds, due to its extensive catabolic pathways (Eltoukhy et al., 2020; Gong et al., 2016).

Bacillus subtilis: Known for its robustness and adaptability, Bacillus subtilis is employed in the bioremediation of heavy metals. This bacterium exhibits metal-resistant properties and can immobilize metals through biosorption, bioaccumulation, and precipitation, reducing their mobility and toxicity in contaminated sites (Abou-Shanab et al., 2008).

Rhodococcus erythropolis: Particularly effective in degrading hydrophobic pollutants, Rhodococcus erythropolis utilizes its unique enzymatic machinery to break down a range of persistent compounds, such as polychlorinated biphenyls (PCBs) and polycyclic aromatic hydrocarbons (PAHs) (Garrido-Sanz et al., 2020; Krivoruchko et al., 2023).

Shewanella oneidensis: This bacterium has garnered attention for its ability to participate in the reduction of heavy metals and radionuclides in anaerobic environments. *Shewanella oneidensis* employs its respiratory capabilities to transform these contaminants into less mobile and less toxic forms (Wu et al., 2019; Liu et al., 2018).

Dehalococcoides mccartyi: This bacterium has earned fame for its unique ability to conduct reductive dechlorination, a process crucial for the detoxification of chlorinated solvents in contaminated groundwater (Solis et al., 2019).

Alcaligenes eutrophus: Renowned for its capacity to accumulate polyhydroxyalkanoates (PHAs), Alcaligenes eutrophus is utilized in bioremediation efforts to remove excess nutrients, such as nitrogen and phosphorus, from wastewater (Jacobsen and Pedersen, 1991).

Geobacter spp.: These bacteria are pivotal players in the bioremediation of subsurface environments contaminated with organic and metal pollutants. Geobacter spp. are capable of coupling the degradation of organic compounds with the reduction of metal ions, thus promoting contaminant immobilization (Jiang et al., 2020; Sekar and DiChristina, 2014).

The selection of the appropriate bacterial species is contingent on the nature of the contaminants, the environmental conditions, and the desired outcome of the bioremediation process. As our understanding of microbial metabolism and genetics deepens, researchers continue to identify novel bacterial candidates and engineer their capabilities to tackle even the most stubborn pollutants. Bacterial bioremediation holds the promise of not only cleaning up contaminated sites but also shaping a more sustainable and harmonious coexistence between human activities and the environment.

3. Fungal Bioremediation

Fungal bioremediation, a branch of biotechnology, has emerged as a promising approach that harnesses the unique abilities of fungi to address a wide range of contaminants. Fungi, as versatile organisms, have shown remarkable potential in remediating pollutants through various mechanisms, including bioaccumulation, biosorption, enzymatic degradation, and transformation (Badia-Fabregat et al., 2015: Anastasi et al., 2013).

Fungi are known for their ability to thrive in diverse environments and metabolize an array of organic and inorganic compounds. Their extensive metabolic capabilities, often exceeding those of bacteria, enable them to degrade complex and recalcitrant pollutants. The mycelial networks of fungi serve as efficient biofilters, facilitating the capture and immobilization of contaminants from air, water, and soil. Additionally, the rich enzymatic arsenal of fungi, including ligninolytic and cellulolytic enzymes, empowers them to degrade challenging pollutants such as aromatic compounds, pesticides, pharmaceuticals, and even recalcitrant synthetic dyes (Zhang et al., 2013; Anastasi et al., 2013).

The mechanisms employed by fungi in bioremediation are multi-faceted. Some fungi, like white-rot fungi, have the remarkable ability to break down lignin, a complex and rigid polymer in plant material, thus aiding in the degradation of persistent organic pollutants. Other fungi possess metal-binding capabilities, facilitating the sequestration of heavy metals from contaminated sites. Fungi can also participate in the process of mycoreme-

diation, where they selectively accumulate and concentrate pollutants, aiding in their subsequent removal (dos Santos Bazanella et al., 2013; Zhang et al., 2013).

Fungal bioremediation offers distinct advantages over traditional methods. It is often cost-effective, requires minimal energy inputs, and generates relatively low amounts of secondary waste. Furthermore, fungi can be utilized in situ, reducing the need for excavation or transport of contaminated materials. As our understanding of fungal physiology, genetics, and interactions with contaminants expands, researchers are engineering fungi to enhance their bioremediation capabilities further. This includes strategies such as genetically modifying fungi to express specific enzymes for targeted degradation or designing consortia of fungi to synergistically tackle complex pollution scenarios (Rodríguez et al., 2013; dos Santos Bazanella et al., 2013).

In this era of ecological imbalance and environmental challenges, fungal bioremediation stands as a beacon of hope. By tapping into the natural abilities of fungi to detoxify and degrade contaminants, we have the potential to rejuvenate ecosystems, restore polluted sites, and pave the way for a more sustainable coexistence between humanity and the environment. This review delves into the intricacies of fungal bioremediation, exploring the diverse fungal species and mechanisms employed in pollution mitigation and highlighting its significance in the larger context of environmental conservation.

3.1. Species in Fungal Bioremediation:

Fungi, with their remarkable adaptability and diverse metabolic capabilities, have gained prominence as valuable agents in bioremediation efforts. Various fungal species have demonstrated their potential to efficiently degrade, transform, or sequester a wide range of pollutants, making them valuable candidates for addressing environmental contamination. The selection of fungal species for bioremediation depends on their affinity for specific contaminants, their growth characteristics, and their adaptability to different environments (Anastasi et al., 2013). Here, we explore some of the key fungal species that have been harnessed for fungal bioremediation:

White-Rot Fungi (Basidiomycetes): White rot fungi (WRF) have emerged as valuable and versatile agents in the field of bioremediation, offering a unique ability to degrade recalcitrant and complex pollutants. Their remarkable enzymatic arsenal and ecological role in breaking down lignin-rich plant material have paved the way for their application in addressing a wide range of environmental contaminants. This article explores the utilization of white rot fungi in bioremediation, highlighting their

mechanisms, advantages, and key applications. White rot fungi are characterized by their ability to produce a diverse array of enzymes, including lignin peroxidases, manganese peroxidases, and laccases. These enzymes work synergistically to degrade complex organic pollutants through oxidative processes. The ligninolytic enzymes produced by WRF have a broad substrate specificity, allowing them to target a variety of pollutants, including aromatic compounds, dyes, pesticides, and even recalcitrant pollutants like polycyclic aromatic hydrocarbons (PAHs) and chlorinated compounds (dos Santos Bazanella et al., 2013; Lladó et al., 2013).

a. *Phanerochaete chrysosporium*: *P. chrysosporium*, a species of white rot fungi, has emerged as a remarkable candidate for bioremediation due to its unique lignin-degrading abilities and versatile enzymatic arsenal. This filamentous fungus has garnered attention for its potential to address environmental pollution by breaking down recalcitrant compounds that are often resistant to conventional degradation methods. One of the key features that sets *P. chrysosporium* apart is its production of ligninolytic enzymes, which play a crucial role in breaking down lignin—a complex and chemically stable component of plant cell walls. The primary lignin-degrading enzymes produced by P. chrysosporium include lignin peroxidase, manganese peroxidase, and laccase. These enzymes work synergistically to dismantle lignin and open up the lignocellulosic matrix. *P. chrysosporium*'s versatility is evident in its ability to degrade a wide range of environmental contaminants (Gu et al., 2016; Zhang et al., 2008; Chen and Ding 2012).

b. *Trametes versicolor*: Trametes versicolor, also known as the turkey tail fungus, is another extensively studied white rot fungus. Its diverse enzyme arsenal, including laccases, lignin peroxidases, and manganese peroxidases, makes it a versatile candidate for bioremediation. *T. versicolor* has been employed in the degradation of phenolic compounds, dyes, and pesticides. Its adaptability to various environmental conditions and ability to form symbiotic interactions enhance its utility in bioremediation strategies (Nowak et al., 2021; Mori et al., 2018; Mallak et al., 2020).

c. *Pleurotus ostreatus*: Pleurotus ostreatus, commonly known as the oyster mushroom, has gained attention not only for its role in mycoremediation but also for its potential in wastewater treatment. While it may not possess the full complement of ligninolytic enzymes seen in other white rot fungi, it still exhibits lignin-degrading capabilities. P. ostreatus is particularly adept at breaking down lignin-rich substrates and has been employed in the treatment of agricultural and industrial wastes (Jiao et al., 2018).

d. *Pleurotus eryngii*: This fungus, commonly known as the King Trumpet or King Oyster mushroom, has garnered attention not only as a culinary delight but also for its potential applications in bioremediation.

This edible mushroom belongs to the genus Pleurotus, which encompasses various species that exhibit ligninolytic capabilities and have been explored for their role in environmental cleanup. *P. eryngii* possesses ligninolytic enzymes, including laccases and peroxidases, which are essential for breaking down complex organic compounds, including lignin-rich substrates. These enzymes enable the mushroom to efficiently degrade lignocellulosic materials, making it a promising candidate for bioremediation applications. One of the significant aspects of *P. eryngii*'s potential lies in its ability to degrade a range of pollutants (Brana et al., 2017; Mau et al., 1998).

e. Ascomycetes and Deuteromycetes: Several fungal species within the Ascomycota and Deuteromycota phyla have shown potential for pollutant degradation. Aspergillus niger is known for its ability to degrade various organic compounds, including petroleum hydrocarbons and pharmaceuticals. Trichoderma species are commonly used for their cellulolytic and chitinolytic activities, making them effective agents for breaking down organic materials (DSouza et al., 2021; Dini et al., 2022).

f. Zygomycetes: Fungi like Rhizopus and Mucor species are utilized for their ability to accumulate and remove heavy metals through biosorption. These fungi can effectively immobilize metals such as cadmium, lead, and zinc from contaminated environments (Awasthi et al., 2017; Asemoloye et al., 2020).

g. Arbuscular Mycorrhizal Fungi (AMF): While traditionally known for their role in promoting plant growth, AMF have also shown potential in bioremediation. These fungi form symbiotic relationships with plant roots and can improve plant tolerance to contaminants, enhancing phytoremediation efforts (Guo et al., 2023).

The effectiveness of fungal bioremediation is influenced by factors such as the composition of the contaminated site, fungal growth conditions, and the nature of pollutants. Advances in genetic engineering and synthetic biology have enabled the modification of fungal strains to enhance their degradation capabilities, opening doors for tailoring fungal species to specific contamination scenarios. Furthermore, the use of fungal consortia, where multiple fungal species work synergistically, has shown promise in addressing complex pollution scenarios. As fungal bioremediation continues to evolve, the selection of appropriate fungal species or strains becomes pivotal to the success of remediation strategies. By harnessing the remarkable metabolic diversity of fungi, researchers and environmental professionals are harnessing nature's inherent power to restore ecosystems and mitigate the impacts of pollution.

4. Algal Bioremediation:

Algae, a diverse group of photosynthetic microorganisms, are not only essential components of aquatic ecosystems but also exhibit remarkable capabilities in removing pollutants from water and air. Their rapid growth rates, efficient nutrient uptake, and ability to synthesize a wide range of bioactive compounds render them ideal candidates for bioremediation applications. Algae can effectively mitigate environmental issues arising from pollutants such as heavy metals, organic compounds, nutrients, and even greenhouse gases.

The use of algae in bioremediation aligns with the principles of sustainable development, as it leverages the natural abilities of these organisms to restore ecosystems and improve the quality of air and water. Algal bioremediation, also known as phytoremediation or algal-based treatment, represents a green and cost-effective solution for remediating contaminated sites, treating wastewater, and addressing other environmental challenges (Chugh et al., 2023; Ugya et al., 2021).

This review delves into the fascinating world of algal bioremediation, exploring the diverse mechanisms by which algae interact with and transform contaminants. We will delve into various algal species, their unique metabolic pathways, and the conditions that optimize their remediation potential. Moreover, we will highlight recent advancements in biotechnology and genetic engineering that enable the enhancement of algae's bioremediation capabilities. Through a comprehensive exploration of algal bioremediation, this review aims to shed light on the significant contributions of algae to the field of environmental restoration. By harnessing the inherent abilities of these microscopic organisms, we can pave the way for more sustainable and effective strategies to address pollution and promote a healthier planet.

4.2. Species Used in Algal Bioremediation:

Algal bioremediation, a subset of bioremediation, harnesses the remarkable capabilities of various algae species to mitigate environmental pollution. Algae are renowned for their ability to photosynthesize, capturing sunlight and utilizing carbon dioxide to synthesize organic matter. This inherent metabolic process allows them to effectively sequester pollutants from water and air, making them valuable tools in remediating diverse contaminants. Here, we explore some of the prominent algae species utilized in algal bioremediation and their roles in addressing environmental challenges (Chugh et al., 2023).

Chlorella spp.: Chlorella is a widely studied genus of green microalgae known for its rapid growth and high nutrient uptake rates. These algae

have demonstrated efficacy in removing heavy metals, such as cadmium, lead, and copper, from contaminated water bodies. Their ability to accumulate metals within their cell walls through biosorption and subsequent precipitation has made them effective agents for heavy metal bioremediation (González et al., 1997; Wang et al., 2013).

Spirulina platensis: Spirulina is a well-known cyanobacterium often referred to as a "superfood." Beyond its nutritional value, Spirulina platensis exhibits promising potential in treating wastewater and remediating pollutants like nitrogen and phosphorus. Its high growth rates and ability to fix nitrogen from the atmosphere enhance its suitability for wastewater treatment applications (Ibrahim et al., 2021; Thengodkar and Sivakami 2010).

Scenedesmus spp.: Scenedesmus is a genus of green algae that has gained attention for its capability to remove nutrients, such as nitrogen and phosphorus, from agricultural runoff and municipal wastewater. These algae can accumulate nutrients within their cells, effectively reducing the nutrient load in water bodies and preventing eutrophication (Kafil et al., 2022; Oliveira et al., 2019).

Microcystis aeruginosa: This cyanobacterial species is known for its ability to proliferate and form harmful algal blooms (HABs) in water bodies. However, under controlled conditions, Microcystis can be harnessed for the removal of contaminants like heavy metals and organic pollutants. This approach transforms a potential ecological threat into a bioremediation asset (Deng et al., 2020; Cheraghpour et a., 2020).

Ulva lactuca (Sea Lettuce): This macroalgae species is utilized in phytoremediation efforts to address nutrient pollution in coastal areas. *Ulva lactuca* can efficiently absorb excess nutrients like nitrogen and phosphorus, thereby preventing the deterioration of marine ecosystems due to eutrophication (Rahhou et al., 2023; Shuang et al., 2017).

These are just a few examples of the many algae species employed in algal bioremediation. The selection of a particular species depends on factors such as the type of pollutant, environmental conditions, and the specific goals of the remediation project. As the field of algal bioremediation advances, researchers continue to explore and optimize the use of diverse algae species, unlocking their potential to contribute to a cleaner and healthier environment.

5. Applications of Yeasts in Bioremediation

Yeast, a type of unicellular fungus, has gained attention in recent years for its potential in bioremediation processes. With their diverse metabolic

capabilities, yeasts are employed in various environmental applications to remove or detoxify pollutants. Yeasts offer several advantages for bioremediation, including their ability to thrive in various conditions, their rapid growth rates, and their capacity to tolerate and metabolize a wide range of pollutants (Nicula et al., 2023).

Heavy Metal Removal: Certain yeast species, such as Saccharomyces cerevisiae, have the ability to accumulate heavy metals from contaminated environments. Through a process called biosorption, yeasts can bind and immobilize heavy metals on their cell surfaces, effectively removing them from water and soil (Massoud et al., 2019).

Organic Pollutant Degradation: Yeasts are used in the biodegradation of various organic pollutants, including hydrocarbons, phenols, and aromatic compounds. Candida spp. and Rhodotorula spp. are examples of yeast species known for their ability to degrade petroleum hydrocarbons and recalcitrant organic pollutants (Gargouri et al., 2019).

Wastewater Treatment: Yeasts are employed in the treatment of industrial and municipal wastewaters. They can remove nutrients like nitrogen and phosphorus through assimilation and can also contribute to the degradation of organic matter (Wang et al., 2018; Dias et al., 2020).

Bioremediation of Xenobiotics: Yeasts are used to detoxify xenobiotic compounds, which are synthetic chemicals not naturally found in the environment. Pichia pastoris and Yarrowia lipolytica are examples of yeasts that can metabolize and degrade xenobiotic pollutants (Nicula et al., 2023; Cherni et al., 2020).

6. Conclusion

In conclusion, microbial bioremediation stands as a powerful and promising approach to address the environmental challenges posed by various contaminants. Microorganisms, including bacteria, fungi, algae and yeast, have demonstrated their ability to degrade, transform, or immobilize pollutants in a wide range of contaminated environments. The versatility of microbial bioremediation lies in the diversity of microbial species, their metabolic capabilities, and their potential for adaptation to changing environmental conditions.

Bacterial bioremediation, with its rapid growth rates and diverse metabolic pathways, offers effective solutions for organic and inorganic pollutant removal. Bacterial species have been harnessed for their proficiency in breaking down complex compounds, detoxifying hazardous materials, and enhancing the overall health of ecosystems.

Fungal bioremediation, on the other hand, capitalizes on the enzymatic prowess of fungi, especially white-rot fungi, in degrading recalcitrant pollutants like lignin and other complex organic compounds. Fungi's ability to accumulate heavy metals and form symbiotic relationships with plants further expands their role in remediating contaminated sites.

Advancements in genetic engineering, synthetic biology, and biotechnology have opened avenues to tailor microbial strains for specific contaminants and environments, improving their bioremediation capabilities. The synergy between microbiology, environmental science, and engineering continues to shape innovative strategies that harness microbial bioremediation for sustainable pollution management.

However, challenges remain, including the optimization of bioremediation conditions, scaling up from laboratory to field applications, and ensuring the long-term sustainability of treated sites. Additionally, the potential ecological impacts of introducing non-native microbial species must be carefully considered.

As our understanding of microbial interactions, metabolic pathways, and environmental processes deepens, microbial bioremediation will continue to evolve as a valuable tool for restoring contaminated ecosystems, safeguarding human health, and contributing to a cleaner and healthier planet. Embracing the intricate capabilities of microorganisms, microbial bioremediation represents a harmonious collaboration between science and nature to address the pressing environmental issues of our time.

References:

Abou-Shanab R.A., Ghanem K., Ghanem N., Al-Kolaibe A. (2008). The role of bacteria on heavy-metal extraction and uptake by plants growing on multi-metal-contaminated soils. World Journal of Microbiology and Biotechnology, 24: 253–262.

Alaira, S., Padilla, C., Alcantara, E., Aggangan, N. (2021). Social Acceptability of the Bioremediation Technology for the Rehabilita-tion of an Abandoned Mined-Out Area in Mogpog, Marinduque, Philippines. Journal of Environmental Science and Management, 24.

Anastasi, A., Tigini, V., Varese, G.C. (2013) The bioremediation potential of different ecophysiological groups of fungi. In: Goltapeh EM et al (eds) Fungi as bioremediators. Fungi as Bioremediators, pp. 29–49.

Asemoloye, M.D., Tosi, S., Daccò, C., Wang, X., Xu, S., Marchisio, M.A., Gao, W., Jonathan, S.G., Pecoraro, L. (1912). Hydrocarbon Degradation and Enzyme Activities of *Aspergillus oryzae* and *Mucor irregularis* Isolated from Nigerian Crude Oil-Polluted Sites. Microorganisms, 30, 8(12), 1912.

Awasthi, S., Srivastava, N., Singh, T., Tiwary, D., Mishra, P.K. *(2017). Biodegradation of thermally treated low density polyethylene by fungus Rhizopus* oryzae NS 5. 3 Biotech, 7(1), 73.

Badia-Fabregat, M., Lucas, D., Gros, M., Rodríguez-Mozaz, S., Barceló, D., Caminal, G., Vicent, T. (2015). Identification of s.ome factors affecting pharmaceutical active compounds (PhACs) removal in real wastewater. Case study of fungal treatment of reverse osmosis concentrate. Journal of Hazardous Materials, 283, 663–671.

Branà, M.T., Cimmarusti, M.T., Haidukowski, M., Logrieco, A.F., Altomare, C. (2017). Bioremediation of aflatoxin B1-contaminated maize by king oyster mushroom (*Pleurotus eryngii*). PLoS One, 12(8), e0182574.

Cervantes-González, E., Guevara-García, M.A., García-Mena, J., Ovando-Medina, V.M. (2019). Microbial diversity assessment of polychlorinated biphenyl–contaminated soils and the biostimulation and bioaugmentation processes. Environmental Monitoring and Assessment, 191, 118.

Chen, B.L., Ding, J. (2012). Biosorption and biodegradation of phenanthrene and pyrene in sterilized and unsterilized soil slurry systems stimulated by *Phanerochaete chrysosporium*. Journal of Hazardous Materials, 229, 159–169.

Cheraghpour, J., Etemadifar, Z., Afsharzadeh, S., Bahador, N. (2020). Assessment of bioremediation potential of *Microcystis aeruginosa* for removal of cadmium and lead ions from aqueous matrices. Iranian Journal of Fisheries Sciences, 19(4), 1994 – 2009.

Cherni, Y., Botta, C., Kasmi, M., Franciosa, I., Cocolin, L., Chatti, A., Trabelsi, I., Elleuch, L. (2020). Mixed culture of *Lactococcus lactis* and *Kluyveromyces marxianus* isolated from kefir grains for pollutants load removal from Jebel Chakir leachate. Water Environment Research, 92, 2041–2048.

Chugh, M., Kumar, L., Shah, M.P., Bharadvaja, N. (2022). Algal Bioremediation of heavy metals: An insight into removal mechanisms, recovery of by-products, challenges, and future opportunities. Energy Nexus, 7, 100129.

Deng, J., Fu, D., Hu, W., Lu, X., Wu, Y., Bryan, H. (2020). Physiological responses and accumulation ability of *Microcystis aeruginosa* to zinc and cadmium: Implications for bioremediation of heavy metal pollution. Bioresource Technology, 303, 122963.

Dias, C., Reis, A., Santos, J.A.L., Lopes Da Silva, T. (2020). Concomitant wastewater treatment with lipid and carotenoid production by the oleaginous yeast *Rhodosporidium toruloides* grown on brewery effluent enriched with sugarcane molasses and urea. Process Biochemistry, 94, 1 – 14.

Dini, I., Alborino, V., Lanzuise, S., Lombardi, N., Marra, R., Balestrieri, A., Ritieni, A., Woo, S.L., Vinale, F. (2022). Trichoderma Enzymes for Degradation of Aflatoxin B1 and Ochratoxin A. Molecules, 20, 27(12), 3959.

dos Santos Bazanella, G.C., Araujo, A.V., Castoldi, R., Maciel, G.M., Inacio, F.D., de Souza, C.G.M., Bracht, A., Peralta, R.M. (2013). Ligninolytic enzymes from white-rot fungi and application in the removal of synthetic dyes. In: Polizeli, T.M., Rai, M., De Lourdes, M., editors. Fungal enzymes. Boca Raton: CRC Press, pp. 258–279.

Dsouza, G.C., Sheriff, R.S., Ullanat, V., Shrikrishna, A., Joshi, A.V., Hiremath, L., Entoori, K. (2021). Fungal biodegradation of low-density polyethylene using consortium of Aspergillus species under controlled conditions. Heliyon, 13,7(5), e07008.

Egorova, D.O., Demakov, V.A., Plotnikova, E.G. (2013). Bioaugmentation of a polychlorobiphenyl contaminated soil with two aerobic bacterial strains. Journal of Hazardous Materials, 261, 378–386.

Gargouri, B., Mhiri, N., Karray, F., Aloui, F., Sayadi, S. (2015). Isolation and Characterization of Hydrocarbon-Degrading Yeast Strains from Petroleum Contaminated Industrial Wastewater. BioMed Research International, 929424.

Garrido-Sanz, D., Sansegundo-Lobato, P., Redondo-Nieto, M., Suman, J., Cajthaml, T., Blanco-Romero, E., Martin, M., Uhlik, O., Rivilla, R. (2020). Analysis of the biodegradative and adaptive potential of the novel polychlorinated biphenyl degrader Rhodococcus sp. WAY2 revealed by its complete genome sequence. Microbial Genome, 6(4), e000363

González, L.E., Cañizares, R.O., Baena, S. (1997) Efficiency of ammonia and phosphorus removal from a colombian agroindustrial wastewater by the microalgae *Chlorella vulgaris* and *Scenedesmus dimorphus*. Bioresource Technology, 60, 259 – 262.

Gu, H., Lou, J., Wang, H., Yang, Y., Wu, L., Wu, J., Xu, J. (2016). Biodegradation, Biosorption of Phenanthrene and Its Trans-Membrane Transport by Massilia sp. WF1 and *Phanerochaete chrysosporium*. Frontiers in Microbiology, 29, 7:38.

Guo, J., Chen, J., Li, C., Wang, L., Liang, X., Shi, J., Zhan, F. (2023). Arbuscular Mycorrhizal Fungi Promote the Degradation of the Fore-Rotating Crop (*Brassica napus* L.) Straw, Improve the Growth of and Reduce the Cadmium and Lead Content in the Subsequent Maize. Agronomy, 13, 767.

Horváthová, H., Lászlová, K., Dercová, K. (2018). Bioremediation of PCB-contaminated shallow river sediments: The efficacy of biodegradation using individual bacterial strains and their consortia. Chemosphere, 193, 270–277.

Ibrahim, S.S., Elsabagh, R., Allam, A., Youssef, G., Fadl, S.E., Abdelhiee, E.Y., Alkafafy, M., Soliman, A., Aboubakr, M. (2021). Bioremediation role of *Spirulina platensis* against deltamethrin-mediated toxicity and its chemical residues in chicken meat. Environmental Science and Pollution Research International, 28(40), 56188 – 56198.

Jacobsen, C.S., Pedersen, J.C. (1991). Mineralization of 2,4-dichlorophenoxyacetic acid (2,4-D) in soil inoculated with *Pseudomonas cepacia* DBO1(-pRO101), *Alcaligenes eutrophus* AEO106(pRO101) and *Alcaligenes eutrophus* JMP134(pJP4): Effects of inoculation level and substrate concentration. Biodegradation, , 2(4)253-63.

Jiang, Z., Shi, M., Shi, L. (2020). Degradation of organic contaminants and steel corrosion by the dissimilatory metal-reducing microorganisms Shewanella and Geobacter spp. International Biodeterioration & Biodegradation, 147, 104842.

Jiao, X., Li, G., Wang, Y., Nie, F., Cheng, X., Abdullah, M., Lin, Y., Cai, Y. (2018). Systematic Analysis of the *Pleurotus ostreatus* Laccase Gene (PoLac) Family and Functional Characterization of PoLac2 Involved in the Degradation of Cotton-Straw Lignin. Molecules, 23(4), 880.

Kafil, M., Berninger, F., Koutra, E., Kornaros, M. (2022). Utilization of the microalga *Scenedesmus quadricauda* for hexavalent chromium bioremediation and biodiesel production. Bioresource Technology, 346, 126665.

Kour, D., Kaur, T., Devi, R., Yadav, A., Singh, M., Joshi, D. (2021). Beneficial microbiomes for bioremediation of diverse contaminated environments for environmental sustainability: Present status and future challenges. Environmental Science and Pollution Research, 28, 24917–24939.

Krivoruchko, A., Kuyukina, M., Peshkur, T., Cunningham, C.J., Ivshina, I. (2023). Rhodococcus Strains from the Specialized Collection of Alkanotrophs for Biodegradation of Aromatic Compounds. Molecules, 28(5), 2393.

Krzmarzick, M.J., Taylor, D.K., Fu, X., McCutchan, A.L. (2018). Diversity and niche of archaea in bioremediation. Archaea, 2018, 3194108.

Liu, L., Li, S., Wang, S., Dong, Z., Gao, H. (2018). Complex Iron Uptake by the Putrebactin-Mediated and Feo Systems in *Shewanella oneidensis*. Applied and Environmental Microbiology, 84(20), e01752-18.

Lladó, S., Covino, S., Solanas, A.M., Vinas, M., Petruccioli, M., Dannibale, A. (2013). Comparative assessment of bioremediation approaches to highly

recalcitrant PAH degradation in a real industrial polluted soil. Journal of Hazardous Materials, 248–249, 407–414.

Mallak, A.M., Lakzian, A., Khodaverdi, E., Haghnia, G.H., Mahmoudi, S. (2020). Effect of *Pleurotus Ostreatus* and *Trametes Versicolor* on Triclosan Biodegradation and Activity of Laccase and Manganese Peroxidase Enzymes. Microbial Pathogenesis, 149, 104473.

Masindi, V., Osman, M.S., Tekere, M. (2021) Water Pollution and Remediation: Heavy Metals. Springer; Berlin/Heidelberg, Germany: Mechanisms and Approaches for the Removal of Heavy Metals from Acid Mine Drainage and Other Industrial Effluents, pp. 513–537.

Massoud, R., Hadiani, M.R., Hamzehlou, P., Khosravi-Darani, K. (2019). Bioremediation of heavy metals in food industry: Application of *Saccharomyces cerevisiae*. Electronic Journal of Biotechnology, 37, 56–60.

Mau, J.L., Lin, Y.P., Chen, P.T., Wu, Y.H., Peng, J.T. (1998). Flavor compounds in king oyster mushrooms *Pleurotus eryngii*. Journal of Agricultural and Food Chemistry, 46(11), 4587–4591.

Mori, T., Sudo, S., Kawagishi, H., Hirai, H. (2018). Biodegradation of Diuron in Artificially Contaminated Water and Seawater by Wood Colonized with the White-Rot Fungus *Trametes Versicolor*. Journal of Wood Science, 64, 690–696.

Nicula, N.O., Lungulescu, E.M., Rîmbu, G.A., Marinescu, V., Corbu, V.M., Csutak, O. (2023). Bioremediation of Wastewater Using Yeast Strains: An Assessment of Contaminant Removal Efficiency. International Journal of Environmental Research and Public Health, 20, 4795.

Nicula, N.O., Lungulescu, E.M., Rîmbu, G.A., Marinescu, V., Corbu, V.M., Csutak, O. (2023). Bioremediation of Wastewater Using Yeast Strains: An Assessment of Contaminant Removal Efficiency. Journal of Environmental and Public Health, 8, 20(6), 4795.

Nowak, M., Zawadzka, K., Szemraj, J., Góralczyk-Bińkowska, A., Lisowska, K. (2021). Biodegradation of Chloroxylenol by *Cunninghamella elegans* IM 1785/21GP and *Trametes versicolor* IM 373: Insight into Ecotoxicity and Metabolic Pathways. International Journal of Molecular Sciences, 22(9), 4360.

Oliveira, A.C., Barata, A, Batista, A.P., Gouveia, L. (2019). *Scenedesmus obliquus* in poultry wastewater bioremediation. Environmental Technology, 40(28), 3735 - 3744.

Rahhou, A., Layachi, M., Akodad, M., El Ouamari, N., Rezzoum, N.E., Skalli, A., Oudra, B., El Bakali, M., Kolar, M., Imperl, J., et al. (2023). The Bioremediation Potential of *Ulva lactuca* (Chlorophyta) Causing Green Tide in Marchica Lagoon (NE Morocco, Mediterranean Sea): Biomass, Heavy Metals, and Health Risk Assessment. Water, 15(7), 1310.

Rodríguez, C.E., Castro-Gutiérrez, V., Chin-Pampillo, J.S., Ruiz-Hidalgo, K.

(2013). On-farm biopurification systems: Role of white-rot fungi in depuration of pesticide-containing wastewaters. FEMS Microbiology Letters, 345, 1–12.

Sekar, R., DiChristina, T.J. (2014). Microbially driven fenton reaction for degradation of the widespread environmental contaminant 1,4-dioxane. Environmental Science and Technology, 48, 12858-12867.

Sharma, P., Pandey, A.K., Kim, S.H., Singh, S.P., Chaturvedi, P., Varjani, S. (2021). Critical review on microbial community during in-situ bioremediation of heavy metals from industrial wastewater. Environmental Technology and Innovation, 24, 101826.

Shuang, Q., ShiJian, G., Champagne, P., Robertson, R.M. (2017). Potential of *Ulva lactuca* for Municipal Wastewater Bioremediation and Fly Food. Desalination and Water Treatment, 91, 23 – 30.

Solis, M.I.V., Abraham, P.E., Chourey, K., Swift, C.M., Löffler, F.E., Hettich, R.L. (2019). Targeted detection of *Dehalococcoides mccartyi* microbial protein biomarkers as indicators of reductive dechlorination activity in contaminated groundwater. Scientific Reports, 22, 9(1), 10604.

Thengodkar, R.R.M., Sivakami, S. (2010). Degradation of Chlorpyrifos by an alkaline phosphatase from the *Cyanobacterium Spirulina platensis*, Biodegradation, 21, 637 - 644.

Ugya, A.Y., Ajibade, F.O., Hua, X. (2021). The efficiency of microalgae biofilm in the phycoremediation of water from River Kaduna. Journal of Environmental Management, 1(295), 113109

Wang, K., Brown, R.C., Homsy, S. et al. (2013). Fast pyrolysis of microalgae remnants in a fluidized bed reactor for bio-oil and biochar production. Bioresource Technology, 127, 494 - 499.

Wang, Y., Qiu, L., Hu, M. (2018). Application of yeast in the wastewater treatment. E3S Web Conference, 53: 04025.

Wu, H., Wu, Q., Zhang, J., Gu, Q., Wei, L., Guo, W., He, M. (2019). Chromium ion removal from raw water by magnetic iron composites and *Shewanella oneidensis* MR-1. Scientific Reports, 9(1), 3687.

Zhang, K., Xu, Y., Y., Hua, X.F., Han, H.L., Wang, J N., Wang, J. et al. (2008). An intensified degradation of phenanthrene with macroporous alginate-lignin beads immobilized *Phanerochaete chrysosporium*. Biochemical Engineering Journal, 41, 251–257.

Zhang, Y., Xie, J., Liu, M., Tian, Z., He, Z., van Nostrand, J.D., Ren, L., Zhou, J., Yang, M. (2013). Microbial community functional structure in response to antibiotics in pharmaceutical wastewater treatment systems. Water Resources, 47, 6298–6308.

CHAPTER 2

COMPARISON OF SOUS-VIDE COOKING METHOD WITH SOME TRADITIONAL COOKING METHODS IN TERMS OF MEAT TEXTURE AND SDS-PAGE PROFILE

Emel OZ[1]

1 Doç. Dr., Atatürk Üniversitesi, Ziraat Fakültesi, Gıda Mühendisliği Bölümü emel.oz@atauni.edu.tr

Introduction

Meat is an important foodstuff for humans' diet because of its rich nutritional elements. However, meat is also a material that is highly sensitive to various quality deteriorations (Zhou et al., 2010). Cooking is an important technique that has been used since ancient times to preserve meat quality and safety and increase its shelf life. With cooking, the meat's water content decreases, sarcoplasmic, myofibrillar and connective tissue proteins are denatured, and thus meat texture and quality change (Tornberg, 2005; Barbera and Tassone, 2006).

One of the important parameters that play a role in consumer preference is meat texture. Textural properties are closely related to changes in proteins (Larrea et al., 2006). Sarcoplasmic proteins have been reported to affect meat quality parameters including color, texture, and water holding capacity (Marcos et al., 2010). In myofibrillar proteins, it has been reported that due to denaturation during cooking, the hydrophobic environment increases and this affects the water retention capacity (Berhe et al., 2014).

Meat texture is a highly variable characteristic of meat that is affected by many factors such as cooking temperature, time, and method. Cooking methods can be classified as low-temperature cooking methods applied below 100 ºC and high-temperature cooking methods applied above 100 ºC (Angel-Rendon et al., 2020). Some cooking methods such as high-temperature grill and oven are frequently preferred for cooking meat (Babür and Gürbüz, 2015). However, these methods may cause the formation of some hazardous compounds that pose a risk to human health (Öz and Zikirov, 2015). In recent years, as a result of increasing consumer awareness on the food-health relationship, the trend towards cooking methods such as sous-vide, which involves low temperature application, has increased (Angel-Rendon et al., 2020). The basis of the sous-vide method is; it is the application of heat at a controlled temperature in a water bath to a food packaged under vacuum and then quickly cooling the food to 0-3 ºC (Vaudagne et al., 2008). In this method, meat samples are cooked for a long time at temperatures varying between 50-80 ºC, depending on the characteristics and size of the meat (Baldwin, 2012). It has been mentioned that the sous-vide method is advantageous in terms of flavor profile and textural properties (Vaudagne et al., 2008).

Herein, the effects of grill, oven cooking and sous-vide cooking methods on the water content, cooking loss, texture and SDS-PAGE profiles of M. *Longissimus thoracis et lumborum* muscle were determined.

Material and Method

Material and cooking methods

M. *Longissimus thoracis et lumborum* muscles (24h post mortem) were used as material. Muscles brought to the laboratory under cold chain were cut into slices of 2 cm in thickness after removing the visible fat and connective tissues.

Sous-vide, grill (on a hot plate) and oven cooking techniques were used to cook samples. Cooking temperatures were 80 ºC for sous-vide (Öz and Zikirov, 2015), 180 ºC for grilling (on a hot plate) and oven cooking (Öz and Çelik, 2015). All cooking methods were based on an internal temperature of 71 ºC, which is accepted as the microbial safety limit for beef by USDA - FSIS (Anon., 2020).

Water content

The water content was determined by drying the 10 g samples weighed in the cups in an oven at 102-105°C until a constant weight (Gökalp ve ark. 2010).

Cooking loss

The change in the weight of the samples cooked with different methods was calculated as a percentage, and the cooking loss values were determined (Oz and Zikirov, 2015).

SDS-PAGE profile of sarcoplasmic/ myofibrillar proteins

The method reported by Oz and Kaya (2019) was used for this analysis. Briefly, the samples were homogenized in a 30 mM phosphate buffer (pH 7.4). The homogenate was centrifuged at 10000 g for 20 min at 4 °C, and the supernatant was stored as the sarcoplasmic protein fraction after filtration. Then, the pellet obtained was homogenized with 100 mM phosphate buffer (pH 7.4). The homogenate was centrifuged at 10000 g for 20 min at 4 °C, and the supernatant was collected as the myofibrillar protein fraction. The concentration of the fractions was determined by the Bradford method and then mixed with 50 mM Tris buffer. The mixture was kept at 100 °C for 5 min and stored at −18 °C.

For the separation of proteins, 5% loading gel and 12% separation gel were used. Then, the samples were loaded into gel wells, and run at 100 V. After that the gel was then stained with a staining solution. After staining, the dye was removed with a wash solution until the gel background became clear. The molecular weights of the bands were evaluated using the protein standard in the Image Lab 6.0 program.

Texture profile analysis

The texture profile of the samples including hardness, springiness, cohesiveness and chewiness were determined at room temperature using a texture profile analyzer and aluminum P/50R probe (Yeşilyurt, 2020).

Statistical analysis

The research was carried out according to the randomized complete blocks trial plan with 3 replications, based on three different cooking methods (sous-vide, grill and oven). Statistical analysis was performed to evaluate the significance of differences between groups.

Results and discussion

Water content and cooking loss of meat cooked with different cooking methods

The water contents of the samples are presented in Table 1. Different cooking methods had a significant ($P<0.01$) effect on the water content of the meat, and the water content of the samples varied between 65.11-68.99%. While the highest water content was detected in meat samples cooked with the sous-vide method, the average water content of the samples cooked with the grill and oven methods did not differ statistically from each other. The high-water content of meats cooked with the sous-vide method is thought to be related to the fact that these samples are cooked in a vacuum-sealed plastic package. Indeed, it has been stated that in the sous-vide cooking method, packaging can be a factor that prevents the evaporation of water in meat (Baldwin, 2012; Modzelewska-Kapituła et al., 2019). In addition, protein denaturation during cooking may also have affected this result. Aaslyng et al. (2003) reported that, as a result of protein denaturation during cooking, the water content of meat decreases with less water retention in the protein structures.

Table 1. *Water content and cooking losses of meats cooked with different methods (mean ± SD)*

Cooking method	Water content (%)	Cooking loss (%)
Sous-vide	68.99±0.38^{a}	19.79±1.50^{b}
Grill	65.11±1.37^{b}	30.20±2.04^{a}
Oven	66.02±0.78^{b}	27.80±1.61^{a}
Sign.	**	**

SD: Standard deviation, *: $P<0.05$, **: $P<0.01$
Different letters in the same column are significantly different.

As can be seen from the Table 1, different cooking methods had a significant ($P<0.01$) effect on the cooking loss of meat, and the values var-

ied between 19.79-30.20%. While the highest and lowest cooking losses were determined in the samples cooked with grill and sous-vide methods, respectively, the cooking loss values of the samples cooked with the oven method did not differ statistically from those of the samples cooked with the grill method. It has been stated that cooking loss varies depending on many factors such as cooking method and cooking surface (Alfaia et al., 2010). It is thought that the low cooking loss detected in the samples cooked with the sous-vide method may be related to the low temperature applied in this method and the fact that the samples were packaged before cooking. In addition, this result may be related to the fact that this cooking method causes lower levels of denaturation in meat proteins.

Changes in myofibrillar and sarcoplasmic protein profile of meat cooked with different cooking methods

The SDS-PAGE profile of myofibrillar proteins of meat cooked with different methods is presented in Figure 1. Accordingly, it was evaluated that the samples generally had similar myofibrillar protein profiles. In all treatment groups, high band intensity was detected in proteins with molecular weights of 56, 43, 39, 38.4 and 37 kDa, and low band intensity was detected in proteins with molecular weights of 27, 25, 17 and 14.4 kDa. The heavy myosin form, weighing 200 kDa, of myosin, one of the most important myofibrillar proteins of meat, was not observed in any sample. It is thought that the density difference observed between different protein molecules in the current study may be related to the different thermal tolerances of protein fractions. Indeed, Wen et al. (2015) reported that actin and myosin, the two most important myofibrillar proteins of meat, responded differently to the cooking process. Additionally, they stated that the thermal tolerance of myosin decreased significantly at 60 ºC, while actin maintained its stability.

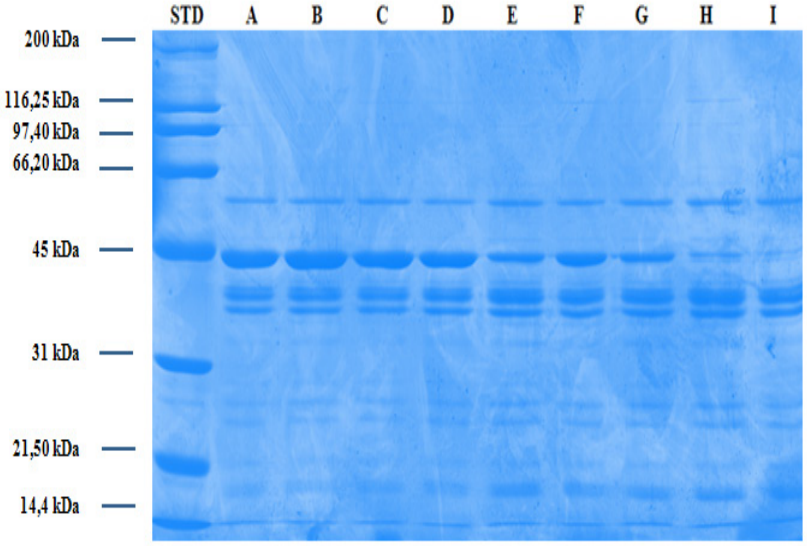

Figure 1. *SDS-PAGE electrophoretogram of myofibrillar proteins of meat cooked with different methods*

STD: It shows the protein standard in the range of 200-14.4 kDa.
A, B, C: Samples cooked with sous-vide method, D, E, F: Samples cooked with grill method, G, H, I: Samples cooked with oven method

In this current study, the density of the 43 kDa protein band (actin) varied between treatment groups, the highest band density was observed in the samples cooked with the sous-vide method, and the lowest band density was observed in the samples where the oven cooking method was applied. This result can be related to the aggregation of the protein. Kajak-Siemaszko et al. (2011) reported that decreases in protein band densities could be observed due to the inability of large polymerized protein clusters to enter the gel pores as a result of cooking. Dai et al. (2013) reported that the low band density observed due to aggregation was related with a high denaturation rate. In this respect, it can be said that the sous-vide cooking method applied in the current research causes lower levels of protein denaturation in meat compared to grill and oven cooking methods. On the other hand, while the protein band weighing 17 kDa could not be detected in samples cooked with sous-vide, it exhibited low band intensity in samples with grill and oven cooking methods. Dai et al. (2014) reported that some low molecular weight protein bands resulting from myosin degradation products could be observed because of the cooking process.

The SDS-PAGE profile of sarcoplasmic proteins of meat cooked with different methods is presented in Figure 2. Accordingly, it was evaluated that there were only 3 protein bands in cooked meats with molecular

weights of 27, 17 and 14.4 kDa. Sarcoplasmic proteins, known as soluble proteins of the sarcoplasm; They are low molecular weight proteins containing various enzymes, pigments and regulatory proteins (Tornberg, 2005). It has been reported that these proteins generally aggregate at 40 - 60 ºC (Wen et al., 2015). Considering the internal temperature of 71 ºC applied in the current study, this explains the sarcoplasmic protein profile observed in the present study.

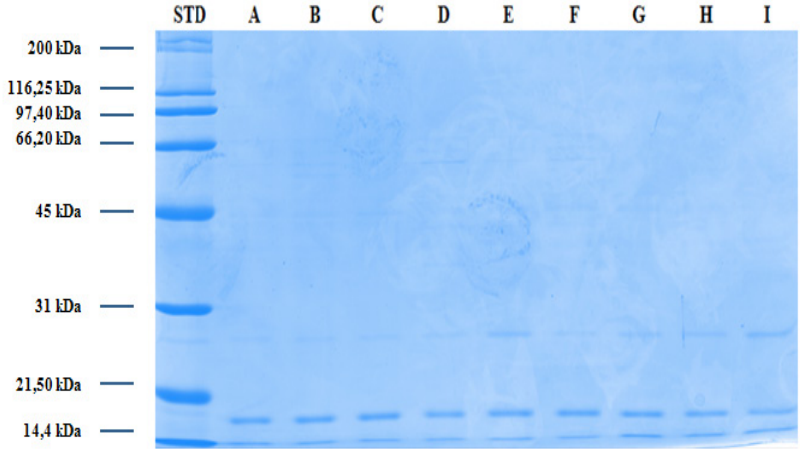

Figure 2. *SDS-PAGE electrophoretogram of sarcoplasmic proteins of meats cooked with different methods*

STD: It shows the protein standard in the range of 200-14.4 kDa.
A, B, C: Samples cooked with sous-vide method, D, E, F: Samples cooked with grill method, G, H, I: Samples cooked with oven method

According to the sarcoplasmic protein electrophoretogram, protein bands weighing 17 and 14.4 kDa were detected in all cooking methods, while the protein molecule weighing 27 kDa was not observed in the samples with sous-vide cooking method. This may be related to the fact that the saturated steam in the sous-vide bag causes further expansion of this protein.

Texture profile of meats cooked with different cooking methods

Data on the texture profile of meat are presented in Table 2. Accordingly, the springiness, cohesiveness and chewiness properties of meats cooked with different methods did not show a statistically significant difference from each other. However, different cooking methods had a significant ($P<0.05$) effect on the hardness value. While the lowest and highest hardness values were detected in the samples cooked with the sous-vide

and grill methods, respectively, the hardness values of the samples cooked with the oven method did not differ statistically from the hardness values of the samples cooked with the sous-vide and grill methods.

Table 2. *Texture profile of meats cooked with different methods (mean ± SD)*

Cooking method	Hardness (N)	Springiness (mm)	Cohesiveness	Chewiness (N.mm)
Sous-vide	225.48±64.52^{b}	0.75±0.11^{a}	0.69±0.06^{a}	125.82±64.79^{a}
Grill	323.68±22.01^{a}	0.80±0.09^{a}	0.73±0.09^{a}	194.97±62.81^{a}
Oven	262.99±20.71^{ab}	0.77±0.03^{a}	0.69±0.01^{a}	140.18±64.79^{a}
Sign.	*	Ns	ns	ns

SD: Standard deviation, *: P<0.05, ns: Not significant
Different letters in the same column are significantly different.

It is thought that the lower hardness of samples cooked with the sous-vide method compared to other cooking methods may be related to the lower temperature applied in this method and the fact that this method causes a more moderate denaturation in meat proteins. King et al. (2003) reported that rapid heating caused significant shortening of myofibrils and a decrease in sarcomere length. On the other part, it was observed that meat with high hardness also had high cooking losses. This confirms the idea that cooking loss can affect the degree of hardness of meat. It has been stated that the denaturation of proteins during meat cooking causes a decrease in the amount of water retained in the meat, and as a result of this, the observed cooking loss affects the hardness value (Chiavaro et al., 2009).

Conclusion

The use of different cooking methods affected the water content, cooking loss and hardness of the samples statistically. The highest water content, lowest cooking loss and hardness value were determined in the samples cooked by the sous-vide method. Myofibrillar and sarcoplasmic proteins of meats cooked with different methods generally showed similar SDS-PAGE profiles. However, some protein band densities differed depending on the cooking method. In the light of the SDS-PAGE profile results, it can be said that the sous-vide cooking method has a more moderate effect on the denaturation of meat proteins compared to other cooking methods.

Acknowledgment

This research was supported by the Atatürk University (Project No: 2020-8555). In addition, this research presented in part at the International 19 May Innovative Scientific Approaches Congress-V, Samsun, Turkey, May 19, 2021.

References

Aaslyng, M.D., Bejerholm, C., Ertbjerg, P., Bertram, H.C. & Andersen, H.J. (2003). Cooking loss and juiciness of pork in relation to raw meat quality and cooking procedure. *Food Quality and Preference*, 14, 277-288.

Alfaia, C.M.M., Alves, S.P., Lopes, A.F., Fernandes, M.J.E., Costa, A.S.H., Fontes, C.M.G.A., Castro, M.L.F., Bessa, R.J.B. & Prates, J.A.M. (2010). Effect of cooking methods on fatty acids, conjugated isomers of linoleic acid and nutritional quality of beef intramuscular fat. *Meat Science*, 84 (4), 769-777.

Ángel-Rendón, S.V., Filomena-Ambrosio, A., Hernández-Carrión, M., Llorca, E., Hernando, I., Quiles, A. & Sotelo-Díaz, I. (2020). Pork meat prepared by different cooking methods. A microstructural, sensorial and physicochemical approach. *Meat Science*, 163, 108089.

Babür, T.E. & Gürbüz, Ü. (2015). Geleneksel pişirme yöntemlerinin et kalitesine etkileri. *Journal of Tourism and Gastronomy Studies*, 3-4, 58-64.

Baldwin, D.E. (2012). Sous vide cooking: A review. *International Journal of Gastronomy and Food Science*, 1(1), 15-30.

Barbera, S. & Tassone, S. (2006). Meat cooking shrinkage: Measurement of a new meat quality parameter. *Meat Science*, 73, 467-474.

Berhe, D.T., Engelsen, S.B., Hviid, M.S. & Lametsch, R. (2014). Raman spectroscopic study of effect of the cooking temperature and time on meat proteins. *Food Research International*, 66, 123–131.

Chiavaro, E., Rinaldi, M., Vittadini, E. & Barbanti, D. (2009). Cooking of pork Longissimus dorsi at different temperature and relative humidity values: Effects on selected physico-chemical properties. *Journal of Food Engineering*, 93, 158-165.

Dai, Y., Miao, J., Yuan, S.Z., Liu, Y., Li, X.M. & Dai, R.T. (2013). Colour and sarcoplasmic protein evaluation of pork following water bath and ohmic cooking. *Meat Science*, 93, 898–905.

Gökalp, H.Y., Kaya, M. & Zorba, Ö. (2010). Et ürünleri işleme mühendisliği Atatürk Üniversitesi, Yayın No: 786. Atatürk Üniversitesi Ziraat Fakültesi Ofset Tesisi. Erzurum.

Kajak-Siemaszko, K., Aubry, L., Peyrin, F, Bax, M.L., Gatellier, P., Astruc, T., Przybylski, W., Jaworska, D., Gaillard-Martinie, B. & Sante-Lhoutellier, V. (2011). Characterization of protein aggregates following a heating and freezing process. *Food Research International*, 44, 3160−3166.

King, D.A., Dikeman, M.E., Wheeler, T.L., Kastner, C.L. & Koohmaraie, M. (2003). Chilling and cooking rate effects on some myofibrillar determinants of tenderness of beef. *Journal of Animal Science*, 81, 1473-1481.

Larrea, V., Hernando, I., Quiles, A., Lluch, M.A. & Perez-Munuera, I. (2006). Changes in proteins during Teruel dry-cured ham processing. *Meat Science*, 74, 586–593.

Marcos, B., Kerry, J.P. & Mullen, A.M. (2010). High pressure induced changes on sarcoplasmic protein fraction and quality indicators. *Meat Science*, 85, 115-120.

Modzelewska-Kapituła, M., Pietrzak-Fiećko, R., Tkacz, K., Draszanowska, A. & Więk, A. (2019). Influence of sous vide and steam cooking on mineral contents, fatty acid composition and tenderness of *semimembranosus* muscle from Holstein- Friesian bulls. *Meat Science*, 157, 107877.

Oz, E. & Kaya, M. (2019). The proteolytic changes in two different types of pastırma during the production. *Journal of Food Processing and Preservation*, 43 (8), e14042.

Öz, F. & Zikirov, E. (2015). The effects of sous-vide cooking method on the formation of heterocyclic aromatic amines in beef chops. *LWT-Food Science and Technology*, 64, 120-125.

Oz, F., & Celik, T. (2015). Proximate composition, color and nutritional profile of raw and cooked goose meat with different methods. *Journal of food processing and preservation*, 39(6), 2442-2454.

Tornberg, E. (2005). Effects of heat on meat proteins – implications on structure and quality of meat products. *Meat Science*, 70(3), 493-508.

Vaudagna, S.R., Pazos, A.A., Guidi, S.M., Sanchez, G., Carp, D.J. & Gonzalez, C.B. (2008). Effects of salt addition on sous vide cooked whole beef muscles from Argentina. *Meat Science*, 79(3), 470–482.

Wen, S., Zhou, G., Li, L., Xu, X., Yu, X., Bai, Y. & Li, C. (2015). Effect of cooking on in vitro digestion of pork proteins: A peptidomic perspective. *Journal of Agricultural and Food Chemistry*, 63, 250−261.

Yeşilyurt, H. (2020). İncir (*ficus carica l.*) kabuğu ununun yağ ikamesi ve fonksiyonelleştirici olarak köfte üretiminde kullanim potansiyeli. Yüksek Lisans Tezi, Fen Bilimleri Enstitüsü, Ondokoz Mayıs Üniversitesi, Samsun.

Zhou, G.H., Xu, X.L. & Liu, Y. (2010). Preservation technologies for fresh meat–A Review. *Meat Science*, 86, 119–128.

CHAPTER 3

LOTUS FIBER

Suat CANOĞLU[1], Ayberk ŞİT[2]

1 Prof.Dr., Marmara University, Faculty of Technology, Department of Textile Engineering, Recep Tayyip Erdoğan Campus, Istanbul / Türkiye scanoglu@marmara.edu.tr / ORCID: 0000-0002-1604-9875
2 Marmara University, Faculty of Technology, Department of Textile Engineering, Recep Tayyip Erdoğan Campus, Istanbul / Türkiye ayberksit@marun.edu.tr / ORCID: 0009-0008-9116-9800

1. INTRODUCTION

In the Intergovernmental Panel on Climate Change (IPCC), held in 2007, scientists declared that one of the most important causes of climate change is carbon dioxide gas emission. As a result, trend towards sustainability has increased worldwide. It has become inevitable to consider the concept of sustainability from design stage to recycle of a product. In this process, various sustainable production approaches have been put forward. Elimination of harmful effects on human health during production process, reducing waste, increasing production of recyclable products, planning and implementing product design process in accordance with these strategies and developing production processes that save materials and energy are examples of these approaches [1].

Figure 1. Lotus flower and leaf [7]

The United Nations General Assembly designated 2009 as the International Year of Natural Fibers (IYNF) and focused on raising awareness around the world about natural fibers [2]. Increased environmental aware-

ness due to growing of environmental problems on a global scale and unsustainable consumption of petroleum resources, have raised the demand for environmentally friendly, biodegradable and sustainable materials [3,4]. Efforts are increasing in textile sector to realize production of materials from environmentally friendly fibers and to reduce processes that pollute the nature. Fibers used in production of environmentally friendly products are important. There is a need for production made from renewable plant-derived fibers. These products are recyclable and biodegradable [5].

Lotus is an aquatic perennial distributed in Asia, North America and Australia. It has been cultivated for more than 2000 years [6]. *Figure 1* shows lotus flower and leaf [7].

Lotus fiber is an aromatic, natural and cellulosic fiber obtained from lotus plant. Lotus fibers have yellowish white color and soft touch [8]. It stands out as it is completely organic and environmentally friendly [5]. Lotus fibers have a self-cleaning property [7].

Process of extracting fiber from lotus plant has been practiced since 1910. Today, lotus fibers are used in sustainable luxury industry. Italy-based Loro Piana and Cambodia-based Samatoa are among the brands that use lotus fiber in sustainable luxury sector [5].

In the next parts of this chapter, subjects such as extraction of lotus fiber, its properties, structure and application areas will be examined.

2. EXTRACTION OF LOTUS FIBER

First step in the fiber extraction process from lotus plant is collection of lotus stems. Shallow cuts are made on the outside of the stems with help of a knife. Then, lotus stems are broken. Broken lotus stems are twisted to extract the fibers and are obtained by systematically pulling the fibers [5]. The fibers are extracted by twisting and breaking lotus stems one by one in 5 cm section [9]. In addition, fiber can be obtained from lotus rhizomes. Process of extraction fiber from plant rhizomes is carried out by folding and breaking rhizomes. Then, the lotus fibers are exposed [9].

Various processes such as biological, chemical and biochemical methods can be applied to lotus stems in order to obtain lotus fibers. Biological extraction method consists of dipping lotus stems in water. Lotus stems soften with the help of bacteria in water. Afterwards, fibers are obtained from softened lotus stems. Lotus stems can also dip in enzymes and semi-cellulosic chemicals. This method is called biochemical extraction [9]. In a study in which the chemical method was applied, lotus stems that were washed, dried at room temperature and cut were placed in sodium hydroxide (NaOH) solution and treated under microwave irradiation. Plant

stems were washed with deionized water. Then, samples were separated after lotus stems were squeezed and rinsed. After these processes, fibers were dried at 50°C [10].

3. PROPERTIES AND STRUCTURE OF LOTUS FIBER

In this section, physical and chemical properties and structure of lotus fiber will be examined.

3.1. Physical Properties and Structure

Wang et al. (2008) investigated basic physical properties of lotus fiber such as linear density, volumetric density and moisture regain rate. According to this study, volumetric density of lotus fiber was found as 1.1848 g/cm^3. This value was lower than volumetric density of cotton, wool and ramie fibers but similar to volumetric density of acrylic fibers. Linear density value of the fiber was found to be 1.55 dtex. This result showed that lotus fiber has a fine structure. Fine structure of the fiber contributes to yarn strength and evenness for yarns produced from lotus fiber. In the study, it was determined that moisture regain value of the fiber was 12.32%. Lotus fibers regain moisture at a higher rate than cotton and silk fibers but at a lower rate than wool fibers [11]. In *Table 1*, volumetric density and moisture regain values of various fibers compared with lotus fiber in the chapter are given [11,12].

Table 1. *Volumetric density and moisture regain values of various fibers [11,12]*

Fiber Type	**Volumetric Density *(g/cm^3)***	**Moisture Regain *(%)***
Cotton	1.55	7 – 8.5
Wool	1.30	13 – 19
Silk	1.34	11
Acrylic	1.19	1.2 – 2
Lotus	1.1848	12.32

Pandey et al. (2020) stated that the lotus fiber used in their study had an average fineness of 0.22 tex (2.2 dtex). Fibers showed an average elongation of 1.95% and average moisture content of the fiber was 11.3%. In addition, average tenacity of the fibers was 13.41 g/tex. Average moisture content of the fiber was higher than moisture content of cotton fiber. High moisture value is due to amount of -OH groups. Increase in moisture content in the fiber provides that body perspiration is removed into the atmosphere and increasing moisture content is recommended for high comfort [13].

Pan et al. (2011) stated that Young's modulus and average breaking tenacity of lotus fibers were similar to cotton fibers. In addition, elongation

value of lotus fiber was close to elongation value of flax fiber. It was determined that average strength of lotus fiber was 2.23 cN/dtex and average Young's modulus of the fiber was 78.5 cN/dtex. Average elongation of the fibers was found to be 2.6%. Moisture regain value of lotus fibers was up to 12.3% and average fineness value was 0.91 dtex. It was noted that the fineness of lotus fibers ranged between 0.56 - 1.81 dtex, strength was between 1.07 - 5.25 cN/dtex, modulus was between 12.9 - 144.1 cN/dtex and elongation value was between 1.88 - 4.07%. Various physical properties of untreated lotus fibers are shown in *Table 2* [8].

Table 2. *According to a study, physical properties of lotus fibers [8]*

Parameter	**Average**	**Range**
Fineness *(dtex)*	0.91	0.56 – 1.81
Strength *(cN/dtex)*	2.23	1.07 – 5.25
Modulus *(cN/dtex)*	78.5	12.9 – 144.1
Elongation *(%)*	2.60	1.88 – 4.07

Chen et al. (2012) explained that breaking strength of lotus fibers was 3.44 cN/dtex, initial modulus was 146.81 cN/dtex and breaking elongation was 2.75% [14].

Yuan et al. (2012) noted that lotus fiber strength gradually increased from wet state to dry state. It was also explained that elongation of the fiber at break gradually decreased as it changed from wet state to dry state [15].

Liu et al. (2009) explained that lumen structure seen in cotton fiber was not seen in cross section of lotus fiber. Cross section of lotus fiber has a slightly oval or elliptical shape [16]. Chen et. al (2012) stated that the fiber had a spiral shape in longitudinal direction [14]. Lotus fibers are naturally crimped [13].

Ananthi et al. (2023) investigated thermal comfort properties of knitted fabrics produced from bamboo fiber, lotus fiber and their blends (100% lotus, 67% lotus - 37% bamboo, 50% lotus - 50% bamboo, 37% lotus - 67% bamboo and 100% bamboo). It was observed that increase in lotus fiber ratio in the fabric increased water vapor permeability, air permeability and thermal conductivity of the fabric but decreased its thermal resistance. Fabrics produced from lotus fiber are more suitable for production of summer wear in terms of thermal comfort. Length of lotus fibers used in the study was 451 mm, fineness was 1.62 dtex, strength was 4.05 cN/tex (0.405 cN/dtex), elongation was 2.19%, volumetric density was 1.08 g/cm^3 and moisture regain value was 7.04% [17].

In a study, it was stated that fiber length was not affected by lotus peduncle length or thickness. 61% of the fibers used in the study ranged between

20-55 cm, 30% ranged between 56-140 cm and 9% ranged between 12-19 cm. Average length value of the fibers was determined as 46.72 cm [13].

3.2. Chemical Properties and Structure

The main component of lotus fiber is cellulose [14]. It was seen that the fiber contains 41.4%±0.29% cellulose, 25.87±0.64% hemicellulose and 19.56±0.32% lignin [8]. Examples of other components in the fiber structure are fat waxy, ash, pectin, hydrotrope and amino acids [14]. When chemical structure of flax fiber is examined, it is seen that the fiber contains 70-85% of cellulose, 18.5% of hemicellulose and 2-3% of lignin [12]. Lotus fiber contains higher amounts of lignin and hemicellulose compared to other common plant fibers [8].

Surfaces with a contact angle less than 90° are hydrophilic, and surfaces with a contact angle more than 90° are hydrophobic [7]. It was seen that fabric produced from lotus fiber had a water contact angle of 145±0.05° [18].

In a study using cellulase enzyme, it was noted that non-cellulosic impurities on the fiber surface were removed by treating fabric produced from lotus fibers with cellulase enzyme. An increase in the wettability of the fabric was observed. As a result of the process, weight loss occurred in the fabric. Optimum conditions for the treatment were stated to be 2% enzyme concentration, 1:20 MLR (Material to Liquor Ratio), 5.5 pH, 55°C temperature and 60 minutes. Water contact angle of the fabric treated with cellulase enzyme under optimum conditions decreased to 30±0.02° [18].

Studies have shown that crystallinity of lotus fiber is 48% [8,14]. Crystallinity of cotton fiber is between 65-70% [19]. Ratio of crystalline region in the fiber has an effect on properties of the fiber such as absorbency, dyeability and touch [12].

In a study, it was noted that the behavior of lotus fiber against various chemicals was similar to that of cotton fiber. Both are cellulosic fibers and chemically similar to each other. Although lotus fiber is tolerant to alkalis, it is sensitive to concentrated acids. Lotus fiber was unaffected by treatment with acetic acid, the fiber was disintegrated by treatment with hydrochloric acid and completely dissolved by treatment with sulfuric acid. As stated, lotus fiber was unaffected by alkali treatment with sodium hydroxide. No effect on fiber was observed as a result of treatment with carbon tetrachloride. In addition, the fiber turned brown as a result of treatment with metacresol [13].

4. APPLICATION AREAS OF LOTUS FIBER

Lotus fibers have a delicate structure therefore production should be done carefully. Fabric production processes are carried out in the form of handmade. Fabric production from lotus fiber is time consuming and amount of fabric produced becomes limited [5]. Lotus fibers are used in production of garments, accessories such as bags and scarves, vegan leather, table linen, chemical-free food packaging material and various medical textiles [2,9]. It can be used as substitute of cotton fiber. It is also available in blends with other sustainable fibers [9].

In *Figure 2*, woven fabric produced from lotus fiber is shown [20]. Fabrics produced from lotus fiber have a similar appearance with blend of silk and linen [5]. *Figure 3* shows a scarf and *Figure 4* shows a garment produced from lotus fiber [20].

Figure 2. *Woven fabric produced from lotus fiber [20]*

Figure 3. *A scarf produced from lotus fiber [20]*

Figure 4. *A garment produced from lotus fiber [20]*

5. CONCLUSION

In this chapter, lotus fibers were examined for their physical and chemical properties and evaluated for their structures. Volumetric density, linear density, length, moisture regain rate, elongation, strength, modulus, crystallinity, water contact angle and chemical properties of the fiber were investigated. Fiber properties were compared with different fibers. In addition, application areas of the fibers were examined. Lotus fiber, a cellulose-based fiber, is one of the most sustainable and rare fibers. It is obtained from lotus plant. In recent years, increasing emphasis on sustainable fibers

in textile sector also contributes to awareness of lotus fibers. Thanks to values such as fineness and moisture regain, lotus fibers have superior comfort properties. Process from obtaining lotus fiber to fabric production requires high effort. It can be said that fabrics produced from lotus fiber has a high value. In this chapter, it is aimed to examine subjects such as extraction of lotus fiber, its properties, structure and application areas, to provide information about lotus fiber and to increase its recognition.

REFERENCES

[1] Yavuz, V.A. (2010) Sürdürülebilirlik Kavramı ve İşletmeler Açısından Sürdürülebilir Üretim Stratejileri. *Mustafa Kemal Üniversitesi Sosyal Bilimler Enstitüsü Dergisi*, 7(14), 63-86.

[2] Mahapatra, N.N. (2017) Processing of lotus fiber in textile industries. *Colourage*, 64(11), 74-76.

[3] Wu, M., Shuai, H., Cheng, Q., Jiang, L. (2014) Bioinspired Green Composite Lotus Fibers. *Angewandte Chemie International Edition*, 53, 3358-3361.

[4] Netravali, A.N., Chabba, S. (2003) Composites get greener. *Materials Today*, 6, 22-29.

[5] Gardetti, M.A., Muthu, S.S. (2015) The Lotus Flower Fiber and Sustainable Luxury. In *Handbook of Sustainable Luxury Textiles and Fashion*. Gardetti, M.A., Muthu, S.S. (eds.); Springer, Singapore.

[6] Zhu, M., Liu, T., Guo, M. (2016) Current Advances in the Metabolomics Study on Lotus Seeds. *Frontiers in Plant Science*, 7, 891.

[7] Özdoğan, E., Demir, A., Seventekin, N. (2006) Lotus Etkili Yüzeyler. *Tekstil ve Konfeksiyon*, 16(1), 287-290.

[8] Pan, Y., Han, G., Mao, Z., Zhang, Y., Duan, H., Huang, J., Qu, L. (2011) Structural characteristics and physical properties of lotus fibers obtained from Nelumbo nucifera petioles. *Carbohydrate Polymers*, 85(1), 188-195.

[9] Pandey, R., Dubey, A., Sinha, M.K. (2023) Lotus fibre drawing and characterization. In *Sustainable Fibres for Fashion and Textile Manufacturing*. Nayak, R. (ed.); Elsevier, Cambridge, USA.

[10] Cheng, C., Guo, R., Lan, J., Jiang, S. (2017) Extraction of lotus fibres from lotus stems under microwave irradiation. *Royal Society Open Science*, 4(9), 170747.

[11] Wang, J., Yuan, X., He, J., Gan, Y., Chen, D. (2008) Physical property of lotus fibers. *Journal of Textile Research*, 29(12), 9-11.

[12] Başer, İ. (1992) Elyaf Bilgisi. Marmara Üniversitesi Teknik Eğitim Fakültesi Döner Sermaye İşletmesi Matbaa Birimi, İstanbul, Türkiye.

[13] Pandey, R., Sinha, M.K., Dubey, A. (2020) Cellulosic fibers from Lotus (Nelumbo nucifera) peduncle. *Journal of Natural Fibers*, 17(2), 298-309.

[14] Chen, D.S., Gan, Y.J., Yuan, X.H. (2012) Research on Structure and Properties of Lotus Fibers. *Advanced Materials Research*, 476-478, 1948-1954.

[15] Yuan, X.H., Gan, Y.J., Chen, D.S., Ye, Y.J. (2012) Analysis on mechanical properties of lotus fibers. *Advanced Materials Research*, 476-478, 1905-1909.

[16] Liu, D., Han, G., Huang, J., Zhang, Y. (2009) Composition and structure study of natural Nelumbo nucifera fiber. *Carbohydrate Polymers*, 75, 39-43.

[17] Ananthi, P., Jemina Rani, P.C., Priyalatha, S., Prakash, C. (2023) Investigation on Influence of Blend Proportion on Comfort Characteristics of Bamboo/Lotus Knitted Fabrics. *Journal of Natural Fibers*, 20(1), 2153192.

[18] Vajpayee, M., Dave, H., Singh, M., Ledwani, L. (2022) Cellulase Enzyme Based Wet-Pretreatment of Lotus Fabric to Improve Antimicrobial Finishing with A. indica Extract and Enhance Natural Dyeing: Sustainable Approach for Textile Finishing. *ChemistrySelect*, 7(25), e202200382.

[19] Reddy, N., Yang, Y. (2008) Characterizing natural cellulose fibers from velvet leaf (Abutilon theophrasti) stems. *Bioresource Technology*, 99(7), 2449-2454.

[20] Samatoa (2022) *https://samatoa.lotus-flower-fabric.com/buy/sustainable/textile/pure-lotus-fabric/* [Accessed 24 May 2023].

CHAPTER 4

ACTIVATION FUNCTIONS USED IN ARTIFICIAL NEURAL NETWORKS

İsmail AKGÜL[1]

1 Asst. Prof. Dr., Department of Computer Engineering, Faculty of Engineering and Architecture, Erzincan Binali Yıldırım University, Erzincan, Türkiye, E-mail: iakgul@erzincan.edu.tr, ORCID: 0000-0003-2689-8675

1. Introduction

The human brain consists of billions of biological/natural neurons connected. A neuron receives input from other neurons and produces output, stimulating subsequent neurons. Biological neurons form the Biological Neural Network (BNN) by establishing connections between them. Artificial neurons are created with computational models inspired by biological neurons. Artificial neurons that imitate the neurons in BNNs also establish connections between them, forming an Artificial Neural Network (ANN). In an ANN consisting of artificial neurons, outputs are calculated as a function of inputs. In each artificial neuron, multiplication and addition operations are performed with parameters such as input data, weight, and bias. In addition, each artificial neuron has an Activation Function (AF) hyperparameter that performs activation processes. In this chapter, firstly, an overview of the structure of ANNs is presented and then the AFs used in ANNs are discussed.

2. Artificial Neural Networks (ANN)

ANN was developed as a generalization of mathematical models of biological nervous systems. According to the basic assumption of theoretical neurophysiology, the nervous system is a network consisting of neurons, each of which has a soma and an axon (McCulloch and Pitts, 1943). Figure 1 shows the structure of a biological neuron.

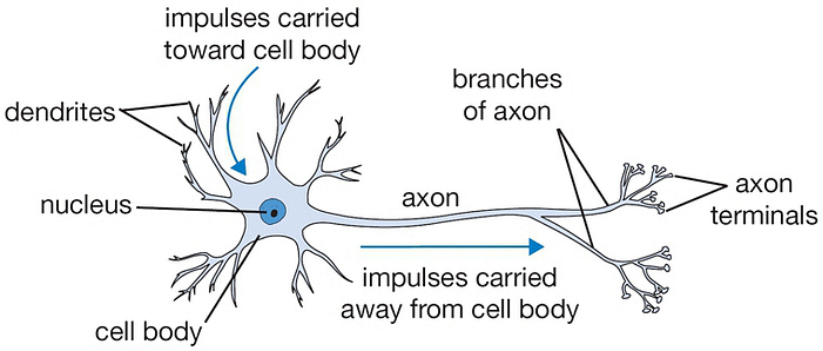

Figure 1. *Structure of a biological neuron (Medium, 2023a)*

The human brain, consisting of more than 10 billion interconnected neurons, is capable of parallel computing cognitive and perceptual actions and control activities. In Figure 1, tree-like nerve fiber networks called dendrites are connected to the cell body or soma where the cell nucleus is located. A single long fiber called an axon extends from the cell body. This

fiber eventually divides into ribbons and sub-strands and connects to other neurons via synaptic terminals or synapses (Abraham, 2005). In this way, signals are sent, and other neurons are activated. Similarly, artificial neurons are a computational model inspired by natural neurons. (Gershenson, 2003).

ANN is modeled based on BNN. Similar to the connection of neurons in a BNN, ANN consists of connecting nodes. At each node, signals such as the number of inputs and outputs, input and output weights, and AFs are processed (Zou et al., 2009). The basic building block of ANN is the artificial neuron. In other words, it is a simple mathematical model. There are three simple rules in the mathematical model of the neuron which are multiplication, addition, and activation. In the artificial neuron, at the input each input value is multiplied by weights, in the middle the pre-weighted inputs and biases are collected, and at the output this sum passes through the AF, also called the transfer function (Krenker et al., 2011). Figure 2 shows the structure of an artificial neuron, and Figure 3 shows the mathematical model of an artificial neuron.

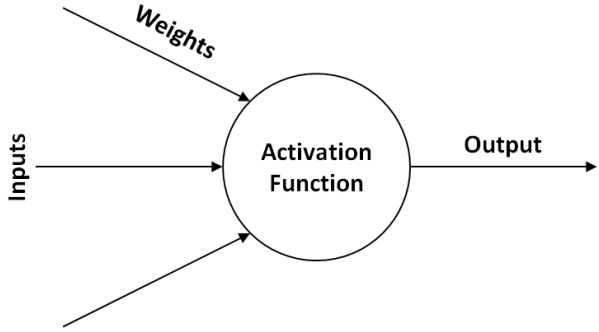

Figure 2. *Structure of an artificial neuron*

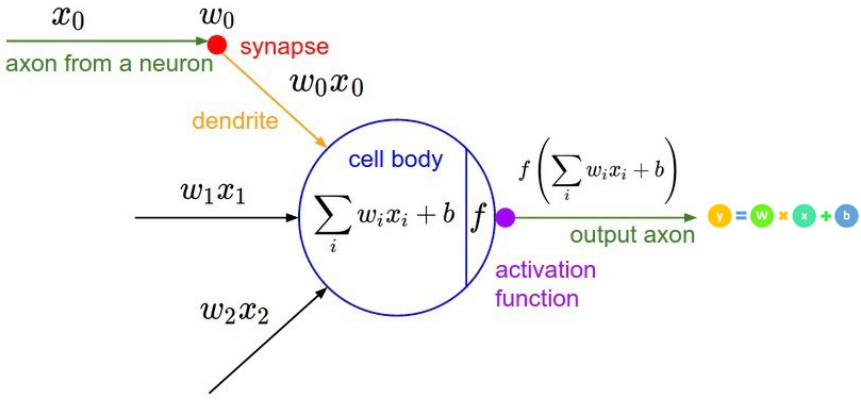

Figure 3. *Mathematical model of an artificial neuron (Medium, 2023a)*

In Figure 3, x represents input data, w represents weight, b represents bias, f represents AF and y represents output value. After the multiplication of all inputs and weights in each artificial neuron is collected, the bias value is added, and the output is obtained by subjecting it to the AF. Each neuron is connected in series and parallel, forming the neural network.

If a neural network consists of a single layer, it is called a single-layer ANN. A single-layer ANN contains only input and output layers. If a neural network consists of many neurons and hidden layers, it is called a multilayer ANN (Veri Bilimi Okulu, 2023). The basic architecture of ANN consists of three types of neuron layers: input, hidden, and output (Abraham, 2005). Figure 4 shows the multilayer ANN structure.

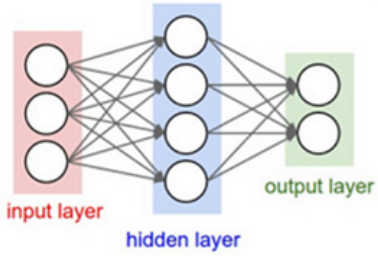

Figure 4. *Multilayer ANN structure (Medium, 2023a)*

Figure 4 shows a three-layer ANN model consisting of input, hidden, and output layers. Each layer can contain many artificial neurons. An ANN structure is formed as a result of connecting artificial neurons to each other.

ANN is one of the Artificial Intelligence (AI) methods that aims to gain self-learning ability by modeling the human brain architecturally. Information is kept in its memory thanks to the neurons in its structure that imitate BNNs, and the neurons in the layers are connected thanks to weights. ANN has a distributed architecture and processes information in parallel. It is used in many areas such as classification, prediction, and modeling (Yılmaz and Kaya, 2019).

ANNs, one of the important tools of machine learning, whose use has become widespread in neuroscience, offer powerful techniques for data analysis (Yang and Wang, 2020). ANNs, which are massively parallel systems, consist of many simple processors connected. ANNs are inspired by BNNs and attempt to use some of the organizational principles believed to be used in humans (Jain et al., 1996). Recent advances in ANNs have revealed the power to optimize millions of synaptic weights from millions of observations to work robustly in real-world applications (Hasson et al., 2020). ANNs have been applied to many fields, from speech recognition to

protein structure prediction, and from cancer classification to gene prediction (Krogh, 2008).

3. Activation Functions (AF)

AF is the function that converts input signals into output signals in an artificial neuron (Pratiwi et al., 2020). In ANNs, each neuron typically has a nonlinear AF (Agostinelli et al., 2014). The task of the AF is to help learn complex mappings by transforming input data that cannot be linearly separated into more linearly separable abstract features (Sharma et al., 2017; Dubey et al., 2022). AF plays an important role in the training process and model performance of an ANN (Rasamoelina et al., 2020). When ANNs are designed, many hyperparameters directly affect the performance of the model. It is important to decide on the selection of hyperparameters such as the number of layers, number of neurons, optimization algorithm, learning rate, and AF to be used in the model. AFs are one of the important hyperparameters that directly affect the performance of the model.

Many AFs are used in the layers of ANNs. In this section, Step, Linear, Sigmoid, Tanh, ReLU, Swish, and Softmax AFs are included. Information is presented about AFs, which have an important role in the training and performance of the ANN model and provide an output based on the inputs in ANN.

3.1. Step Function

Step is the simplest AF used when creating a binary classifier (Sharma et al., 2017). Its derivative always equals zero (Tatraiya et al., 2023). Since it has a fundamental problem such as non-differentiability, it cannot be used to calculate error coefficients in backpropagation ANNs (Asaad and Ali, 2019). Sigmoid is used instead of Step (Ying, 1990). The mathematical expression of the Step function is shown in Equation 1, and the plot of the Step function and its derivative is shown in Figure 5.

$$f(x) = \begin{cases} 0, & x < 0 \\ 1, & x \geq 0 \end{cases} \tag{1}$$

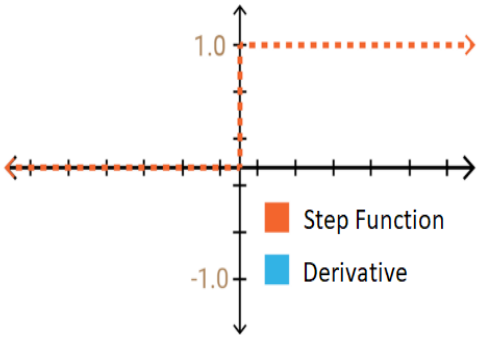

Figure 5. *Step function and derivative (Medium, 2023b, Towards Data Science, 2023)*

As shown in Equation 1 and Figure 5, the Step function has a structure that produces binary values (0 or 1). The derivative of the Step function is zero. Since it is not differentiable, it is not preferred to be used in hidden layers and is generally used in output layers. It can only solve binary classification problems.

3.2. Linear Function

Linear is an AF proportional to the input whose equation resembles a straight line (Feng and Lu, 2019). It is directly proportional to the input. Its derivative is not zero but equal to the value of the constant used. It is not preferred because the error cannot be improved due to the same gradient value in each iteration of the ANN. It can be used for simple tasks. Linear function can be used to eliminate the disadvantage of zero gradient in the Step function (Sharma et al., 2017). It is used in the output layer in regression problems (Sivri et al., 2022). The mathematical expression of the Linear function is shown in Equation 2, and the plot of the Linear function and its derivative is shown in Figure 6.

$$f(x) = x \tag{2}$$

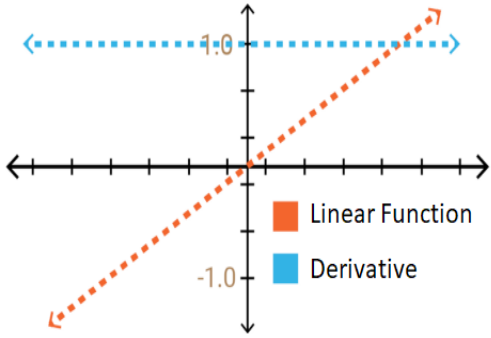

Figure 6. *Linear function and derivative (Medium, 2023b, Towards Data Science, 2023)*

As shown in Equation 2 and Figure 6, the Linear function has a structure that produces values between -∞ and ∞. The derivative of the Linear function equals a constant value. It is not preferred because its derivative is equal to a constant value and is generally used in very simple tasks.

3.3. Sigmoid Function

Sigmoid is one of the oldest AFs used in ANNs (Kamalov, 2021). It is the AF that is most useful for training data between 0 and 1 (Sibi et al., 2013). It is nonlinear and has a regular derivative (Rasamoelina et al., 2020). Thanks to the derivative of the Sigmoid, the error coefficient used to propagate the error in ANNs can be calculated (Asaad and Ali, 2019). The mathematical expression of the Sigmoid function is shown in Equation 3, and the plot of the Sigmoid function and its derivative is shown in Figure 7.

$$f(x) = \frac{1}{1+e^{-x}} \tag{3}$$

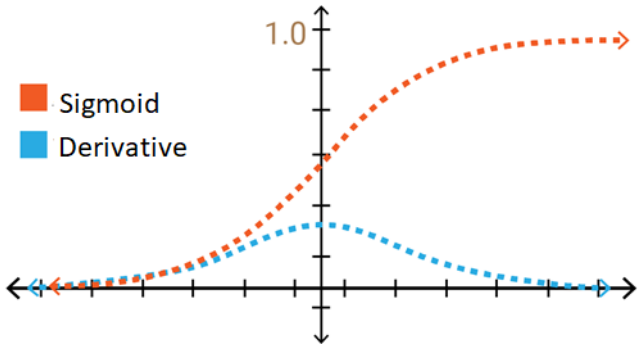

Figure 7. *Sigmoid function and derivative (Medium, 2023b, Towards Data Science, 2023)*

As shown in Equation 3 and Figure 7, the Sigmoid function has a structure that produces values between 0 and 1. Hence, it compresses the data between 0 and 1. The Sigmoid function has a derivative. Therefore, the Sigmoid is preferred instead of the Step, whose derivative is equal to zero, and the Linear, whose derivative is equal to a constant number. The Sigmoid is a nonlinear differentiable function and is generally used in output layers in binary classification problems.

3.4. Hyperbolic Tangent (Tanh) Function

Tanh is one of the AFs commonly used instead of the Sigmoid to train ANNs in regression problems from the late 1990s to the early 2000s (Jagtap and Karniadakis, 2023). It is nonlinear and differentiable everywhere (Kılıçarslan et al., 2021; Ding et al., 2018). The Tanh is similar in shape to the Sigmoid, but the Sigmoid has limits from 0 to 1, while the Tanh has limits from -1 to +1 (Kukreja et al., 2016). Compared to the Sigmoid, the gradient is steeper. It is preferred over the Sigmoid because it has gradients that are not limited to moving in a particular direction and is zero-centered (Tatraiya et al., 2023). The mathematical expression of the Tanh function is shown in Equation 4, and the plot of the Tanh function and its derivative is shown in Figure 8.

$$f(x) = \frac{(e^{x} - e^{-x})}{(e^{x} + e^{-x})} \tag{4}$$

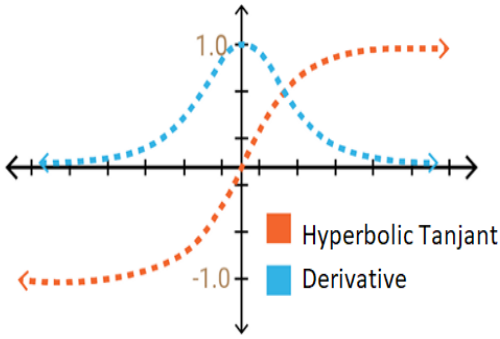

Figure 8. *Tanh function and derivative (Medium, 2023b, Towards Data Science, 2023)*

As shown in Equation 4 and Figure 8, the Tanh function has a structure that produces values between -1 and 1. Tanh is quite similar to the Sigmoid. The Tanh, whose derivative is steeper than the Sigmoid, provides more efficient learning because it can take more values. Therefore, it is almost always superior to the Sigmoid. Tanh is a nonlinear differentiable function and is generally used in hidden layers in binary classification problems.

3.5. Rectified Linear Unit (ReLU) Function

ReLU is one of the most used AFs in ANNs (Surekcigil Pesch et al., 2022). At input values less than zero, the output is equal to zero, and at input values greater than zero, the output is equal to the input (Stursa and Dolezel, 2019; Bai, 2022). Since the ReLU only propagates gradients when the input is positive, activating ANNs with the ReLU is simpler than Sigmoid and Tanh. Therefore, using the ReLU makes ANN less regular compared to others (Zhang et al., 2023). It has become the default AF, having been widely used in ANNs since 2012. Although the ReLU is popular, the fact that input values less than zero are exactly zero prevents negative values from propagating throughout the network (Chieng et al., 2018). The mathematical expression of the ReLU function is shown in Equation 5, and the plot of the ReLU function and its derivative is shown in Figure 9.

$$f(x) = \begin{cases} 0, & x < 0 \\ x, & x \geq 0 \end{cases} \tag{5}$$

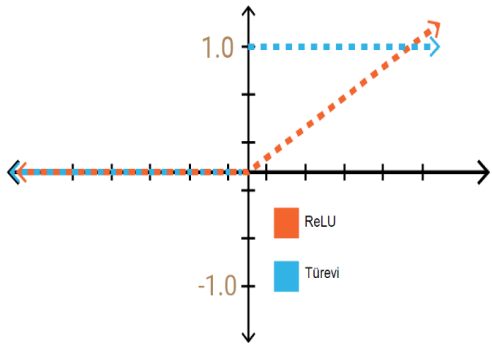

Figure 9. *ReLU function and derivative (Medium, 2023b, Towards Data Science, 2023)*

As shown in Equation 5 and Figure 9, the ReLU function has a structure that produces values between 0 and ∞. It produces zero at values of x less than zero, and x at values of x greater than zero. At negative values, neurons take the value zero, which significantly reduces the computational load. Therefore, the ReLU is preferred over Sigmoid and Tanh in multilayer ANNs. It is a very popular and effective AF. On the one hand, the fact that neurons take the value of zero at negative values is a disadvantage of the ReLU. Because, at values of x less than zero, the derivative is zero, so learning does not occur in these regions. ReLU is a nonlinear differentiable function and is generally used in hidden layers in multilayer ANNs.

3.6. Leaky ReLU Function

Leaky ReLU is a continuous, unbounded, zero-centered, and low-computational AF (Gustineli, 2022). It is a modified version of the classic ReLU. At input values less than zero, the output will have a small slope. Although this causes slowness, it can solve the problem of neurons not learning by reducing the problem of dead neurons (Xu et al., 2020). The Leaky ReLU, which is fast and simple to calculate, helps prevent saturation problems that may occur in Sigmoid and Tanh (Mahima et al., 2023). Like the ReLU, the Leaky ReLU is also a very popular AF. Its difference from the ReLU is that the Leaky ReLU can also be differentiated at values less than zero (Dubey and Jain, 2019). The Leaky ReLU, which was developed to prevent the problem of vanishing gradients in training ANNs, performs similarly to the ReLU. This shows that the non-zero slope of the Leaky ReLU over the entire domain does not significantly affect ANN training (Maas et al., 2013). The mathematical expression of the Leaky ReLU function is shown in Equation 6, and the plot of the Leaky ReLU function and its derivative is shown in Figure 10.

$$f(x) = \begin{cases} 0.01x, & x < 0 \\ x, & x \geq 0 \end{cases} \tag{6}$$

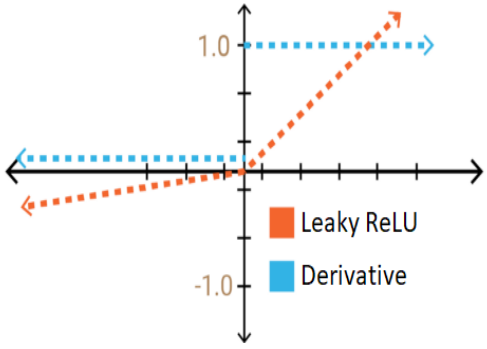

Figure 10. *Leaky ReLU function and derivative (Medium, 2023b, Towards Data Science, 2023)*

As shown in Equation 6 and Figure 10, the Leaky ReLU function has a structure that produces values between -∞ and ∞. It produces a value, albeit small, at values of x less than zero. Since the Leaky ReLU, unlike the ReLU, also processes values less than zero, learning occurs at every stage, but the processing load is high. Although the Leaky ReLU is slightly better than the ReLU because learning occurs at each stage, the ReLU is more popular due to the higher processing load. The Leaky ReLU is a nonlinear differentiable function and is generally used in hidden layers in multilayer ANNs.

3.7. Swish (A Self-Gated) Function

Swish is a hybrid AF proposed as a combination of input and Sigmoid (Nwankpa et al., 2018). It was suggested by Google in 2017 (Zhu and Chen, 2020). It is a non-monotonic function (Biswas et al., 2022; Mercioni and Holban, 2023), and its most important difference from other AFs is that it is not monotonic (Koçak and Şiray, 2022). This means the value of the function may decrease even if the values of the inputs increase (Sharma et al., 2017). The Swish outperforms the ReLU and its versions in many tasks (Kumar, 2022), due to its features of having no upper and lower bounds, being smooth, and being non-monotonic (Hu et al., 2022). The mathematical expression of the Swish function is shown in Equation 7, and the plot of the Swish function and its derivative is shown in Figure 11.

$$f(x) = x * sigmoid(x) \tag{7}$$

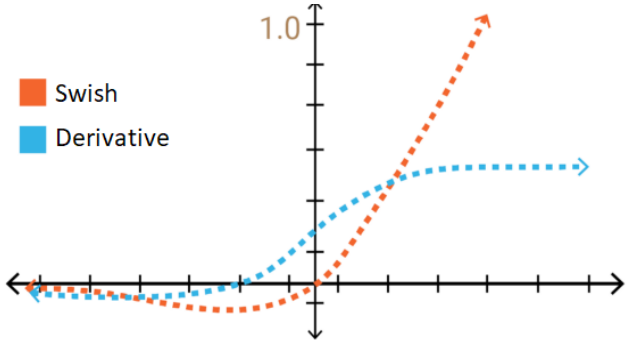

Figure 11. *Swish function and derivative (Medium, 2023b, Towards Data Science, 2023)*

As shown in Equation 7 and Figure 11, the Swish function has a structure that produces values between -∞ and ∞. It is very similar to the Sigmoid and produces as output the multiplication of the inputs and the Sigmoid. While the ReLU does not process values less than zero, the Swish, like the Leaky ReLU, also processes values less than zero. Therefore, in the Swish, learning occurs in every region, just like the Leaky ReLU. Its difference from the Leaky ReLU is that the values it receives in the negative region are nonlinear. It performs better than the ReLU in most problems. The Swish is a nonlinear differentiable function and is generally used in hidden layers in multilayer ANNs.

3.8. Softmax Function

Softmax is an AF commonly used in ANNs (Mahima et al, 2023). To represent a classification problem in ANNs, the Softmax is usually used in the last layer (Raghuram et al., 2022). It outputs the dependent probabilities corresponding to each input (Emanuel et al., 2023). Represents the probability, between 0 and 1, that the input matches a particular class. Thus, the output can be interpreted as a possibility (Velonis and Vergos, 2022). The Softmax, which is similar to the Sigmoid, is an extension of the Sigmoid for more than two values (Bouchard, 2007). Its difference from the Sigmoid is that the Sigmoid is useful in binary classification problems, while the Softmax is useful in multiple classification problems (Sharma, 2019). Softmax is seen as the Sigmoid with more classes. Used to determine the probability of more classes at the same time (Mercioni and Holban, 2020). The mathematical expression of the Softmax function is shown in Equation 8.

$$f(x_i) = \frac{e^{x_i}}{\sum_{j=1}^{n} e^{x_j}} \tag{8}$$

As shown in Equation 8, the Softmax function has a structure that produces values between 0 and 1. It is very similar to the Sigmoid and produces the probability result of each class as output. Its difference from the Sigmoid is that it gives the probability of each input belonging to a class by normalizing the sum of the outputs up to 1. In ANNs with more than two classifications, the Softmax is preferred instead of the Sigmoid. The Softmax is a nonlinear differentiable function and is generally used in output layers in multiple classification problems.

4. Conclusions

ANN is one of the AI methods that aims to gain learning ability by taking the human brain as an example. It contains artificial neurons in its structure. Thanks to artificial neurons, information is kept in its memory, and neurons are connected thanks to weights. In each artificial neuron, the input data is subjected to the activation process after being subjected to operations such as multiplication and addition with weight and bias parameters. AF is an important hyperparameter that directly affects the performance of the ANN and provides output based on input. In this chapter, firstly, an overview of the structure of ANNs is presented. Then, Step, Linear, Sigmoid, Tanh, ReLU, Leaky ReLU, Swish, and Softmax AFs used in ANNs are explained in detail.

Due to the problem that the derivative of the Step is zero and the derivative of the Linear is equal to a constant value, these two AFs are not used much in ANNs. The Sigmoid is preferred Instead of these two functions.

The Sigmoid has a smooth derivative. It is generally used in output layers in binary classification problems. In more than two classification problems, Softmax is preferred instead of Sigmoid. Both Sigmoid and Softmax are generally used in the output layers and not in the hidden layers. The Sigmoid is used in binary classification and the Softmax is used in multiple classifications.

The Tanh is very similar to the Sigmoid. Since its derivative is steeper and can take more values, it has been used frequently instead of the Sigmoid in previous years. The Tanh is not preferred much today and has been replaced by the ReLU. The ReLU is one of the most popular AFs used in multilayer ANNs today. In the ReLU, neurons take the value of zero at negative values, which reduces the processing load. Therefore, the ReLU is preferred instead of Sigmoid and Tanh.

The Leaky ReLU is derived from the ReLU. Although it provides a solution to the problem of the ReLU not learning at negative values, it is a function that has a similar effect to the ReLU in terms of performance. Since the Leaky ReLU also processes negative values, it is slower than the ReLU in terms of speed. Therefore, the ReLU is preferred instead of Leaky ReLU.

Swish is proposed as a combination of input and Sigmoid. Its main difference from other functions is that it is not monotonic. Like Leaky ReLU, it also processes negative values and provides learning in every region. Unlike the Leaky ReLU, the values it takes in the negative region are nonlinear and it performs better than the popular ReLU in most problems. The Swish is a function that produces successful results, like the ReLU.

As a result of the investigations, it was seen that Step and Linear functions are not preferred in ANNs, and the Tanh function is not used much anymore. It was concluded that Sigmoid and Softmax in the output layers of ANNs, and ReLU and Swish in the hidden layers of ANNs are the best AFs to be used.

References

Abraham, A. (2005). Artificial Neural Networks. *Handbook of Measuring System Design*; Sydenham, P.H., Thorn, R., Eds.; John Wiley & Sons, Ltd.: Hoboken, NJ, USA.

Agostinelli, F., Hoffman, M., Sadowski, P., & Baldi, P. (2014). Learning activation functions to improve deep neural networks. *arXiv preprint arXiv:1412.6830*. https://doi.org/10.48550/arXiv.1412.6830

Asaad, R. R., & Ali, R. I. (2019). Back Propagation Neural Network (BPNN) and sigmoid activation function in multi-layer networks. *Academic Journal of Nawroz University*, *8*(4), 216-221. https://doi.org/10.25007/ajnu.v8n4a464

Bai, Y. (2022). RELU-function and derived function review. In *SHS Web of Conferences* (Vol. 144, p. 02006). EDP Sciences. https://doi.org/10.1051/shsconf/202214402006

Biswas, K., Kumar, S., Banerjee, S., & Pandey, A. K. (2022, June). ErfAct and Pserf: Non-monotonic Smooth Trainable Activation Functions. In *Proceedings of the AAAI Conference on Artificial Intelligence* (Vol. 36, No. 6, pp. 6097-6105). https://doi.org/10.1609/aaai.v36i6.20557

Bouchard, G. (2007, December). Efficient bounds for the softmax function and applications to approximate inference in hybrid models. In *NIPS 2007 workshop for approximate Bayesian inference in continuous/hybrid systems* (Vol. 6).

Chieng, H. H., Wahid, N., Ong, P., & Perla, S. R. K. (2018). Flatten-T Swish: a thresholded ReLU-Swish-like activation function for deep learning. *arXiv preprint arXiv:1812.06247*. https://doi.org/10.26555/ijain.v4i2.249

Ding, B., Qian, H., & Zhou, J. (2018, June). Activation functions and their characteristics in deep neural networks. In *2018 Chinese control and decision conference (CCDC)* (pp. 1836-1841). IEEE. https://doi.org/10.1109/CCDC.2018.8407425

Dubey, A. K., & Jain, V. (2019). Comparative study of convolution neural network's relu and leaky-relu activation functions. In *Applications of Computing, Automation and Wireless Systems in Electrical Engineering: Proceedings of MARC 2018* (pp. 873-880). Springer Singapore. https://doi.org/10.1007/978-981-13-6772-4_76

Dubey, S. R., Singh, S. K., & Chaudhuri, B. B. (2022). Activation functions in deep learning: A comprehensive survey and benchmark. *Neurocomputing*. https://doi.org/10.1016/j.neucom.2022.06.111

Emanuel, R. H., Docherty, P. D., Lunt, H., & Möller, K. (2023). The effect of activation functions on accuracy, convergence speed, and misclassification confidence in CNN text classification: a comprehensive exploration. *The Journal of Supercomputing*, 1-21. https://doi.org/10.1007/s11227-023-05441-7

Feng, J., & Lu, S. (2019, June). Performance analysis of various activation functions in artificial neural networks. In *Journal of physics: conference series* (Vol. 1237, No. 2, p. 022030). IOP Publishing. https://doi.org/10.1088/1742-6596/1237/2/022030

Gershenson, C. (2003). Artificial neural networks for beginners. *arXiv preprint cs/0308031*.

Gustineli, M. (2022). A survey on recently proposed activation functions for Deep Learning. *arXiv preprint arXiv:2204.02921*. https://doi.org/10.48550/arXiv.2204.02921

Hasson, U., Nastase, S. A., & Goldstein, A. (2020). Direct fit to nature: an evolutionary perspective on biological and artificial neural networks. *Neuron*, *105*(3), 416-434. https://doi.org/10.1016/j.neuron.2019.12.002

Hu, H., Liu, A., Guan, Q., Qian, H., Li, X., Chen, S., & Zhou, Q. (2022). Adaptively customizing activation functions for various layers. *IEEE Transactions on Neural Networks and Learning Systems*. https://doi.org/10.1109/TNNLS.2021.3133263

Jagtap, A. D., & Karniadakis, G. E. (2023). How important are activation functions in regression and classification? A survey, performance comparison, and future directions. *Journal of Machine Learning for Modeling and Computing*, *4*(1). https://doi.org/10.1615/JMachLearnModelComput.2023047367

Jain, A. K., Mao, J., & Mohiuddin, K. M. (1996). Artificial neural networks: A tutorial. *Computer*, *29*(3), 31-44. https://doi.org/10.1109/2.485891

Kamalov, F., Nazir, A., Safaraliev, M., Cherukuri, A. K., & Zgheib, R. (2021, November). Comparative analysis of activation functions in neural networks. In *2021 28th IEEE International Conference on Electronics, Circuits, and Systems (ICECS)* (pp. 1-6). IEEE. https://doi.org/10.1109/ICECS53924.2021.9665646

Kılıçarslan, S., Adem, K., & Çelik, M. (2021). An overview of the activation functions used in deep learning algorithms. *Journal of New Results in Science*, *10*(3), 75-88. https://doi.org/10.54187/jnrs.1011739

Koçak, Y., & Şiray, G. Ü. (2022). Performance evaluation of swish-based activation functions for multi-layer networks. *Artificial Intelligence Studies*, *5*(1), 1-13. https://doi.org/10.30855/AIS.2021.05.01.01

Krenker, A., Bešter, J., & Kos, A. (2011). Introduction to the artificial neural networks. *Artificial Neural Networks: Methodological Advances and Biomedical Applications. InTech*, 1-18.

Krogh, A. (2008). What are artificial neural networks?. *Nature biotechnology*, *26*(2), 195-197. https://doi.org/10.1038/nbt1386

Kukreja, H., Bharath, N., Siddesh, C. S., & Kuldeep, S. (2016). An introduction to artificial neural network. *Int J Adv Res Innov Ideas Educ*, *1*, 27-30.

Kumar, R. (2022). APTx: better activation function than MISH, SWISH, and

ReLU's variants used in deep learning. *arXiv preprint arXiv:2209.06119*. https://doi.org/10.51483/IJAIML.2.2.2022.56-61

Maas, A. L., Hannun, A. Y., & Ng, A. Y. (2013, June). Rectifier nonlinearities improve neural network acoustic models. In *Proc. icml* (Vol. 30, No. 1, p. 3).

Mahima, R., Maheswari, M., Roshana, S., Priyanka, E., Mohanan, N., & Nandhini, N. (2023, July). A Comparative Analysis of the Most Commonly Used Activation Functions in Deep Neural Network. In *2023 4th International Conference on Electronics and Sustainable Communication Systems (ICESC)* (pp. 1334-1339). IEEE. https://doi.org/10.1109/ICESC57686.2023.10193390

McCulloch, W. S., & Pitts, W. (1943). A logical calculus of the ideas immanent in nervous activity. *The bulletin of mathematical biophysics*, *5*, 115-133. https://doi.org/10.1007/BF02478259

Medium (2023a) "Yapay Sinir Ağı Nedir?", https://ayyucekizrak.medium.com/şu-kara-kutuyu-açalim-yapay-sinir-ağları-7b65c6a5264a Accessed: 13.09.2023.

Medium (2023b) "Derin Öğrenme İçin Aktivasyon Fonksiyonlarının Karşılaştırılması", https://ayyucekizrak.medium.com/derin-öğrenme-için-aktivasyon-fonksiyonlarının-karşılaştırılması-cee17fd1d9cd Accessed: 13.09.2023.

Mercioni, M. A., & Holban, S. (2020, May). The most used activation functions: Classic versus current. In *2020 International Conference on Development and Application Systems (DAS)* (pp. 141-145). IEEE. https://doi.org/10.1109/DAS49615.2020.9108942

Mercioni, M. A., & Holban, S. (2023, June). A Brief Review of the Most Recent Activation Functions for Neural Networks. In *2023 17th International Conference on Engineering of Modern Electric Systems (EMES)* (pp. 1-4). IEEE. https://doi.org/10.1109/EMES58375.2023.10171705

Nwankpa, C., Ijomah, W., Gachagan, A., & Marshall, S. (2018). Activation functions: Comparison of trends in practice and research for deep learning. *arXiv preprint arXiv:1811.03378*. https://doi.org/10.48550/arXiv.1811.03378

Pratiwi, H., Windarto, A. P., Susliansyah, S., Aria, R. R., Susilowati, S., Rahayu, L. K., ... & Rahadjeng, I. R. (2020, February). Sigmoid activation function in selecting the best model of artificial neural networks. In *Journal of Physics: Conference Series* (Vol. 1471, No. 1, p. 012010). IOP Publishing. https://doi.org/10.1088/1742-6596/1471/1/012010

Raghuram, S., Bharadwaj, A. S., Deepika, S. K., Khadabadi, M. S., & Jayaprakash, A. (2022, December). Digital Implementation of the Softmax Activation Function and the Inverse Softmax Function. In *2022 4th International Conference on Circuits, Control, Communication and Computing (I4C)* (pp. 64-67). IEEE. https://doi.org/10.1109/I4C57141.2022.10057747

Rasamoelina, A. D., Adjailia, F., & Sinčák, P. (2020, January). A review of ac-

tivation function for artificial neural network. In *2020 IEEE 18th World Symposium on Applied Machine Intelligence and Informatics (SAMI)* (pp. 281-286). IEEE. https://doi.org/10.1109/SAMI48414.2020.9108717

Sharma, O. (2019, February). A new activation function for deep neural network. In *2019 international conference on machine learning, big data, cloud and parallel computing (COMITCon)* (pp. 84-86). IEEE. https://doi.org/10.1109/COMITCon.2019.8862253

Sharma, S., Sharma, S., & Athaiya, A. (2017). Activation functions in neural networks. *Towards Data Sci*, *6*(12), 310-316.

Sibi, P., Jones, S. A., & Siddarth, P. (2013). Analysis of different activation functions using back propagation neural networks. *Journal of theoretical and applied information technology*, *47*(3), 1264-1268.

Sivri, T. T., Akman, N. P., & Berkol, A. (2022, June). Multiclass classification using arctangent activation function and its variations. In *2022 14th International Conference on Electronics, Computers and Artificial Intelligence (ECAI)* (pp. 1-6). IEEE. https://doi.org/10.1109/ECAI54874.2022.9847486

Stursa, D., & Dolezel, P. (2019, June). Comparison of ReLU and linear saturated activation functions in neural network for universal approximation. In *2019 22nd International Conference on Process Control (PC19)* (pp. 146-151). IEEE. https://doi.org/10.1109/PC.2019.8815057

Surekcigil Pesch, I., Bestelink, E., de Sagazan, O., Mehonic, A., & Sporea, R. A. (2022). Multimodal transistors as ReLU activation functions in physical neural network classifiers. *Scientific Reports*, *12*(1), 670. https://doi.org/10.1038/s41598-021-04614-9

Tatraiya, P., Priyadarshi, H., Singh, K., Mishra, D., & Shrivastava, A. (2023, May). Applicative Analysis Of Activation Functions For Pneumonia Detection Using Convolutional Neural Networks. In *2023 IEEE IAS Global Conference on Emerging Technologies (GlobConET)* (pp. 1-8). IEEE. https://doi.org/10.1109/GlobConET56651.2023.10149937

Towards Data Science (2023) "Comparison of Activation Functions for Deep Neural Networks", https://towardsdatascience.com/comparison-of-activation-functions-for-deep-neural-networks-706ac4284c8a Accessed: 13.09.2023.

Velonis, K., & Vergos, H. T. (2022, November). A comparison of Softmax proposals. In *2022 International Conference on Electrical, Computer, Communications and Mechatronics Engineering (ICECCME)* (pp. 1-6). IEEE. https://doi.org/10.1109/ICECCME55909.2022.9988065

Veri Bilimi Okulu (2023) "Yapay Sinir Ağı(Artificial Neural Network) Nedir?", https://www.veribilimiokulu.com/yapay-sinir-agiartificial-neural-network-nedir/ Accessed: 13.09.2023.

Xu, J., Li, Z., Du, B., Zhang, M., & Liu, J. (2020, July). Reluplex made more practical: Leaky ReLU. In *2020 IEEE Symposium on Computers and*

communications (ISCC) (pp. 1-7). IEEE. https://doi.org/10.1109/ISCC50000.2020.9219587

Yang, G. R., & Wang, X. J. (2020). Artificial neural networks for neuroscientists: a primer. *Neuron*, *107*(6), 1048-1070. https://doi.org/10.1016/j.neuron.2020.09.005

Yılmaz, A., & Kaya, U. (2019). Derin öğrenme (1. Baskı). *İstanbul: Kodlab*.

Ying, X. (1990, June). Role of activation function on hidden units for sample recording in three-layer neural networks. In *1990 IJCNN International Joint Conference on Neural Networks* (pp. 69-74). IEEE. https://doi.org/10.1109/IJCNN.1990.137548

Zhang, S., Lu, J., & Zhao, H. (2023). Deep Network Approximation: Beyond ReLU to Diverse Activation Functions. *arXiv preprint arXiv:2307.06555*. https://doi.org/10.48550/arXiv.2307.06555

Zhu, J., & Chen, Z. (2020, November). Comparative analysis of various new activation functions based on convolutional neural network. In *Journal of Physics: Conference Series* (Vol. 1676, No. 1, p. 012228). IOP Publishing. https://doi.org/10.1088/1742-6596/1676/1/012228

Zou, J., Han, Y., & So, S. S. (2009). Overview of artificial neural networks. *Artificial neural networks: methods and applications*, 14-22. https://doi.org/10.1007/978-1-60327-101-1_2

CHAPTER 5

COMPARISON THE BIOREMEDIATION ABILITY OF M. ARTHROSPHOREA AND M. RADIOTOLERANS ON PYROXSULFONE HERBICIDE AND THEIR EFFECT ON MORTALITY OF DAPHNIA MAGNA[1]

Gokhan Onder ERGUVEN[2], Volkan KORKMAZ[3], Duygu TEKIN[4]

1 This study was supported by Munzur University, Scientific Research Coordinatorship Unit with the project numbered YLMUB021-15

2 Doç. Dr., Munzur University, Faculty of Economics and Administrative Sciences, Department of Political Science and Public Administration, Department of Urbanization and Environmental Issues, Tunceli, Turkey gokhanondererguven@gmail.com ORCID:0000-0003-1573-080X

3 Dr. Öğr. Üyesi, Munzur Unıversity, Faculty of Health Sciences, Department of Nursing, Tunceli, Turkey vkorkmaz@munzur.edu.tr ORCID:0000-0003-2022-6851

4 Çevre Yüksek Mühendisi, Munzur University, Graduate School of Education, Department of Environmental Engineering, Tunceli, Turkey duygu.duztas@gmail.com ORCID: 0000-0003-1708-2244

Introduction

Herbicides, which belong to a group of weed killer pesticides, are used continuously even in non-agricultural environments such as agricultural fields, homes, sports fields and other urban green spaces (Choudri et al., 2020). According to Sharma et al. (2020), it is inevitable that there will be serious consequences for the environment and humanity as a result of these uses.

Many herbicides are persistent in nature. Bacteria can bioremediate toxic effects of herbicides in a naturally engineered way. Controlling micro-organisms is an effective approach for a possible and imminent future cultivation with herbicides. According to Herbicide the remaining agriculture is targeted (detoxification), less targeted or designed to be removed from this education, for the polluted dreams of the last ostensibly effective technology is exploited (Sidhu et al., 2019).

Weeds are a fairly common group of all crop pests that invade crop fields each year. In every crop system, weeds present multidimensional problems that compete for water, space, nutrients and sunlight, negatively impacting crop production (Adetunji et al., 2019).

In modern farming systems, management of weeds is important to ensure abundant crop yields and its main purpose is to obtain maximum yield while minimizing cost (Guo et al., 2021). Therefore, due to the inadequate weed control capability of previous methods, herbicide application has become an important part of weed management programs in agriculture. Herbicide technology provides an effective and relatively inexpensive means of weed control, significantly reducing the heavy financial burden and contributing to increasing average yields since its adoption (Andrew et al., 2015). Currently, herbicides are widely applied as the primary weed control strategy for agricultural crops (Duke, 2015).

One of the methods of removing pesticides from the liquid environment is biological remediation, and biological remediation is a natural process. In this process, microorganisms can survive by breaking down an herbicide. Most bacteria live in soil, air, and aquatic environments, but it is possible to modify them in such a way that herbicides degrade with increasing speed. These properties of bacteria can be used as an inexpensive and useful technology to break down herbicides. In recent years, most of the studies on the biodegradation process of herbicides have been carried out in the areas where these herbicides are applied. Worldwide research has been conducted to identify pollutants and microorganisms capable of degrading pesticides in soil, water and air (Erguven, 2017).

Water fleas are important inhabitants of the aquatic ecosystem's food chain, and for this reason, they are widely used in ecotoxicological studies

with their rapid growth rate, high reproductive potential, short life cycle and indicator feature (Martins et al., 2007; Korkmaz et al., 2021). One of the most widely used bioassays internationally for toxicity screening of chemicals and monitoring the toxicity of wastewater and polluted waters is the acute toxicity test with daphnid crustaceans, especially *Daphnia magna* (Persoone, 2019).

Daphnia is one of the most widely used and oldest living test organisms in biological research. Parthenogenetic reproduction, high fertility levels, short life cycles and body sizes provide great advantages for their use in scientific studies (Ebert, 2005). Daphnia is a food source for some fish and invertebrates. Because of these features, Daphnia plays an important role by preparing energy transfer worldwide (Miner et al., 2012). The fact that Daphnia species are very suitable for laboratory studies has allowed them to be used in different disciplines such as ecotoxicology and evaluation (Wu et al., 2019). Daphnia species are test organisms often used to investigate the toxic effects of many chemicals in the water system (Edition, 2002). *D. magna* has an important role in aquatic ecosystems; There are many studies used to evaluate the toxic effects of pollutants (Bao et al., 2020).

The main objective of the study is to reveal out the bioremediation capacity of *M. arthrosphorea, M. radiotolerance* and consortia of these bacteria by the line of COD and TOC parameters that can be an alternative tool for determination of the active substance of the pesticides and determine the toxic effets of these two parameters (COD and TOC) of the pesticide to *D. magna.* The reason for choosing COD and TOC parameters to determine pesticide removal efficiency; It is an easier alternative and cheaper method compared to chromatographic methods in the determination of pesticide active ingredient. For this purpose; in the first step of this study, the bioremediation rates of *M. arthrosphorea, M. radiotolerance* and consortia of these bacteria were followed by COD and TOC reductions in solutions of pyroxasulfone herbicide prepared at concentrations recommended for use in agricultural areas. In the second step, the toxicity shown on *D. Magna* was analyzed for 96 hours in the solutions prepared before bioremediation and in the final sample obtained after bioremediation.

Material and methods

Agricultural soil choosen for bacterial isolation

The agricultural soil used for isolation of the bacteria were taken from Turgutbey village in Kirklareli province, Thrace region of Turkey (41^0, $27^{\prime}$, $30^{\prime\prime}$ N; 27^0, $23^{\prime}$, $12^{\prime\prime}$ E) in 18 May 2021. The temperature of the soil and air were 21 and 23^0 respectively. The Pyhsical and chemical characteristics of the soil sample is shown in Table 1.

Table 1. *Properties of agricultural soil*

Parameter	Value	Properties
Saturation	% 51.9	Loamy
EC	1072 mS/cm	Saltless
Clay	32 mg/l	Calcareous
Organic material (content)	11.52 mg/l	Medium
Potassium	38 mg/l	High
Phosphorus	0.037 mg/l	Low

Approximately 10 g soil sample taken from the agricultural land was diluted up to 10^6 in 0.8% isotonic water. After dilution, 0.1 ml samples were taken and inoculated into sterile plate count agar medium under aseptic conditions in a laminar flow. After inoculation, the petri dishes were taken to the incubator at 27°C and the incubation of these bacteria that will carry out the bioremediation activity in the study was completed. Bacteria growing on petri dishes were coded as A for sunflower field and B for wheat field and enriched by incubating subaraud dextrose broth for bacterial colonies by using loops under sterile conditions in the planting cabinet.

Bacteria used in the study

To identify the bacteria species, Phire Hot Start II DNA Polymerase was employed. PCR bands in various lengths (1000–3000 bp) were used with bacterial 16S ribosomal primers. 16S rRNA forward primers were determined as "AGA GTT TGA TCC TGG CTC AG," and 16S rRNA reverse primers were determined as "ACG GCT ACC TTG TTA CGA CTT." In BLAST program, bacteria species were identified as JCM2831 for *M. radiotolerans* and FN870023 for *M. arthrosphaerae* with an identity rate over 99% (Erguven et al., 2021).

Thermal Cycle Conditions: 1 cycle: 98°C-5 min, 40 cycle: 98°C-5 s, 72°C-20 s, 1 cycle 72∘C-4min, 4°C-∞. Identification of bacteria isolated was carried out in line with 16S RNA Universal Primers 27F (AGAGTTTGATCCTGGCTCAG-; *Escherichia coli* positions 8–27), 16S rRNA universal primers 27F (AGAGTTTGATCCTGGCTCAG; *Escherichia coli* positions 8–27), and 1492R (TACGGYTACCTTGTTACGACTT - positions 1492–1512) (Weisburg et al., 1991). Final Concentrations. They are as follows: total reaction volume 20 μL; 1X Phire animal tissue PCR tampon (contains dNTPs and $MgCl_2$)/0.5 μm forward primer, 0.5 μm adverse primer, Phire Hot Start II DNA polymerase and H_2O were used.

According to the bacterrial identify results, *Methylobacterium radiotolerans* and *Microbacterium arthrosphaerae* species are choosen since their identity rates are over 99%.

The accession numbers of the *Methylobacterium radiotolerans* and *Microbacterium arthrosphaerae* species were JCM2831 and FN870023 respectively.

The reason for choosing these bacterial species is that these bacteria have previously shown effective COD and TOC removal on different pesticides, and the use of pyroxcasufone herbicide has been increasing in recent years to increase crop yield in a country like Turkey which economy is based on agriculture.

Removal of Pyroxasulfone by bioremediation

The herbicide pyroxasulfone is obtained from local market in Turkey and was prepared in 250 ml flasks as 375, 500, 750 and 1000 ppm, based on the recommended concentrations for the use of farmers.

In order to determine the bioremediation activities of bacteria in their pyroxasulfone environment, individual colonies and mixtures of these bacteria were taken into the Sabouraud dextrose broth medium, where they were enriched and multiplied (Approximately 1ml of bacteria includes 10^6 colony forming unit (CFU) in cultute media). The culture media created separately by adding pyroxasulfone to the bacterial solution prepared in 0.8% sterile isotonic solution were set to 27^0C in a Ttyitech brand ZHWY-2008 model shaker incubator. Chemical oxygen demand (COD) and total organic carbon (TOC) analyzes were performed on the samples taken every 24 hours. The reason for choosing the COD and TOC parameters of pyrxasulfone for monitoring the decreasing of the pesticides is, the determination methods of them is cheaper than determination of active material of pyroxasulfone. In the study, Cat. 23459-52 model COD kits were used. While the standard method 5220B closed reflux method was preferred for COD measurements, the high temperature burning method specified in Standard Method 5310B was used for the TOC test (APHA, 1998). It was expected that the pyroxasulfone herbicide to be used in the study followed up with 24-hour intervals would be equal to the recommended chemical oxygen demand value used in the agricultural land. When the recommended COD value of pyroxasulfone herbicide reached 700 ppm at the end of 120 hours, 1 ml cultures taken from this enriched medium were inoculated into the pesticide and measurements were started. The experiments lasted 8 days in total.

In order to determine the initial COD and TOC values of the pyroxasulfone medium, immediately after the cultures taken from the enriched bacterial medium into the pyroxasulfone solutions were added at the concentrations determined due to the growth in the agar medium, they were filtered with 0.45µm filter paper and a sterile funnel, and the COD and

TOC values in the filtrate were determined. measurements were made. During the experiments, 1 drop of 1N H_2SO_4 was added to the filtrates in order to prevent the activity of bacterial colonies.

Adaptation of *Daphnia magna* to the environment

The test organisms *D. magna* used in the experiment were obtained from Cip dam lake in Elazig Province of Turkey from coordinates of 38^0, $40^{\prime}$, $41^{\prime\prime}$ N; 39^0, $4^{\prime}$, $4^{\prime\prime}$ E. Species determination made by morphological properties (Korkmaz et al., 2021). *D. magna* used in the experiment was taken to the laboratory and stocked in a 120 L aquarium and kept at 16–18°C (± 1) temperature and 16:8 hours light: dark photoperiod for one month to adapt to laboratory conditions. It has been observed that the daily mortality rate during adaptation is less than 10%. Water fleas were regularly fed once a day with a mixture of dry spirulina powder and baker's yeast (*Saccharomyces cerevisiae*), and the aquarium water was regularly aerated with an air pump. In addition, 25% of the water was renewed every seven days.

Mortality on *Daphnia magna*

During *D. magna* adaptation, the daily mortality rate was found to be less than 10%. *D. magna* was fed once daily with a mixture of dry spirulina powder and baker's yeast (*Saccharomyces cerevisiae*) periodically, and the aquarium water was regularly aerated with an air pump. In addition, 25% of the water was renewed at a rate of 1/7. Six experimental groups were designed for mortality assessment.

For this purpose, 350 mL filtered samples were taken from the environments with the best treatment performance seen and from the untreated media (Natural living water at 11^{th} day as control media, 375, 500, 750 and 1000 ppm for treated and unterated media) and mortality rates were determined. Ten first-stage juvenile daphnia individuals were pipetted into polycarbonate cups and after gentle transfer to these cups, the water temperature in each polycarbonate cup was adjusted to 20 °C (± 1). An air conditioner and changes in water temperature were checked regularly. Test organisms were not fed during the experiment and a light:dark photoperiod of 16:8 hours was maintained. Three replications were made for each experimental group. The number of dead water fleas in each bowl was counted after 24, 48, and 72 hours. At the end of the test period (72 hours), mortality rates were calculated as a percentage in each experimental group (Babu et al., 2015)

Results

Results of bioremediation studies

In the study, the results of the bioremediation activities of the mixtures and individual cultures of microorganisms showing bioremediation activity were collected under two separate headings as system efficiency and actual yield. The reason for separating the study in this way is that while bioremediation activities occur in the system efficiency, the way the microorganisms are introduced into the system is together with the medium and there is a load of COD and TOC originating from the medium. The actual yield is based on the bioremediation activity of the pure pesticide COD and TOC values at 375, 500, 750 and 1000 ppm concentrations.

Removal efficiencies of the system

The removal efficiencies of the system are the removal of COD and TOC from the nutrient medium containing pesticides and microorganisms. The bioremediation test results regarding the COD parameters taken from the system belonging to the shaking culture conditions are given in fig 1, and the results regarding the TOC parameter are given in fig 2.

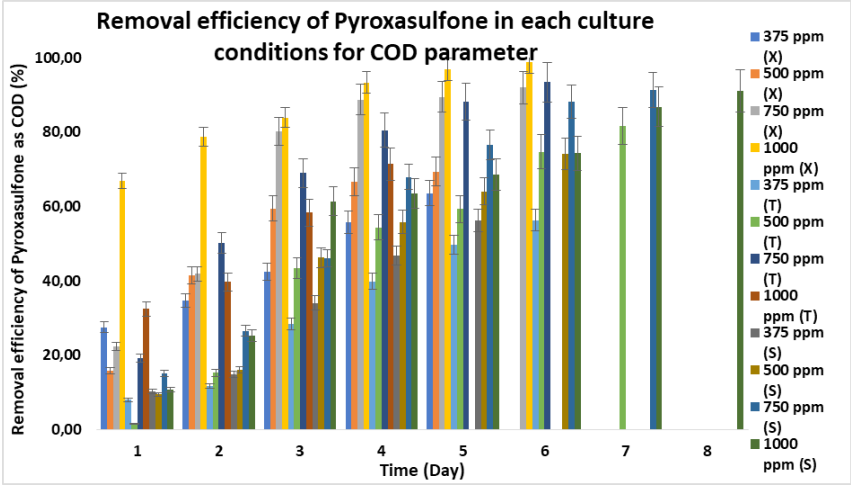

Figure 1. *The bioremediation efficiency in the COD parameter demonstrated by the consortium (X), M. arthrosphaerae (S) and M. radiotolerance (T) on the pyroxasulfone herbicide (T bars on the figures indicate that the data are statistically significant)*

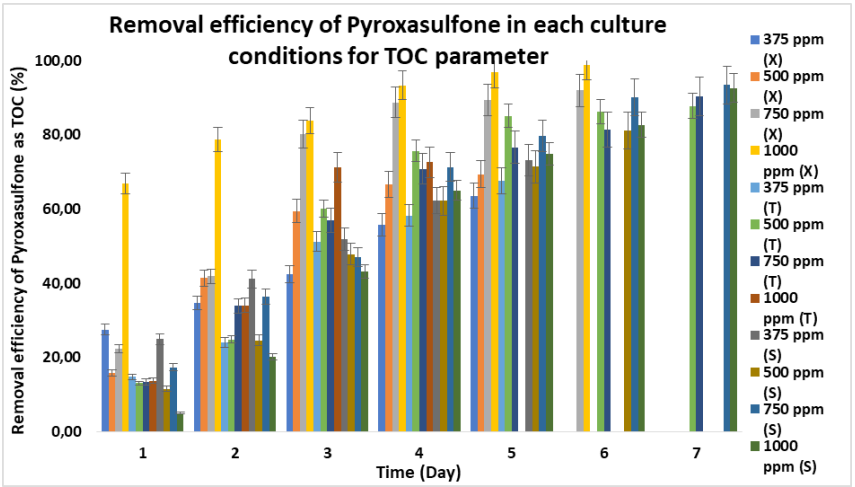

Figure 2. *The bioremediation efficiency in the TOC parameter demonstrated by the consortium (X), M. arthrosphaerae (S) and M. radiotolerance (T) on the pyroxasulfone herbicide (T bars on the figures indicate that the data are statistically significant)*

The bioremediation performance yields of the consortia consisting of a mixture of *M. radiotolerans* and *M. arthrosphorea* species of pyroxasulfone herbicide at 375, 500, 750 and 1000 ppm concentrations were 64, 69, 92 and 99 %, respectively, at the end of 5, 5, 6 and 6 days in the established system. Accordingly, the best removal efficiency was achieved by decreasing from 3446 ppm COD value to 35 ppm at 1000 ppm concentration at the end of the 6th day. The removal efficiencies at other concentrations ranged from 1868 ppm to 680 ppm at 375, 500, and 750 ppm for this parameter, respectively; from 2454 ppm to 750 ppm; It is from 2872 ppm to 230 ppm (Fig. 1).

The study was also carried out in both types of microorganisms separately. Considering the removal of COD in *M. arthrosphorea* species, at the end of the 6th day, from 2460 ppm to 563 ppm with a 77% removal at 375 ppm; From 2628 ppm at 500 ppm to 449 ppm at the end of the 7th day with a removal rate of 83%; It was observed that at 750 ppm it decreased from 2700 ppm to 189 ppm at the end of the 6th day and finally from 2766 ppm at the end of the 4th day at 1000 ppm to 987 ppm with a removal efficiency of 64%. Accordingly, the best removal efficiency of *M. arthrosphorea* was achieved at 750 ppm at the end of the 6th day at the COD level (Fig. 1).

When the removal efficiency of the other species, *M. radiotolerans*, at the level of COD is examined, at the end of the 5th, 6th, 7th and 8th days, at 375, 500, 750 and 1000 ppm, it ranges from 2432 ppm to 817 ppm with a removal efficiency of 66%, respectively; From 2768 ppm to 634 ppm

with a removal efficiency of 77%; It was determined that it decreased from 3120 ppm to 250 ppm and from 3410 ppm to 307 ppm. *M. radiotolerans* strain achieved the best COD removal with 92% at the end of the 7th day in the system (Fig. 1).

Considering the decrease in the total organic carbon parameter, different results from COD stand out in terms of both time and removal efficiency. The main reason for this is that the COD is larger than the TOC. As it is known, COD is the energy requirement for the chemical breakdown of organic matter (in this study, the organic matter in question refers to an organic load from both pesticide and nutrient media in the system). TOC, on the other hand, contains all the carbonaceous substances originating from the pesticide and microorganism in the system.

Considering the TOC removal shown by the consortium in the system, the values of 2070, 2320, 2780 and 3010 ppm at 375, 500, 750 and 1000 ppm reach 557 ppm with 74% yield, respectively, at the end of the 5, 6, 7 and 8th days; to 441 ppm with a yield of 81%; witnessing a decrease of 93% to 195 ppm and finally from 3010 ppm to 228 ppm. Accordingly, the best removal efficiency in consortia is from 2780 ppm to 195 ppm at 750 ppm at the end of the 7th day with a 93% efficiency (Fig. 2)

Fig 2. shows the bioremediation performance of *M. arthrosphorea* species on the basis of TOC at the end of the 5, 7, 7 and 4th days, respectively, in 375, 500, 750 and 1000 ppm pyroxasulnfone herbicides. Accordingly, the removal amounts and yields range from 68 % to 2040 ppm to 661 ppm, from 88% to 2220 ppm to 270 ppm, from 2390 ppm to 230 ppm, and finally from 2410 ppm to 660 ppm. It is in the decreasing direction towards ppm. As can be understood from these results, the best removal efficiency in this system is from 2390 ppm to 230 ppm in an environment of 750 ppm with 90% at the end of the 7th day (Fig. 2)

M. radiotolerance species in the system, the TOC values of 2072, 2352, 2722 and 3040 ppm read at 375, 500, 750 and 1000 ppm concentrations of the herbicide in question, and 73% at the end of the 5th, 6th, 7th and 7th days, respectively. decreased to 554, 441, 177 and 93 ppm with removal efficiencies of 81, 94 and 93. As it can be understood from these results, the best TOC removal belongs to 750 ppm pesticide from 2722 ppm to 177 ppm with 94% at the end of the 7th day for *M. radiotolerans* strain (Fig. 2). The obtained values were found to be statistically significant (Fig. 1 and Fig. 2)

Actual removal yields

The actual yield is the decrease in the COD and TOC values belonging to the pesticide only. Actual removal efficiencies of only pesticides under shaken culture conditions are given in fig. 9 for the COD parameter related

to the results of bioremediation activities of both the consortium and microorganisms, and fig. 10 for the TOC parameter.

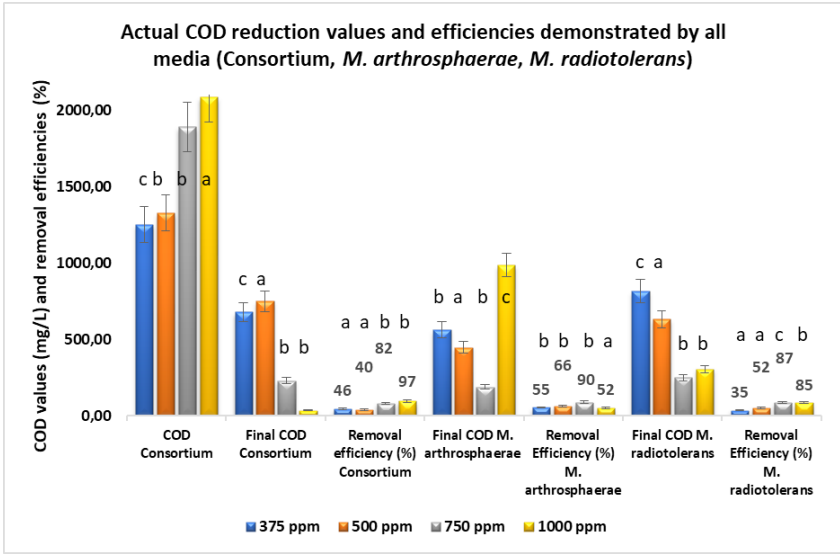

Figure 3. *Actual COD reduction values and efficiencies of M. arthrosphaerae, M. radiotolerans and consortia of them at different concentrations (T bars on the figures indicate that the data are statistically significant)*

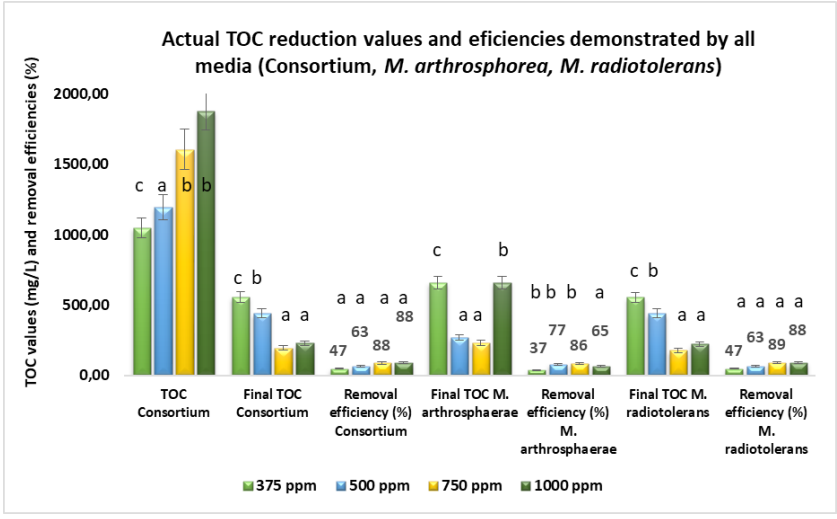

Fig. 4 *Actual TOC reduction values and efficiencies of M. arthrosphaerae, M. radiotolerans and consortia of them at different concentrations (T bars on the figures indicate that the data are statistically significant)*

The initial COD values of consortia decreases to 46, 40, 82 and 97%, respectively. Accordingly, the best actual removal is 97% for 1000 ppm medium. The actual removal efficiencies of *M. arthrosphorea* species on COD parameter was determined with 90% in 750 ppm medium. The actual COD values of *M. radiotolerance* shows a a removal efficiency of 87% (Fig. 3).

When the actual TOC removal of consortia is analyzed, based on the values the best removal efficiency was determined as 88% at the end of the 7th day at 750 and 1000 ppm. Actual TOC removal results also showed that *M. arthrosphorea* species achieved the best TOC based real removal at the end of the 7th day in a media of 750 ppm as 86%. *M. radiotolerance* species really reached its best removal efficiency with an efficiency of 89% at the end of the 7th day (Fig. 4).

Statistically analysis

SPSS version PASW Statistics 18 was performed for analysis of all datas (SPSSInc., Chicago, IL, USA). The datas were analyzed by analysis of variance (ANOVA) and the datas presented are the averages of the results of three replicates with a standard error (SE).

*Statistical differences according to two-tailed independent T test between different bioremediation time (1 day, 7 days) in same groups *$P < 0.05$, and different letters on bar (a, b, c) show statistical differences of Duncan's multiple range test among all application groups in the same exposure time, abc $P < 0.05$. Values represent mean ± SE, $n = 10$.

Mortality results

Considering the findings at the end of 96 hours in terms of mortality rates; Mortality rates of 80% and 70% in 375 ppm treated and untreated media; 100% and 80% in 500 ppm treated and untreated media; 95 and 40% in 750 ppm treated and untreated media; Finally, it was determined that it was 75-50% in 1000 ppm treated and untreated media. Accordingly, the highest mortality rate was observed in the treated 500 ppm application group (100%); the lowest mortality rate was determined as 750 ppm untreated treatment group (40%). Mortality rates were observed to be higher in treated media due to increasing concentrations. It is thought that this situation is caused by the toxic effects of the by-products of the pesticides after their nutrients are broken down. No mortality rate was observed in the control group, indicating that there were no problems with the living conditions and population health of the test organisms used in the experiment (Fig. 5).

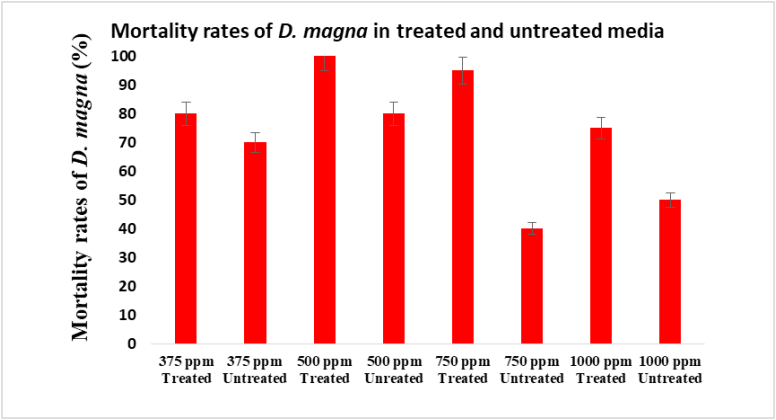

Fig. 5 *Rates of mortality outcomes in treated and untreated media by pyroxasulfone on D. magna*

Discussion

The biodegradation of pesticides depends on pesticide residues and their application time and the activities of microorganisms. Erguven and Yıldırım (2019) also found that *Methylobacterium radiotolerans* and *Microbacterium arthrosphaerae* strains completed Imidacloprid bioremediation after 18 days. For the COD parameter, it was determined as 52%, 96% and 99% with 20, 40 and 80 ml bacteria consortium, respectively, while the BOD_5 removal rates were determined as 88, 79 and 50% in the same period (Erguven and Yildirim, 2019).

According to most researchers, some microorganisms have a tolerance to pesticides. In another research study, *B. cereus, B. subtilis, B. melitensis, K. species, P. aeroginosa, P. fuorescence* and *S. marcescens* were able to decompose 46-72% of chlorpyrifos as the sole carbon source in a sedimentary environment after three weeks (Lakshmi et al., 2008). Another bioremediation study on persistent organic pollutants was performed by immobilized *Candida tropicalis*. In this study, the rate of bioremediation increased with time. As a result of this study, it was understood that bacterial strains can remain active in bioreactors during bioremediation activities (Lin et al., 2015). This means that bioremediation can be an efficient and alternative method to improve environmental pollution. It is recommended to use microorganisms for the elimination of the toxic effects of pesticides. After pesticides are given to the receiving environment, their negative effects on contaminated areas can also be investigated with important environmental parameters such as BOD_5 and COD.

This study is about the use of bacteria isolated from agricultural soil. The microorganisms used in many researches before are the species isolated from the activated sludge of pesticide producing companies. The difference of this research study from the others is that the microorganisms were isolated from the agricultural field.

Bioremediation process of herbicide residues; It is related to the activity and nutritional requirements of the microorganism (Erguven and Yildirim, 2016). It has been determined that Penicillium-type enzymes can metabolize micro-pollutants such as herbicides and eliminate the toxic effects of the chemicals they contain by breaking down lignin by 76% in 15 days and 94% in 30 days (Siripong et al., 2009). Literature studies in aerobic and anaerobic plants, in which mixed bacterial media are used in experiments, have shown that endosulfan can be biodegraded up to 96% (Kumar and Philip, 2006). Góngora-Echeverría et al. (2020) investigated the degradation of glyphosate in pure strains and microbial consortium (Gongora et al., 2020)+

They have revealed bioremediation efficiency through grafting even in remediation of contaminated agricultural soils. *Pseudomonas nitroreducens*, Ochrobactrum sp. B18 and *Pseudomonas citronellolis* strains achieved a removal efficiency of more than 90% in agricultural areas with glyphosate herbicide with the ADA-23B consortium.

Erguven and Yildirim (2016) investigated the bioremediation rate of chlorsulfuron herbicide by reducing COD. they determined that. In a study on chlorpyrifos, which is biodegraded by soil bacteria (Erguven and Yildirim, 2016). Tatar et al. (2020) examined the toxicity of metomyl insecticide before and after bioremediation. As a result of their studies, at the end of 8 days, *Ochrobactrum thiophenivorans* and *Sphingomonas melonis* decreased their COD parameters by 94.7% and 96.8% (Tatar et al., 2020). Belal and Elkhateeb (2014) also conducted a study on the bioremediation of pendimethalin, another diniroaniline group. This study was investigated with *Pseudomonas putida* bacteria isolated from soil contaminated with pendimethalin by 16S rDNA method. After one month, they observed that the entire concentration of 100 µg/ml pendimethalin was removed by this bacterium.

Similarly, Belal and Elkhateeb (2014) determined in their biological removal study with *Phanerochaete chrysosporium* that pendimethalin at 100 ppm concentration was removed by 56% in aquatic organisms. They achieved a removal efficiency of 75% at the end of 7 days, 85% and 95% at the end of 14, 21 and 28 days.

Since herbicides are widely used around the world, besides their use to control terrestrial and aquatic plants, it is also of great importance to

evaluate the toxic potential against other non-target species (Williams et al., 2000). It is also known that Daphnia species are more sensitive to toxic chemicals than other creatures such as fish, birds and mammals. This is associated with increased sensitivity of the respective sodium channel, smaller bodies, and increased risk with increased metabolic differential and decreased metabolic rate (Korkmaz et al., 2021).

The response level of Daphnia is related to the level of contamination and the duration of exposure to toxic substances (Ren et al., 2009). It has been reported that daphnia's juveniles are more sensitive to toxic pollutants than adults (Hanazato, 1991). Daphnia cannot treat direct incoming primary wastewater. However, theoretically, the inhibition of Daphnia may be due to the presence of COD or biochemical oxygen demand, toxicity of organic matter, oxygen depletion due to heterotrophic growth stage or a combination of these (Pous et al., 2020). We examined mortality by exposure at short exposure times (24, 48, 72 and 96 hours).

Since pyroxasulfone is not degraded, increased mortality rates in environments with high removal efficiency may be due to the effects of stress and changes in various organs, enzymes or metabolites like the serine conjugate, DMIT [5, 5-dimethyl-4, 5-dihydroisoxazole-3-thiol (DMIT)] &Ser (Zhang et al., 2023). Similarly, Aghoghovwia and Izah (2018) reported that environmental toxicants can affect various organs or systems of *D. magna* (Aghoghovwia and Izah, 2018). Colomer et al. (2019) suggested that, *Daphnia magna* can survive longer when exposed to foreign matter than in quiescent conditions, provided that food concentrations do not limit their biodegradation capacity. Erguven et al (2022) studied bioremediation performance of *S. melonis* with 180 ppm methomyl insecticide. According to their results, the bioremediation efficiency of this bacteria was 88% and 91% for TOC and COD parameters in 10.5 days respectively. They explained this significant decrease as follows: As the *S. melonis* concentration given to the system increases, decomposed metabolites of the pesticide and medium are formed, and therefore these metabolites increase the TOC and COD values. In this article, despite the decrease in COD and TOC values, *D. magna* deaths did not decrease, which is the by-product of metabolites. According to the results of the COD and TOC values, there is no statistically significiant differencies between datas.

Conclusion

This is the first study on the bioremediation of pyroxasulfone herbicide, prepared at recommended concentrations for use in agricultural lands, with newly isolated *M. arthrosphorea* and *M. radiotolerans* soil bacteria and their consortia in agitated environments at COD and TOC levels. The study also evaluated the mortality of untreated and biologically treated Py-

roxasulfone herbicide on *Daphnia magna*.

In the study, a solution was proposed for the farmers who use or will use this herbicide by using pyroxasulfone at the concentrations recommended for use in agricultural land, to rehabilitate their receiving environment. In addition, bioremediation removal was followed by COD and TOC, which are an alternative to expensive chromatographic methods.

According to the results obtained from the study, both bacterial species and their consortia showed an effective removal efficiency and their use is recommended. Considering the mortality results, the high mortality rates seen in environments with the highest removal rate are that the final products of the decomposed pesticide have a toxic effect on *Daphnia magna*. In this context, it has been understood that such studies should definitely be continued with mortality tests and the by-products of pesticide species targeted for removal should be examined after degradation. It will also be possible to work on field applications with high budgets.

References

Adetunji C.O., Oloke J.K., Bello O.M., Pradeep M., Jolly R.S. (2019). Innovation. Isolation, structural elucidation and bioherbicidal activity of an eco-friendly bioactive 2 (hydroxymethyl) phenol, from *Pseudomonas aeruginosa* (C1501) and its ecotoxicological evaluation on soil. *Environmental Technology and Innovation*, 13:304–317. https://doi.org/10.1016/j.eti.2018.12.006

Aghoghovwia O.A., Izah S.C. (2018). Toxicity of glyphosate based herbicides to fingerlings of Heterobranchus bidorsalis. *International Journal of Avian & Wildlife Biology*, 3: 397–400. https://doi.org/10.15406/ijawb.2018.03.00127

Andrew I., Storkey J., Sparkes D. (2015). A review of the potential for competitive cereal cultivars as a tool in integrated weed management. *Weed Research,* 55:239–248. https://doi.org/10.1111/wre.12137

APHA. Standard methods for the examination of water and wastewater. 20th ed. Washington DC: American Public Health Association; 1998

Babu S.S., Mohandass C., Vijayaraj A.S., Dhale M.A. (2015). Detoxification and color removal of Congo Red by a novel Dietzia sp. (DTS26) – a microcosm approach. *Ecotoxicology and Environmental Safety*, 114: 52–60. https://doi.org/10.1016/j.ecoenv.2015.01.002

Bao S., Pan B., Wang L., Cheng Z., Liu X., Zhou Z., Nie X. (2020). Adverse effects in *Daphnia magna* exposed to e-waste leachate: Assessment based on life trait changes and responses of detoxification-related genes. *Environmental Research*, 188: 109821. https://doi.org/10.1016/j.envres.2020.109821

Belal E.B., Elkhateeb N.M. (2014). Biodegradation of pendimethalin residues by *P. chrysosporium* in aquatic system and soils. *Journal of Biological Chemistry and Environmental Sciences*, 9: 383–400. https://doi.org/ 10.5897/AJMR12.1919

Choudri B.S., Charabi Y., Al-Nasiri N., Al-Awadhi T. (2020). Pesticides and herbicides. *Water Environment Research*, 92: 1425–1432. https://doi.org/10.1002/wer.1380

Colomer J., Muller M., Barcelona A., Serra T. (2019). Mediated food and hydrodynamics on the ingestion of microplastics by *Daphnia magna*. *Environmental Pollution*, 251: 434–441. https://doi.org/10.1016/j.envpol.2019.05.034

Duke S.O. (2015) Perspectives on transgenic, herbicide-resistant crops in the United States almost 20 years after introduction. *Pest Management Science*, 71:652–657. https://doi.org/10.1002/ps.3863

Ebert D. (2005). Ecology, Epidemiology, and Evolution of Parasitism in Daphnia. National Library of Medicine. *National Center for Biotechnology Information.*

Edition F. (2002.) Methods for measuring the acute toxicity of effluents and receiving waters to freshwater and marine organisms. https://www.epa.gov/sites/default/files/2015-08/documents/acute-freshwater-and-marine-wet-manual_2002.pdf Accessed 6 October 2022

Erguven G.O. (2017). Role of Some Selected Fungi Cultures on Bioremediation of Herbicide Chlorsulfuron. *Journal of Tekirdag Agricultrural Faculty*, 14 (02):110-118.

Erguven G.O., Serdar O., Tanyol M., Yildirim N.C., Yildirim N., Durmus B. (2022) The Bioremediation Capacity of *Sphingomonas melonis* for Methomyl-Contaminated Soil Media: RSM Optimization and Biochemical Assessment by *Dreissena polymorpha*. *Chemistry Selec*t 7: e202202105.

Erguven G.O., Tatar S., Serdar O., Yildirim N.C. (2021). Evaluation of the efficiency of chlorpyrifos-ethyl remediation by *Methylobacterium radiotolerans* and *Microbacterium arthrosphaerae* using response of some biochemical biomarkers. *Environmental Science and Pollution Research*, 28:2871–2879. https://doi.org/10.1007/s11356-020-10672-9

Erguven G.O., Yildirim N. (2016). Efficiency of some soil bacteria for chemical oxygen demand reduction of synthetic chlorsulfuron solutions under agiated culture conditions. *Cellular and Molecular Biology*, 62: 92–96. https://doi.org/10.14715/cmb/2016.62.6.17

Erguven G.O., Yildirim N. (2019). The evaluation of imidacloprid remediation in soil media by two bacterial strains. *Current Microbiology*, 76(12):1461–1466. https://doi.org//10.1007/s00284-019-01774-w

Góngora-Echeverría V.R., García-Escalante R., Rojas-Herrera R., Giácoman-Vallejos G., Ponce-Caballero C. (2020) Pesticide bioremediation in liquid media using a microbial consortium and bacteria-pure strains isolated from a biomixture used in agricultural areas. *Ecotoxicology and Environmental Safety*, 200: 110734. https://doi.org/10.1016/j.ecoenv.2020.110734

Guo Y., Cheng L., Long W., Gao J., Zhang J., Chen S., Pu H., Hu M. (2021). Synergistic mutations of two rapeseed AHAS genes confer high resistance to sulfonylurea herbicides for weed control. *Theoretical and Applied Genetics*, 133:2811–2824. https://doi.org/10.1007/s00122-020-03633-w

Hanazato T. (1991). Effects of long and short-term exposure to carbaryl on survival, growth and reproduction of *Daphnia ambigua*. *Environmental Pollution*, 74: 139–148.

Korkmaz V., Yildirim N., Erguven G.O., Durmus B., Nuhoglu Y. (2021). The biyoremediation of glyphosate in soil media by some newly isolated bacteria: The COD, TOC removal efficiency and mortality assessment for *Daphnia magna*. *Environmental Technology and Innovation*, 22: 1-9. https://doi.org/10.1016/j.eti.2021.101535

Kumar M., Philip L. (2006). Adsorption and desorption characteristics of hydrophobic pesticide endosulfan in four Indian soils. *Chemosphere* 62:1064–

1077. https://doi.org/10.1016/j.chemosphere.2005.05.009

Lakshmi C.V., Kumar M., Khanna S. (2008). Biotransformation of chlorpyrifos and bioremediation of contaminated soil. *International Biodeterioration Biodegradation* 62(2): 204–209. https://doi.org/10.1016/j.ibiod.2007.12.005

Lin J., Gan L., Chen Z., Naidu R. (2015). Biodegradation of tetradecane using Acinetobacter venetianus immobilized on bagasse. *Biochemical Engineering Journal,* 100: 76–82. https://doi.org/10.1016/j.bej.2015.04.014

Martins J., Teles O., Vasconcelos V. (2007). Assays with *Daphnia magna* and *Danio rerio* as alert systems in aquatic toxicology. *Environment International*, 33: 414-425. https://doi.org/10.1016/j.envint.2006.12.006

Miner B.E., De Meester L., Pfrender M.E., Lampert W., Hairston Jr N.G. (2012). Linking genes to communities and ecosystems: Daphnia as an ecogenomic model. *Proceedings of the Royal Society B: Biological Sciences*, 279: 1873–1882. https://doi.org/10.1098/rspb.2011.2404

Persoone G., Baudo R., Cotman M., Blaise C., Thompson K., Moreira-Santos M., Vollat B., Torokne A., Han T. (2009). Review on the acute *Daphnia magna* toxicity test – Evaluation of the sensitivity and the precision of assays performed with organisms from laboratory cultures or hatched from dormant eggs. *Knowledge and Management of Aquatic Ecosystems*, 393(1): 29. https://doi.org/10.1051/kmae/2009012

Pous N., Hidalgo M., Teresa S., Colomer J., Colprim J., Salvadó V. (2020). Assessment of zooplankton-based eco-sustainable wastewater treatment at laboratory scale. *Chemosphere* 238: 124683. https://doi.org/10.1016/j.chemosphere.2019.124683

Ren Z., Li Z., Ma M., Wang Z., Fu R. (2009). Behavioral responses of *Daphnia magna* to stresses of chemicals with different toxic characteristics. *Bulletin of Environmental Contamination and Toxicology*, 82: 310. . https: //doi.org/10.1007/s00128-008-9588-1

Sharma A., Shukla A., Attri K., Kumar M., Kumar P., Suttee A., Singh G., Barnwal R.P., Singla N. (2020). Global trends in pesticides: A looming threat and viable alternatives. *Ecotoxicology and Environmental Safety*, 201: 110812. https:// doi: 10.1016/j.ecoenv.2020.110812.

Sidhu G.K., Singh S., Kumar V., Dhanjal D.S., Datta S., Singh J. (2019). Toxicity, monitoring and biodegradation of organophosphate pesticides: a review. *Critical Reviews in Environmental Science and Technology*, 49: 1135-1187. https://doi.org/10.1080/10643389.2019.1565554

Siripong P., Oraphin B., Sanro T., Duanporn P. (2009). Screening of fungi from natural sources in Thailand for degradation of polychlorinated hydrocarbons. American-Eurasian Journal of Agricultural & Environmental Sciences, 5: 466–472.

Tatar S., Yildirim N.C., Serdar O., Erguven G.O. (2020). Can toxicities induced by insecticide methomyl be remediated via soil bacteria *Ochrobactrum thio-*

phenivorans and *Sphingomonas melonis*? *Current Microbiology,* 77:1301–1307. https://doi.org/10.1007/s00284-020-02042-y

Weisburg W.G., Barns S.M., Pelletier D.A., Lane. D.J. (1991). 16S ribosomal DNA amplification for phylogenetic study. *Journal of Bacteriology*, 173 (2): 697–703.

Williams G.M., Kroes R., Munro I.C. (2000). Safety evaluation and risk assessment of the herbicide Roundup and its active ingredient, glyphosate, for humans. *Regulatory Toxicology and Pharmacology*, 31:117–165. https://doi.org/10.1006/rtph.1999.1371

Wu D., Liu Z., Cai M., Jiao Y., Li Y., Chen Q., Zhao Y. (2019). Molecular characterisation of cytochrome P450 enzymes in waterflea (*Daphnia pulex*) and their expression regulation by polystyrene nanoplastics. *Aquatic Toxicology*, 217:105350. https://doi.org/10.1016/j.aquatox.2019.105350

Zhang J.J., Niu Y., Ma C., Zhao T., Wang H., Yan Z., Zhou L., Liu X., Piao F., Du N. (2023). Accumulation and metabolism of pyroxasulfone in tomato seedlings. *Ecotoxicology and Environmental Safety*, 254: 114765. https://doi.org/10.1016/j.ecoenv.2023.114765

CHAPTER 6

NAVIGATING UNCERTAINTY: FROM TYPE-1 TO INTERVAL TYPE-2 FUZZY LOGIC IN DECISION MAKING

Baris SANDAL[1], Ayfer ERGIN[2]

1 Rsch Asst Dr. Istanbul University-Cerrahpaşa, Faculty of Engineering, Department of Mechanical Engineering, Istanbul, TÜRKİYE e-mail: bsandal@iuc.edu.tr ORCID ID: 0000-0003-1078-7786

2 Asist. Prof. Dr. Istanbul University-Cerrahpaşa, Faculty of Engineering, Maritime Transportation Management Engineering, Istanbul, TÜRKİYE e-mail: ayfersan@iuc.edu.tr ORCID ID: 0000-0002-6276-4001

1. Introduction:

Fuzzy Logic (FL) emerges as a potent tool for addressing the intricacies and uncertainties inherent in the real world. Its mode of information processing often transcends precise boundaries, making it a frequently adopted paradigm. Type-1 Fuzzy Sets (T1FSs), a widely applied branch of FL, excels in handling uncertainty and imprecision with notable success. However, when confronted with the need to address more complex and extensive ranges of uncertainty, Type-2 Fuzzy Sets (T2FS) logic comes into play (Mendel & Wu, 2002). Fuzzy sets have aroused great interest both in industry and academia, leading to fruitful research across various fields (John & Coupland, 2007).

Taking into account the advantages and disadvantages of each approach, comprehending their effectiveness under specific conditions can provide invaluable insights into solving real-world problems fraught with uncertainty. It is within the purview of this study to shed light on these intricate aspects of FL and guide practitioners and researchers in making informed decisions regarding its application.

The primary objective of this study is to delve into the distinct application domains and performance characteristics of both FL approaches. Firstly, we embark on elucidating the concept of FL while underscoring its paramount significance. The fundamental motivation behind the adoption of FL lies in its intrinsic ability to effectively tackle uncertainties within complex systems and the real world (Türkşen, 2002). Secondly, we meticulously scrutinize the advantages and disadvantages of Interval Type-2 Fuzzy Sets (IT2FSs). The capacity of IT2FS to handle broader intervals of uncertainty and operate within these intervals is particularly vital when dealing with intricate problems (Mendel, 2018). However, it is noteworthy that these advantages might necessitate increased computational power, which can be considered a potential drawback.

This study is organized into several sections, each dedicated to a specific facet of FL and its application domains. The subsequent section, " Concept of Fuzzy Sets and Applications" delves into the core concepts of FL, providing a comprehensive understanding of its principles and significance. Following this, the chapter explores " Applications of Type-1 Fuzzy Sets " highlighting their prowess in handling moderate uncertainty scenarios and examines applications in this field. Moving forward, the discussion extends to " Applications of Type-2 Fuzzy Sets " emphasizing their critical role in addressing extensive and intricate uncertainty ranges and highlighting applications that are new to the literature. The chapter then scrutinizes " Interval Type-2 Fuzzy Sets" shedding light on their advantages and computational considerations. Finally, the concluding section synthesizes

the insights gained and paves the way for the subsequent chapters, which delve deeper into methodologies, practical applications, and computational aspects of FL.

2. Concept of Fuzzy Sets and Applications

Traditional approaches often prove inadequate in handling the inherent imprecision and vagueness found in information obtained from humans.

These classical methods are limited in their ability to capture the complexity of human thought processes. FL emerges as a method that closely mimics human reasoning and can replicate the ambiguities present in human thinking (Ergin, 2021). The development and application of fuzzy set theory have significantly advanced our ability to model complex real-world phenomena, while simultaneously yielding invaluable insights into the realms of decision-making and artificial intelligence. FL, closely aligned with fuzzy set theory, represents a powerful methodology that closely mirrors human reasoning processes, making it adept at navigating the nuances and ambiguities inherent in many real-world scenarios.

By emulating human thought patterns, particularly in situations characterized by imprecision and vagueness, FL has emerged as a versatile tool with broad-ranging applications. This synergy between fuzzy set theory and FL not only enhances our comprehension of intricate systems but also plays a pivotal role in shaping the landscape of artificial intelligence, enabling machines to approach problem-solving tasks with a human-like capacity to grapple with uncertainty and complexity.

Type-1 Membership Functions (T1MFs) are preferred due to their straightforward conceptual understanding and computational efficiency in transforming input variables into fuzzy counterparts. Among the numerous available shapes for membership functions (MFs), the Gaussian, trapezoidal and triangle shapes are the most prevalent choices in practical applications.

In T1FS, it is assumed that the form of the MF that is created by the designer for the given problem is a certain one. As a result, T1FSs cannot handle uncertainty effectively due to their deterministic nature. Thus, the inherent imprecision in the shape of the MF leads to persistent uncertainty.

Within a fuzzy sets, various forms of uncertainty can manifest, and T1FSs are ill-suited to model these uncertainties comprehensively or mitigate their impact due to their rigid MFs. Mendel and Wu identified four primary sources of such uncertainties: 1) the employment of specialized terminology in the antecedent and consequent segments of rules, which may introduce uncertainty; 2) The consequents may constitute a spread of

outcomes, usually illustrated in the form of a histogram; 3) measurements have the potential to be influenced by noise; and 4) similarly, noisy characteristics may be present in tuning data (Mendel & Wu, 2002).

In contrast, T2FSs provide the capability to model uncertainty in the MF by representing its boundaries as fuzzy. In essence, Type-2 Membership Functions (T2MFs) inherently possess fuzziness. This capacity to model the level of uncertainty within the MF is Achieved through the introduction of an additional third dimension that arises from the fuzzy boundaries of T2MFs.

In this context, T2FSs prove to be better suited for addressing and managing such uncertainties (Mendel & Wu, 2002). Nevertheless, comprehending and utilizing T2FSs poses several challenges, as we will elucidate. Regrettably, T2FSs are more intricate to employ and grasp compared to their type-1 counterparts. Consequently, their adoption has not yet achieved widespread acceptance.

2.1. Applications of Type-1 Fuzzy Sets

Fuzzy logic has established itself as a prominent paradigm in scientific research and publications across diverse domains, encompassing fields such as engineering disciplines (Arık & Bilgiç, 2022; Ozer, Hacioglu, & Yagiz, 2016), control systems (Taskin & Hacioglu, 2020; Taskin, Hacioglu, & Yagiz, 2017), medical diagnosis (Sandal, Hacioglu, Salihoglu, & Yagiz, 2023), image processing (Bloch, 2015), natural language processing (Gupta, Jain, & Joshi, 2018), and decision support systems (Kumar, Singh, & Singh, 2013). Where, it not only enables the development of sophisticated algorithms and intelligent systems but also plays a transformative role in enhancing decision-making processes, reflecting its pervasive presence in both the theoretical foundations of academic studies and practical, real-world implementations.

T1FS is extensively utilized across a wide spectrum of academic disciplines. In the academic sphere, T1FS is harnessed to tackle issues characterized by ambiguity, model intricate systems, and enhance the decision-making process. Moreover, it finds application within the domain of multi-criteria decision-making (MCDM) procedures, seamlessly integrating with various other MCDM methodologies (Pedrycz, Ekel, & Parreiras, 2011) Academic inquiries that amalgamate T1FS with MCDM techniques aim to enhance the efficiency and realism of decision-making endeavors (Skalna et al., 2015). These studies provide application-centric approaches to intricate decision-making challenges that often involve multiple criteria and inherent uncertainties.

FL approach can be integrated with many multi-criteria decision making methods. This integration approach is widely adopted to yield comprehensive and realistic outcomes when confronting complex real-world

decision-making problems. This is attributed to the inherent presence of uncertainty and imprecise information in numerous decision-making processes, where FL serves as a potent tool for effectively managing such uncertainties.

T1FS stands out as a versatile and flexible tool with extensive applications across various domains. Its proficiency in handling ambiguity, modeling complex systems, and enhancing decision-making processes renders it a valuable asset in both academic research and numerous practical disciplines. The domains where T1FS is commonly in decision making utilized include the following:

Finance and Economics: T1FS is employed in financial forecasting and risk management, particularly when dealing with uncertain financial data. In their study, Celik and Ozok endeavored to model the pivotal process of selecting a shipping registry, employing analytical methodologies within the multidisciplinary framework of ship management. The study harnessed the Fuzzy Analytical Hierarchy Process (FAHP) method, grounded in Chang's scope analysis. The research discerned that within the decision-making process, economic considerations, with a particular focus on tax-related and bank finance expenses, emerged as the prevailing determinants (M. Celik, Er, & Ozok, 2009). The financial performance of three Taiwanese liner companies has been assessed using the Fuzzy Technique for Order Preference by Similarity to Ideal Solution (FTOPSIS) method (Wang, 2014). Park et al. utilized the FAHP method in their ship acquisition decision-making process (Park, Seo, Kim, & Ha, 2018).

Transport and Logistics: T1FS is the preferred choice in domains like transport management, routing, fleet management, and logistics operations, particularly when dealing with uncertain data. Notably, the maritime sector has witnessed a threefold growth over the last 30 years (Yasa, Ergin, Ergin, & Alkan, 2016). This expansion has prompted researchers to shift their focus toward the maritime sector. For the selection of dry port locations in China, an integration of FAHP and Elimination and Choice Expressing Reality (ELECTRE) methods has been implemented (Ka, 2011). The FTOPSIS method was applied in the selection of a harbor, taking into consideration environmental factors (A Ergin & Eker, 2019). Sahin et al. have developed a model for selecting the most suitable shipyard in the shipbuilding industry. This model combines FAHP with game theory principles to address challenges ship owners face when choosing among different shipyards. By considering factors like capacity, quality, cost, delivery time, and other crucial elements, it helps decision-makers prioritize these factors (Sahin, Yazir, Soylu, & Yip, 2021). Unver et al. conducted an examination of 46 maintenance activities related to two-stroke marine diesel engines within the propulsion systems of commercial vessels. This

examination was carried out employing the FAHP method, while also considering various risk levels (Ünver, Altın, & Gürgen, 2021). Tuncel et al. utilized FAHP to uncover potential risk factors in the Electronic Nautical Charts (ENCs) preparation process (Tunçel, Arslan, & Akyüz, 2023). Studies in the fastest-growing segment of the maritime industry, container transport, (Ergin & Ergin, 2018) utilize fuzzy methods. Onut et al. utilized the Fuzzy Analytical Network Process (FANP) method to make container port selection (Onut, Tuzkaya, & Torun, 2011). The transshipment container port choise problem has been addressed using the Fuzzy Multiple Criteria Decision Making Method (FMCDM) (Chou, 2007). With the application of the FAHP method, ocean container selection has been conducted (Ergin, 2021).

Energy and Resource Management: In the domains of energy generation, resource allocation, and energy efficiency analysis, T1FS is employed to address a multitude of criteria and uncertainties. Heo et al. utilized the FAHP method to facilitate the necessary decisions for enhancing the utilization of new and renewable energy sources in Korea, and to determine the relevant criteria and factors for this purpose (Heo, Kim, & Boo, 2010). To ascertain Turkey's energy plan, Strengths, Weaknesses, Opportunities and Threats (SWOT) analysis was employed to identify the main and sub-criteria, and then the weights of these criteria were ascertained using the ANP method. Finally, the FTOPSIS method was applied to rank the strategies (Ervural, Zaim, Demirel, Aydin, & Delen, 2018). For the selection of alternative renewable energy sources in the Istanbul region, the FAHP and Fuzzy VlseKriterijumska Optimizacija I Kompromisno Resenje (FVIKOR) methods were integrated (Kaya & Kahraman, 2010).

Industrial Engineering and Production Management: T1FS is extensively utilized in industrial engineering problems, encompassing optimization of production processes, quality control, and inventory management. In Turkey, a study on supplier selection in the white goods sector was conducted using the FAHP method, involving Kahraman et al. (Kahraman, Cebeci, & Ulukan, 2003). Kahraman et al. utilized FAHP to determine the catering company that maximizes customer satisfaction (Kahraman, Cebeci, & Ruan, 2004). In their research, they investigate the prioritization of measurement dimensions and the path to achieving the best performance by employing fuzzy logic methods, specifically FAHP and FTOPSIS, for the evaluation of multidimensional performance (Sun, 2010). Güngör et al. have conducted personnel selection by employing the FAHP, which takes into account both qualitative and quantitative criteria (Güngör, Serhadlıoğlu, & Kesen, 2009). The facility location selection problem of a Turkish textile company was addressed in this study by employing the FAHP and the FTOPSIS methods. The main aim was to illustrate how these two fuzzy

methods could be utilized in the decision-making process and to examine their similarities and differences by presenting the obtained results (Ertuğrul & Karakaşoğlu, 2008).

Environmental Engineering and Sustainability: T1FS is commonly employed in the assessment of environmental impacts, waste management, and environmental sustainability efforts. Ren and Lutzen have introduced a FMCDM for technology selection aimed at mitigating emissions from ships. This approach offers a decision-making structure that incorporates environmental, economic, and social sustainability criteria, employing a combination of FAHP and VlseKriterijumska Optimizacija I Kompromisno Resenje (VIKOR) methods to assess the performance of various alternative technologies (Ren & Lützen, 2015). Besikci et al. employed the FAHP method within the scope of the Ship Energy Efficiency Management Plan to assess the energy-saving potential in the maritime industry and reduce ship fuel consumption by addressing environmental and economic concerns (Beşikçi, Kececi, Arslan, & Turan, 2016).

2.2. Applications of Type-2 Fuzzy Sets

IT2FSs can be integrated with MCDMs, and this integration can be useful, particularly when addressing complex and uncertain problems, to achieve better results. The integration between IT2FS and MCDMs can vary depending on the specific problem and application. Here are some examples of this integration:

Industrial Engineering and Production Management: These integrated methods are frequently utilized, particularly in applications related to supply chain management, such as supplier selection studies. One of the earliest integrations of these two methods occurred in the context of supplier selection for supply chain management. Kahraman et al. have developed the Interval Type-2 Fuzzy AHP (IT2FAHP) method for the first time and introduced it to the literature. They have applied this method to supplier selection (Kahraman, Öztayşi, Sarı, & Turanoğlu, 2014). A company engaged in the production of household appliances, Ecer, utilized the IT2FAHP method to carry out green supplier selection (Ecer, 2022). Chen and Lee have introduced the Interval Type-2 Fuzzy TOPSIS (IT2FTOPSIS) method to address fuzzy multi-attribute group decision-making problems using IT2FSs (Chen & Lee, 2010). Abdullah and Zulkifli have proposed the integration of FAHP and Interval Type-2 Fuzzy DEMATEL (IT2FDEMATEL) methods in human resource management (Abdullah & Zulkifli, 2015). Faced with the challenges stemming from the geographical dispersion of its head office, retail stores, and manufacturing plant, the company for an information system selection using the IT2FAHP (Oztaysi, 2015). Onar et al. proposed using the IT2FAHP method for defining the

weights of criteria in the strategic decision-making process and recommended using the FTOPSIS method to select the best strategy (Cevik Onar, Oztaysi, & Kahraman, 2014).

Transport and Logistics: In the maritime and transport sectors, there are innovative examples of the use of these integrations in various applications. Soner et al. employed IT2FAHP to ascertain the criteria weights for the bulk carrier hatch cover selection problem, followed by Interval Type-2 Fuzzy VIKOR (IT2FVIKOR) for ranking the alternatives (Soner, Celik, & Akyuz, 2017). The integration of IT2FAHP and TOPSIS methods was employed for determining the ship loader type of dry bulk cargo vessels (E. Celik & Akyuz, 2018). Kiraci and Akan have integrated the IT2FAHP and IT2FTOPSIS methods to ascertain criteria weights and rank alternative choices for the aviation selection of airline companies. This integration has facilitated the aircraft selection process for Kiraci and Akan's airline companies (Kiracı & Akan, 2020). In public transportation, a T2FS framework has been integrated with the AHP and TOPSIS methods to assess customer satisfaction (Öztürk, 2021).

Environmental Engineering and Finance: IT2FS and MCDM methods have found applications in environmental and financial domains. Oztasi and Kahraman integrated the IT2FAHP and IT2TOPSIS methods for selecting renewable energy sources (Öztayşi & Kahraman, 2017). The Delphi method and IT2FAHP methods have been employed in conjunction to determine public expectations from water treatment facilities (Yildiz, Ayyildiz, Taskin Gumus, & Ozkan, 2021). The performance of Real Estate Investment Trusts (REITs) listed on Borsa Istanbul has been evaluated using a methodology that combines IT2FAHP and Data Envelopment Analysis (DEA) (Yilmaz, Kusakci, Tatoglu, Icten, & Yetgin, 2019).

3. Interval Type-2 Fuzzy Sets

In the Boolean system, the value 1 represents absolute truth, while the value 0 signifies absolute falsehood, demonstrated as

$$\mu_A(x) = 1 \; if \; x \in A \tag{1}$$

$$\mu_A(x) = 0 \; if \; x \notin A \tag{2}$$

Fuzzy set theory, was first introduced by Lotfi A. Zadeh in 1965 as a response to the limitations of traditional set theory, has revolutionized our ability to handle and quantify uncertainty and vagueness in various fields of study (Zadeh, 1996). At its core, fuzzy set theory allows us to represent

the degree of truthfulness or falsity of a value through the concept of a membership degree. This measure of membership determines the degree to which an element, identified as 'x,' pertains to a fuzzy set, conventionally labelled as 'A' .

Within the realm of FL, values can exhibit a wide spectrum of truthfulness, ranging from absolute falsity to absolute truthfulness. Membership values within the range of (0, 1) represent the partial degrees of truthfulness and falsity. These membership degrees are computed using a MF, which, in simpler terms, serves as a subjective measure of an element's association with the set. When the membership value is 0, it signifies absolute falsity, representing complete non-membership in the set. Conversely, a membership value of 1 signifies absolute truthfulness, indicating full membership in the set.

As a consequence, Lotfi A. Zadeh devised the notion of type-n fuzzy sets, which incorporate T1FSs and T2FSs (Zadeh, 1971). These sets serve as a foundation for fuzzy theory, allowing for the calculation of membership degrees. Specifically, when working with A, a T1FS, we use Equation (3) to determine membership characteristics.

$$A = \{(x, \mu_A(x) \mid x \in X\} \tag{3}$$

The MF is represented as $\mu_A(x)$, where $x' \in X$, as follows:

$$\mu_A(x) \rightarrow [0,1] \tag{4}$$

In simpler terms, the process involves the conversion of input variables into fuzzy variables. The MF serves as the defining element, assigning a real number value within the [0-1] range to represent the degree of membership of variable 'x' within the fuzzy set. A plethora of MFs has been developed to accommodate various types of fuzzy sets. Among these, T1MFs reign supreme in terms of both widespread use and recognition.

T2FSs are characterized by their three-dimensional structure and rely on Zadeh's extension principle for operations such as union, intersection, and complement. Consequently, T2FSs tend to be more challenging to comprehend and require more complicated and lengthy calculations when compared to T1FSs. This complexity has limited their widespread adoption.

T1MFs use linear functions to define boundaries, while T2MFs establish boundaries as intervals between the upper and lower membership

functions (UMF and LMF), illustrated in Figure 1-a. The UMF is denoted by an overbar, and the LMF is indicated by an underbar. The area enclosed within these fuzzy boundaries is named to as the Footprint of Uncertainty (FOU), as shown in Figure 1-b. Both the UMF and LMF essentially consist of two T1MFs that define the extents of the FOU within a T2MF. The UMF characterizes the FOU subset with the highest membership degree, whereas the LMF characterizes the FOU subset with the lowest membership degree.

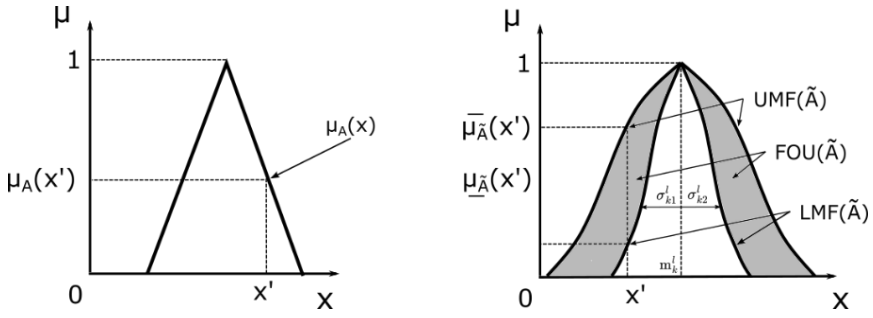

Figure 1: *MF Representations for a) Type-1 Triangular and b) Type-2 Gaussian (Ergin & Sandal, 2023)*

There are four mathematical representations for a T2FS, as outlined by Mendel in 2014: a) A collection of individual points, as depicted in Equation (5). b) A union of vertical slices over the entire domain X, where each vertical slice is a T1FS (a secondary MF), as depicted in Equation (6). c) A union of wavy slices, where each wavy slice represents an embedded T2FS. d) A fuzzy union of horizontal slices over the interval [0, 1], where each horizontal slice bears resemblance to an IT2FS raised to the level of α (Mendel, 2013).

The symbol Ã is used to denote a T2FS, which can be formulated as

$$\tilde{A} = \left\{ \left((x,u), \mu_{\tilde{A}}(x,u) \right) \middle| \forall\, x \in X, \forall u \in J_x \subseteq [0,1] \right\} \tag{5}$$

$$\tilde{A} = \int_{x \in X} \int_{u \in J_x} \frac{\mu_{\tilde{A}}(x,u)}{(x,u)}, \quad J_x \subseteq [0,1] \tag{6}$$

In this context, the primary and secondary variables of T2FS are x and u correspondingly, respectively. Furthermore, J signifies the secondary MF. At each specific value of $x = x'$, $\mu_{\tilde{A}}(x',u)$ represents the vertical cross-section of $\mu_{\tilde{A}}(x,u)$, and the T2MF of $\tilde{A}$ is formally expressed as

$$\mu_{\tilde{A}}(x = x', u) \equiv \mu_{\tilde{A}}(x') = \int_{u \in J_{x'}} \frac{f_{x'}(u)}{u}, \quad J_{x'} \subseteq [0,1] \tag{7}$$

Here, $x \in X$, $u \in J_{x'} \subseteq [0,1]$, and $0 \leq \mu_{\tilde{A}}(x,u) \leq 1$, as described by Mendel and John (Mendel & John, 2002). Additionally, $f_{x'}(u)$ signifies the magnitude of the secondary MF, where $f_{x'}(u) \subseteq [0,1]$.

When $\mu_{\tilde{A}}(x,u) = 1$, $\tilde{A}$ is considered as an IT2MF. Since the third dimension of general T2FSs does not provide any additional information, it is considered unnecessary and can be considered as a special case of T2FS, as illustrated below:

$$\tilde{A} = \int_{x \in X} \int_{u \in J_x} \frac{1}{(x,u)}, \quad J_x \subseteq [0,1] \tag{8}$$

$$\mu_{\tilde{A}}(x = x', u) \equiv \mu_{\tilde{A}}(x') = \int_{u \in J_{x'}} \frac{1}{u}, \quad J_{x'} \subseteq [0,1] \tag{9}$$

Categorically, an IT2FS can be regarded as a particular kind of a T2FS. Due to the ease of use and minimal calculation requirements, IT2FSs are frequently utilized. In IT2FSs, the third dimension does not carry significant information, as it is assumed to remain constant. Consequently, the third dimension is disregarded, and only the FOU is utilized to define IT2FSs. The MF, as a result of the characteristics of T2FS boundaries, can assume values within the [0-1] range along a vertical line between the upper-bound $\overline{\mu_{\tilde{A}}}(x')$ and the lower-bound $\underline{\mu_{\tilde{A}}}(x')$ a departure from the crisp numbers used in the case of T1FSs.

In Equations (10) and (11), it is clear that the UMF represents the portion of the FOU with the highest membership degree, whereas the LMF represents the portion of the FOU with the lowest membership degree.

$$\overline{\mu}_{\tilde{A}}(x) \equiv \overline{FOU}(\tilde{A}), \quad \forall x \in X \tag{10}$$

$$\underline{\mu}_{\tilde{A}}(x) \equiv \underline{FOU}(\tilde{A}), \quad \forall x \in X \tag{11}$$

Let $\tilde{Q}$ as an arbitrary interval T2MF. The following equation can be used to calculate the membership degrees for its lower and upper limits

$$\mu_{\tilde{Q}_k^l}(x_k) = \int_{q^l \in \left[\underline{\mu}_{\tilde{Q}_k^l}(x_k), \overline{\mu}_{\tilde{Q}_k^l}(x_k)\right]} 1/q^l \tag{12}$$

The MFs within IT2FSs can assume various forms. Additionally, there exist classical types of MFs, including triangular, trapezoidal, Gaussian,

and sigmoid types, which are akin to those employed in T1FSs. If we denote the Gaussian MF as $\tilde{g}_k^l(x_k)$, we can express a similar equation, as outlined by Liang and Mendel in 2000 (Liang & Mendel, 2000).

$$\mu_{\tilde{Q}_k^l}(x_k) = \int_{v^l \in \left[\mu_{\underline{X}_k^l}(x_k), \mu_{\overline{X}_k^l}(x_k)\right]} 1/v^l \tag{13}$$

For a Gaussian MF with a fixed mean m_k^l and a uncertain standard deviation that falls within the range $[\sigma_{k1}^l, \sigma_{k2}^l]$, the MF is represented by Equation (14).

$$\mu_k^l(x_k) = exp\left[-\frac{1}{2}\left(\frac{x_k - m_k^l}{\sigma_k^l}\right)^2\right], \quad \sigma_k^l \in \left[\sigma_{k1}^l, \sigma_{k2}^l\right] \tag{14}$$

4. Interval Type-2 Fuzzy Numbers

In everyday life, the term "about" is commonly employed to pragmatically represent numerical values for which the precise or well-defined magnitude remains uncertain or undefined. However, it is crucial to acknowledge that the interpretation of this "about" expression can exhibit variations among different individuals. In scenarios where uncertainties are inherent, such as due to measurement errors or linguistic ambiguities, the numerical value under consideration inherently carries an element of indistinctness.

To enhance the clarity and practical utility of such inherently vague concepts and to encapsulate their intuitive significance in a manner that accommodates diverse perspectives, it becomes conceivable to depict this numerical value as a fuzzy set. This approach, grounded in the mathematical framework of FL, leads to the creation of what is referred to as a fuzzy number (FN) (Dijkman, van Haeringen, & de Lange, 1983; Mendel, 2017).

Interval Type-2 Fuzzy Numbers (IT2FNs) have risen to prominence in scientific research, primarily owing their success to the utilization of two-dimensional MFs. These two-dimensional MFs enable a more comprehensive representation of model uncertainties, resulting in a significant reduction in complexity when dealing with IT2FNs. Consequently, mathematical operations involving IT2FNs are streamlined and simplified. This computational advantage has positioned IT2FNs at the forefront of scientific investigation, especially when contrasted with the computational intricacies associated with Type-2 Fuzzy Numbers (T2FNs). In recent decades, IT2FNs have garnered increased attention and have become a focal point of research endeavors

Liang and Mendel introduced IT2FNs in their pioneering work (Liang & Mendel, 2000). The Mendel-John Representation Theorem for IT2FSs states that an IT2FS can be represented as the union of embedded T1FSs covering its FOU. This theorem allows us to leverage T1FS mathematics to comprehend IT2FSs efficiently, resulting in significant time savings in learning.

Defining an IT2FN lacks consensus, unlike the well-established definition of a Type-1 Fuzzy Number. The uncertainty arises because an IT2FS is characterized by two T1FSs: LMF and UMF, offering diverse interpretations. Hamrawi and Coupland (2009) define two kinds:

- A perfectly normal IT2FN is an IT2FS both of whose LMF and UMF of its FOU are type-1 fuzzy numbers
- A normal IT2FN is an IT2FS only whose UMF of its FOU is a type-1 fuzzy number

"perfectly normal interval type-2 fuzzy numbers" are the appropriate representations of numbers and linguistic terms, preserving specificity without introducing uncertainty. While consensus may vary, adhering to Hamrawi-Coupland designations is advisable (Mendel, 2017).

An IT2FS, represented as $\tilde{A}$ and bounded by two T1FSs known as the LMF and UMF, is denoted as $\tilde{A} = (A^l, A^u)$.

In the realm of IT2FSs, specific categorizations have been established based on the characteristics of these sets. When an IT2FS features both its UMF and LMF as type-1 fuzzy numbers, it is classified as a Perfect Interval Type-2 Fuzzy Number. On the other hand, if the UMF is a type-1 fuzzy number while the LMF is a Fuzzy Sub Number (FSN), the IT2FS is denoted as an IT2FN. Lastly, when both the UMF and LMF are FSNs, the IT2FS is referred to as an Interval Type-2 Fuzzy Sub Number.

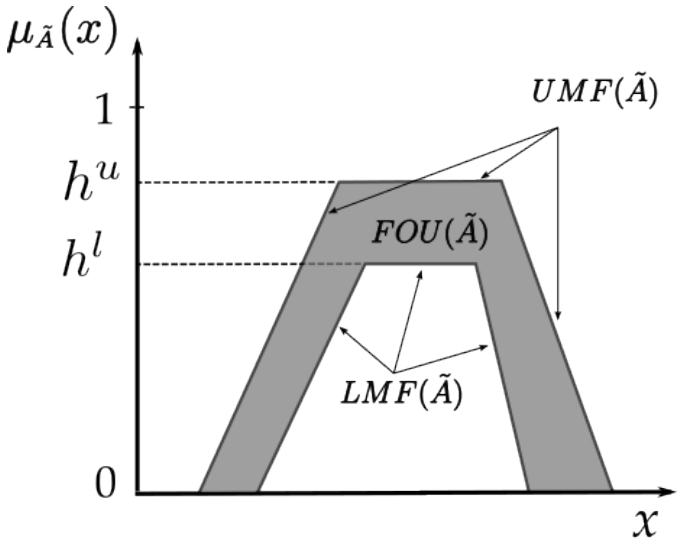

Figure 2: *UMF, LMF and FOU for the IT2FN with heights of h^l and h^u*

General Interval Type-2 Trapezoidal Fuzzy Numbers (GIT2TrFNs) provide a foundational framework for arithmetic operations and ranking of IT2FNs, characterized by their boundaries defined by straight lines, as illustrated in Figure 2. In this context, General Interval Type-2 Triangular Fuzzy Numbers (GIT2TFNs) emerge as a special case within the GIT2TrFN category.

GIT2TrFNs can serve as exemplary model for performing arithmetic operations and ranking among IT2FNs characterized by linear boundary profiles. It is worth noting that analogous procedures can be readily derived for GIT2TFNs using the provided information for GIT2TrFN.

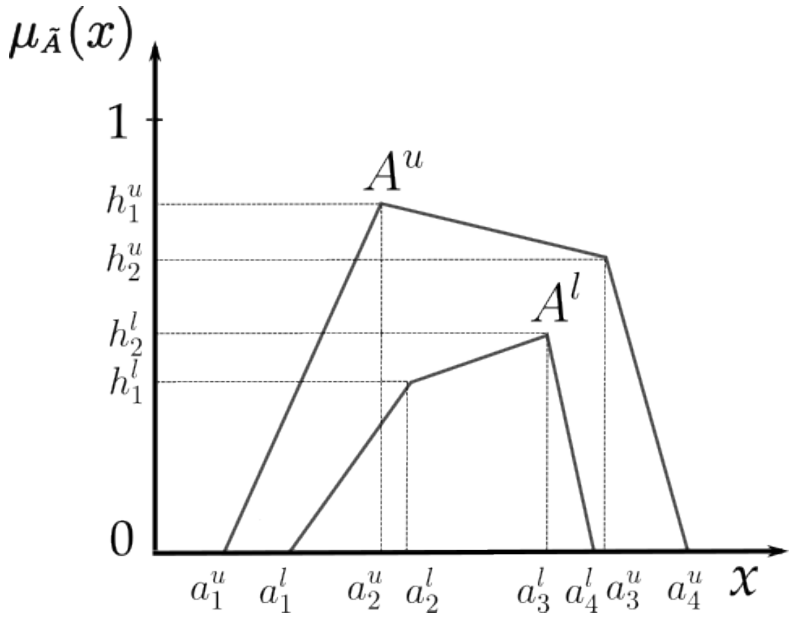

Figure 3: *The upper trapezoidal membership function A^u and the lower trapezoidal membership function A^l of the interval type-2 fuzzy set $\tilde{A}$*

GIT2TrFN is illustrated in Figure 3 and denoted as $\tilde{A} = (A^l, A^u) = \left((a_1^l, a_2^l, a_3^l, a_4^l, h_1^l, h_2^l), (a_1^u, a_2^u, a_3^u, a_4^u, h_1^u, h_2^u)\right)$ and its associated MFs for A^l and A^ucan be characterized as follows, respectively:

$$\mu_{A^l}(x) = \begin{cases} \mu_{A_1^l}(x) = h_1^l \frac{x - a_1^l}{a_2^l - a_1^l} & a_1^l \le x \le a_2^l \\ \mu_{A_2^l}(x) = (h_2^l - h_1^l)\frac{x - a_2^l}{a_3^l - a_2^l} + h_1^l & a_2^l \le x \le a_3^l \\ \mu_{A_3^l}(x) = h_2^l \frac{a_4^l - x}{a_4^l - a_3^l} & a_3^l \le x \le a_4^l \\ \mu_{A_4^l}(x) = 0 & x \le a_1^l, x \ge a_4^l \end{cases} \quad (15)$$

and

$$\mu_{A^u}(x) = \begin{cases} \mu_{A_1^u}(x) = h_1^u \frac{x - a_1^u}{a_2^u - a_1^u} & a_1^u \le x \le a_2^u \\ \mu_{A_2^u}(x) = (h_2^u - h_1^u)\frac{x - a_2^u}{a_3^u - a_2^u} + h_1^u & a_2^u \le x \le a_3^u \\ \mu_{A_3^u}(x) = h_2^u \frac{a_4^u - x}{a_4^u - a_3^u} & a_3^u \le x \le a_4^u \\ \mu_{A_4^u}(x) = 0 & x \le a_1^u, x \ge a_4^u \end{cases} \quad (16)$$

when $h_1^l = h_2^l = h^l$, $h_1^u = h_2^u = h^u$, and $h_1^l = h_2^l = h_1^u = h_2^u = 1$ It is termed as an Interval Type-2 Flat Trapezoidal Fuzzy Number (IT2FTrFN) and Perfect Interval Type-2 Trapezoidal Fuzzy Number (PIT2TrFN), respectively.

For GIT2TrFNs, some arithmetic operations and ranking are defined as follows, where

$$\tilde{A} = (A^l, A^u) = \left((a_1^l, a_2^l, a_3^l, a_4^l, h_{1A}^l, h_{2A}^l), (a_1^u, a_2^u, a_3^u, a_4^u, h_{1A}^u, h_{2A}^u)\right)$$

and

$$\tilde{B} = (B^l, B^u) = \left((b_1^l, b_2^l, b_3^l, b_4^l, h_{1B}^l, h_{2B}^l), (b_1^u, b_2^u, b_3^u, b_4^u, h_{1B}^u, h_{2B}^u)\right)$$

and k is the crisp value (Javanmard & Mishmast Nehi, 2019; Türkşen, 2002; Wang & Lee, 2008).

Addition Operation:

$$\begin{aligned}\tilde{A} \oplus \tilde{B} &= (A^l \oplus B^l, A^u \oplus B^u) \\ &= (a_1^l + b_1^l, a_2^l + b_2^l, a_3^l + b_3^l, a_4^l + b_4^l, \min\{h_{1A}^l, h_{1B}^l\}, \min\{h_{2A}^l, h_{2B}^l\}), \\ &\quad (a_1^u + b_1^u, a_2^u + b_2^u, a_3^u + b_3^u, a_4^u + b_4^u, \min\{h_{1A}^u, h_{1B}^u\}, \min\{h_{2A}^u, h_{2B}^u\})\end{aligned} \tag{18}$$

Subtraction Operation:

$$\begin{aligned}\tilde{A} \ominus \tilde{B} &= (A^l \ominus B^l, A^u \ominus B^u) \\ &= (a_1^l - b_4^l, a_2^l - b_3^l, a_3^l - b_2^l, a_4^l - b_1^l, \min\{h_{1A}^l, h_{1B}^l\}, \min\{h_{2A}^l, h_{2B}^l\}), \\ &\quad (a_1^u - b_4^u, a_2^u - b_3^u, a_3^u - b_2^u, a_4^u - b_1^u, \min\{h_{1A}^u, h_{1B}^u\}, \min\{h_{2A}^u, h_{2B}^u\})\end{aligned} \tag{19}$$

Multiplication Operation:

$$\tilde{A} \otimes \tilde{B} = \left((c_1^l, c_2^l, c_3^l, c_4^l, h_{1C}^l, h_{2C}^l), (c_1^u, c_2^u, c_3^u, c_4^u, h_{1C}^u, h_{2C}^u)\right) \tag{20}$$

where

$$c_1^l = min\{a_1^l \times b_1^l, a_1^l \times b_4^l, a_4^l \times b_1^l, a_4^l \times b_4^l\}$$

$$c_2^l = min\{a_2^l \times b_2^l, a_2^l \times b_3^l, a_3^l \times b_2^l, a_3^l \times b_3^l\}$$

$$c_3^l = max\{a_2^l \times b_2^l, a_2^l \times b_3^l, a_3^l \times b_2^l, a_3^l \times b_3^l\}$$

$$c_4^l = max\{a_1^l \times b_1^l, a_1^l \times b_4^l, a_4^l \times b_1^l, a_4^l \times b_4^l\}$$

$$h_{1C}^{l} = min\{h_{1A}^{l}, h_{1B}^{l}\}$$

$$h_{2C}^{l} = min\{h_{2A}^{l}, h_{2B}^{l}\} \tag{21}$$

$$c_1^u = min\{a_1^u \times b_1^u, a_1^u \times b_4^u, a_4^u \times b_1^u, a_4^u \times b_4^u\}$$

$$c_2^u = min\{a_2^u \times b_2^u, a_2^u \times b_3^u, a_3^u \times b_2^u, a_3^u \times b_3^u\}$$

$$c_3^u = max\{a_2^u \times b_2^u, a_2^u \times b_3^u, a_3^u \times b_2^u, a_3^u \times b_3^u\}$$

$$c_4^u = max\{a_1^u \times b_1^u, a_1^u \times b_4^u, a_4^u \times b_1^u, a_4^u \times b_4^u\}$$

$$h_{1C}^{u} = min\{h_{1A}^{u}, h_{1B}^{u}\}$$

$$h_{2C}^{u} = min\{h_{2A}^{u}, h_{2B}^{u}\}$$

Scalar Multiplication Operation:

$$if\ k \geq 0 \quad k\tilde{A} = (kA^l, kA^u) = \left((ka_1^l, ka_2^l, ka_3^l, ka_4^l, kh_{1A}^l, kh_{2A}^l), (ka_1^u, ka_2^u, ka_3^u, ka_4^u, kh_{1A}^u, kh_{2A}^u)\right) \tag{22}$$

$$if\ k \leq 0 \quad k\tilde{A} = (kA^l, kA^u) = \left((ka_4^l, ka_3^l, ka_2^l, ka_1^l, kh_{1A}^l, kh_{2A}^l), (ka_4^u, ka_3^u, ka_2^u, ka_1^u, kh_{1A}^u, kh_{2A}^u)\right) \tag{23}$$

Ranking of IT2FNs:

Ranking methods, similarity measures, and uncertainty measures are among the cornerstone concepts in the domain of IT2FSs. While similarity and uncertainty measures have extensive methodologies and research attention, the situation differs significantly for ranking methods. Compared to their counterparts, ranking methods for IT2FSs are limited (Lee & Chen, 2008; Mitchell, 2006; Wu & Mendel, 2009). and underscore the ongoing need for novel approaches (Javanmard & Mishmast Nehi, 2019; Kahraman et al., 2014).

The significance of ranking within the IT2FS framework cannot be overstated, given its pivotal role in aiding decision-making processes and facilitating a deeper understanding of fuzzy systems. The scarcity of established ranking methods highlights the exciting opportunities for further research and innovation in this area. As researchers continue to delve into the complexities of IT2FSs, the quest for improved ranking techniques remains an active and vital pursuit, reflecting the dynamic nature of this field.

In the following, Lee and Chen's ranking method (Lee & Chen, 2008) proposed for IT2TrFSs is presented. For a interval type-2 trapezoidal fuzzy sets

$$\tilde{A}_i = \left(A_i^l, A_i^u\right) = \left(\left(a_{i1}^l, a_{i2}^l, a_{i3}^l, a_{i4}^l, h_{1A_i}^l, h_{2A_i}^l\right), \left(a_{i1}^u, a_{i2}^u, a_{i3}^u, a_{i4}^u, h_{1A_i}^u, h_{2A_i}^u\right)\right) \quad (24)$$

the ranking value, denoted as Rank($\tilde{A}$), is defined as follows.

$$\begin{aligned} Rank(\tilde{A}) = {} & M_1(\tilde{A}_i^l) + M_1(\tilde{A}_i^u) + M_2(\tilde{A}_i^l) + M_2(\tilde{A}_i^u) + M_3(\tilde{A}_i^l) + M_3(\tilde{A}_i^u) \\ & - \frac{1}{4}\left(S_1(\tilde{A}_i^l) + S_1(\tilde{A}_i^u) + S_2(\tilde{A}_i^l) + S_2(\tilde{A}_i^u) + S_3(\tilde{A}_i^l) + S_3(\tilde{A}_i^u) + S_4(\tilde{A}_i^l) + S_4(\tilde{A}_i^u)\right) \\ & + H_1(\tilde{A}_i^l) + H_1(\tilde{A}_i^u) + H_2(\tilde{A}_i^l) + H_2(\tilde{A}_i^u) \end{aligned} \quad (25)$$

$M_p(\tilde{A}_i^j) = \frac{a_{ip}^j + a_{ip+1}^j}{2}$ denotes the average of the elements a_{ip}^j and $a_{i(p+1)}^j$ for $1 \le p \le 3$,

$S_q(\tilde{A}_i^j) = \sqrt{\frac{1}{2}\sum_{k=q}^{q+1}\left(a_{ik}^j - \frac{1}{2}\sum_{k=q}^{q+1} a_{ik}^j\right)^2}$ denotes the standart deviation for $1 \le q \le 3$,

$H_p(\tilde{A}_i^j)$ denotes the membership value of the element $a_{i(p+1)}^j$ in the trapezoidal MF $\tilde{A}_i^j$ for $1 \le p \le 2$, $j \in \{U, L\}$ and $1 \le i \le n$

5. Conclusion

This study presents a comprehensive exploration of the T1FS and IT2FS approaches in terms of various application domains. To begin with, it is evident that T1FS finds successful application in numerous domains where dealing with uncertainty and non-definitive data is a requirement. This approach is distinguished by its lower computational costs and simpler rule structures, rendering it adept at managing imprecise data. In contrast, IT2FS exhibits the capacity to handle more extensive uncertainty intervals, making it particularly suitable for tackling intricate and uncertain problems. Nevertheless, it may necessitate increased computational resources and is often associated with more complex rule structures, presenting certain inherent drawbacks.

Both approaches offer distinct advantages in specific application domains. While T1FS, with its lower computational costs and simpler rule structures, is proficient at handling certain types of problems, IT2FS shines when it comes to managing larger uncertainty intervals and effectively solving complex problems. Consequently, the choice between these approaches may hinge on the specific problem at hand and the goals to be achieved.

With a profound comprehension of the strengths and weaknesses inherent in each approach, their applicability within specific domains becomes increasingly apparent. Furthermore, this study has underscored the significant contributions of IT2FS applications to critical sectors such as engineering disciplines, supply chain management, maritime, transport and finance. These applications serve as potent tools for navigating uncertainty and making well-informed decisions in these pivotal sectors. Consequently, the findings of this study underscore the substantial impact on the advancement of these critical industries and underscore the promising potential for future IT2FS applications within them.

In conclusion, the synthesis of these findings reaffirms the enduring relevance of FL as an invaluable instrument for decision-makers seeking innovative solutions to the ever-evolving challenges of the digital era. FL continues to provide more effective solutions to the challenges of decision making in situations of uncertainty.

References

Abdullah, L., & Zulkifli, N. (2015). Integration of fuzzy AHP and interval type-2 fuzzy DEMATEL: An application to human resource management. *Expert systems with Applications, 42*(9), 4397-4409.

Arık, A. E., & Bilgiç, B. (2022). Fuzzy control of a landing gear system with oleo-pneumatic shock absorber to reduce aircraft vibrations by landing impacts. *Aircraft Engineering and Aerospace Technology*(ahead-of-print).

Beşikçi, E. B., Kececi, T., Arslan, O., & Turan, O. (2016). An application of fuzzy-AHP to ship operational energy efficiency measures. *Ocean Engineering, 121*, 392-402.

Bloch, I. (2015). Fuzzy sets for image processing and understanding. *Fuzzy Sets and Systems, 281*, 280-291.

Celik, E., & Akyuz, E. (2018). An interval type-2 fuzzy AHP and TOPSIS methods for decision-making problems in maritime transportation engineering: the case of ship loader. *Ocean Engineering, 155*, 371-381.

Celik, M., Er, I. D., & Ozok, A. F. (2009). Application of fuzzy extended AHP methodology on shipping registry selection: The case of Turkish maritime industry. *Expert systems with Applications, 36*(1), 190-198.

Cevik Onar, S., Oztaysi, B., & Kahraman, C. (2014). Strategic decision selection using hesitant fuzzy TOPSIS and interval type-2 fuzzy AHP: a case study. *International Journal of Computational intelligence systems, 7*(5), 1002-1021.

Chen, S.-M., & Lee, L.-W. (2010). Fuzzy multiple attributes group decision-making based on the interval type-2 TOPSIS method. *Expert systems with Applications, 37*(4), 2790-2798.

Chou, C.-C. (2007). A fuzzy MCDM method for solving marine transshipment container port selection problems. *Applied Mathematics and Computation, 186*(1), 435-444.

Dijkman, J. G., van Haeringen, H., & de Lange, S. J. (1983). Fuzzy numbers. *Journal of Mathematical Analysis and Applications, 92*(2), 301-341. doi:https://doi.org/10.1016/0022-247X(83)90253-6

Ecer, F. (2022). Multi-criteria decision making for green supplier selection using interval type-2 fuzzy AHP: a case study of a home appliance manufacturer. *Operational Research, 22*(1), 199-233.

Ergin, A. (2021). A fuzzy AHP approach to evaluating differences between ocean container carriers and their customers. *International Journal of Shipping and Transport Logistics, 13*(3-4), 402-421.

Ergin, A., & Eker, I. (2019). Application of Fuzzy Topsis Model for Container Port Selection Considering Environmental Factors.

Ergin, A., & Ergin, M. F. (2018). Reduction of Ship Based CO2 Emissions from Container Transportation. *International Journal of Computational and Ex-*

perimental Science and Engineering, 4(3), 1-4.

Ergin, A., & Sandal, B. (2023). Mobbing among seafarers: Scale development and application of an interval type-2 fuzzy logic system. *Ocean Engineering, 286*, 115595.

Ertuğrul, İ., & Karakaşoğlu, N. (2008). Comparison of fuzzy AHP and fuzzy TOPSIS methods for facility location selection. *The International Journal of Advanced Manufacturing Technology, 39*(7-8), 783-795.

Ervural, B. C., Zaim, S., Demirel, O. F., Aydin, Z., & Delen, D. (2018). An ANP and fuzzy TOPSIS-based SWOT analysis for Turkey's energy planning. *Renewable and Sustainable Energy Reviews, 82*, 1538-1550.

Gupta, C., Jain, A., & Joshi, N. (2018). Fuzzy logic in natural language processing–a closer view. *Procedia computer science, 132*, 1375-1384.

Güngör, Z., Serhadlıoğlu, G., & Kesen, S. E. (2009). A fuzzy AHP approach to personnel selection problem. *Applied Soft Computing, 9*(2), 641-646.

Heo, E., Kim, J., & Boo, K.-J. (2010). Analysis of the assessment factors for renewable energy dissemination program evaluation using fuzzy AHP. *Renewable and Sustainable Energy Reviews, 14*(8), 2214-2220.

Javanmard, M., & Mishmast Nehi, H. (2019). Rankings and operations for interval type-2 fuzzy numbers: a review and some new methods. *Journal of Applied Mathematics and Computing, 59*, 597-630.

John, R., & Coupland, S. (2007). Type-2 fuzzy logic: A historical view. *IEEE computational intelligence magazine, 2*(1), 57-62.

Ka, B. (2011). Application of fuzzy AHP and ELECTRE to China dry port location selection. *The Asian Journal of Shipping and Logistics, 27*(2), 331-353.

Kahraman, C., Cebeci, U., & Ruan, D. (2004). Multi-attribute comparison of catering service companies using fuzzy AHP: The case of Turkey. *International Journal of Production Economics, 87*(2), 171-184.

Kahraman, C., Cebeci, U., & Ulukan, Z. (2003). Multi-criteria supplier selection using fuzzy AHP. *Logistics information management*.

Kahraman, C., Öztayşi, B., Sarı, İ. U., & Turanoğlu, E. (2014). Fuzzy analytic hierarchy process with interval type-2 fuzzy sets. *Knowledge-Based Systems, 59*, 48-57.

Kaya, T., & Kahraman, C. (2010). Multicriteria renewable energy planning using an integrated fuzzy VIKOR & AHP methodology: The case of Istanbul. *Energy, 35*(6), 2517-2527.

Kiracı, K., & Akan, E. (2020). Aircraft selection by applying AHP and TOPSIS in interval type-2 fuzzy sets. *Journal of Air Transport Management, 89*, 101924.

Kumar, D., Singh, J., & Singh, O. P. (2013). A fuzzy logic based decision support system for evaluation of suppliers in supply chain management practices.

Mathematical and Computer Modelling, 58(11-12), 1679-1695.

Lee, L.-W., & Chen, S.-M. (2008). *Fuzzy multiple attributes group decision-making based on the extension of TOPSIS method and interval type-2 fuzzy sets.* Paper presented at the 2008 international conference on machine learning and cybernetics.

Liang, Q., & Mendel, J. M. (2000). Interval type-2 fuzzy logic systems: theory and design. *IEEE Transactions on fuzzy systems, 8*(5), 535-550.

Mendel, J. M. (2013). General type-2 fuzzy logic systems made simple: a tutorial. *IEEE Transactions on fuzzy systems, 22*(5), 1162-1182.

Mendel, J. M. (2017). Uncertain rule-based fuzzy systems. *Introduction and new directions, 684*.

Mendel, J. M. (2018). Comparing the performance potentials of interval and general type-2 rule-based fuzzy systems in terms of sculpting the state space. *IEEE Transactions on fuzzy systems, 27*(1), 58-71.

Mendel, J. M., & John, R. B. (2002). Type-2 fuzzy sets made simple. *IEEE Transactions on fuzzy systems, 10*(2), 117-127.

Mendel, J. M., & Wu, H. (2002). *Uncertainty versus choice in rule-based fuzzy logic systems.* Paper presented at the 2002 IEEE World Congress on Computational Intelligence. 2002 IEEE International Conference on Fuzzy Systems. FUZZ-IEEE'02. Proceedings (Cat. No. 02CH37291).

Mitchell, H. (2006). Ranking type-2 fuzzy numbers. *IEEE Transactions on fuzzy systems, 14*(2), 287-294.

Onut, S., Tuzkaya, U. R., & Torun, E. (2011). Selecting container port via a fuzzy ANP-based approach: A case study in the Marmara Region, Turkey. *Transport Policy, 18*(1), 182-193.

Ozer, H. O., Hacioglu, Y., & Yagiz, N. (2016). Suppression of structural vibrations using PDPI+ PI type fuzzy logic controlled active dynamic absorber. *Journal of the Brazilian Society of Mechanical Sciences and Engineering, 38*, 2105-2115.

Oztaysi, B. (2015). A Group Decision Making Approach Using Interval Type-2 Fuzzy AHP for Enterprise Information Systems Project Selection. *Journal of Multiple-Valued Logic & Soft Computing, 24*.

Öztayşi, B., & Kahraman, C. (2017). Evaluation of renewable energy alternatives using hesitant fuzzy TOPSIS and interval type-2 fuzzy AHP. In *Renewable and Alternative Energy: Concepts, Methodologies, Tools, and Applications* (pp. 1378-1412): IGI Global.

Öztürk, F. (2021). A hybrid type-2 fuzzy performance evaluation model for public transport services. *Arabian Journal for Science and Engineering, 46*(10), 10261-10279.

Park, K.-S., Seo, Y.-J., Kim, A.-R., & Ha, M.-H. (2018). Ship acquisition of shipping companies by sale & purchase activities for sustainable growth: Ex-

ploratory fuzzy-AHP application. *Sustainability, 10*(6), 1763.

Pedrycz, W., Ekel, P., & Parreiras, R. (2011). *Fuzzy multicriteria decision-making: models, methods and applications*: John Wiley & Sons.

Ren, J., & Lützen, M. (2015). Fuzzy multi-criteria decision-making method for technology selection for emissions reduction from shipping under uncertainties. *Transportation Research Part D: Transport and Environment, 40*, 43-60.

Sahin, B., Yazir, D., Soylu, A., & Yip, T. L. (2021). Improved fuzzy AHP based game-theoretic model for shipyard selection. *Ocean Engineering, 233*, 109060.

Sandal, B., Hacioglu, Y., Salihoglu, Z., & Yagiz, N. (2023). Fuzzy Logic Preanesthetic Risk Evaluation of Laparoscopic Cholecystectomy Operations. *The American Surgeon, 89*(3), 414-423.

Skalna, I., Rebiasz, B., Gawel, B., Basiura, B., Duda, J., Opila, J., & Pelech-Pilichowski, T. (2015). Advances in fuzzy decision making. *Studies in Fuzziness and Soft Computing, 333*.

Soner, O., Celik, E., & Akyuz, E. (2017). Application of AHP and VIKOR methods under interval type 2 fuzzy environment in maritime transportation. *Ocean Engineering, 129*, 107-116.

Sun, C.-C. (2010). A performance evaluation model by integrating fuzzy AHP and fuzzy TOPSIS methods. *Expert systems with Applications, 37*(12), 7745-7754.

Taskin, Y., & Hacioglu, Y. (2020). Robust and Intelligent Control Techniques for Twin Rotor System. In *Handbook of Research on Advanced Mechatronic Systems and Intelligent Robotics* (pp. 401-420): IGI Global.

Taskin, Y., Hacioglu, Y., & Yagiz, N. (2017). Experimental evaluation of a fuzzy logic controller on a quarter car test rig. *Journal of the Brazilian Society of Mechanical Sciences and Engineering, 39*, 2433-2445.

Tunçel, A. L., Arslan, Ö., & Akyüz, E. (2023). An Application of Fuzzy AHP Using Quadratic Mean Method: Case Study of ENC Preparation Process for Intended Voyages. *Journal of ETA Maritime Science, 11*(1).

Türkşen, I. B. (2002). Type 2 representation and reasoning for CWW. *Fuzzy Sets and Systems, 127*(1), 17-36.

Ünver, B., Altın, İ., & Gürgen, S. (2021). Risk ranking of maintenance activities in a two-stroke marine diesel engine via fuzzy AHP method. *Applied Ocean Research, 111*, 102648.

Wang, Y.-J. (2014). The evaluation of financial performance for Taiwan container shipping companies by fuzzy TOPSIS. *Applied Soft Computing, 22*, 28-35.

Wang, Y.-J., & Lee, H.-S. (2008). The revised method of ranking fuzzy numbers with an area between the centroid and original points. *Computers*

& Mathematics with Applications, 55(9), 2033-2042. doi:https://doi.org/10.1016/j.camwa.2007.07.015

Wu, D., & Mendel, J. M. (2009). A comparative study of ranking methods, similarity measures and uncertainty measures for interval type-2 fuzzy sets. *Information sciences, 179*(8), 1169-1192. doi:https://doi.org/10.1016/j.ins.2008.12.010

Yasa, H., Ergin, M. F., Ergin, A., & Alkan, G. (2016). Importance of Inert Gases for Chemical Transportation. *PROCEEDINGS BOOK*, 825.

Yildiz, A., Ayyildiz, E., Taskin Gumus, A., & Ozkan, C. (2021). A framework to prioritize the public expectations from water treatment plants based on trapezoidal type-2 Fuzzy Ahp method. *Environmental Management, 67*(3), 439-448.

Yilmaz, M. K., Kusakci, A. O., Tatoglu, E., Icten, O., & Yetgin, F. (2019). Performance evaluation of real estate investment trusts using a hybridized interval type-2 fuzzy AHP-DEA approach: the case of Borsa Istanbul. *International Journal of Information Technology & Decision Making, 18*(06), 1785-1820.

Zadeh, L. A. (1971). Quantitative fuzzy semantics. *Information sciences, 3*(2), 159-176.

Zadeh, L. A. (1996). Fuzzy sets. In *Fuzzy sets, fuzzy logic, and fuzzy systems: selected papers by Lotfi A Zadeh* (pp. 394-432): World Scientific.

CHAPTER 7

METALLIC BIOMATERIALS PRODUCTION BY SELECTIVE LASER MELTING

Safiye İPEK AYVAZ[1]

1 Öğr. Gör. Dr. Manisa Celal Bayar University, Turgutlu Vocational School, Department of Machinery and Metal Technologies, 45140 Manisa, Turkey, E-mail:safiye.ipek@cbu.edu.tr, Orcid id: orcid.org/0000-0001-7385-7388

1. INTRODUCTION

Due to various diseases, accidents or congenital causes, artificial tissues/organ, orthoses and prostheses are implanted through surgical interventions. Metallic biomaterials are the first choice for needs where mechanical reliability is at the forefront(J. Zhang et al., 2019; L. C. Zhang et al., 2016a). However, in the field of implantology, the realization of the design and production of biomaterials with complex geometry and porous structure, which are specific to the patient and suitable for his anatomy, is an important limitation for the use of traditional methods in this field. For this reason, 3D additive manufacturing methods are needed (Bobik et al., 2020; Davoodi et al., 2022; Prasad et al., 2017; Yang et al., 2020).

Selective laser melting (SLM), one of the 3D manufacturing methods, was first developed by Carl Deckard at the University of Texas in his master's thesis (Mazzoli, 2013). It was later used in Germany in the 1990s by the Fraunhofer Institute for Laser Technology (Gao et al., 2023; Yap et al., 2015). As shown schematically in Figure 1, in the SLM technique, a high-energy laser beam locally melts the metallic powders on which it is focused. The molten powders are then rapidly solidified. This process is continued layer by layer to produce the final product(Song et al., 2015; J. Zhang et al., 2019; W. neng Zhang et al., 2020).

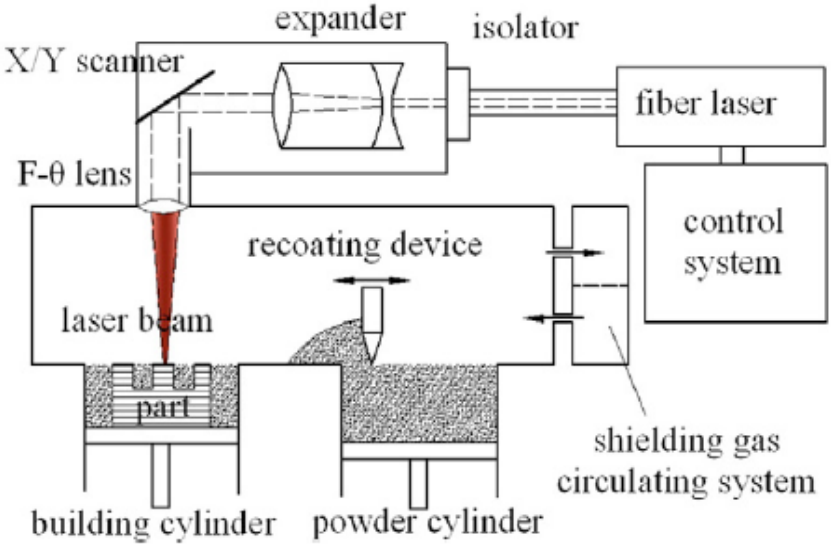

Figure 1. *Schematic representation of part production with SLM (Y. Liu et al., 2015).*

The ability to produce customized, complex and intricate structures layer by layer are important advantages of SLM technology. However, layered, rapid heating and cooling, and the transformation from powder to melt and then to solid, lead to inhomogeneous phase transformations, microstructures and thermal stresses (Fang et al., 2020). As a result, especially residual stresses make it difficult to control mechanical properties. The physical mechanism causing residual stresses is shown in Figure 2. In order to eliminate residual stresses and to obtain a homogeneous microstructure and to improve mechanical properties, appropriate heat treatments should be applied after production (Guoqing et al., 2018a; Im et al., 2022a; Kajima et al., 2018).

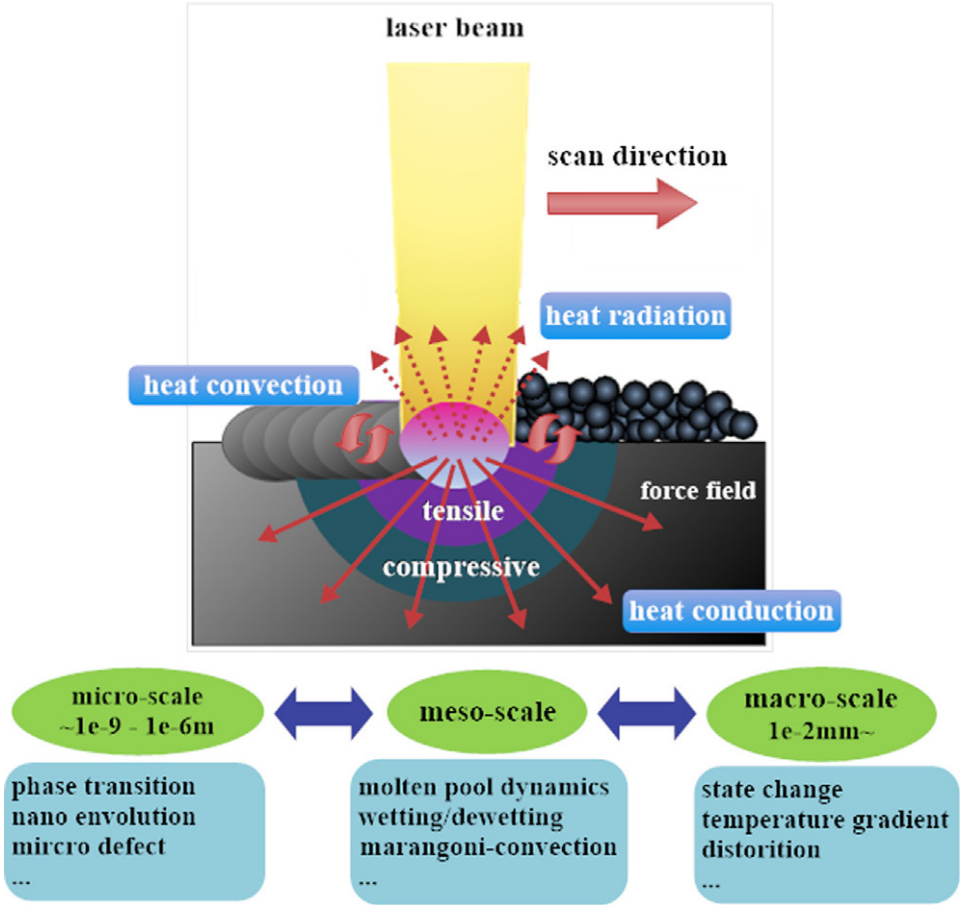

Figure 2. *Mechanism generating residual stresses in production with SLM technique (Fang et al., 2020)*

The mechanical properties of the specimens produced with SLM are closely related to the porosity ratio as well as the residual stress. The density and porosity ratio of the specimen vary with the laser energy density (LED) (Greco et al., 2020; Tang et al., 2020; Tonelli et al., 2020; Yu et al., 2021). LED [J mm^{-3}] is directly correlated with laser power (P) [W] and inversely correlated with scanning speed (v) [mm s^{-1}], scanning space (h) [mm] and layer thickness (d) [mm] and its equation is given in Equation 1.

$$LED = \frac{P}{vhd}$$

Studies in the literature have focused on the effect of LED, heat treatments on mechanical properties, biocompatibility of the implant and antibacterial activity in the production of metallic biomaterials with SLM technology.

2. METALLIC BIOMATERIALS PRODUCED BY SLM TECHNIQUE

2.1. Titanium and Its Alloys

The Young's modulus of human bone varies between 4-30 GPa. In general, metals have a high Young's modulus. The mismatch in Young's modulus causes a biocompatibility called stress shielding effect. Titanium and its alloys have a lower Young's modulus compared to other metallic biomaterials (Aufa et al., 2022; L. C. Zhang et al., 2016b; L. C. Zhang & Attar, 2016). For this reason, they are widely used as implant materials. Figure 3 shows real bone and a Ti alloy implant of the same size and geometry produced by the SLM technique.

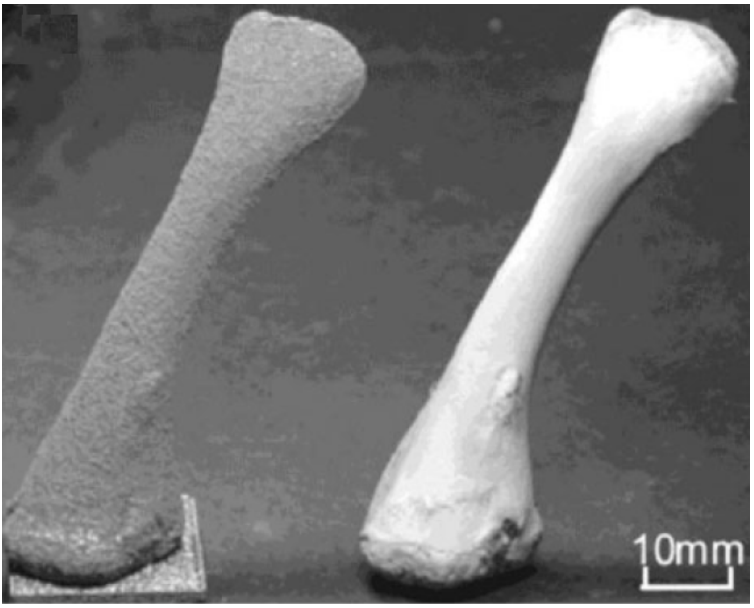

Figure 3. *Ti alloy implant produced with SLM and original bone (Osakada & Shiomi, 2006).*

Bartolomeu et al. produced Ti6Al4V alloy implants by SLM technique with 90W of laser power, 600 mm/s of speed, 70 μm of scan spacing and 30 μm of layer thickness. Implant-bone interaction tests were performed on the specimens produced with the SLM technique and Ti alloy implants produced with traditional production methods. As a result of the tests, higher kinetic friction coefficient and adherent bone tissue were detected in the specimens produced by SLM technique (Bartolomeu et al., 2019). Li et al. produced Ti35Zr28Nb scaffolds with high mechanical properties, corrosion resistance and biocompatibility Yan et al. produced Ti-15Ta alloy by SLM technique by adding Zr at various ratios to Ti-15Ta alloy. Mechanical tests showed that Ti-15Ta-10.5Zr alloy has a Young's modulus very close to bone (42.93 ± 3.28 GPa), while histological analysis proved that it is suitable for use in artificial hip joints and bone implants (Yan et al., 2016). Chlebus et al. investigated the mechanical properties of Ti-6Al-7Nb alloy produced by SLM. As a result of the study, it was reported that the SLM technique exhibits high anisotropic properties in production and that post-production heat treatments are needed to minimize the negative effects of this (Chlebus et al., 2011). Luo et al. investigated the effect of Cu addition at different ratios on the cytocompatibility of Ti6Al4V implants fabricated with SLM. The studies showed that SLM implants exhibited good cytocompatibility even at 6 wt. % Cu supplementation (Luo et al., 2018). Li et al. produced Ti6Al4V alloys with 75% porosity by SLM

technique. The tests showed that SLM implants have good biocompatibility and osteogenic ability. (J. Li et al., 2019). Rajendran and Pattanayak investigated the antimicrobial activity of macro-micro/nano-porous SLM Ti6Al4V alloy samples (Rajendran & Pattanayak, 2022). Guo et al. examined the effect of Cu addition on the antibacterial properties of SLM Ti6Al4V alloy implants. It was reported that all samples produced with different Cu addition rates showed good cytocompatibility, while 4-6% Cu addition was found to have very high antibacterial properties (L. Liu et al., 2017).

2.2. CoCr and Its Alloys

Implants are required to have high corrosion resistance against blood and other body fluids. In addition, the wear resistance of joint implants or dental implants must also be excellent. CoCr based alloys are also prominent in these implant applications due to their high corrosion and wear resistance (Acharya et al., 2021; Saini et al., 2021a, 2021b). Figure 4 shows an ankle joint made of SLM CoCr alloy.

Figure 4. *SLM CoCr Based Ankle Joint (Lu et al., 2023)*

CoCr alloys generally have a γ phase with a surface-centered cubic (FCC) structure and another ε phase with a hexagonal tight packing (HSP) structure after SLE fabrication (Guoqing et al., 2018b; Im et al., 2022b). The proportion of ε phase is important in determining the mechanical properties of Co-Cr-Mo alloys. Strength increases with increasing ε phase ratio. It has also been reported that the higher the ε phase, the higher the wear resistance (Guoqing et al., 2018b). However, the increase of ε phase decreases the cold workability and toughness of Co-Cr alloys.

Hedberg et al. investigated the effect of manufacturing parameters on the corrosion resistance of CoCrMo dental implants produced by SLM technique. In the study, when SLM samples were compared with cast sam-

ples, it was determined that the implants produced with SLM technique had higher corrosion resistance (Hedberg et al., 2014). Mace et al. investigated the corrosion resistance of low carbon forged CoCrMo alloy and SLM CoCrMo alloy implants. As a result of the tests, no significant difference was found between these two dental implants produced by different methods in terms of corrosion resistance (Mace et al., 2022). Guoqing et al. examined the biocompatibility of SLM CoCrMo alloys. In the study, it was reported that SLM specimens showed higher blood compatibility compared to cast specimens (Guoqing et al., 2018). Ren et al. reported that they formed an antibacterial film on Cu-added CoCr alloys produced by SLM and obtained similar mechanical properties, corrosion resistance and biocompatibility between these samples and CoCr alloys (Ren et al., 2016). Luo et al. They added 3% Cu to CoCrW alloys and produced them by SLM technique. It is reported that Cu reinforcement improves the corrosion and wear resistance of CoCrW alloys (Luo, Wu, et al., 2018).

2.3. 316L Stainless Steel

316L is widely used in the biomedical field due to their high strength, corrosion resistance and biocompatibility (Dewidar'.' et al., n.d.). SLM 316L stainless steel alloy has started to be used in implant production due to the fact that the implant suitable for the patient's needs can be produced much faster and easier than traditional methods. (Bartolomeu et al., 2017). Figure 5 shows a knee joint produced with SLM.

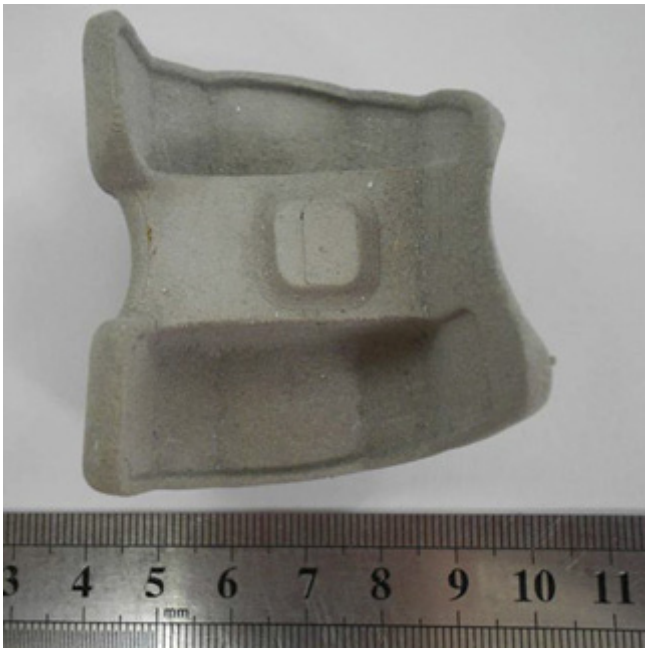

Figure 5. *SLM 316L knee joint (Xie et al., 2013).*

Bartolomeu et al. comparatively investigated the mechanical and tribological properties of 316L stainless steel alloy implants produced by SLM, hot pressing and conventional casting methods. It was reported that SLM 316L parts have higher mechanical properties and wear performance due to the fine-grained microstructure after fabrication (Bartolomeu et al., 2017). Kong et al. reported that 316L stainless steel implants produced with SLM have high corrosion resistance and biocompatibility (Kong et al., 2018). Capek et al. reported that 316L stainless steel alloy implants with similar mechanical properties and Young's modulus of trabecular bone can be manufactured porously with SLM technique (Čapek et al., 2016). Xu et al. reported by finite element analysis that 316L stainless steel alloys with 300 μm diameter porous structure produced by SLM technique exhibited similar mechanical properties to human bone (Xu et al., 2023). Hoa et al. HAp reinforced 316L stainless steel matrix composites were fabricated by SLM technique. HAp reinforced specimens were found to have finer grained microstructure and higher hardness than unreinforced specimens (Hao et al., 2009). Luo et al. investigated the effect of HAp coating on biocompatibility in 316L stainless steel alloys produced by SLM. In the study, it was determined that HAp coated samples did not show cell cytotoxicity and had higher biocompatibility than uncoated samples (Luo, Jia, et al., 2018).

2.4. Biodegradable Zn and Mg Alloys

Metallic alloys such as Ti, CoCr and Pt are widely used as implant materials due to their high biocompatibility. However, these implants need to be removed with a second operation after treatment (Haghshenas, 2017; Shahin et al., 2019). Mg alloy implants begin to dissolve simultaneously with the healing of the tissue in which they are implanted and disappear at the end of healing without the need for a second operation. For this reason, they are called biodegradable (Krishnan et al., 2022; Shahin et al., 2019). Figure 6 shows the dissolution process of the Mg rod implant at week 18. Similar to Mg alloys, Zn alloys are also biodegradable metallic biomaterials (Wen et al., 2018).

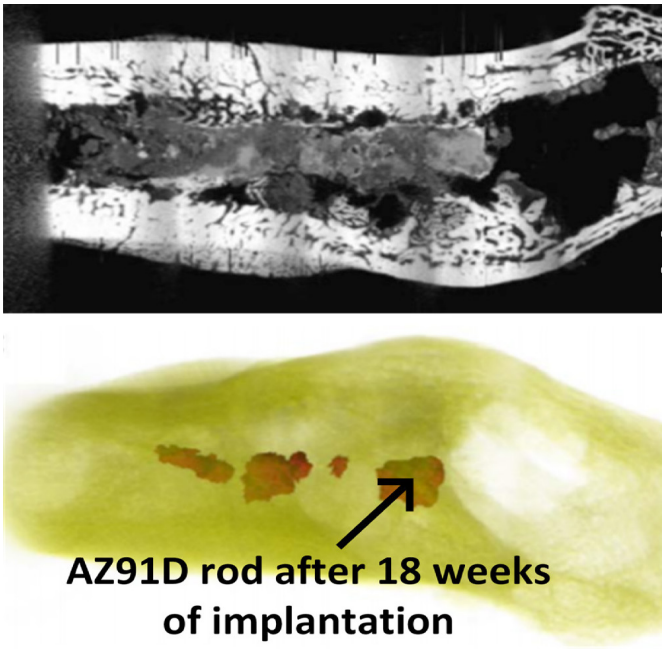

Figure 6. *Mg rod implant degradation process*

Ng et al. found that Mg implants produced with SLM exhibited mechanical properties closer to human bone than conventional Mg ingots (Ng et al., 2011). Suchy et al. investigated the corrosion resistance of SLM WE43 magnesium alloys in simulated body fluid (SBF). It was reported that the corrosion resistance of SLM alloys was lower than that of extruded samples (Suchý et al., 2021). Wu et al. reported that the hardness and elastic modulus of ZK60 magnesium alloys produced with SLM were closer to human bone compared to conventional Ti, CoCr and Fe alloy implants (Wu et al., 2021). Lovasiova et al. reported that the corrosion resistance of SLM WE43 magnesium alloys needs improvement but their biocompatibility is good (Lovašiová et al., 2022). Wen et al. produced biodegradable Zn alloy samples by SLM technique. As a result of their investigations, they reported that SLM Zn samples exhibited better mechanical properties than those produced by other methods (Wen et al., 2018). Wang et al. found that SLM pure Zn specimens exhibited higher mechanical properties compared to conventional specimens (Wang et al., 2022). Wagas et al. found that Zn10Mg alloy implants produced by the SLM technique have much better mechanical properties than those produced by the traditional casting method and provide the necessary qualification for biomedical use (Waqas et al., 2023).

2.5. NiTi Shape Memory Alloy

Shape memory alloys are smart materials that can retain their original shape by converting thermal energy into mechanical energy. NiTi alloys have the best shape memory capability. For this reason, they have many advanced engineering applications, especially in biomedicine (Jalali et al., 2023; Khoo et al., 2018). Figure 7 shows the biomedical applications of shape memory alloys.

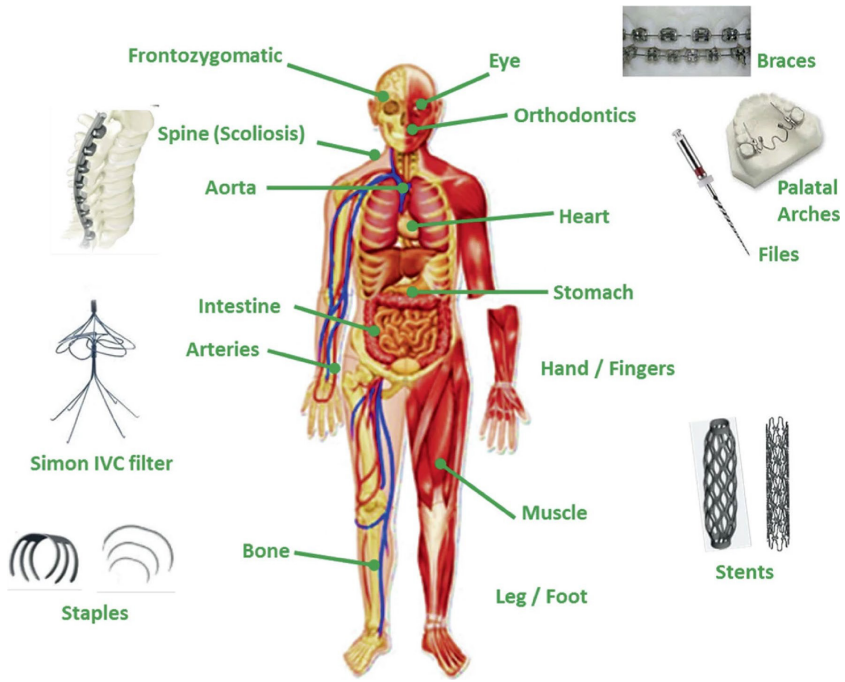

Figure. Biomedical applications of shape memory alloys (Jalali et al., 2023).

Andani et al. produced NiTi alloy specimens with porous structure by SLM technique. In their studies, it was reported that the elastic modulus can be reduced by 86% with the change in the amount of pore (Taheri Andani et al., 2017). Lu et al. produced NiTi alloys with porous structure, similar to the mechanical properties of human bone and high biocompatibility by SLM technique (Lu et al., 2021).

3. RESULTS

The production of metallic biomaterials with SLM has been shown to have some advantages specific to the production method:

- The mechanical properties of metallic biomaterials produced by SLM are generally higher than those produced by conventional methods (Bartolomeu et al., 2019; Bartolomeu et al., 2017; Suchý et al., 2021;

Waqas et al., 2023).

- The corrosion resistance of metallic biomaterials produced with SLM is generally higher than those produced by conventional methods (Hedberg et al., 2014; Mace et al., 2022).

- In production with SLM, mechanical properties can be made closer to human bone by realizing production in porosity structure (Lu et al., 2021; Taheri Andani et al., 2017; Xu et al., 2023).

- Biocompatibility and antibacterial activity can be increased by making different reinforcements to the metallic biomaterial alloy in SLM production (L. Liu et al., 2017; Luo, Jia, et al., 2018)

References

Bartolomeu, F., Buciumeanu, M., Pinto, E., Alves, N., Carvalho, O., Silva, F. S., & Miranda, G. (2017). 316L stainless steel mechanical and tribological behavior—A comparison between selective laser melting, hot pressing and conventional casting. *Additive Manufacturing*, *16*, 81–89. https://doi.org/10.1016/j.addma.2017.05.007

Čapek, J., Machová, M., Fousová, M., Kubásek, J., Vojtěch, D., Fojt, J., Jablonská, E., Lipov, J., & Ruml, T. (2016). Highly porous, low elastic modulus 316L stainless steel scaffold prepared by selective laser melting. *Materials Science and Engineering C*, *69*, 631–639. https://doi.org/10.1016/j.msec.2016.07.027

Dewidar'.', M. M., Khalil', K. A., & Lim3, J. K. (n.d.). *Science Press Processing and mechanical properties of porous 3 16L stainless steel for biomedical applications*. www.sciencedirect.com

Guoqing, Z., Yongqiang, Y., Changhui, S., Fan, F., & Zimian, Z. (2018). Study on Biocompatibility of CoCrMo Alloy Parts Manufactured by Selective Laser Melting. *Journal of Medical and Biological Engineering*, *38*(1), 76–86. https://doi.org/10.1007/s40846-017-0293-6

Haghshenas, M. (2017). Mechanical characteristics of biodegradable magnesium matrix composites: A review. In *Journal of Magnesium and Alloys* (Vol. 5, Issue 2, pp. 189–201). National Engg. Reaserch Center for Magnesium Alloys. https://doi.org/10.1016/j.jma.2017.05.001

Hao, L., Dadbakhsh, S., Seaman, O., & Felstead, M. (2009). Selective laser melting of a stainless steel and hydroxyapatite composite for load-bearing implant development. *Journal of Materials Processing Technology*, *209*(17), 5793–5801. https://doi.org/10.1016/j.jmatprotec.2009.06.012

Hedberg, Y. S., Qian, B., Shen, Z., Virtanen, S., & Odnevall Wallinder, I. (2014). In vitro biocompatibility of CoCrMo dental alloys fabricated by selective laser melting. *Dental Materials*, *30*(5), 525–534. https://doi.org/10.1016/j.dental.2014.02.008

Jalali, M., Mohammadi, K., Movahhedy, M. R., Karimi, F., Sadrnezhaad, S. K., Chernyshikhin, S. V., & Shishkovsky, I. V. (2023). SLM Additive Manufacturing of NiTi Porous Implants: A Review of Constitutive Models, Finite Element Simulations, Manufacturing, Heat Treatment, Mechanical, and Biomedical Studies. In *Metals and Materials International* (Vol. 29, Issue 9, pp. 2458–2491). Korean Institute of Metals and Materials. https://doi.org/10.1007/s12540-023-01401-1

Khoo, Z. X., Liu, Y., An, J., Chua, C. K., Shen, Y. F., & Kuo, C. N. (2018). A review of selective laser melted NiTi shape memory alloy. In *Materials* (Vol. 11, Issue 4). MDPI AG. https://doi.org/10.3390/ma11040519

Kong, D., Ni, X., Dong, C., Lei, X., Zhang, L., Man, C., Yao, J., Cheng, X., & Li, X. (2018). Bio-functional and anti-corrosive 3D printing 316L stain-

less steel fabricated by selective laser melting. *Materials and Design*, *152*, 88–101. https://doi.org/10.1016/j.matdes.2018.04.058

Krishnan, R., Pandiaraj, S., Muthusamy, S., Panchal, H., Alsoufi, M. S., Ibrahim, A. M. M., & Elsheikh, A. (2022). Biodegradable magnesium metal matrix composites for biomedical implants: synthesis, mechanical performance, and corrosion behavior - a review. In *Journal of Materials Research and Technology* (Vol. 20, pp. 650–670). Elsevier Editora Ltda. https://doi.org/10.1016/j.jmrt.2022.06.178

Lovašiová, P., Lovaši, T., Kubásek, J., Jablonská, E., Msallamová, Š., Michalcová, A., Vojtěch, D., Suchý, J., Koutný, D., & Alzubi, E. G. H. (2022). Biodegradable WE43 Magnesium Alloy Produced by Selective Laser Melting: Mechanical Properties, Corrosion Behavior, and In-Vitro Cytotoxicity. *Metals*, *12*(3). https://doi.org/10.3390/met12030469

Lu, H. Z., Ma, H. W., Luo, X., Wang, Y., Wang, J., Lupoi, R., Yin, S., & Yang, C. (2021). Microstructure, shape memory properties, and in vitro biocompatibility of porous NiTi scaffolds fabricated via selective laser melting. *Journal of Materials Research and Technology*, *15*, 6797–6812. https://doi.org/10.1016/j.jmrt.2021.11.112

Luo, J., Jia, X., Gu, R., Zhou, P., Huang, Y., Sun, J., & Yan, M. (2018). 316L stainless steel manufactured by selective laser melting and its biocompatibility with or without hydroxyapatite coating. *Metals*, *8*(7). https://doi.org/10.3390/met8070548

Luo, J., Wu, S., Lu, Y., Guo, S., Yang, Y., Zhao, C., Lin, J., Huang, T., & Lin, J. (2018). The effect of 3 wt.% Cu addition on the microstructure, tribological property and corrosion resistance of CoCrW alloys fabricated by selective laser melting. *Journal of Materials Science: Materials in Medicine*, *29*(4). https://doi.org/10.1007/s10856-018-6043-7

Mace, A., Khullar, P., Bouknight, C., & Gilbert, J. L. (2022). Corrosion properties of low carbon CoCrMo and additively manufactured CoCr alloys for dental applications. *Dental Materials*, *38*(7), 1184–1193. https://doi.org/10.1016/j.dental.2022.06.021

Ng, C. C., Savalani, M., & Man, H. C. (2011). Fabrication of magnesium using selective laser melting technique. *Rapid Prototyping Journal*, *17*(6), 479–490. https://doi.org/10.1108/13552541111184206

Ren, L., Memarzadeh, K., Zhang, S., Sun, Z., Yang, C., Ren, G., Allaker, R. P., & Yang, K. (2016). A novel coping metal material CoCrCu alloy fabricated by selective laser melting with antimicrobial and antibiofilm properties. *Materials Science and Engineering C*, *67*, 461–467. https://doi.org/10.1016/j.msec.2016.05.069

Shahin, M., Munir, K., Wen, C., & Li, Y. (2019). Magnesium matrix nanocomposites for orthopedic applications: A review from mechanical, corrosion, and biological perspectives. In *Acta Biomaterialia* (Vol. 96, pp. 1–19). Acta Materialia Inc. https://doi.org/10.1016/j.actbio.2019.06.007

Suchý, J., Klakurková, L., Man, O., Remešová, M., Horynová, M., Paloušek, D., Koutný, D., Krištofová, P., Vojtěch, D., & Čelko, L. (2021). Corrosion behaviour of WE43 magnesium alloy printed using selective laser melting in simulation body fluid solution. *Journal of Manufacturing Processes*, *69*, 556–566. https://doi.org/10.1016/j.jmapro.2021.08.006

Taheri Andani, M., Saedi, S., Turabi, A. S., Karamooz, M. R., Haberland, C., Karaca, H. E., & Elahinia, M. (2017). Mechanical and shape memory properties of porous Ni50.1Ti49.9 alloys manufactured by selective laser melting. *Journal of the Mechanical Behavior of Biomedical Materials*, *68*, 224–231. https://doi.org/10.1016/j.jmbbm.2017.01.047

Wang, C., Hu, Y., Zhong, C., Lan, C., Li, W., & Wang, X. (2022). Microstructural evolution and mechanical properties of pure Zn fabricated by selective laser melting. *Materials Science and Engineering: A*, *846*. https://doi.org/10.1016/j.msea.2022.143276

Waqas, M., He, D., Tan, Z., Yang, P., Gao, M., & Guo, X. (2023). A study of selective laser melting process for pure zinc and Zn10mg alloy on process parameters and mechanical properties. *Rapid Prototyping Journal*. https://doi.org/10.1108/RPJ-04-2022-0138

Wen, P., Jauer, L., Voshage, M., Chen, Y., Poprawe, R., & Schleifenbaum, J. H. (2018). Densification behavior of pure Zn metal parts produced by selective laser melting for manufacturing biodegradable implants. *Journal of Materials Processing Technology*, *258*, 128–137. https://doi.org/10.1016/j.jmatprotec.2018.03.007

Wu, C. L., Zai, W., & Man, H. C. (2021). Additive manufacturing of ZK60 magnesium alloy by selective laser melting: Parameter optimization, microstructure and biodegradability. *Materials Today Communications*, *26*. https://doi.org/10.1016/j.mtcomm.2020.101922

Xie, F., He, X., Cao, S., & Qu, X. (2013). Structural and mechanical characteristics of porous 316L stainless steel fabricated by indirect selective laser sintering. *Journal of Materials Processing Technology*, *213*(6), 838–843. https://doi.org/10.1016/j.jmatprotec.2012.12.014

Xu, S., Ma, H., Song, X., Zhang, S., Hu, X., & Meng, Z. (2023). Finite Element Simulation of Stainless Steel Porous Scaffolds for Selective Laser Melting (SLM) and Its Experimental Investigation. *Coatings*, *13*(1). https://doi.org/10.3390/coatings13010134

CHAPTER 8

A NEW APPROACH TO WEB BASED EXPERT SYSTEMS: ONLINE RULE ADDITION

Yenal ARSLAN[1]

1 Dr. Öğr. Üyesi, Ankara Yıldırım Beyazıt Üniversitesi Mühendislik ve Doğa Bilimleri Fakültesi, Yazılım Mühendisliği Bölümü, Ankara, Orcid Id: 0000- 0002-1776-6091, yenalarslan@aybu.edu.tr

1. INTRODUCTION

Expert systems, a sub branch of the artificial intelligence which emerged to produce machinery and software which can think and act like human beings, are known as the systems which can respond to users like human experts in a specific field. In other words, the expert system means turning the data, based on knowledge and experience of an expert in a field, into a program which can advise for and decide on a certain problem to be solved in the same field [1].

Traditional expert systems, in the beginning, used to operate in local and standalone computers, main frames or artificial intelligence machinery [2]. This had many disadvantages, in addition to certain superiorities such as efficiency, flexibility and reliability of expert systems, including:

- Cost. Although they were cheaper than human experts, mainframe and artificial intelligence machines were highly priced indeed.
- Performance issues. Problems with the performance occurred from time to time due to interworking of the knowledge base and the inference mechanism in local computers.
- Accessibility. Problems were experienced in accessing the target user audience at the end of operation.
- Platform dependence. Expert systems did not operate on all platforms, they could only operate in operating systems compatible with the respective protocol.

Application and information update. Separate updates in local computers required a huge amount of time and cost.

Development and more common use of the internet technologies, however, opened new doors in developing expert systems [3]. Researches started since the 2000s to look for answers to the question of developing web based expert systems. This would release the expert systems from the foregoing limitations. Below are some of the studies on web based expert systems.

Grupe, in one of his studies, turned an expert system, which was created with traditional methods, able to act like a decision support system in election of universities and departments according to the disposition of high school students, into a web based expert system. It was able to reach more students and achieve significant success as the expert system was web based [4].

Li et al. discussed in the beginning of their study the limitations and

immaturity of web based expert systems and then detailed their study. The researchers developed a web based expert system which provided farmers with information about diagnosis and treatment of fish diseases identified at fish farms in China. In the end, they created a complex system which included many software techniques such as java script, java, vb script, Ms sql server and ASP to remove the limitations of web based expert systems they discussed in the beginning [5].

Thomson and Willoughby, in their study, presented a web based expert system written with the perl language which gave opinions about using harmful pesticide to farmers in the United Kingdom [6].

Li developed a system called Webstra which was able to give answers such as the decision support system in market planning for companies and underlined that Webstra was a web based expert system created as hybrid using the group delphi technique [7]

Duan et al. in the introduction part of their study, defined expert systems as the branch of the artificial intelligence with the highest level of commercial success, addressed limitations of traditional expert systems as well as advantages of newly commissioned web based expert systems and compared some of them to each other. They reviewed in detail 3 web based expert systems called WITS, Fish-Expert, IMIS and listed their advantages and disadvantages respectively [8].

Kim et al. developed a link based expert system using CGI technologies and java scripts. Accordingly, each inference or entries from the user are received or presented with the web browser screens opened through predefined links with the production rules method [9].

Dunstan made a study which transformed an area in which expert information is provided with XML files into a web based expert system with the prologue interpreter in the background and shared this expert information with the end user. The study presented a web-based system which provided information about the university education system to university students [10].

Hasan and Isaac addressed insufficiency of methodology and research techniques in developing an expert system and stated that the web based expert system is a multidisciplinary area and a web engineer is required in addition to the field expert, information engineer and software developer to develop a web based expert system. Hasan and Isaac used MAS-CommonKADS agent-based knowledge base development methodology for the expert system and MS ASP.Net MVC technology for the user interface in their study. The researchers used their method to develop a web based expert system which provided producers with information about diagnosis

and treatment of the sugar cane disease in India [11].

Engin at al. developed two educational expert systems for a university. The first expert system is a course advising system which recommends courses to undergraduate students. The second system suggests scholarships to undergraduate students based on their eligibility. Both systems were implemented and tested with Oracle Policy Automation (OPA) software. And they serve their study to students via web application. As a result, they reduced workload on the faculty members [12].

Basciftci and Avuclu developed a web based expert system to diagnose cancer risk according to the symptomps in an individual [13].

It was observed that an established methodology is missing in developing web based expert systems in the studies in literature. Studies are generally made using CGI technology and java applet technology. These two technologies have both advantages and disadvantages compared to each other.

Hunington stated that performance problems might occur in the servers as the servers send a new form to the end user every time the end user sends a new entry level in web based expert systems using CGI technology, and the servers cannot memorize on time basis which information has been received from whom in the inference mechanism of the servers and when there is an error in the system, the end users need to reenter the concerned information. He, therefore, stated that it might be more efficient to use java applets in web based expert systems. Here, downloading java applets to the computer of the end user would prevent performance problems in the servers during operation of the expert system [14].

However, the study focused on developing a new methodology due to time, slowness and security problems associated with downloading java applets to the computer of the end user and the fact that web browsers do not support older java versions with rapid development of java versions. There are a few reasons for the rare use of web based expert systems in literature. One of them is that web technologies and developing applications with these technologies are a new technology compared to traditional expert system programming. Therefore, the expert system shells which had been commonly used in local computers could not be transferred to web-based systems. Another obstacle to developing web based expert systems is that the inference mechanisms of expert systems process only a single inference at the same time and with this inference, they keep information in the memory of the machines with the stack logic. The fact that memory using capacity of expert systems is naturally high and they only serve to a single server at the same time has become the biggest obstacle to transferring expert systems to the web environment and researchers developed

various methodologies to overcome this problem.

In the study, a central expert system shell which was not developed in literature before, was able to conduct all inference mechanisms from the server at the center and serve multiple people in multiple areas using asp.net and mssql server. The web based expert system shell developed is a new methodological approach and this approach is believed to make important contributions to science in leading the current complexion of concepts and methodologies.

2. DESIGNING USYAPP

2.1. Providing Information

It is very important to acquire information in establishing information systems and there are various ways to obtain information [15]. While designing USYAAP to provide information, experts and catalogued books on metals in literature [16], previously published articles and dissertations and the book Surface Engineering Against Abrasion by Dr. Özkan Sarıkaya were benefitted from [17].

2.2. Creating the Knowledgebase

The production rules method, one of the methods of presenting information, was used while creating the knowledge base [18]. Here, the attributes, conditions, rules and actions were defined separately [19]. The diagram of the tables used in the knowledge base is provided in Figure 1 below. Pid means project ID. The Pid column was placed to present multiple expert systems in the same knowledge base structure, it means the abrasion expert system and the medical expert system can operate in the system at the same time, accordingly abrasion is Pid=P1 and the medical expert system is Pid=P2. Therefore, the USYAAP web based expert system can be used as shell. In the attributes table, Nadi means the name of the attribute and Nid is the single indication of the attribution to be used in all expert system inferences. In the conditions table, Sid is the single indication of the condition and the condition column is the area where indications are entered to show on which conditions the considered condition will be active.

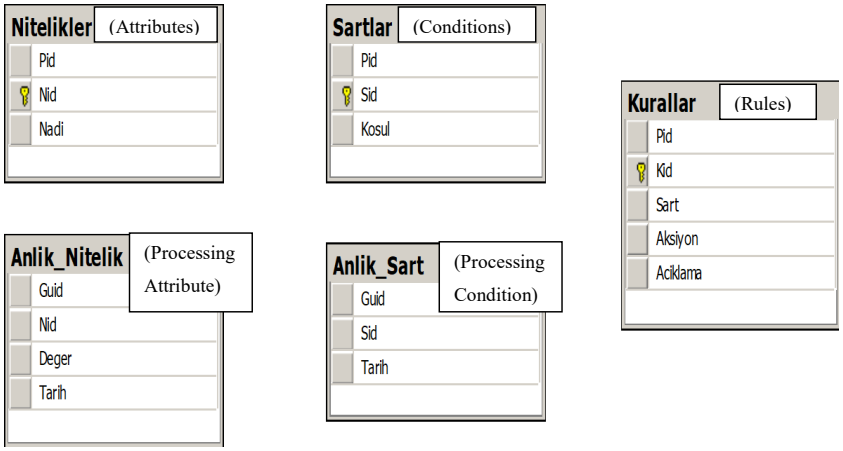

Figure 1. Knowledge Base Diagrams

The Lisp language was used in the study to show the conditions [20]. An example condition line can be used to provide further explanation. In table 1, the condition numbered 27 taken from the knowledge base.

Table 1. *Condition number 27*

P1	S27	(*(*(=N1,Corrosion,),(=N6,High_Temperature_Corrosion,),),(=N7,Carbide,),)

To explain the line provided in the example, N1 attribute should take the corrosion value in order to active the rule number 27 in P1 expert system, N6 attribute should take High_Temperature_Corrosion value and N7 should take Carbide value, when all these three conditions are met, the rule no 27 will be activated. The condition can be stated in terms of the production rules as S27 = (N1=Corrosion and N6=High_Temperature_Corrosion) and N7=Carbide. The condition in the dual tree structure can be demonstrated as in Figure 2 [21].

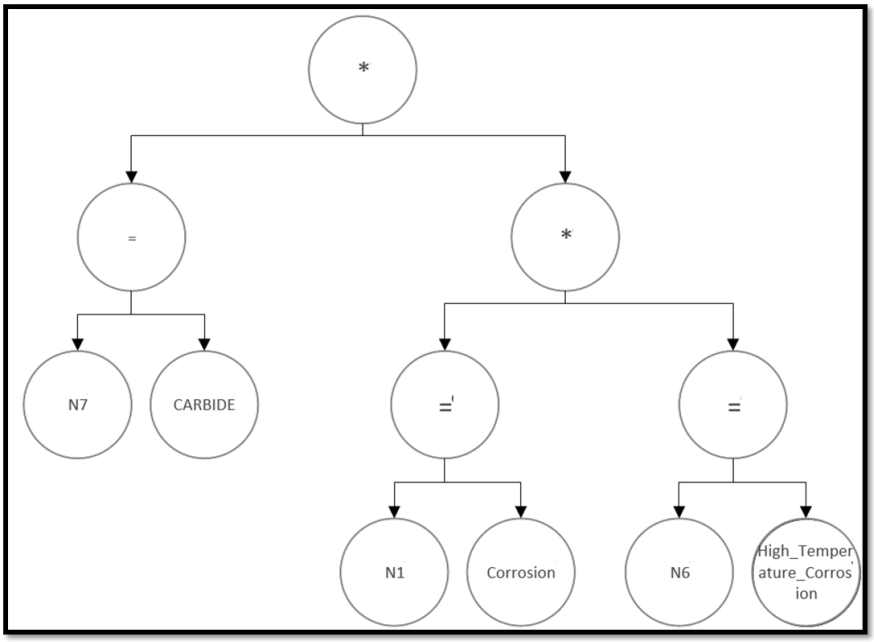

Figure 2. *Conditions in the dual tree format*

The rule pointed by this condition should be read in order to make the condition in this example a full production rule.

Rules are listed in the Rules table in the knowledge base. Kid is the single indication of the rule. The condition column is the condition which would activate the rule. Action describes what to do when the rule is active. If action is not defined in a rule, that rule is defined is the last rule by the expert system inference mechanism and the expert system is terminated by showing on the description screen in the description section. In the table 2, it is stated that when S2 condition is met for K2 rule in P1 domain, it is active and when K2 rule is active, there is no action defined, and thus, the related rule is the last rule according to the forward chaining principle. In the description section, there is the inference to be provided to the user.

Table 2. *Condition number 2*

P1	K2	S2	NoAction	In case of hollowing corrosion, the metal should be made of a very hard material resistant to corrosion and a solid material resistant to impact.

In the study, rules, conditions and attributes are completely flexible and the expert system can be modified or the new ones can be included by

the information engineer managing the expert system without recollecting the application or even during operation of the expert system, the expert system will notice and consider these modifications or inclusions. In order to do this, it is required to log into USYAAP application with the information engineer role and to click open the expert system administration panel.

In the Instant_Attribute table, the values of attributes entered by the end user in this session are kept singularly. Guid is the abbreviation of Globally Unique ID in English, written in the unique 16-byte hexadecimal format. In the study, the computer creates each expert system session started by the user. Therefore, with this algorithm, multiple persons can work on different sessions on the same expert system at the same time which is not available in literature. Multiple persons can even work on separate expert systems on multiple fields. It is possible by the web-based operation of the expert system, ability to identify single IDs for each session and keep the project ID for each knowledge base.

In the Instant_Condition table, as in the Instant_Attribute table, conditions activated are included after the attribute values entered by the end user in this session.

Moreover, USYAAP also keeps database tables to give reference to the end user.

2.3. Creating the Inference Mechanism

The modus ponens technique, one of the inference principles, was used while designing the inference mechanism. Among the search techniques, the breath first search technique was used in the first place. The forward chaining method, one of the inference control strategies, was used [22]. The Lisp language was used while creating the rules.

The operating logic of the inference mechanism starts with the first rule identified by the information engineer. In USYAAP program, this rule begins with the question “Which kind of corrosion mechanism are you dissatisfied with in your system?”. There are 4 concepts in the system, namely attributes, conditions, rules and action.

The system controls if conditions are met to activate a rule. Rules are maintained in the Rules table in the database.

Conditions are maintained in the Conditions table in the database. In order to determine if a condition is met, the system controls if the attributes in the conditions are as required (if the provisions are met). Attributes are maintained in the Attributes table in the database. In order for the entire system to take an action, an attribute needs to have a value. Therefore, the first attribute entry in the system begins with the answer to the first ques-

tion determined by the information engineer. The operating logic of the inference mechanism of the system developed can be outlined as follows.

- Entering a value for an attribute.
- Controlling and activating conditions compliant with the value entered.
- Activating the rules in compliance with the conditions activates and executing the actions.

The flow diagram of the expert system developed is in Figure 3.

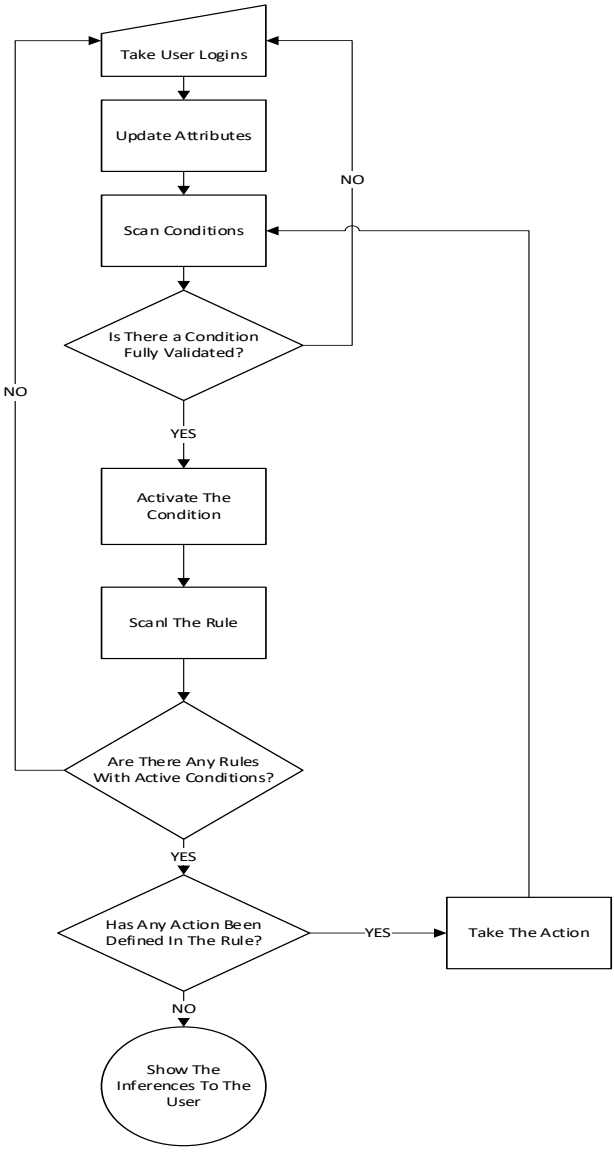

Figure 3. *USYAAP expert system flow diagram*

The system is based on activating a single rule at one time. The information engineer can create verification or in other words, solution tables to ensure information accuracy and consistency in the knowledge base. If multiple rules are active at the same time in the system, the system will execute the action of the rule it sees the first. The general flow of the system is outlined in Figure 4. Accordingly, an attribute can be an input of multiple provisions or one or more provisions can be an input of a condition. One condition only addresses one rule and one rule only triggers one action.

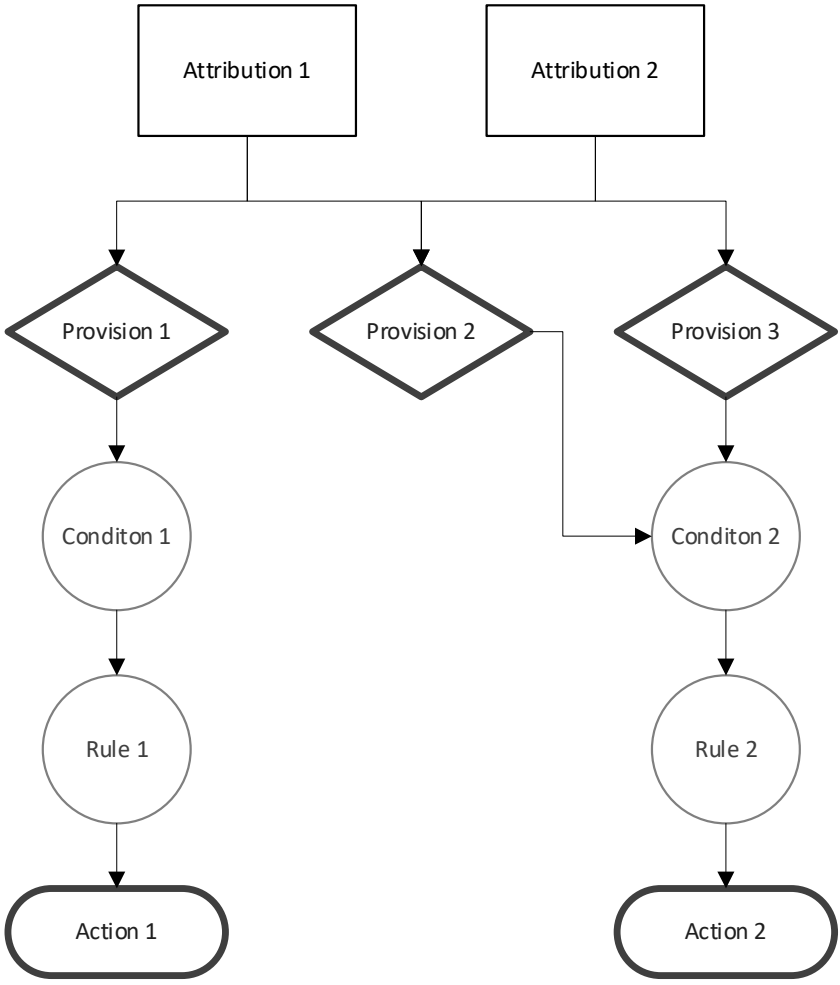

Figure 4. *Symbolic representation of the inference mechanism*

USYAAP has superiorities over the expert systems in literature.

• It is a web based expert system on contrary to many expert systems. Therefore, it is platform independent and can be operated from any

kind of computer.

- It can serve multiple end users at the same time on contrary to many expert systems. It can do this by maintaining the operating memory not in the memory but in the database.
- It is possible to enter new attributes, conditions and rules without recollecting the program on contrary to many expert systems.
- Reports can be created retrospectively as USYAAP records all end user operations since its establishment.
- USYAAP can be used as a shell. If the rules of other expert fields are added instead of corrosion, an expert system is created for the concerned expert field, it is not necessary to change any codes in the program while doing this.

2.4. Updating information in USYAAP

In order to update information in USYAAP, it is necessary to log into the system as the information engineer. In USYAAP, differently from traditional expert systems, information update can be practically made by the information engineer without deployment.

The information engineer, after logging into the Administration Panel with the authorized user, it is possible to make 3 main administrative operations as shown in Figure 5. The first of them is the Expert System Management section. In this section, the information engineer can add new rules, cases and conditions to the expert system. In the second section, the information engineer can add new materials to the Material Catalogue by clicking on the Identify Material and in the third section, it is possible to enter technical properties of materials according to the entered temperature and heat treatment through the Enter Test Data link.

Figure 5. *Launching the administration panel*

When the information engineer clicks on the Expert System Management link, three section will appear, namely the list of rules, the list of conditions and the list of attributes. The information engineer can change any rule, condition or attribute or add new ones (Figure 6, Figure 7, Figure 8).

Figure 6. *Operations which can be done by the information engineer at the Administration Panel*

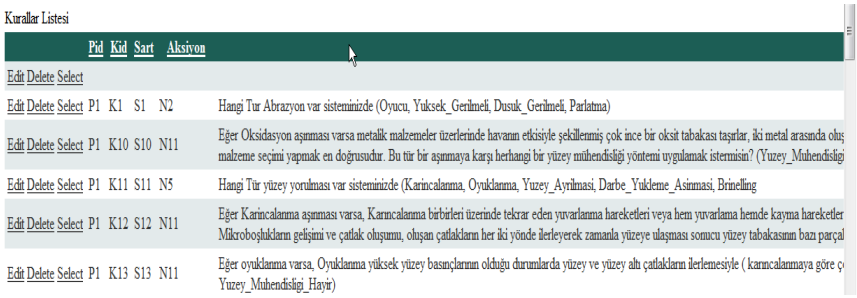

Kurallar Listesi

	Pid	Kid	Sart	Aksiyon	
Edit Delete Select					
Edit Delete Select	P1	K1	S1	N2	Hangi Tur Abrazyon var sisteminizde (Oyucu, Yuksek_Gerilmeli, Dusuk_Gerilmeli, Parlatma)
Edit Delete Select	P1	K10	S10	N11	Eğer Oksidasyon aşınması varsa metalik malzemeler üzerlerinde havanın etkisiyle şekillenmiş çok ince bir oksit tabakası taşırlar, iki metal arasında oluş malzeme seçimi yapmak en doğrusudur. Bu tür bir aşınmaya karşı herhangi bir yüzey mühendisliği yöntemi uygulamak istermisin? (Yuzey_Muhendisligi
Edit Delete Select	P1	K11	S11	N5	Hangi Tür yüzey yorulması var sisteminizde (Karincalanma, Oyuklanma, Yuzey_Ayrilmasi, Darbe_Yukleme_Asinmasi, Brinelling
Edit Delete Select	P1	K12	S12	N11	Eğer Karincalanma aşınması varsa, Karıncalanma birbirleri üzerinde tekrar eden yuvarlanma hareketleri veya hem yuvarlama hemde kayma hareketler Mikroboşlukların gelişimi ve çatlak oluşumu, oluşan çatlakların her iki yönde ilerleyerek zamanla yüzeye ulaşması sonucu yüzey tabakasının bazı parçal
Edit Delete Select	P1	K13	S13	N11	Eğer oyuklanma varsa, Oyuklanma yüksek yüzey basınçlarının olduğu durumlarda yüzey ve yüzey altı çatlakların ilerlemesiyle (karıncalanmaya göre ç Yuzey_Muhendisligi_Hayir)

Figure 7. *Representation of the rules in the expert system*

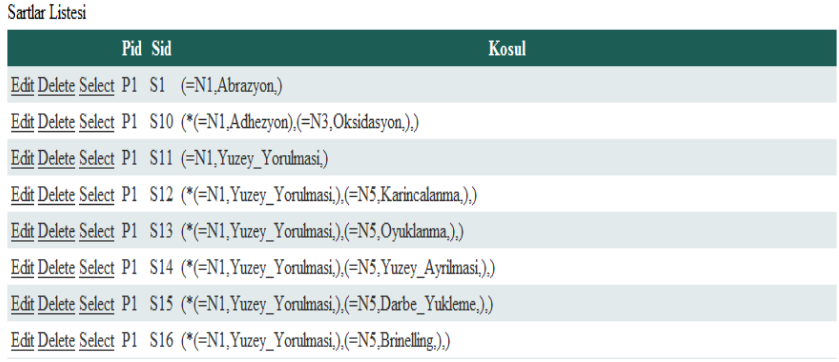

Sartlar Listesi

	Pid	Sid	Kosul
Edit Delete Select	P1	S1	(=N1,Abrazyon,)
Edit Delete Select	P1	S10	(*(=N1,Adhezyon),(=N3,Oksidasyon,),)
Edit Delete Select	P1	S11	(=N1,Yuzey_Yorulmasi,)
Edit Delete Select	P1	S12	(*(=N1,Yuzey_Yorulmasi,),(=N5,Karincalanma,),)
Edit Delete Select	P1	S13	(*(=N1,Yuzey_Yorulmasi,),(=N5,Oyuklanma,),)
Edit Delete Select	P1	S14	(*(=N1,Yuzey_Yorulmasi,),(=N5,Yuzey_Ayrilmasi,),)
Edit Delete Select	P1	S15	(*(=N1,Yuzey_Yorulmasi,),(=N5,Darbe_Yukleme,),)
Edit Delete Select	P1	S16	(*(=N1,Yuzey_Yorulmasi,),(=N5,Brinelling,),)

Figure 8. *Representation of the conditions in the expert system*

The distinctive advantage of the system is the ability to enter attributes, conditions and rules without engaging with the complexity of the expert system and inference system by logging into the web based expert system as the administrator without the need for any deployment even during operation.

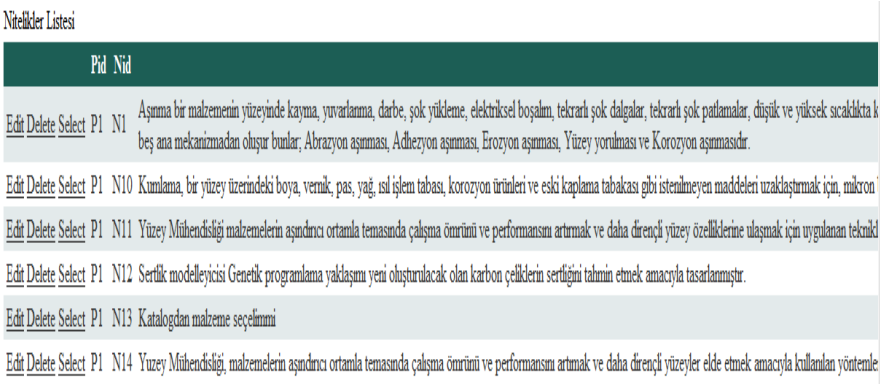

Nitelikler Listesi

	Pid	Nid	
Edit Delete Select	P1	N1	Aşınma bir malzemenin yüzeyinde kayma, yuvarlanma, darbe, şok yükleme, elektriksel boşalım, tekrarlı şok dalgalar, tekrarlı şok patlamalar, düşük ve yüksek sıcaklıkta k beş ana mekanizmadan oluşur bunlar; Abrazyon aşınması, Adhezyon aşınması, Erozyon aşınması, Yüzey yorulması ve Korozyon aşınmasıdır.
Edit Delete Select	P1	N10	Kumlama, bir yüzey üzerindeki boya, vernik, pas, yağ, isil işlem tabası, korozyon ürünleri ve eski kaplama tabakası gibi istenilmeyen maddeleri uzaklaştırmak için, mikron
Edit Delete Select	P1	N11	Yüzey Mühendisliği malzemelerin aşındırıcı ortamla temasında çalışma ömrünü ve performansını artırmak ve daha dirençli yüzey özelliklerine ulaşmak için uygulanan teknikl
Edit Delete Select	P1	N12	Sertlik modelleyicisi Genetik programlama yaklaşımı yeni oluşturulacak olan karbon çeliklerin sertliğini tahmin etmek amacıyla tasarlanmıştır.
Edit Delete Select	P1	N13	Katalogdan malzeme seçelimmi
Edit Delete Select	P1	N14	Yuzey Mühendisliği, malzemelerin aşındırıcı ortamla temasında çalışma ömrünü ve performansını artırmak ve daha dirençli yüzeyler elde etmek amacıyla kullanılan yöntemle

Figure 9. *Representation of attributes in the expert system*

3. CONCLUSION

In this study, a web based expert system (USYAAP) has been developed, which givers information to users, warns them about selection of accurate materials and offers material recommendations to end users thanks to a wide material database with an aim to remove or minimize corrosion mechanisms which cause a serious amount of cost and time in the corrosion field. The production rules method among the methods of information presentation was used while creating the knowledge base in USYAAP, the modus ponens technique among the inference principles while designing the inference mechanism, the breath first technique among the search techniques and the forward chaining method among the inference control strategies were used.

Furthermore, the most significant property of the system is the ability to change the rules during runtime. While many web based expert systems do require termination and restart of the system to change the rules, USYAAP does not.

In the study, a new approach has been brought to web based expert systems which do not have many examples in literature and have a problem of methodology confusion, and a field independent expert system shell has been developed. The web based expert system developed is distinguished from traditional expert systems with the following specifications.

- It can be accessed from anywhere through the internet and it is platform independent. Each user can access the expert system, as independent from the platform (Windows, Linux, Unix, Apple etc.), through web browsers from their computers or mobile devices.
- Users do not need to download any file to their computers (java applet, temp files etc.).
- Information update can be made practically by the information engineer and even the end users without reinstalling the program pack to the server.
- Multiple users can centrally use the concerned shell in multiple fields at the same time.

The system has been created with an approach which can operate with the mutual question and answer method to ensure proximity to the natural language. Accordingly, the end user can operate the system as if talking to a human expert. In further studies, user inputs can be acquired without using the keyboard by using the natural language processing techniques.

REFERENCES

[1] P. Jackson, Introduction to expert systems, Addison-Wesley, 1990.

[2] Y. Duan, J. S. Edwards, and M. X. Xu, "Web-based expert systems: Benefits and challenges," *Inf. Manag.*, vol. 42, no. 6, pp. 799–811, 2005.

[3] D. J. Power, "Web-based and model-driven decision support systems: concepts and issue," no. January 2000, 2000.

[4] F. H. Grupe, "An Internet-based expert system for selecting an academic major: www.MyMajors.com," *Internet High. Educ.*, vol. 5, no. 4, pp. 333–344, 2002.

[5] D. Li, Z. Fu, and Y. Duan, "Fish-Expert: A web-based expert system for fish disease diagnosis," *Expert Syst. Appl.*, vol. 23, no. 3, pp. 311–320, 2002.

[6] A. J. Thomson and I. Willoughby, "A web-based expert system for advising on herbicide use in Great Britain," *Comput. Electron. Agric.*, vol. 42, no. 1, pp. 43–49, 2004.

[7] S. Li, "A Web-enabled hybrid approach to strategic marketing planning: Group Delphi a Web-based expert system," *Expert Syst. Appl.*, vol. 29, no. 2, pp. 393–400, 2005.

[8] Y. Duan, J. S. Edwards, and M. X. Xu, "Web-based expert systems: Benefits and challenges," *Inf. Manag.*, vol. 42, no. 6, pp. 799–811, 2005.

[9] W. Kim, Y. U. Song, and J. S. Hong, "Web enabled expert systems using hyperlink-based inference," *Expert Syst. Appl.*, vol. 28, no. 1, pp. 79–91, 2005.

[10] N. Dunstan, "Generating domain-specific web-based expert systems," *Expert Syst. Appl.*, vol. 35, no. 3, pp. 686–690, 2008.

[11] S. S. Hasan and R. K. Isaac, "An integrated approach of MAS-CommonKADS, Model-View-Controller and web application optimization strategies for web-based expert system development," *Expert Syst. Appl.*, vol. 38, no. 1, pp. 417–428, 2011.

[12] G. Engin *et al.*, "Rule-based expert systems for supporting university students," *Procedia Comput. Sci.*, vol. 31, pp. 22–31, 2014.

[13] F. Başçiftçi and E. Avuçlu, "An expert system design to diagnose cancer by using a new method reduced rule base," *Comput. Methods Programs Biomed.*, vol. 157, pp. 113–120, 2018.

[14] D. Huntington, "Web-based expert systems are on the way: Java-based Web delivery," *PC AI*, vol. 14, pp. 34–36, Dec. 2000.

[15] E. Oztemel, "Bilginin Elde Edilmesi ve Derlenmesi", *Otomasyon*, p. 46-47, 1997.

[16] *Karbon Celikleri*,Asil Celik Teknik Yayınları, 1990.

[17] Ö. Sarıkaya, *Aşınmaya karşı yüzey mühendisliği yöntemleri*. y.y, 2007.

[18] J. C. Giarratano, G. Riley, Expert Systems: Principles and Programming, 3 rd ed., PWS Publishing Company, pp. 547, 1998.

[19] A. Barr, E. Feigenbaum, C. Roads, "The Handbook of Artificial Intelligence", *Comput. Music J.*, vol. 1, 1982.

[20] J. Liebowitz, "The Handbook of Applied Expert Systems", *Crc Pres LLC*, pp 22-25, 1998.

[21] I. Bindoff, T. Ling, B.H. Kang, Multiple classification ripple round rules: A preliminary study, in: Lect. Notes Comput. Sci. (Including Subser. Lect. Notes Artif. Intell. Lect. Notes Bioinformatics), 2009.

[22] N. Allahverdi, *Uzman Sistemler Bir Yapay Zeka Uygulaması*, Atlas Yayın Dağıtım, 78, 2002.

CHAPTER 9

EXAMINATION OF PRECIOUS METAL CONTENTS AND RECOVERY METHODS OF WASTE ELECTRICAL AND ELECTRONICAL EQUIPMENTS

Burcu TAN[1]

1 Dr., Çanakkale Onsekiz Mart University School of Graduate Studies, 17020, Çanakkale, Türkiye, burcu.tan88@gmail.com, ORCID : 0000-0003-4661-9661

1. INTRODUCTION

The manufacturing of electronic equipment is growing quickly on a global scale. With industrialization, economic growth, technological advancement, and affluent lifestyles, the dependence on electronic equipment has increased (Shagun et al., 2013).

Today, the almost universally accepted definition of WEEE is expressed by the European Union WEEE Directive. "WEEE" is defined as "discarded products, including subgroups, consumables, and all parts" in the WEEE Directive of the European Union (22/96/EC, (2003).

The fastest-growing category of waste in the world is waste electrical and electronic equipment. Electronic wastes (sometimes referred to as "e-wastes") are the remnants from the use of electronic devices (ED) such as computers, cell phones, televisions, fans, refrigerators, washing machines, and air conditioners (Rautela et al., 2021). In 2019, roughly 53.6 metric tonnes (Mt) of e-waste were produced globally, reported to the International Solid Waste Association (ISWA). The production of e-waste in Asia, America, and Europe in 2019 was 24.9 million tons, 13.1 million tons, and 12 million tons, respectively (Andeobu et al., 2021). The amount of e-waste generation is rising by around 2 million metric tons (Mt) annually on a global scale. In 2030, there will likely be 74 Mt of electronic waste generated (Chacraborty et al., 2022a). However, several noble metals, like Pd and Au, are found in these e-wastes; a ton of old mobile phones contains 368 g of Au and 287 g of Pd, which is more than the amount found in mineral ores and has a significant economic worth (Andrade et al., 2022) Forti et al. (2020) estimate that there are about $14 billion worth of precious metals (PMs) in e-waste, but that only $4 billion worth has been recovered.

Due to the approximately 30% amount of metals of this hazardous but otherwise beneficial waste, numerous studies illustrating the process pathways for recycling it have been published. Silver and gold are crucial components of contacts, bonding wires, and switches in the field of electronics, whereas palladium is used in computer hard disk drives (Ding et al., 2019; Diaz et al., 2016; Ning et al., 2023). These PMs are highly catalytically active and ductile (Shi et al., 2021).

E-waste may comprise roughly 70 elements from the periodic table due to the chemically rich yet complex the structure of electrical and electronical equipments. E-waste is a significant secondary source of common metals, PMs, and rare earth elements (REEs) because of its accumulated quantities and material composition (Lixandru et al., 2017). A report from the United States Environmental Protection Agency (USEPA), the metals—Ni, Cu, Cr, Hg, Cd, As Pb and Zn—have the greatest adverse effects

on the environment and are the most widespread (Wang & Chen, 2006). If discarded improperly, outdated electronics can leach lead and other materials into the ground and soil. These materials' toxic composition endangers both human health and the environment (Huang et al., 2009; Shagun et. al, 2013).

Therefore, from an economic and environmental perspective, recycling e-waste is essential. Recycling end-of-life (EoL) goods could help to improve sustainable management of e-wastes and at the very least reduce the environmental footprint and associated negative effects (Ottoni et al., 2020).

2. PMs RECOVERY FROM WEEs

Pertaining to the management of WEEs;

- Ensuring that WEEs are designed to be environmentally friendly, starting from the production phase, and that measures are taken to limit the amount of WEEs,
- During the recycling phase, ensuring the registered collection, separation, reuse, recycling and recovery of WEEs using appropriate and effective methods,
- Legal legislation, market structure, technological know-how and awareness that will ensure production and recycling processes must be ensured (Sayman, 2016).

In the hierarchy of e-waste treatment, reuse of the entire device is encouraged first, followed by remanufacturing, material recovery through recycling, and, as the final option, disposal by landfilling and incineration It is also hazardous to burn municipal solid waste in traditional incinerators along with electronic waste. When flame-retardants are burned, for instance, copper acts as a catalyst to cause the generation of dioxin. As flame retardants with bromine (BFRs) are being burned at low temperatures, this is very concerning (Cui &Zhang, 2008).

Metals have greater benefits for the environment and the economy during the recovery process.

These benefits may include the following (Aydın, 2011; Karataş, 2018):

- reducing down the use of primary resources,
- Reducing solid waste production,
- Material recovery from non-metals (plastic, etc.),
- Recovery of ferrous metals like iron, non-ferrous metals like steel, aluminum, and copper, and PMs like gold, silver, palladium, etc.

2.1 Components of WEEs

The preliminary treatment of e-waste mostly involves mechanical processes and disassembly to improve the PMs content. However, PMs cannot be completely recovered through mechanical recycling (Kang &Schoenung, 2006). Metals comprise approximately 60% of e-waste, followed by plastics at 15% and metal-plastic combination at 5% (Ari, 2015& Kaya, 2019).

Following mechanical processing and separation of WEEE components, iron typically leads the metallic portion, followed by copper, aluminum, and PMs (typically less than 1%). A device's component-specific availability of metals also varies. Six illustrative components or EDs are shown in Table 1 lists the amount of metals present (Regel-Rosocka, 2018)

Table 1. Component weight estimates (wt% or ppm) in illustrative EDs (Hagelüken &Corti, 2010).

Devices	Ag, ppm	Al, percentage	Au, ppm	Cu, percentage	Fe, percentage	Pd, ppm	Plastics, percentage
MB	280	15	20	12	30	10	28
PCB	900	5	200	18	7	80	23
MP	3000	3	320	13	7	120	43
PA	150	1	12	21	23	4	47
DVDP	115	2	15	5	62	4	24
C	260	5	50	3	4	5	61

Abr., C: calculator, DVDP: DVD player, MB: monitor board, MP: mobile phone, PA: Portable audio, PCB: PC-board.

Pretreatment processes are applied for the recycling of plastics containing WEEE. Pre-shredding and post-shredding methods at the pre-treatment stage are widely used in the recycling of plastics. In cases where plastics cannot be separated by type, they are reused or recycled as different plastic complexes. Plastic complexes can be used as energy sources or reducing agents for the recovery of metals in foundries with high emission control systems (Tuncer, 2014).

The majority of electronic systems nowadays employ PCBs, which are an essential component of electronic gadgets. The primary components of PCB assemblies are integrated circuits and yellow-green cards. A variety of metallic elements, including PMs, are combined with epoxy resin to create PCB, a copper-clad layer (Duan et al., 2011).

The most economically appealing component of WEEE, PCBs contribute around 3-5% of its total weight. waste PBSs (WPCBs) are a complex mixture of hazardous chemicals, nonmetals, and metals (Jiang et al., 2012). More than ten times as pure as rich minerals, PMs are found in

PCBs, in particular (Zhou & Qiu, 2010). There are significant amounts of base and PMs in used printed circuit boards. The concentration ranges (g/kg) for copper, iron, aluminum, nickel and palladium in waste WPCB in past research were 100–350, 10–100, 50–50, 1–10, 0.01–0.035, 0.02–0.150, and 0.01–0.12 respectively (Yamane et al., 2011).

Table 1 A typical PCB contents

Substance	Quantity (%)
Glass fiber	45-50
Integrated circuit	10-25
PMs	0-4
Copper	15-20
Another metals (Ni, Pb. Etc.)	~5-30

Mobile electronics that are nearing the end of their useful lives include a variety of base and PMs in concentrations that are higher than those present in mineral ores, including Au, Cu, Ag, Pd and Ni (Ghosh et al. 2015). Mobile phones typically include 3.5 kg of silver, 340 g of gold, 130 g of platinum, and 130 kg of copper each ton (Hagelüken et al., 2008). REEs, which can be collected and recycled, are also found in small but considerable amounts in the speakers, vibrators, and hard disks of mobile electronic gadgets (Buchert et al., 2012).

2.2 Methods of Recovery of PMs

Physical, thermochemical, pyrometallurgical, hydrometallurgical, biohydrometallurgical, and combination methods are some of the e-waste treatment processes that are utilized to recover metals (Chakraborty, 2022b).

2.2.1 Mechanical and physical techniques

One of the most crucial elements in the process is pretreatment methods for recovering electronic waste. Mechanical and physical procedures are part of pretreatment. Mechanical and physical processes; These include separation procedures based on the material's unique physical characteristics, such as disassembly, shredding, classification, gravity separation, magnetic separation, and electrostatic separation (Yazıcı, 2012). Because the whole process requires a lot of energy, applying mechanical techniques to the reuse of metals is not a viable option (Veglio et al., 2003). Prior to metallurgical operations, physical methods are typically used for pre-separation and enrichment. Pre-treated WEEE may be integrated into hydrometallurgical or pyrometallurgical processes.

2.2.2 Hyrometallurgical techniques

The processes of ion exchange, solvent extraction, electrochemistry, and leaching can be used to recover PMs. The waste is mechanically pretreated before the metals are dissolved with a suitable reagent, the charged leach solution is purified, and the metals are then recovered using hydrometallurgical procedures (Tuncuk et al., 2012). One of the most crucial techniques used in the separation and/or purification of many elements is the solvent extraction method, which is one of the hydrometallurgical techniques and is based on the notion of dispersing a substance at a given rate between two immiscible or partially mixed liquids (Lee et al., 2019).

In the recycling process to recover pure metals, the electrochemical procedure is a crucial stage. Both the initial extraction of metals from their mines (electrowinning) and the later refinement of metals to high purity (electropurification) utilise the electrochemical process. By using electrochemical methods that are based on the fundamental chemistry and electrochemistry laws, such as the principle of cathodic reduction of metal ions on the cathode of an electrochemical cell, many metals can be recovered (Murali et al., 2022).

Leaching is the process of dissolving metals after reactants with strong solvent characteristics are used to treat feed that is rich in PMs. The feed may be formed up of secondary sources like casting or scrap or it may be formed up of a primary source like ore or metal concentrate. The enhanced metal-containing solution is put through recovery procedures after the leaching procedure. The process of leaching depends greatly on the solvent to be employed. The physical and chemical characteristics of the primary or secondary source, as well as the solvent's selectivity to the metal to be recovered, must all be taken into consideration when choosing a solvent (Lin et al., 2023).

2.2.3 Pyrometallurgical techniques

Pyrometallurgy is a conventional technology that has been used for a long time to recover metal from WEEE; nevertheless, selective recovery of individual metals is very challenging with this method since this approach lacks selective behavior specific to the required metal. In order to recover non-ferrous metals, pyrometallurgy processes typically entail burning while being exposed to specific gases, melting in an arc furnace, melting in a high temperature furnace, or melting in copper smelting furnaces. Important metals present in electronic scrap, such as copper, silver, gold, and palladium, are frequently recovered using the smelter method. Instead of being recovered during the copper smelting process, iron and aluminum are oxidized in the slag. Melting furnaces are where this procedure takes place. The optimum method for processing waste complex polymer con-

tent and recovering material and energy is pyrolysis (Kaya, 2016).

2.2.4 Biohydrometallurgical techniques

Biometallurgical techniques are currently used as one approach for recovering metal from WEEE. Through sorption and complexing mechanisms, natural materials with biological origins can retain significant quantities of metal content. To recover metals, particularly Cu and Au, from very low concentrated ore concentrations, an alternate method is to use bio-hydrometallurgical methods. Due to their low investment costs, reduced environmental effect, low energy consumption, and improved control over conventional pyrometallurgical and hydrometallurgical processes, researchers have concentrated on bio-hydrometallurgy investigations and other metal recovery studies (Adentunji et al., 2023; Thakur & Kumar, 2023).

In comparison to pyrometallurgical procedures, hydrometallurgical methods have lower initial investment costs, a smaller negative impact on the environment, and higher metal recovery rates (Yazici et al., 2009).

2.2.5 Disposal techniques

The majority of nations frequently dispose of their waste in landfills. In the past, landfills were frequently employed; today, disused mines or temporary pits are frequently exploited. A sanitary and reasonably affordable way to dispose of waste items can be found in a landfill that is adequately planned and maintained. Storage facilities that are old, poorly made, or poorly maintained can have a number of detrimental consequences on the environment, including the release of harmful gases into the atmosphere, the dispersal of trash, the unchecked development of pests, and leaking (Ian, 2008).

Incineration is a disposal technique that involves burning waste. Waste materials are transformed into heat, gas, steam, and ash using this approach. Solid, liquid, and gaseous wastes are disposed of by small- and large-scale incineration processes in industry. The incineration of hazardous waste is seen to be an appropriate means of disposal. Its use is frowned upon in most nations since it results in the generation of gaseous pollutants that are hazardous to the environment as a result of improper burning; yet, it is extensively employed in nations where there is little or no flat ground appropriate for storage (Baka, 2019; Ghulam & Abushammala, 2023).

2.3 Studies on the Recovery of PMs from WEEEs.

Mobile electronics contain a little amount of gold, yet they are responsible for the largest share of the recoverable value of all e waste. The development and optimization of hydrometallurgical, non-cyanide, processes

concentrating on the recovery of valuable metals are currently the subject of intensive research based on this fact.

Birloaga et al. (2013), in their work, present the process of leaching WPCBs to recover gold through thioureation with the present laboratory-scale experimental study. An oxidative leaching pre-treatment was carried out in order to eliminate base metals because preliminary experiments have showed that copper negatively impacts the extraction of goldThe leaching process indicated that Cu may be removed with up to 90% efficiency. After 75% Cu was removed from WPCBs with particle sizes less than 2 mm using the twofold oxidative leaching technique, the optimization studies led to a gold extraction efficiency of 69%. After removing the copper, Figure 1 illustrates the particle sizes and illustrates the effectiveness of gold extraction.

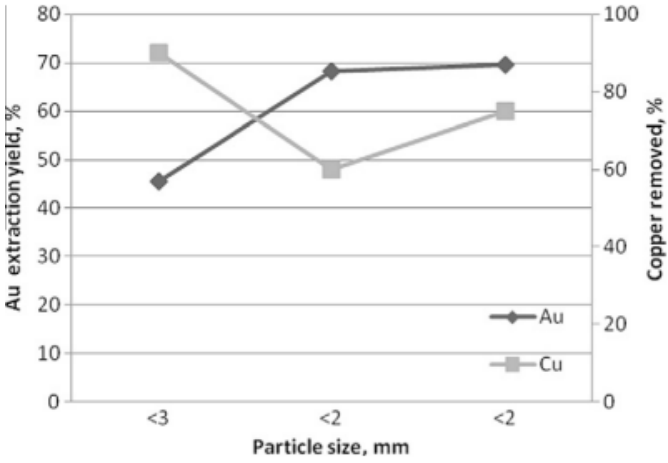

Fig. 1 Efficacy of gold extraction and a comparison of gold particle size followed copper removal.

The research of gold recovery from electronic waste material with a high copper content under ambient circumstances was the focus of Torres and Lapidus's (2016) study. In pretreatments with peroxide and HCl or citrate, over 90% of the copper was extracted. After barely an hour of reaction, the solid copper extraction waste was exposed to thiourea solutions in the second leaching process for gold recovery, which removed more than 90% of the gold. Figure 2 depicts the leaching of gold from WPCB during a three-hour period using 0.4 M Thiourea solutions at pH 1.5.

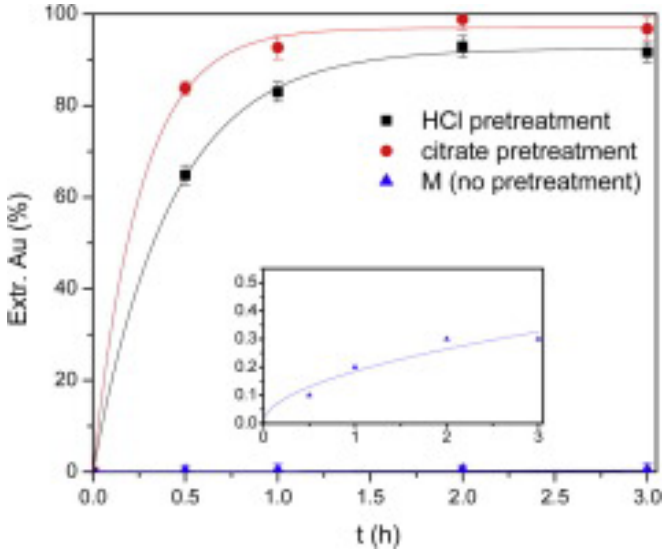

Fig. 2 Leaching of gold from WPCB

In their experiments, Photharin et al. (2022), have demonstrated a different method of recovering gold from electronic waste that makes use of cyanide secreted by microorganisms that are involved in the bioleaching process. The cyanogenic plant cassava, which contains cyanogenic glucosides, is not currently utilized as a source of bio-lixiviants. The production of cassava, a basic food, is rising to keep up with demand for food worldwide. They created a method to remove cyanide from freshly harvested cassava leaves, an agricultural waste. The cyanide concentration reached 120 ppm after several extractions, which was higher than the cyanide concentration created by cyanogenic bacteria. Finally, they demonstrated that the extract could remove gold from electronic trash with 69% more efficiency than the KCN solution control. The amount of electronic trash was optimized, and the recovery rate was 26.9%. It was determined that this rate was comparable to the biodegradation of cyanogenic bacteria. Fig. 3 illustrates the process.

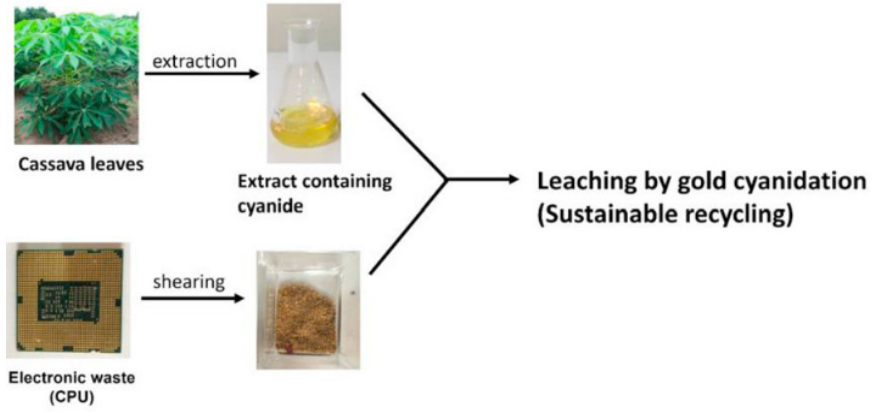

Fig. 3 Leaching by gold cyanidation

Bourgeois et al. (2020), focused on recovering palladium from WP-CBs. Palladium is an alloy of silver, thus diluted nitric acid was used to dissolve it without any difficulty. Base metals, primarily copper and iron, and palladium were combined to form a solution. A solvent extraction process was then applied to this solution. After precipitation with ammonia, a ca. 1 g/L Pd(II) aqueous solution with a 99.4% purity is finally obtained, from which palladium is directly separated as dichlorodiammine palladium(II) salt (Pd(NH3)2Cl2). Overall, palladium is quantitatively recovered from the leaching solution and was not found in the solid residue that was left behind. Fig. 4 illustrates illustrate the process's leaching stage, as well as the solids and solution produced.

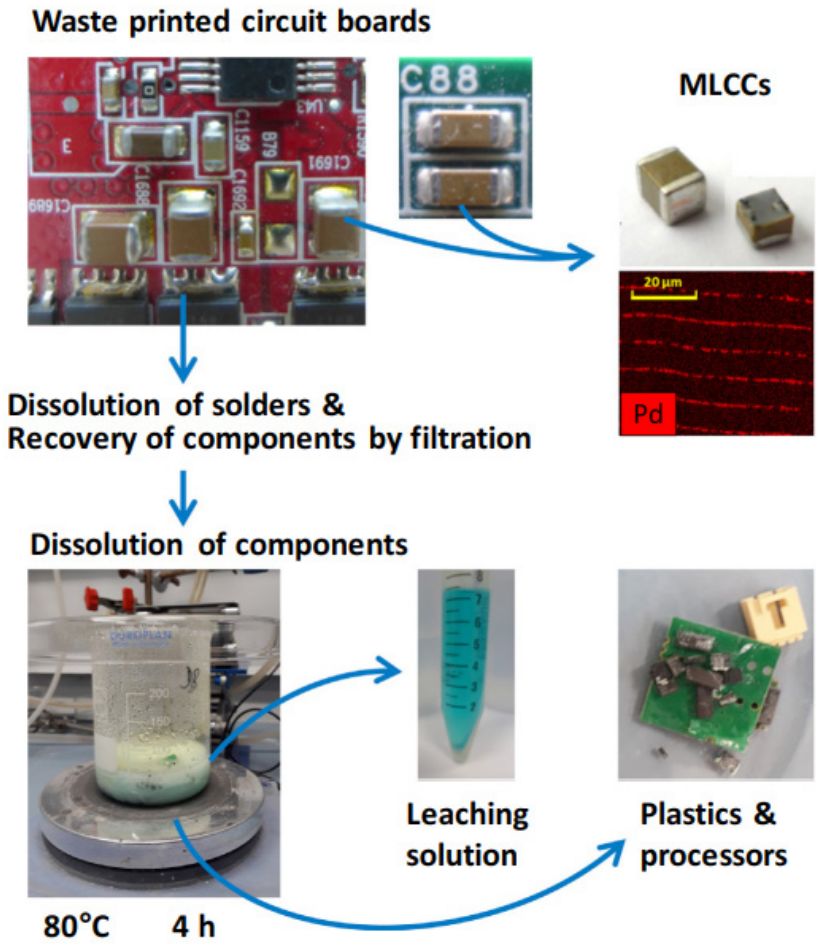

Fig. 4 Process steps

Ning et al. (2023), in order to look into the selective extraction of Au(III) and Pd(II) from hydrochloric acid media, the researchers synthesized a p-tert-butyl-thiacalix[4]arene tetrathioamide (TBTAT). With 100% extractability from 0.1 M hydrochloric acid media for 1 hour, TBTAT demonstrated exceptional extraction performance for Au(III) and Pd(II). Thiourea enabled the effective removal of gold and palladium from the loaded organic phase at the same time. Indicating the remarkable reusability of TBTAT for extraction of Au(III) and Pd(II) from HCl medium, the extractabilities of Au(III) and Pd(II) remained 100% after being reused five times.

An environmentally friendly, acid-free method for the selective recovery of palladium from used printed circuit boards (PCBs) has been success-

fully developed by Zhang & Zhang (2014). Initially, the copper recovery technique was used to enhance the palladium, which was then dissolved in a unique solution of $CuSO_4$ and NaCl. 96.9% of the palladium was recovered overall during the dissolution-extraction-stripping process. As a result, this work created a safe and efficient procedure for selective palladium recovery from used printed circuit boards. Figure 5 illustrates the flow chart for the extraction of palladium and enrichment of the metal from used PCBs.

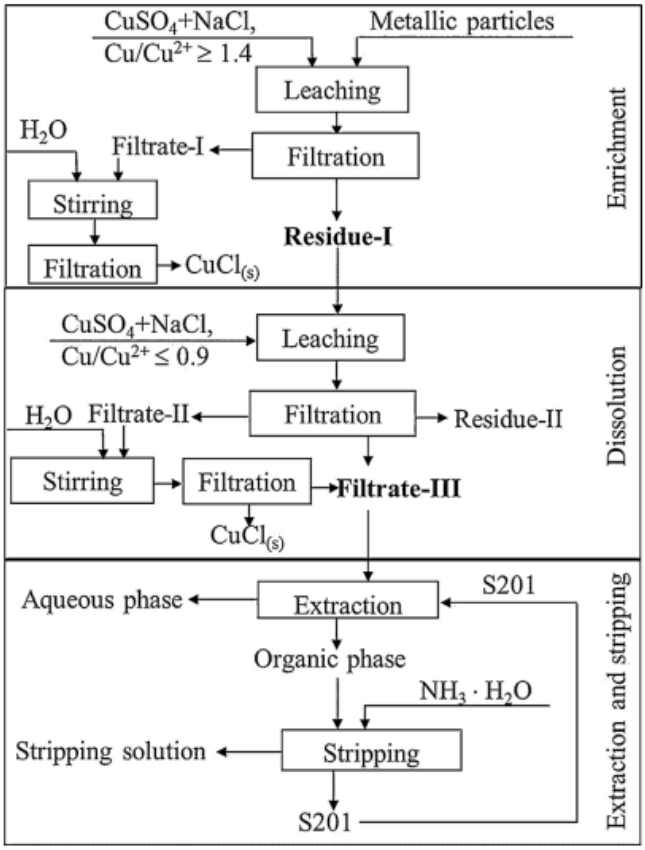

Fig. 5 Flow diagram for recovering and enriching palladium from used PCBs.

Wu (2008), utilized acid thiourea leaching and Zn/Fe exchange to extract gold and silver from waste PCBs after using two times oxidizing acid leaching as a pretreatment to recover base metals. In conclusion, nitrogen oxides are less dangerous air pollutants than the conventional oxidizing acid leaching technique, as demonstrated by twice the oxidative acid leaching pretreatment. Copper, gold, and silver all leach at rates of 97.6%, 95.1%, and 80%, respectively.

Cao & Xiao (2005), extracted gold, palladium, and silver from waste PCBs discovered in cell phones using calcine leaching method. Because of this, their research revealed that the recovery rates for gold, palladium, and silver were each over 95%.

3. CONCLUSION

Numerous industrial sectors make extensive use of PMs. Recycling PMs from secondary sources is crucial due to dwindling natural resources and rising demands that conflict with their economic value. WEEEs aren't waste, garbage, or poison. WEEEs should never be unlawfully disposed. Municipal dumping grounds, parks, rivers, lakes, and oceans, among other places, shouldn't serve as an e-waste cemetery. Recycling materials results in substantial energy savings. Due to the vast manufacture of electronic gadgets in response to worldwide demand, the amount of WEEEs are currently growing every day. WEEEs needs to be managed properly since it contains metals that are hazardous for the environment. The risk of metals pollution from WEEEs can be reduced if metals can be extracted from it and treated properly. The goal of this research is to help the scientific community, policy makers etc. identify the gaps in establishing a cleaner, safer, and more affordable recycling process. It is also expected to raise awareness about the e-waste problem and WEEE management.

REFERENCES

22/96/EC, (2003). Directive of European Parliament and of The Council of 27 January 2003 on Waste Electrical and Electronic Equipment (WEEE), Joint Declaration of The European Parliament, The Council and The Commission Relating to Article 9., Official Journal, L037: 0024-39

Adentunji, A.I., Oberholster, P.J., Erasmus, M. (2023). Bioleaching of metals from e-waste using microorganism: A review. Minerals, 13 (6), 828.

Andreobu, L., Wibowo, S., Grandhi, S. (2021). An assessment of e-waste generation and environmental management of selected countries in Africa, Europe and North America: A systematic review. Science of The Total Environment, 792, 148078.

Andrade, D.F., Castro, J.P., Garcia, J.A., Machado, R.C., Pereira-Filho, E.R., Amarasiriwardena, D. (2022). Analytical and reclamation Technologies for identification and recycling of precious materials from waste computer and mobile phones. Chemosphere, 286(2), 131739.

Ari, V. (2015) A review of Technology of Metal Recovery from Electronic Waste. E-Waste Transition-From Pollution ro Resource, 121-157.

Aydin, B. (2011). Recycling of electrical and electronic equipment waste, Master's Thesis, Institute of Science and Technology, Suleyman Demirel University.

Baka, B. (2019). Recovery pf precious metals from electronic waste. Masters's Thesis, Graduate School of Natural and Applied Sciences, Yıldız Technical University, İstanbul.

Birloaga, I., Michelis, I.D., Ferella, F., Buzatu, M., Veglio, F. (2013). Study on the influence of various factors in the hydrometallugical processing of waste printed circuit boards for copper and gold recovery. Waste Management, 33(4), 935-941.

Bourgeois, D., Lacanau, V., Mastretta, R., Contino-Pepin, C., Meyer, D. (2020). A simple process fort he recovery of Palladium from wastes of printes circuit boards. Hydrometallurgy, 191, 105241.

Buchert, M., Manhart A., Bleher, D., Pingel, D. 2012. Recycling Critical Raw Materials from Waste Electronic Equipment. Öko-Institut eV, Freiburg.

Cao, R., Xiao, S. (2005). Recovery of gold, palladium and silver fromwaste mobile phone, Precious Metals. 26, 13–15,

Chakraborty, S.C., Quamruzzaman, M., Zaman, M.W.U., Alam, M., Hossain D., Pramanik, B.K., Nguyen, L.N., Nghiem, L.D., Ahmed, M.F., Zhou, J.L., Mondal, I.H., Hossain, M.A., Johir, M.A.H., Ahmed, M.B., Sithi, J.A., Zargar, M., Moni, M.A. (2022a). Metals in e-waste: Occurrence, fate, impacts and remediation Technologies. Process Safety and Environmental Protection, 162, 230-252.

Chakraborty, S.C., Zaman, M.W.U., Hoque, M., Qamruzzaman, M., Zaman, J.U., Hossain, D., Pramanik, B.K., Nguyen, L.N., Nghiem, L.D., Mofijur, M.

(2022b). Metals extraction processes from electronic waste: constraints and opportunities. Environmental Science and Pollution Research, 29, 32651-32669.

Cui, J., Zhang, L. (2008). Metallurgical recovery of metals from electronic waste: A review. Journal of Hazardous Materials, 158, 228-256.

Diaz, L.A., Lister, T.E., Parkman, J.A., Clark G.G. (2016). Comprehensive process fort he recovery of value and critical materials from electronic waste. Journal of Cleaner Production, 125, 236-244.

Ding, Y., Zhang, S., Liu, Bo, Zheng, H., Chang C., Ekberg, C. (2019). Recovery of precious metals from electronic waste and spent catalysts: A review. Resources, Conservation & Recycling, 141, 284-293.

Duan, H., Hou, K., Li, J., Zhu, X. (2011). Examining the technology acceptance for dismantling of waste printed circuit boards in light of recycling and environmental concerns. Journal of Environmental Management, 92, 392-399.

Forti, V. Balde, C.P., Kuehr, R., Bel, G. (2020). The global e-waste monitor 2020: quantities, flows and the circular economy potential. United Nations University (UNU)/United Nations Institute for Training and Research (UNITAR) – co-hosted SCYCLE Programme, International Telecommunication Union (ITU) & International Solid Waste Association (ISWA), Bonn/Genova/Amsterdam. 3, 1-120.

Ghosh, B., Ghosh, M.K., Parhi, P., Mukherjee, P.S., Mishra, B.K. (2015). Waste printed circuit boards recycling: an extensive assessment of current status. Journal of Cleaner Production, 94, 5-19.

Ghulam, S.T., Abushammala, H. (2023). Challenges and opportunities in the management of electronic waste and its impact on human health and environment. Sustainability, 15 (3), 1837.

Hagelüken, C., Corti, C.W. (2010). Recycling of gold from electronics: cost-effective use through "Design for Recycling".. Gold Bulletin;43, 209–20.

Hagelüken, C., Meskers, C.E.M. (2008). Mining our computers- opportunities and challenges to recover scarce and valuable metals from end-of-life electronic devices. Electronics Goes Green 2008. Fraunhofer IRB Verlag, Berlin, 623-628.

Huang, K., Guo, J., Xu, Z. (2009). Recycling of waste printed circuit boards: A review of current technologies and treatment status in China. Journal of Hazardous Materials, 164(2,3), 399-408.

Ian, H. (2008). Dumping, burning and landfill, Electronic Waste Management, 27, 75-90.

Jiang, P., Harney, M., Song, Y., Chen, B., Chen, B., Chen, Q., Chen, T. Lazarus, G., Lawrence, H.D., Korzenski, M.B. (2012). Improving the end-of-life for electronic materials via sustainable recycling methods. Procedia Environmental Sciences, 16, 485-490.

Kang, H.Y., Schoenung, J.M. (2006). Economic analysis of electronic waste recycling: modeling the cost and revenue of a materials recovery facility in California. Environmental Science & Technology, 40(5), 1672-1680.

Karataş, O. (2018). Recycling of electronic waste and it's effects on human life. Graduate School of Natural and Applied Sciences, Izmır Katıp Celebi University.

Kaya, M. (2016). Recovery of metals from electronic waste by physical and chemical recycling processes. Proceeding Part VII, 18th International Conference on Waste Management, Recycling and Environment (ICWMRE 2016), Barcelona, 939-950.

Kaya, M. (2019). E-waste and e-waste recycling. Electronic Waste and Printed Circuit Board Recycling Technologies. Springer, Cham. 1-32.

Lee, H., Bae, M., Lee, E., Mishra, B. (2019). Copper extraction from flue dust electronic by electrowinning and ion exchange process- Urban mining: characterization and recycling of solid wastes, The Minerals, Metals & Materials Society, 71 (7), 2360-2367.

Lin, P.J., Werner, J., Ali, Z.A., Bertucci, L., Groppo, J. (2023). Kinetic and modeling of counter-burrent leaching of waste random-access memory chips in a Cu-NH_3-SO_4 system utilizing Cu(II) as an oxidizer. Materials, 16(8), 6274.

Lixandru, A., Venkatesan, P., Jinsson, C., Poenaru, I., Hall, B., Yang, Y., Gutfleisch, O. (2017). Identification and recovery of rare-earth permanent magnets from waste electrical and electronical equipment. Waste Management, 68, 482-489.

Murali, A., Zhang, Z.L., Shine, A.E., Free, M.L., Sarswat, P.K. (2022). E-wasted derived sustainable Cu recovery using solvent extraction and electrowinning followed by thiosulfate-based gold and silver extraction. Journal of Hazardous Materials Advances, 8, 100196.

Ning, S., Xie, R., Zeng, L., Tang, K. (2023). Process Safety and Environmental Protection, 178, 595-604.

Ottoni, M., Dias, P., Xavier L.H. (2020). A circular approach to the e-waste valorization through urban mining in Rio de Janerio, Brazil. Journal of Cleaner Production, 261, 120990.

Photharin, Y., Wangngae, Ngivprom, U., Chansaenpak, K., Kamkaew, A., Lai, R.Y. (2022). Extract od cassava waste as a lixiviant for gold leaching from electronic waste. Green Chemistry Letters and Reviews, 15(2), 437-448.

Rautela, R., Arya, S., Vishwakarma, S., Lee, J., Kim, K.H., Kumar, S. (2021). E-waste management and its effects on the environmental and human health. Science of the Total Environment, 773, 145623.

Regel-Rosocka, M. (2018). Electronic wastes. De Gruyter Physical Sciences Reviews, 20180020.

Sayman, R.Ü. (2016). T.R. Ministry of Environment and Urbanization, Waste

Electrical and Electronic Equipment Control Regulation, Municipality Implementation Guide- REC Türkiye.

Shagun, Kush, A., Arora, A. (2013). Proposed solution of e-waste management. International Journal of Future Computer and Communication, 2(5), 490-493.

Shi, W., Hu, Y., Lan, T., Zhang, X., Cao, J. (2021). Recovery of Pd(II) in chloride solutions by solvent extraction with new vinyl sulfide ploymer extractamts. Hydrometallurgy, 204, 105716.

Thakur, P., Kumar, S. (2023). Exploring bioleaching potential of indigenous Bacillus sporothermodurans ISO1 for metals recovery from PCBs through sequential leaching process. Waste Management & Research, 41 (7), 1255-1266.

Torres, R., Lapidus, G.T. (2016). Copper leaching from electronic waste fort he improvement of gold recycling. Waste Management, 57, 131-139.

Tuncer, E., (2014). The Selection of The Best Management Technology to Recycle Precious Metals from Electric and Electronic Equipment, Master's Thesis, ITU Department of Environmental Engineering Environmental Sciences and Engineering Programme, Istanbul.

Tuncuk, A., Stazi, V., Akcil, A., Yazici, E.Y., Deveci, H. (2012). Aqueous metal recovery techniques from e-scarp: Hydrometallurgy in recycling. Mineral Engineering, 25, 28-37.

Wang, J., Chen, C. (2006). Biosorption of metals by Saccharomyces cerevisiae: A review. Biotechnology Advances, 24, 427-451.

Wu, J. Selectively leaching gold fromwaste printed circuit boards with thiourea, Donghua University, Shanghai, 2008

Veglio, F., Quaresima, R., Fornari, P., Ubaldini, S. (2003) Recivery of valuable metals from electronic and galvanic industrial wastes by leaching and electrowinning. Waste Management, 23, 245-252.

Yamane, L.H., de Moraes, V.T., Espinosa, D.C.R., Tenorio, J.A.S. (2011). Recycling of WEEE: characterization of spent printed circuit boards from mobile phones and computers. Waste Management, 31, 2553-2558.

Yazici, E.Y., Deveci, H., Akcil, A. (2009) Recovery from recycling: e-wastes, Recycling Industry, 26, 59-62.

Yazici, E.Y. (2012). Recovery of Metals from Electronic Wastes by Physical and Hydrometallurgical Methods, Master's Thesis, KTÜ Institute of Science and Technology

Zhang, Z., Zhang, F.S., Selective recovery of Palladium from waste printed circuit boards by a novel non-acid process. Journal of Hazardous Materials, 279, 46-51.

Zhou, Y., Qui, K. (2010). A new technology for recycling materials from waste printed circuit boards. Journal of Hazardous Materials, 175, 823-828.

CHAPTER 10

SOLAR RADIATION MODELS BASED ON CLOUDINESS

Mine Tulin ZATEROGLU[1]

1 Dr., Cukurova University, Vocational School of AOSB Technical Sciences, Department of Electrical and Energy, Adana, Turkiye; mtzateroglu@cu.edu.tr; ORCID ID: 0000-0002-1050-6174

Introduction

In recent years, all humanity has been facing the effects of climate change. Today's climate change is entirely caused by the consumption of fossil fuels. Struggles are being made to reduce the effects of climate change and solutions are being produced. To overcome this problem, it is recommended to use renewable energy sources instead of fossil fuel consumption. Solar energy is one of the renewable energy sources and this basic energy source is clean and needed for life on Earth.

Solar radiation is a significant element in the phenomenon of climate change in terms of agriculture and hydrological cycle. In order to determine the climate change's economic effect, causes, and driving factors, it is mainly significant to analyze the variations in solar radiation and specify its related factors. In present century, the major contributors to climate change are the increases in greenhouse gases originated from anthropogenic emissions in atmosphere. The main source of anthropogenic emissions is the consumption of fossil fuels used in power plants, transportation, industrial processess, electricity, heating. These activities cause an increase in greenhouse gases emissions. By using renewable energy sources, a reduction in greenhouse gases can be obtained in mitigation of climate change.

Solar radiation which is the main energy source for our planet's life is an essential factor in the climate system by affecting environmental, ecological and climatological structures. The incoming solar radiation has impacts on various mechanisms such as photosynthesis of plants, carbon uptake, agriculture, surface temperature change, especially hydrological cycle (Liepert et al., 2004; Budyko, 1969; Obryk et al., 2018).

Earth's climate is influenced by variations in concentrations of aerosols and anthropogenic emissions (Fiore et al., 2012; Arneth et al., 2009; Ramanathan and Feng, 2009;). The impact of variations in emissions on aerosols and their related climatological effects are uncertain (Chalmers et al., 2012; Penner et al., 2010). Atmospheric aerosols may lead to variations in radiative balance of Earth, visibility of atmosphere, air pollution and acid deposition, As a result of the interaction between aerosol and climate, aerosols reflect and absorb the solar radiation which flows to the Earth and also affect the clouds' optical properties (Lohmann and Feichter, 2005). Because of their large spatiotemporal changeability, clouds lead to highly uncertainties when interpreting and estimating the climate system (Eastman and Warren, 2013; Zhai et al., 2015).

Earth's energy balance and incoming solar radiation are associated with human habitat, global warming, hydrological cycle and climate of Earth,

and has a significant effect in human activities and also climate change (Trenbert and Fasullo, 2013; Hoskis and Valdes, 1990). Clouds is attenuated the amount of solar radiation reaching the surface of Earth, however aerosols have also an important role and may be dominant under particular situations (Fountoulakis et al., 2019; Neher et al., 2019).

Clouds cover the Earth's surface and are the planet's most influential protection againist solar beams (Boucher et al., 2013). Cloudiness (or cloud cover) and cloud types have contributions on changes in solar radiation. The effect of clouds on solar radiation over their radiative impacts is important in Earth's energy balance. In addition, this impact changes regionally. The changes in cloudiness are a significant act in variations of solar radiation (Long et al., 2009; Pfeifroth et al., 2018). Clouds affect the hydrological cycle and Earth's radiation balance (Södergren et al., 2018; Radley et al., 2014; Walker et al., 2018). In addition, some researchers examined the variations in solar radiation under cloudy and cloud-free conditions (Liepert, 1997; Kazadzis et al., 2018; Ohmura, 2009; Antuna-Marrero et al., 2019; Kumari and Goswami, 2010)

The cause of decadal variations of solar radiation is mainly based on atmospheric transparency for ages. The driving factors of atmospheric transparency are mainly variations in cloud characteristics such as cloud optical properties and cloudiness, and additionally aerosols' optical properties and concentrations, the amount of air pollutants in the atmospheric environment. The largest contributors to the decrease in surface solar radiation are an increment in cloud optical depth and the transition from cloudless sky to cloudy sky (Liepert and Tegen, 2002). Aerosols come from anthropogenic and natural emissions in the atmosphere while some of them are producted by its precursors ,such as nitrogen oxides, sulphur dioxides etc., which undergo interactions with other atmospheric elements. Clouds and atmospheric aerosols affect solar radiation both independently of each other but both factors go interaction with each other (Myhre et al., 2013; Ramanathan et al., 2001). In particular, as a result of this interaction, the lifetime of aerosol particle in atmosphere is influenced by a cloud, while similarly the lifetime and optical property of a cloud may vary due to aerosols. Furthermore, aerosols behave like cloud condensation nuclei and could change the albedo, lifetime, heigth and amount of clouds (Wang et al., 2018; Christensen et al., 2020; Liu et al., 2018; Adebiyi and Zuidema, 2018; (Twomey et al 1984; Andreae et al 2004, Perlwitz and Miller 2010; Ma et al., 2009).

Furthermore, atmospheric elements such as atmospheric aerosols, air pollutants and climate variables interact each other in atmospheric environment (Bose and Roy Chowdhury, 2023; Haddad and Vizakos, 2021; Zateroglu, 2021a-d, 2022, 2023a-d). Atmospheric aerosols are an impor-

tant factor in changing of solar radiation e.g. especially decreasing effect (Che et al., 2005; Liang and Xia, 2005; Li et al., 2018; Shi et al., 2008; Zhang et al., 2013). They influence the atmosphere's radiative transmissivity (Myhre et al., 2013; Ramanathan et al., 2001). Additionally, several studies have shown that clouds have influences on surface solar radiation and sunshine duration (Yang et al., 2013; Xia, 2010; Wang et al., 2011). Some researchers examined quantitively the impacts of cloudiness for different cloud types on variations of surface solar radiation and sunshine duration (Xia, 2010; Wang et al., 2011). Some cloud types such as low cloud cover cause a variability in sunshine duration (Xia, 2010). Further, the decreasing in cloud types cirrostratus and cirrus contributed to the increasing in surface solar radiation (Wang et al., 2011). Low and high clouds have different effects on solar radiation. Thick clouds, that is low, reflect the solar radiation that comes to Earth, and cause the Earth's surface becomes cool. But, thin clouds, that is high, transmit the solar radiation which comes from space to Earth and catch the long-wave (infrared) radiation that Earth emits, then radiate this radiation back and so Earth's surface warms. Furthermore, convective cloud types due to their forcings of albedo and greenhouse, do not cause the warming or cooling of Earth's surface.

In some studies, both aerosol and clouds have effects on surface solar radiation and the combined impacts are investigated. For instance, a decrement in cloudiness and mostly aerosol optical depth cause an increment in surface solar radiation (Li et al., 2018). The interactions between aerosols and clouds and also cloud properties' changes are dominant driving factors in surface solar radiation changes (Tang et al., 2017). According to another study, the reduction in air pollution such as anthropogenic emissions, and clouds are the major causes of the variations in surface solar radiation (Wang et al., 2013).

The data of solar radiation is crucial in a given location to define the solar energy potential needed for many applications e.g. industrial activities, production of electricity, cooling and heating purposes. The value of solar radiation is measured at ground-based meteorological stations of Turkish State Meteorological Service. But it can be also obtained as satellite data from different satellite products.

In some conditions, such as when data is absence or unavailable or inaccessible, or measurements cannot be made in remote areas where the station is not available, the data of solar radiation is estimated by using various constructed models. Some methods such as artificial neural networks, random forest, and other machine learning methods have been used to estimate solar radiation data by several researchers (Jiang, 2008; Leirvik and Yuan, 2021; Zhou, 2017; Sun et al., 2016).

Methods

Kasten-Czeplak Model

This model was developed by Kasten and Czeplak in 1980 has only one input parameter, cloudiness. By this model, global solar radiation data is estimated using cloudiness data for cloud-free and cloudy skies as shown below;

$$I_{gc} = A.sin\alpha_s - B \tag{1}$$

$$I_g = I_{gc}\left(1 - C\left(\frac{N}{8}\right)^D\right) \tag{2}$$

where I_g and I_{gc} determine the horizontal global radiation (in W/m^2) for cloudy sky and cloud-free sky respectively. N shows the hourly cloud cover (in octas). Also, the letters A, B, C, D denote the coefficients of regression depend on the regional data. In this model, I_g / I_{gc} is not depend on the angle of solar altitude.

Kasten and Czeplak in 1980 utilized hourly data and arranged the original formula for Hamburg as follows;

$$I_{gc} = 910sin\alpha_s - 30 \tag{3}$$

$$I_g = I_{gc}\left(1 - 0.75\left(\frac{N}{8}\right)^{3.4}\right) \tag{4}$$

Similar to Hamburg formula of Kasten and Czeplak, some researchers operated the Kasten-Czeplak model by replacing their regional appropirate coefficients to the general formula, as shown in Equation 1-2, in many territories (Paulescu and Schlett 2004).

Furthermore, in onother research, a modification has made in Kasten-Czeplak model and introduced as three built models (Younes and Muneer, 2007) which are expressed in Equations 5-7;

$$I_g = I_{gc}\left[a_0 + a_1\left(\frac{N}{8}\right) + a_2\left(\frac{N}{8}\right)^2\right]^{b_0} \tag{5}$$

$$I_g = I_{gc}\left[a_0 + a_1\left(\frac{N}{8}\right) + a_2\left(\frac{N}{8}\right)^2\right]^{\left(b_0 + b_1\left(\frac{N}{8}\right)\right)} \tag{6}$$

$$I_g = I_{gc}\left[a_0 + a_1\left(\frac{N}{8}\right) + a_2\left(\frac{N}{8}\right)^2\right]^{\left(b_0 + b_1\left(\frac{N}{8}\right) + b_2\left(\frac{N}{8}\right)^2\right)} \quad (7)$$

where a_0, a_1, a_2, and b_0, b_1, b_2 determine the regression coefficients which are appropirate for studied region.

In addition, to improve the Kasten-Czeplak formula, Badescu (2002) added the zenith angle parameter which was not involved. Modified model that has the new contributor is shown in Equation 8;

$$I_g = I_{gc}\left(\alpha + \beta\left(\frac{N}{8}\right)^{\gamma}\right) x\, cos^{\varepsilon-1}\theta_z \quad (8)$$

where the parameters α, β, γ, and ε expresses the regression coefficients provided by using regional data to modified formula.

In order to obtain another formula by improving general form of Kasten-Czeplak model, Badescu and Dumitrescu (2014) developed Equations 9-11 shown below;

$$I_g = I_{gc}\left[1 - \alpha\left(\frac{N}{8}\right)^{\gamma}\right] + I_{go}\beta\left(\frac{N}{8}\right)^{\varepsilon} \quad (9)$$

$$I_g = I_{gc}\left[1 - \alpha\left(\frac{N}{8}\right)^{\gamma}\right] + I_{go}\left(\frac{N}{8}\right)^{\varepsilon} \quad (10)$$

$$I_g = I_{gc}\left[1 - \alpha\left(\frac{N}{8}\right)^{\gamma}\right] + I_{go}\beta\left(\frac{N}{8}\right)^{\varepsilon \cos \alpha_s \varphi} \quad (11)$$

In the new constructed formulas, the coeeficients were obtained according to the localized data that utilized in the related study.

Paltridge-Proctor Model

The Paltridge-Proctor model was constructed to predict solar radiation by using the parameters loud factor, daylength and angle of solar zenith (Paltridge and Proctor, 1976). The study used the daily and hourly solar radiation data to build the equations for diffuse radiation (I_d) and beam radiation (I_b) in different locations of Australia. These expressions were indicated in Equations 12-14;

$$I_b = 3.2248\left(1 - exp\left(-0.075(90 - \theta_z)\right)\right) \quad (12)$$

$$I_d = 0.00913 + 0.0125(90 - \theta_z) + 0.723CF \quad (13)$$

$$CF = \frac{n_1 + 4.5n_2 + 7.5n_3}{(n_1 + n_2 + n_3)} \quad (14)$$

where the parameters respectively n_1, n_2, and n_3 denote the day's number in any month in Oktas; CF determines the cloud factor (between 0-1); θ_z shows the angle of solar zenith.

In this model, horizontal daily total global solar radiation for monthly mean is calculated different locations of Australia by using Equation 15;

$$H = (1 - CF). \int_{sunrise}^{sunset} I_b(\theta_z) \cos\theta_z \, dt + \int_{sunrise}^{sunset} I_b(\theta_z) \cos\theta_z \, dt \quad (15)$$

Furthermore, in another research, an application for Paltridge-Proctor Model was analyzed by Daneshyar (1978). In the rearranged model, the hourly diffuse radiation was estimated for Tehran, Iran as shown in Equation 16;

$$I_d = 0.00515 + 0.00758(90 - \theta_z) + 0.43677CF \quad (16)$$

Moreover, a new model was presented by Sabziparvar (2008) instead of original Paltridge-Proctor model. In this model, the original model was modified by adding two parameters called as the altitude variable and the sun-earth distance variable. The relationship after the modification of original model was used to estimate the daily global solar radiation and shown in Equation 17;

$$H = 1.01K_{ES}(1 - CF)K_{ADR} \int_{sunrise}^{sunset} I_b(\theta_z) \cos\theta_z \, dt + K_{ADF} \int_{sunrise}^{sunset} I_b(\theta_z) \cos\theta_z \, dt \quad (17)$$

where K_{ADF} expressess the diffuse radiation; K_{ADR} indicates the radiation of direct beam; K_{ES} defines the sun-earth distance variable. These factors are calculated by Equations 18-20 as indicated below;

$$K_{ES} = \left(1 + 0.033 \times \cos\left(\frac{2\pi(n - 0.5)}{365}\right)\right) \quad (18)$$

$$K_{ADR} = \left(1 + 0.07\left(h - h_{ref}\right)\right) \quad (19)$$

$$K_{ADF} = \left(1 + 0.1\left(h - h_{ref}\right)\right) \quad (20)$$

In these equations, the parameter h_{ref} shows the reference value of height and the parameter h defines the height of sea-level (in km) for a given location.

Zhang-Huang Model

The Zhang-Huang model has been constructed by regarding some meteorological variables (Zhang and Huang, 2002). Wind speed, temperature, cloudiness and relative humidity have been included in the model to estimate hourly global solar radiation. The relationship was indicated in Equation (21) and built by using Beijing and Guangzhou dataset.

$$I_g = \left(I_{sc} \sin \alpha_s \left(a_0 + a_1\left(\frac{N}{10}\right) + a_2\left(\frac{N}{10}\right)^2 + a_3(T_n - T_{n-3}) + a_4.RH + a_5.V + d\right)\right)/k \quad (21)$$

Where T_n is the temperature at hour n and T_{n-3} is the temperatures at hour n-3; N denotes the cloudiness (between 0-10); the parameters k, d, a_0, a_1, a_2, a_3, a_4, a_5 define the coefficients of regression; V is the wind speed; RH is the relative humidity.

The present Zhang-Huang model was rearranged by Zhang et al. by removing wind speed from the model because of its weak impact on solar radiation (Zhang et al. 2003). The modified formula was indicated in Equation (22) as shown below;

$$I_g = \left(I_{sc} \sin \alpha_s \left(a_0 + a_1\left(\frac{N}{10}\right) + a_2\left(\frac{N}{10}\right)^2 + a_3(T_n - T_{n-3}) + a_4.RH + d\right)\right)/k \quad (22)$$

Zhang et al. (2003) obtained the coefficients of the modified model by using the dataset belong to various regions in China.

Lam Li Model

This model includes solar altitude parameter and is built by researchers Lam and Li, in estimating hourly global solar radiation data (Lam and Li, 1998). The relationships are indicated in Equations 23-24;

$$I_g = A_0 - B_0\left(\frac{N}{8}\right) + C_0 \sin \alpha_s \quad (23)$$

$$I_g = 217 - 485\left(\frac{N}{8}\right) + 696 \sin \alpha_s \quad (24)$$

where the parameter α_s denotes the angle of solar altitude. The coefficients A_0, B_0, and C_0 are generated by using regional hourly cloudiness and solar radiation dataset for Hong Kong.

Similarly, in another study, Lam-Li model was operated by Younes and Muneer (2007) for Aldergrove data in United Kingdom and constructed the new Lam-Li model shown in Equation 25;

$$I_g = 210.7 - 346.3\left(\frac{N}{8}\right) + 630.5 \sin \alpha_s \quad (25)$$

In this equation, regression coefficient were obtained for Aldergrove dataset.

Nielsen Model

The Nielsen model is formed by Nielsen et al. in Copenhagen (Nielsen et al., 1981). In this model, the measurements of cloudiness, solar radiation and the angle of solar altitude belong to Højbakkegård dataset have been utilized to build the relationship shown in Equation 26;

$$I_g = a_0 + a_1 \sin \alpha_s + a_2 sin^3 \alpha_s \quad (26)$$

where the element α_s determines the angle of solar altitude (in rad); the values of coefficients a_0, a_1, a_2 differ according to measurement value of cloudiness (in oktas).

Ehnberg and Bollen (2005) taken into account the different cloudiness situations in predicting solar radiaiton and then improved the Nielsen model (2005). The modified formula is expressed in Equation 27;

$$I_g = \frac{a_0(N) + a_1(N) sin\alpha_s + a_2(N) sin^3\alpha_s - a_3(N)}{a_4(N)} \quad (27)$$

In this new Nielsen model, two parameters are involved into the model to consider the atmospheric condition (Ehnberg and Bollen, 2005).

Conclusion

Availability of solar radiation data is essential in many applications on Earth. The measurement value of this parameter is obtained from not only ground based meterological stations but also satellite products. In the absence of data, various models such as regression based models, machine learning methods are used to estimate the value of data. Firstly, Angstrom-Prescott formula has been operated to predict the solar radiation data by using sunshine duration data. Then this model has been modified by many researchers to provide high accuracy. Furthermore, new alternative relationships have been developed by using other climate variables. One of the cliamte variables is cloudiness which has a key role in Earth' climate. Angstrom-Prescott formula was modified by using cloudiness parameter instead of sunshine duration by some researchers. Then, new models such as Kasten-Czeplak, Zhang-Huang, Paltridge-Proctor, Nielsen and Lam Li were developed by researhers. Finally, the solar radiation models with cloudiness may be a good approach in predicting solar

radiation when there is no data of sunshine duration which provides best results.

References

Adebiyi, A.A., Zuidema, P. (2018). Low cloud cover sensitivity to biomass-burning aerosols and meteorology over the Southeast Atlantic. J. Clim., 31, 4329–4346.

Andreae, M.O., Rosenfeld, D., Artaxo, P., Costa, A.A., Frank, G.P., Longo, K.M., Silva-Dias, M.A.F. (2004). Smoking rain clouds over the Amazo.n Science, 303, 1337–1342.

Antuna-Marrero, J. C., Garcia, F., Estevan, R., Barja, B., Sanchez-Lorenzo, A. (2019). Simultaneous dimming and brightening under all and clear sky at Camagüey, Cuba (1981–2010). Journal of Atmospheric and Solar-Terrestrial Physics, 190, e2020GL092216. 45–53. https:// doi.org/10.1016/j.jastp.2019.05.004

Arneth, A., Unger, N., Kulmala, M., Andreae, M. O. (2009). Clean the Air, Heat the Planet?, Science, 326, 672–673, doi:10.1126/science.1181568

Badescu, V. (2002). A new kind of cloudy sky model to compute instantaneous values of diffuse and global solar irradiance. Theoretical and Applied Climatology 72 (1–2), 127–36. doi:10.1007/s007040200017

Badescu, V., Dumitrescu, A. (2014). New types of simple non-linear models to compute solar global irradiance from cloud cover amount. Journal of Atmospheric and Solar-Terrestrial Physics, 117, 54–70. Elsevier. doi:10.1016/j.jastp.2014.05.010.

Bose, A., Roy Chowdhury, I. (2023). Investigating the association between air pollutants' concent-ration and meteorological parameters in a rapidly growing urban center of West Bengal, India: a statistical modeling-based approach. Model. Earth Syst. Environ. https://doi.org/10.1007/s40808-022-01670-6

Boucher, O., Randall, D., Artaxo, P., Bretherton, C., Feingold, G., Forster, P., et al. (2013). Clouds and aerosols. In Climate change 2013: The physical science basis. Contribution of working group I to the fifth assessment report of the intergovernmental panel on climate change (pp. 571–657). Cambridge University Press.

Budyko, M.I. (1969). The effect of solar radiation variations on the climate of the Earth. Tellus, 21(5), 611–619, doi:10.3402/tellusa.v21i5.10109.

Chalmers, N., Highwood, E. J., Hawkins, E., Sutton, R., Wilcox, L. J. (2012). Aerosol contribution to the rapid warming of near-term climate under RCP 2.6, Geophys. Res. Lett., 39, 2–7, doi:10.1029/2012GL052848

Che, H.Z., Shi, G.Y., Zhang, X.Y., Arimoto, R., Zhao, J.Q., Xu, L., Wang, B., Chen, Z.H. (2005). Analysis of 40 years of solar radiation data from China, 1961–2000. Geophys. Res. Lett., 32, L06803, doi:10.1029/2004gl022322.

Christensen, M.W., Jones, W.K., Stier, P. (2020). Aerosols enhance cloud lifetime and brightness along the stratus-to-cumulus transition. Proc. Natl Acad. Sci. USA 117, 17591–8.

Daneshyar, M. (1978). Solar radiation statistics for Iran. Solar Energy 21 (4):345–49. doi:10.1016/0038-092X(78)90013-0

Eastman, R., Warren, S.G. (2013). A 39-year survey of cloud changes from land stations worldwide 1971–2009: long-termtrends, relation to aerosols, and expansion of the tropical belt. J. Clim., 26, 1286–1303.

Ehnberg, J.S.G., Bollen, M.H.J. (2005). Simulation of global solar radiation based on cloud observations. Solar Energy 78 (2):157–62. doi:10.1016/j.solener.2004.08.016

Fiore, A. M., Naik, V., Spracklen, D. V., Steiner, A., Unger, N., Prather, M., Bergmann, D., Cameron-Smith, P. J., Cionni, I., Collins, W. J., Dalsø ren, S., Eyring, V., Folberth, G. a., Ginoux, P., Horowitz, L. W., Josse, B., Lamarque, J.-F., MacKenzie, I. a., Nagashima, T., O'Connor, F. M., Righi, M., Rumbold, S. T., Shindell, D. T., Skeie, R. B., Sudo, K., Szopa, S., Takemura, T., Zeng, G. (2012). Global air quality and climate., Chem. Soc. Rev., 41, 6663–83, doi:10.1039/c2cs35095e

Fountoulakis, I., Kosmopoulos, P., Papachristopoulou, K., Raptis, I.-P., Mamouri, R.-E., Nisantzi, A., Gkikas, A., Witthuhn, J., Bley, S., Moustaka, A., Buehl, J., Seifert, P., Hadjimitsis, D.G., Kontoes, C., Kazadzis, S. (2021). Effects of Aerosols and Clouds on the Levels of Surface Solar Radiation and Solar Energy in Cyprus. Remote Sensing, 13(12), 2319.

Haddad, K., Vizakos, N. (2021). Air Quality pollutants and their relationship with meteorological variables in four suburbs of Greater Sydney, Australia. Air Quality, Atmosphere & Health, 14, 55-67.

Hoskins, B.J., Valdes, P.J. (1990). On the existence of storm-tracks. J. Atmos. Sci., 47, 1854–1864, https://doi.org/10.1175/1520- 0469(1990)0472.0.CO;2.

Jiang, Y. (2008). Prediction of monthly mean daily diffuse solar radiation using artificial neural networks and comparison with other empirical models. Energy Policy, 36 (10), 3833–3837, doi:10.1016/J.ENPOL.2008.06.030.

Kasten, F., Czeplak, G. (1980). Solar and terrestrial radiation dependent on the amount and type of cloud. Solar Energy 24 (2), 177–189. doi:10.1016/0038-092X(80)90391-6.

Kazadzis, S., Founda, D., Psiloglou, B.E., Kambezidis, H., Mihalopoulos, N., Sanchez-Lorenzo, A., Meleti, C., Raptis, P.I., Pierros, F., Nabat, P. (2018). Long-term series and trends in surface solar radiation in Athens, Greece. Atmos. Chem. Phys., 18, 2395–2411.

Kumari, B.P., Goswami, B.N. (2010). Seminal role of clouds on solar dimming over the Indian monsoon region. Geophysical Research Letters, 37, L06703. https://doi.org/10.1029/2009GL042133

Lam, J.C., Li, D.H.W. (1998). Correlation analysis of solar radiation and cloud cover. International Journal of Ambient Energy 19 (4):187–98. doi:10.1080/01430750.1998.9675305.

Leirvik, T., Yuan, M. (2021). A Machine Learning Technique for Spatial Interpolation of Solar Radiation Observations. Earth and Space Science, 8 (4), doi:10.1029/2020EA001527

Li, J., Jiang, Y.W., Xia, X.G., Hu, Y.Y. (2018). Increase of surface solar irradiance across East China related to changes in aerosol properties during the past decade. Environ. Res. Lett., 13, 34006.

Liang, F., Xia, X.A. (2005). Long-term trends in solar radiation and the associated climatic factors over China for 1961–2000. Ann. Geophys. Ger., 23, 2425–2432.

Liepert, B.G. (1997). Recent changes in solar radiation under cloudy conditions in Germany. International Journal of Climatology, 17(14), 1581–1593.

Liepert, B.G., Feichter, J., Lohmann, U., Roeckner, E. (2004). Can aerosols spin down the water cycle in a warmer and moister world? Geophysical Research Letters, 31(6), doi:10.1029/2003gl019060,

Liepert, B., Tegen, I. (2002), Multidecadal solar radiation trends in the United States and Germany and direct tropospheric aerosol forcing, J. Geophys. Res., 107(D12), 4153, doi:10.1029/2001JD000760.

Liu, Z., Yim, S.H.L., Wang, C., Lau, N.C. (2018). The impact of the aerosol direct radiative forcing on deep convection and air quality in the Pearl River Delta region. Geophysical Research Letters, 45, 4410–4418. https://doi.org/10.1029/2018GL077517

Lohmann, U., Feichter, J. (2005). Global indirect aerosol effects: A review. Atmos. Chem. Phys., 5, 715–737.

Long, C., Dutton, E. G., Augustine, J. A., Wiscombe, W., Wild, M., McFarlane, S. A., Flynn, C. J. (2009). Significant decadal brightening of downwelling shortwave in the continental United States. Journal of Geophysical Research, 114(D10), D00D06. https://doi.org/10.1029/2008jd011263

Ma, Y., Gong, W., Zhu, Z., Zhang, L., Li, P. (2009). Cloud amount and aerosol characteristic research in the atmosphere over Hubei province, China 2009 IEEE Int. Geoscience and Remote Sensing Symp. pp III-631–4

Myhre, G., Lund, C., Samset, B., Storelvmo, T. (2013). Aerosols and their relation to global climate and climate sensitivity. Nature Education Knowledge, 4(5), 7.

Nielsen, L.B., Prahm L.P., Berkowicz, R., Conradsen, K.. (1981). Net incoming radiation estimated from hourly global radiation and/or cloud observations. Journal of Climatology 1 (3):255–72. doi:10.1002/ joc.3370010305.

Neher, I., Buchmann, T., Crewell, S., Pospichal, B., Meilinger, S. (2019). Impact of atmospheric aerosols on solar power. Meteorol. Z., 28, 305–321.

Obryk, M.K., Fountain, A.G., Doran, P.T., Lyons, W.B., Eastman, R. (2018). Drivers of solar radiation variability in the McMurdo Dry Valleys, Antarctica. Scientific Reports, 8 (1), 5002, doi:10.1038/s41598-018-23390-7

Ohmura, A. (2009). Observed decadal variations in surface solar radiation and their causes. Journal of Geophysical Research, 114, D00D05. https://doi. org/10.1029/2008JD011290

Paltridge, G.W., Proctor, D. (1976). Monthly mean solar radiation statistics for Australia. Solar Energy 18 (3):235–43. doi:10.1016/0038- 092X(76)90022-0.

Paulescu, M., Schlett, Z. (2004). Performance assessment of global solar irradiation models under Romanian climate. Renewable Energy 29 (5):767–77. doi:10.1016/j.renene.2003.09.011.

Perlwitz, J., Miller, R.L. (2010). Cloud cover increase with increasing aerosol absorptivity: a counterexample to the conventional semidirect aerosol effect. J. Geophys. Res., 115, 8203.

Pfeifroth, U., Sanchez-Lorenzo, A., Manara, V., Trentmann, J., Hollmann, R. (2018). Trends and variability of surface solar radiation in Europe based on surface-and satellite-based data records. Journal of Geophysical Research: Atmospheres, 123(3), 1735–1754. https://doi. org/10.1002/2017jd027418

Penner, J. E., Prather, M. J., Isaksen, I. S. a., Fuglestvedt, J. S., Klimont, Z., Stevenson, D. S. (2010). Short-lived uncertainty?, Nat. Geosci., 3, 587–588, doi:10.1038/ngeo932

Radley, C., Fueglistaler, S., Donner, L. (2014). Cloud and radiative balance changes in response to ENSO in observations and models. J. Clim., 27, 3100–3113. DOI: 10.1175/JCLI-D-13-00338.1

Ramanathan, V., Crutzen, P., Kiehl, J., Rosenfeld, D. (2001). Aerosols, climate, and the hydrological cycle. Science, 294(5549), 2119–2124. https://doi. org/10.1126/science.1064034

Ramanathan, V., Feng, Y. (2009). Air pollution, greenhouse gases and climate change: Global and regional perspectives, Atmos. Environ., 43, 37–50, doi:10.1016/j.atmosenv.2008.09.063

Sabziparvar, A.A. (2008). A simple formula for estimating global solar radiation in central arid deserts of Iran. Renewable Energy 33(5),1002–10. doi:10.1016/j.renene.2007.06.015.

Shi, G.Y., Hayasaka, T., Ohmura, A., Chen, Z.H., Wang, B., Zhao, J.Q., Che, H.Z., Xu, L. (2008). Data quality assessment and the longterm trend of ground solar radiation in China. J. Appl. Meteorol. Clim., 47, 1006–1016.

Södergren, A.H., McDonald, A.J., Bodeker, G.E. (2018). An energy balance model exploration of the impacts of interactions between surface albedo, cloud cover and water vapor on polar amplification. Clim. Dyn. 51, 1639–1658.

Sun, H., Gui, D., Yan, B., Liu, Y., Liao, W., Zhu, Y., Lu, C., Zhao, N. (2016). Assessing the potential of random forest method for estimating solar radiation using air pollution index. Energy Conversion and Management, 119, 121 – 129, https://doi.org/10.1016/j.enconman.2016.04.051

Tang, W.J., Yang, K., Qin, J., Niu, X.L., Lin, C.G., Jing, X.W. (2017). A revisit to

decadal change of aerosol optical depth and its impact on global radiation over China. Atmos. Environ., 150, 106–115.

Trenberth, K.E., Fasullo, J.T. (2013). Regional energy and water cycles: Transports from ocean to land. J. Climate, 26, 7837–7851, https://doi.org/10.1175/JCLI-D-13-00008.1.

Twomey, S.A., Piepgrass, M., Wolfe, T.L. (1984). An assessment of the impact of pollution on global cloud albedo. Tellus B, 36, 356–366.

Walker T.W.N., Kaiser C., Strasser, F., Herbold, C.W., Leblans, N.I.W., Woebken D, Janssens I A, Sigurdsson, B.D., Richter, A. (2018). Microbial temperature sensitivity and biomass change explain soil carbon loss with warming. Nature Climate Change, 8, 885–889.

Wang, C.H., Zhang, Z.F., Tian, W.S. (2011). Factors affecting the surface radiation trends over China between 1960 and 2000. Atmos. Environ., 45, 2379–2385.

Wang, L, Henderson, M., Liu, B., Shen, X., Chen, X., Lian, L., Zhou, D. (2018). Maximum and minimum soil surface temperature trends over China, 1965–2014. J. Geophys. Res., 123, 2004–2016.

Wang, Y.W., Yang, Y.H., Han, S.M., Wang, Q.X., Zhang, J.H. (2013). Sunshine dimming and brightening in Chinese cities (1955-2011) was driven by air pollution rather than clouds. Clim. Res., 56, 11–20.

Xia, X.G. Spatiotemporal changes in sunshine duration and cloud amount as well as their relationship in China during 1954– 2005. J. Geophys. Res. Atmos. 2010, 115, D00K06, doi:10.1029/2009jd012879.

Yang, S., Shi, G.Y., Wang, B., Yang, H.L., Duan, Y.X. (2013). Trends in Surface Solar Radiation (SSR) and the Effect of Clouds on SSR during 1961–2009 in China. Chin. J. Atmos. Sci., 37, 963–970.

Younes, S., Muneer, T. (2007). Comparison between solar radiation models based on cloud information. International Journal of Sustainable Energy 26 (3):121–47. doi:10.1080/14786450701549824

Zateroglu, M.T. (2021a). Assessment of the effects of air pollution parameters on sunshine duration in six cities in Turkey. Fresenius Environmental Bulletin, 30(02A), 2251-2269.

Zateroglu, M.T. (2021b). The Role of Climate Factors on Air Pollutants (PM10 and SO2). Fresenius Environmental Bulletin, 30(11), 12029-12036.

Zateroglu, M.T. (2021c). Evaluating the Sunshine Duration Characteristics in Association with Other Climate Variables. European Journal of Science and Technology, 29, 200-207, https://doi.org/10.31590/ejosat.1022639.

Zateroglu, M.T. (2021d). Statistical Models For Sunshine Duration Related To Precipitation and Relative Humidity. European Journal of Science and Technology, 29, 208-213. https://doi.org/10. 31590/ejosat.1022962.

Zateroglu, M.T. (2022). Modelling The Air Quality Index For Bolu, Turkey. Car-

pathian Journal of Earth and Environmental Sciences, 17(1), 119– 130. https://doi.org/10.26471/cjees/2022/017/206.

Zateroglu, M.T. (2023a). Comparative Analysis for Atmospheric Oscillations. Çukurova Üniversitesi Mühendislik Fakültesi Dergisi, 38(2), 317-331. https://doi.org/10.21605/cukurovaumfd.1333702

Zateroglu, M.T. (2023b). Estimating the Sunshine Duration Using Multiple Linear Regression in Kocaeli, Turkey. IDOJÁRÁS, 127(3), 285–298. DOI:10.28974/idojaras.2023.3.2

Zateroglu, M.T. (2023c). The Influence of Climatological Variables on Particulate Matter and Sulphur Dioxide. Çukurova Üniversitesi Mühendislik Fakültesi Dergisi, 38(1), 13-24. Doi: 10.21605/cukurovaumfd.1273675

Zateroglu, M.T. (2023d). Estimation of Cloudiness Data Based on Multiple Linear Regression Model. Karadeniz Fen Bilimleri Dergisi, 13(1), 33-41. Doi: 10.31466/kfbd. 1150879.

Zhang, Q.Y., Huang, Y.J. (2002). Development of typical year weather files for Chinese locations. ASHRAE Transaction 108(2).

Zhang, Q., Joe, H., Yang, H., Lou, C. (2003). Development of models to estimate solar radiation for Chinese locations. Journal of Asian Architecture and Building Engineering, 2(2), b35–b41. doi:10.3130/ jaabe.2.b35.

Zhang, H., Yin, Q., Nakajima, T., Makiko, N.M., Lu, P., He, J. (2013). Influence of changes in solar radiation on changes of surface temperature in China. Acta Meteorol. Sin., 27, 87–97.

Zhai, C., Jiang, J.H., Su, H. (2015). Long-term cloud change imprinted in seasonal cloud variation: more evidence of high climate sensitivity. Geophys. Res. Lett., 42, 8729–8737.

Zhou, Q., Flores, A., Glenn, N.F., Walters, R., Han, B. (2017). A machine learning approach to estimation of downward solar radiation from satellite-derived data products: An application over a semi-arid ecosystem in the us. PloS one, 12 (8), e0180 239, doi:10.1371/journal.pone.0180239.

CHAPTER 11

POWER CONVERTERS FOR RENEWABLE ENERGY APPLICATIONS

Tuba ÖZDEMİR ÖGE[1], Firdevs Banu ÖZDEMİR[2], Mecit ÖGE[3]

1 Assoc. Prof. Dr., Bartın University, Bartın University, Faculty of Forestry, Department of Forestry Industry Engineering, Bartin, Turkey. E-mail: tozdemir@bartin.edu.tr, ORCID ID, 0000-0001-6690-7199.
2 Inst. Dr., Kütahya Health Sciences University, Simav Vocational School of Health Sciences, Department of Medical Services and Techniques, Kütahya, Turkey; E-mail: firdevsbanu.ozdemir@ksbu.edu.tr, ORCID ID, 0000-0002-7935-2062.
3 Asst. Prof. Dr., Bartın University, Faculty of Engineering, Architecture and Design, Department of Mechanical Engineering, Bartın, Turkey; E-mail: mecitoge@bartin.edu.tr, ORCID ID, 0000-0001-5243-0828.

1. Introduction

By the ever-increasing energy demand with particular emphasis on clean energy, renewable energy sources have become an indispensable means for energy generation. The term "renewable energy" relates to a sustainable or non-depleting energy source such as the solar energy, wind energy, geothermal energy, etc. The term "alternative energy" is also commonly used to refer to renewable energy sources (Algarni et al., 2023), as it stands for an alternative to conventional energy sources such as hydrocarbon based (fossil) fuels which are known to be more costly or hazardous to environment (Li & Haneklaus, 2022). On the other hand, the use of fossil fuels in energy generation has led to serious environmental considerations due to the increasing impact of green-house effect on the global temperature rise and the resulting climate change (Solomon et al., 2022). Such environmental considerations coupled with the depleting nature of conventional energy sources rendered the use of non-depleting and clean renewable energy sources an important subject both in the industry and academic field, thus increasing number of studies have been published on the efficient use of these energy sources in various fields. The main renewable energy sources are solar energy, wind energy, hydroelectric electric plants, geothermal energy, biomass plants, energy harnessing from oceans and tides, all of which are somehow related with solar energy except for geothermal energy. The energy radiated from the sun in the form of electromagnetic waves amounts to 120.000 TW from its surface which has a perpetual temperature of nearly 5800°K due to the fusion reactions ("Operation and Control of Renewable Energy Systems," 2017). However, the current technology in harnessing this enormous energy potential cannot compete with the energy harnessed from burning the hydrocarbon-based fossil fuels, for which a vast amount of know-how and technology have been developed for more than a century. In this regard, the main issue in harnessing solar power has been the regulation of the electrical energy converted from solar energy to provide non-intermittent DC power for the electrical devices and machines. Wind energy has been harnessed and converted into other types of energy such as electricity by use of wind turbines which vary in size, shape and working principle. They vary in size from small size turbines that suffice to satisfy domestic power needs to wind farms which are composed of large-sized turbines. The common characteristic of renewable energy sources (whether solar power or wind power or other alternative energy sources) is the intermittent nature of the DC voltage level harnessed from these sources (Pavan Kumar et al., 2022). Thus, the main issue in the efficient delivery of renewable energy sources is tackling this intermittent nature of these energy sources through various converter topologies and control techniques by use of power electronics

and electromechanics devices such as DC-DC converters since most of the electrical devices require a continuous or stable voltage level. In addition to tackling the intermittent nature of renewable energy sources which are intrinsically delivered by direct current (DC), most of the modern low, medium, and high DC voltage electric devices are comprised of various circuits and components that are operated by different voltage levels, hence the necessity for conversion of different DC voltage levels between different components. In this regard, a "DC-DC converter", also known as a "voltage regulator" is used to alter the voltage level of a DC source, which is often termed as either stepping up or stepping down. As implied by the name, DC converters are only used for conversion purposes between DC sources, and they are not applicable for alternate current (AC) sources. This study thus aims to provide a general insight into power electronic converters and the semiconductor devices used in converters.

2. Semiconductors Used in Power Converter Devices

2.1 Diode

Semiconductor devices are regarded as controlled or uncontrolled switches. A p-n diode is a two-terminal semiconductor device, based on the principle of p-n junction theory, in which current can flow in single direction which is from anode to cathode. Diodes used as semiconductor devices have several uses such as rectifying the AC to DC as well as detection of radio signals and light. P-N junction principle involves the doping of semiconductors with materials after which the semiconductor has surplus electrons which can be easily removed, and these are known as n-type (negative) region. On the other hand, semiconductors can be also doped with materials that result in a surplus of holes which can readily host electrons and these regions are referred to as p-type (positive) regions. The negative and positive regions of a semiconductor diode can be referred to as cathode and anode of the diode, respectively. In a perfect or ideal diode, the current is allowed to flow in only one direction, whereas in practice, there is always a small amount of current that is allowed to flow in the reverse direction. Figure 1 shows the p-n junction representation, circuit symbol and real appearance of a power diode.

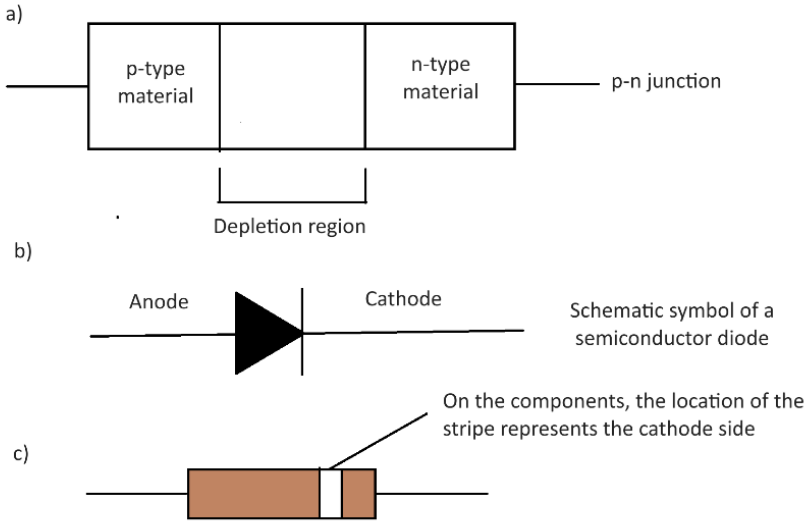

Figure 1. a) *p-n junction representation,* **b)** *schematic appearance and* **c)** *real-life component appearance of a semiconductor p-n junction diode (Diode Operation - Energy Education)*

For a diode, forward bias stands for the condition in which the p-type region of the semiconductor is subjected to positive voltage and the n-type region of the material is subjected to negative voltage. However, the current applied on the diode must overcome a voltage barrier (0.3 V for germanium, and 0.7 V for silicon) to start to flow (Sugii et al., 2005). Inversely, the n-type region of the semiconductor is subjected to a positive voltage and the p-type region of the semiconductor is subjected to a negative voltage in a reverse bias condition.

2.2 Thyristor

A thyristor is a three-terminal device composed of four alternating p and n type p-n junction material layers (PNPN). These power electronic components are used to optimize the closed or open switch conditions for controlling the flow of the power in a circuit (Bryant et al., 2011). This component is usually made of three electrodes, anode, cathode and the gate which is referred to as the control electrode of the component. Thyristor circuits are designed to be able to deliver large currents and to be capable of withstanding large applied voltages (Rashid, 2010). Figure 2 shows the schematic representation and the circuit symbol of a thyristor.

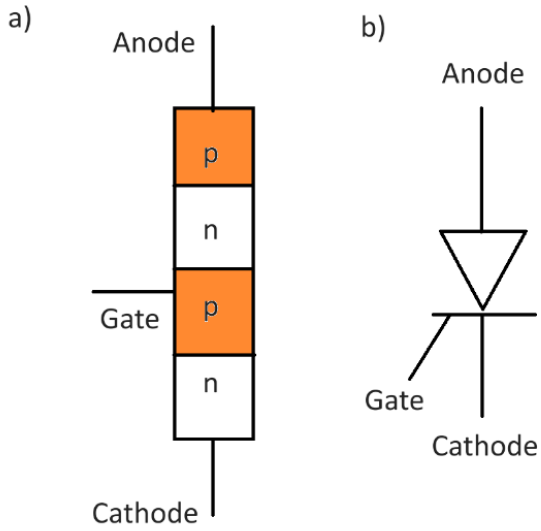

Figure 2. a) *Schematic representation, and* **b)** *circuit symbol of a thyristor.*

Thyristors are categorized as silicon-controlled rectifiers (SCRs), MOS-controlled thyristors (MCTs), gate turn-off thyristors (GTOs), and static induction thyristors (SITh). SCRs are the most common type of thyristors on which no current is present unless the gate is subjected to a pulse when the anode is positively charged as compared to the cathode. In the case of gate turn-off thyristors (GTO), AC is used to turn on and turn off the component via sending a signal to the control gate. Operating states of thyristors are forward conducting, as the primary operating mode; forward blocking in which the current flow is blocked; and reverse blocking mode in which the current passes across the thyristor in opposite direction (What Is a Thyristor and How Does It Work?).

2.3 Power Transistors

The disadvantages of GTOs such as low switching speeds and the requirement of large reverse current flow for turning the component off are addressed by use of power transistors which can be turned on by application of a signal on the base terminal and the on-state is maintained until the control signal is removed. Among all power transistors, bipolar junction transistor (BJT) is the first one to approximate a power switch which is fully controlled. Power transistors can be categorized as bipolar junction transistors (BJTs), insulated-gate bipolar transistors (IGBTs) and metal-oxide-semiconductor field-effect transistors (MOSFETS).

2.3.1 BJT

Transistors are regarded as the building block of power electronics, and they are generally available in two types: Bipolar Junction Transistors (BJTs) and field effect transistors (FETs). As three-terminal semiconductor devices, bipolar junction transistors consist of three distinct semiconductor material layers resembling a sandwich form which is either in P-N-P or N-P-N sequence. The circuit symbols and schematic representations are shown in Figure 3. This current controlled semiconductor device has three terminals, namely the base, the emitter and the collector (Figure 3).

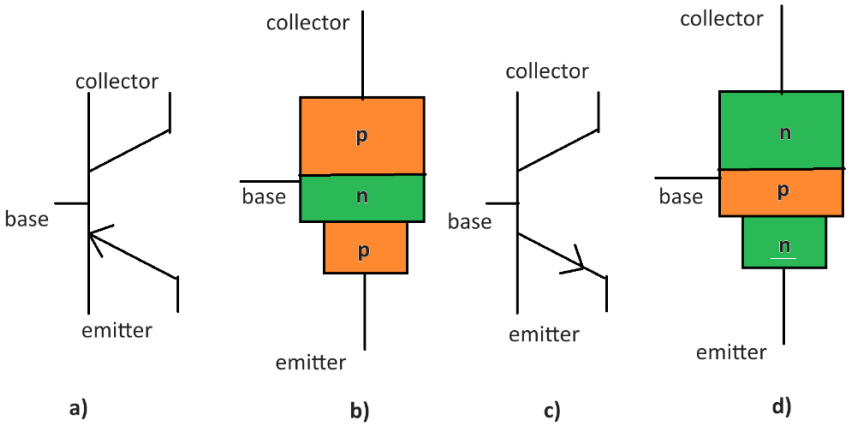

Figure 3. a) *PNP circuit symbol,* **b)** *PNP layout,* **c)** *NPN circuit symbol,* **d)** *NPN layout of BJT*

As opposed to power diodes, BJTs consist of two junctions depending on its forward or reverse bias condition. Based on the state of these junctions on diode models, BJTs can be modeled as in Figure 4. PNP and NPN BJTs differ from each other by the difference in the polarity of the junctions during operation. BJTs are capable to operate in three different regions: namely, the active region, the saturation region and the cut-off region. Also, BJTs are used for switching and amplification purposes. For use as a switch, the BJT is biased such that it works in the cut-off or saturation region, whereas for amplification, it is designed to be biased in the active region (Shur, 2003).

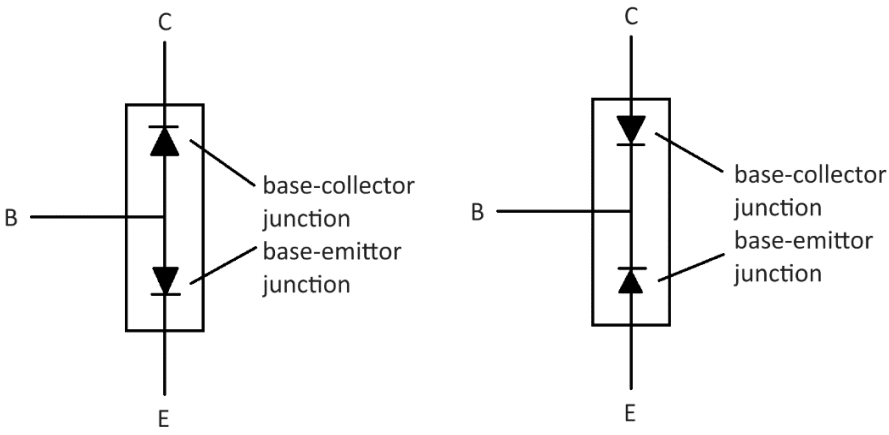

Figure 4. *BJT models relating to diode model based on the junctions.*

2.3.2 MOSFETs

The metal oxide semiconductor field effect transistor (MOSFET) is another three terminal semiconductor device which is also used for switching and amplification of electronic signals. The terminals are referred to as the source, the gate and the drain. It operates on the basis of modification of channel widths through which the charge carriers, electrons and holes, flow. The gate, positioned between the source and the drain, controls the voltage so that the channel width is controlled. The insulation of this electrode (the gate) is ensured by use of an extremely thin metal oxide layer. MOSFETs are categorized as depletion mode MOSFETs (NMOS), and enhancement mode MOSFETs. In the case of depletion mode MOSFETS, an open channel located between the drain and source enables the free charge carriers to flow between these two terminals, in which the carriers are necessarily depleted. When the width of the channel between the source and the drain is reduced, the free carriers are squeezed and forced to flow in the channel. In enhancement mode MOSFETs (E-MOSFET), on the other hand, as the voltage towards the gate cathode is increased, the current flowing from the drain to the source also increases until reaching the maximum level. E-MOSFETs are normally-off-devices, such that, when it is connected, no current flow is available between the drain and the source, hence no voltage in the gate. When the gate terminal is powered, the channel between the drain and source becomes less resistive and as the voltage from the gate to the source is increased, current flow between the drain and the source also increases until the highest current is supplied from the drain to the source. MOSFETS are either N-channel type or P-channel type depending on the substrate material used in the semiconductor. The channel conductivity which relates to the charge carriers depends on the substrate

type used. The circuit diagrams of N-channel and P-channel MOSFETs are shown in Figure 5.

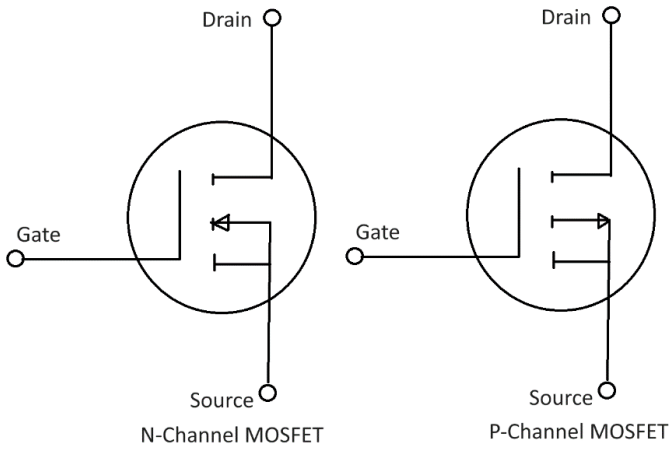

Figure 5. *Schematic representations of N-Channel and P-Channel MOSFETs.*

2.3.3 IGBTs

Insulated gate bipolar transistors (IGBTs) combine the low high switching capabilities of MOSFETs and low conduction losses of BJTs. They are also available as N-channel type and P-channel type. It is a combination of the insulated gate technology of the MOSFET and the output capabilities of the BJT. In power electronics, IGBTs are used in applications such as converters, inverters and power supplies. They provide higher power gain than BJTs and lower input losses than MOSFETs. They have three terminals, also referred to as collector, emitter and gate. Collector and emitter are related to the conductance path whereas the gate is responsible for controlling the device. IGBTs are mostly applied in high-power applications such as electric vehicle motor drives, solar inverters, inductive ovens, UPS (uninterruptible power supplies), etc. The schematic representation of an IGBT is shown in Figure 6.

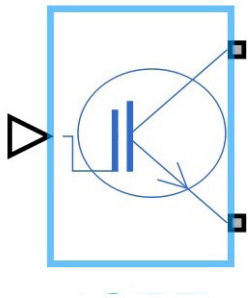

Figure 6. *Schematic representation of an IGBT in ideal switching mode (MATLAB/Simulink representation).*

3. Power Converters

In renewable power generation, electronic converters are used to maintain the desired voltage and frequency levels specific to the subject application or system. In almost all systems powered from renewable sources, the power is stored in batteries which requires power electronic devices for control and regulation purposes. Power electronics is thus essential for delivery of the produced power with the maximum cost-efficiency. Power electronic converters can be categorized as DC-DC converters, DC-AC converters, AC-DC converters and AC-AC converters. AC-AC converters are not addressed in this work since their application related to renewable energy is limited.

3.1 DC-AC Converters (Inverters)

DC-AC converters, widely known as inverters, are used to convert the voltage level of a DC source such as a battery or a fuel cell into an alternating current (AC) output, which is generally a grid load. Therefore, they are essential for conversion purposes in various practical applications where the frequency, amplitude and phase of the output voltage also need to be controlled. Their application area includes various battery systems, variable speed drives and photovoltaic (PV) systems (DC-to-AC Converters (Inverters): Design, Working & Applications). Inverters are categorized as voltage source inverters (VSI) and current source inverters (CSI). They differ from each other by the applied output control methods, input characteristics and compatibility of the load. Conversion of DC to AC voltage is more complicated than AC-DC conversion as this process requires the use of an oscillator to reverse the direction of the current at a specific frequency, which is achieved by use of other circuit components (Difference Between Inverters VSI Vs CSI). In renewable energy generation applications, inverters are required to transform the dc power generated by an alternative energy source such as PV systems or fuel cells into AC power

for direct use either in a grid or an isolated system.

3.2 AC-DC Converters

AC-DC converters, also known as rectifiers, are used to transform alternating current (AC) to variable direct current (DC) output voltage after which a filter is applied to gain unregulated DC voltage through optimization by use of a filter. The main application areas of AC-DC converters, or rectifiers, are electrical consumer devices such as household appliances since almost all non-battery-operated household electronics are run by DC power and supplied by AC power, process control systems used in several industries, defense applications, medical equipment and so on.

3.3 DC-DC Converters for Renewable Energy Applications

DC-DC converters are used to modify the voltage level of a DC source such as a fuel cell, solar panel or a battery. DC-DC converters can be either of non-isolated or isolated type. Their main difference is the use of a transformer or a capacitor in isolated types for separation, whereas no separation is applied, and common ground is used for non-isolated DC-DC converters. Due to their simplicity and cost-efficiency, non-isolated DC-DC converters have found a wider usage for applications where considerations such as voltage inversion or isolation is not a pre-requisite. The operating principle of a DC-DC converter is shown in Figure 7 (What Is a DC-DC Converter ? – X-Engineer.Org).

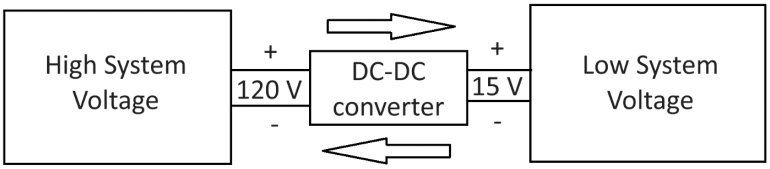

Figure 7. *Operating principle of a DC-DC converter*

Among the other renewable energy generation applications, most of the studies on efficient harnessing of renewable energy sources focuses on the use of power control systems used in solar PV applications. The presence of a suitable DC-DC converter is required to enhance the system efficiency. A DC microgrid can be regarded as a separate system from the main grid which is generally supplied by renewable energy sources such as solar or wind energy to power electronic devices operated by DC, hence the name DC-DC conversion. DC microgrids have crucial importance in providing the users with energy in remote areas such as islands, forests,

hills, etc., as well as in many agricultural applications. Such a micro-scale grid also requires the use of an energy storage system, which is in most cases a hybrid system, bringing about the necessity for application of Energy Management Methods since reduction and optimization of power disturbances and fluctuations is essential for DC powered devices. A vast number of converters have been designed for an efficient and high voltage gain of solar photovoltaic applications. A general classification of DC-DC converters is shown in Figure 8 (Jagadeesh & Indragandhi, 2022).

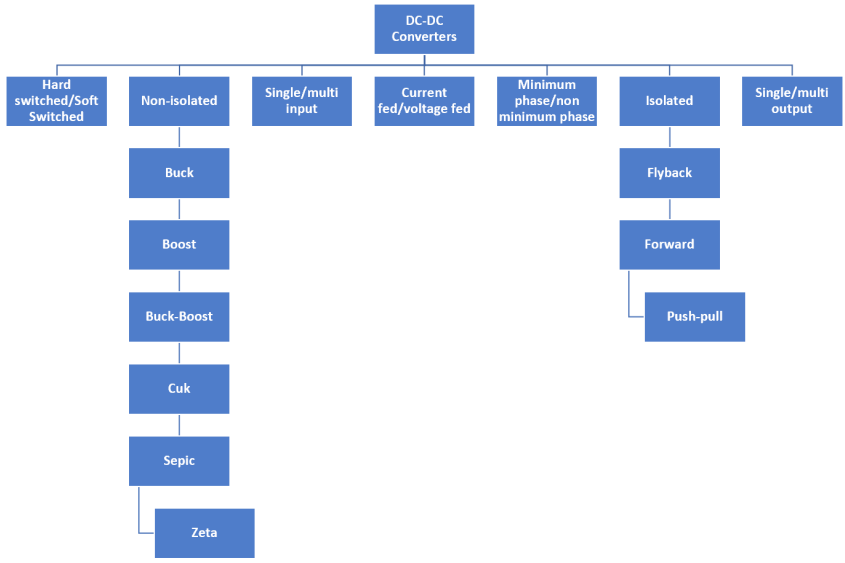

Figure 8. *DC-DC converter types*

Non-isolated type DC-DC converters have been commonly applied in renewable energy applications due to the suitability of their topology for use in standalone and microgrid applications. Among these, DC-DC buck converters steps down the output voltage to a lower level than the input voltage level. DC-DC buck converters have been applied in a variety of solar PV applications including water supply applications in remote areas, MPPT (maximum power point tracking), solar battery chargers as well as off-grid PV systems (Kummara et al., 2019). Some PV applications require a higher voltage level on the load side than the input voltage and in such cases a boost converter is applied which steps up the output voltage level to a higher level than the input voltage level. Boost converters are under the classification of switched-mode power supply equipped with two semiconductors at minimum, namely an inductor and a capacitor. DC-DC

buck-boost converter topology combines the capabilities of buck and boost converters, and they are used in various applications such as standalone and grid-connected PV systems in addition to drive systems. As a result of the efforts to improve the voltage gain of DC-DC converters, various other buck-boost-topology based non-isolated converters have been developed including Cuk and SEPIC converters (Mumtaz et al., 2021).

3.4 AC-AC Converters

AC to AC converters transform an AC voltage level to another AC voltage level. They are categorized as cycloconverters, hybrid matrix converters, matrix converters, AC Voltage controllers and indirect AC-AC converters. They have several applications in motor control and adjustable speed drives, dimming lamps, or heat control and etc.

4. Conclusion

Beside the depletion of conventional energy sources such as fossil fuels, the increasing demand for clean and non-depleting energy sources and ongoing research on these renewable energy sources have prompted the researchers to conduct research on efficient integration and delivery of these power sources into the grid, micro-grid and standalone applications. In line with such efforts, various DC-DC power conversion topologies and strategies have been investigated with an ever-increasing pace. In this regard, the current study aims to provide a general insight into the types of converters used in renewable energy applications and basic information related to the power electronic components used in these semiconductor devices.

References

Algarni, S., Tirth, V., Alqahtani, T., Alshehery, S., & Kshirsagar, P. (2023). Contribution of renewable energy sources to the environmental impacts and economic benefits for sustainable development. *Sustainable Energy Technologies and Assessments*, *56*, 103098. https://doi.org/10.1016/J.SETA.2023.103098

Bryant, A., Santi, E., Hudgins, J., & Palmer, P. (2011). Thyristors. *Power Electronics Handbook: Devices, Circuits,and Applications,Third Edition*, 91–116. https://doi.org/10.1016/B978-0-12-382036-5.00006-9

DC-to-AC Converters (Inverters): Design, Working & Applications. (n.d.). Retrieved October 16, 2023, from https://how2electronics.com/dc-to-ac-converters-inverters-design-working-applications/

Difference Between Inverters VSI Vs CSI. (n.d.). Retrieved October 16, 2023, from https://quick-learn.in/difference-between-inverters-vsi-vs-csi/

Diode operation- Energy Education. (n.d.). Retrieved October 16, 2023, from https://energyeducation.ca/encyclopedia/Diode_operation

Jagadeesh, I., & Indragandhi, V. (2022). Comparative Study of DC-DC Converters for Solar PV with Microgrid Applications. *Energies 2022, Vol. 15, Page 7569*, *15*(20), 7569. https://doi.org/10.3390/EN15207569

Kummara, V. G. R., Zeb, K., Muthusamy, A., Krishna, T. N. V., Prabhudeva Kumar, S. V. S. V., Kim, D. H., Kim, M. S., Cho, H. G., & Kim, H. J. (2019). A Comprehensive Review of DC–DC Converter Topologies and Modulation Strategies with Recent Advances in Solar Photovoltaic Systems. *Electronics 2020, Vol. 9, Page 31*, *9*(1), 31. https://doi.org/10.3390/ELECTRONICS9010031

Li, B., & Haneklaus, N. (2022). The role of clean energy, fossil fuel consumption and trade openness for carbon neutrality in China. *Energy Reports*, *8*, 1090–1098. https://doi.org/10.1016/J.EGYR.2022.02.092

Mumtaz, F., Zaihar Yahaya, N., Tanzim Meraj, S., Singh, B., Kannan, R., & Ibrahim, O. (2021). Review on non-isolated DC-DC converters and their control techniques for renewable energy applications. *Ain Shams Engineering Journal*, *12*(4), 3747–3763. https://doi.org/10.1016/J.ASEJ.2021.03.022

Operation and Control of Renewable Energy Systems. (2017). *Operation and Control of Renewable Energy Systems*. https://doi.org/10.1002/9781119281733

Pavan Kumar, T. V. V., Nabi Mughal, S., Gautamkumar Deshmukh, R., Gopa Kumar, S., Kumar, Y., & Stalin David, D. (2022). A highly consistent and proficient class of multiport dc-dc converter based sustainable energy sources. *Materials Today: Proceedings*, *56*, 1758–1768. https://doi.org/10.1016/J.MATPR.2021.10.458

Rashid, M. H. (2010). Gate Turn-off Thyristors. In *Power Electronics Handbook: Devices, Circuits, and Applications, Third Edition*. Elsevier. https://doi.

org/10.1016/B978-0-12-382036-5.00007-0

Shur, M. (2003). Bipolar Transistors. *Encyclopedia of Physical Science and Technology*, 273–280. https://doi.org/10.1016/B0-12-227410-5/00070-3

Solomon, C. G., Salas, R. N., Malina, D., Sacks, C. A., Hardin, C. C., Prewitt, E., Lee, T. H., & Rubin, E. J. (2022). Fossil-Fuel Pollution and Climate Change — A New NEJM Group Series. *New England Journal of Medicine*, *386*(24), 2328–2329. https://doi.org/10.1056/NEJME2206300/SUPPL_FILE/NEJME2206300_DISCLOSURES.PDF

Sugii, N., Kimura, Y., Kimura, S., Irieda, S., Morioka, J., & Inada, T. (2005). Strained-silicon MOSFET process technology—control of impurity and germanium atoms at the hetero-interface. *Materials Science in Semiconductor Processing*, *8*(1–3), 89–95. https://doi.org/10.1016/J.MSSP.2004.09.072

What is a DC-DC converter ? – x-engineer.org. (n.d.). Retrieved October 16, 2023, from https://x-engineer.org/dc-dc-converter/

What is a thyristor and how does it work? (n.d.). Retrieved October 16, 2023, from https://www.techtarget.com/whatis/definition/thyristor

CHAPTER 12

A REVIEW OF ALOHA-BASED ANTI-COLLISION PROTOCOLS IN RFID SYSTEMS

Mehmet Erkan YUKSEL[1]

1 Doç. Dr., Department of Computer Engineering, Burdur Mehmet Akif Ersoy University, Burdur, Turkey, e-mail: erkanyuksel@mehmetakif.edu.tr, ORCID: 0000-0001-8976-9964

1. Introduction

In recent years, there has been a remarkable surge in the adoption of automatic identification procedures (Auto-ID) across various service industries, including purchasing, distribution logistics, and industrial manufacturing. The primary objective of Auto-ID systems is to provide immediate, dynamic, and secure insights into the movement of objects. Notably, traditional barcode systems, which were once revolutionary and widely used, are now proving inadequate for an ever-expanding range of applications. While barcodes are cost-effective, they suffer from limitations in memory capacity and the inability to adapt programmatically.

A technically viable alternative involves utilizing silicon chips for data storage. In everyday life, electronic data-carrying devices, such as smartphones and bank cards, predominantly rely on physical contact for data exchange. However, the mechanical contact used in these smart cards can be cumbersome. A more flexible approach emerges with contactless data transmission, where information flows wirelessly between the data transport device and the reader. Ideally, the energy required to power the electronic data transport device should also be wirelessly supplied by the reader through contactless technology. This concept underpins the Radio Frequency Identification (RFID) systems. RFID systems convey an object's identity information in the form of a unique numerical serial number through radio frequencies (Erkan, 2010).

Radio Frequency Identification (RFID) constitutes an automatic identification system comprising both readers and tags. The primary function of an RFID reader is to discern and identify objects by reading the unique identification number (ID) affixed to the RFID tag associated with each object. This operation involves the reader transmitting a signal to the tag, eliciting a response in which the tag transmits its ID. Subsequently, the reader undertakes a query of an external database to establish the association between the transmitted ID and the corresponding object. An RFID reader typically comprises essential components: a radio frequency module housing both transmitting and receiving functions, a control unit, and an integrated antenna element. Notably, many RFID readers are equipped with additional interfaces, such as RS 232 or RS 485, to streamline the transfer of data to various external systems, including personal computers and robot control systems. The RFID tag, serving as the data carrier within the RFID system, typically incorporates an antenna element and an embedded electronic microchip. It is of significance to acknowledge that RFID tags lack their own power supply, operating entirely in a passive state when outside the reader's interrogation range. The necessary power for activating these tags is supplied through the antenna element, rendering them self-sustaining (Erkan, 2010).

Within the broader technological landscape, innovations catalyzed by RFID technology have engendered profound transformations in the products, services, and operational processes offered by business entities and institutions. RFID is rapidly supplanting conventional barcode-based identification systems, principally due to its ability to operate without line-of-sight restrictions, enabling the assignment of unique identifiers to each object. Furthermore, in recent years, contactless recognition has matured into an autonomous interdisciplinary domain, transcending traditional classifications. This dynamic field amalgamates expertise from an array of domains, including low, high, and ultra-high-frequency technologies, electromagnetic compatibility, semiconductor technology, data security and cryptography, telecommunications, manufacturing technology, and various other interrelated disciplines.

The perpetual evolution of data communication and information technologies drives the development of systems and their associated management methodologies. In the contemporary, swiftly changing, and intensely competitive landscape, enterprises and institutions must continually adapt, distinguish themselves, and rejuvenate their products, services, communication strategies, and business methodologies to maximize the efficient use of their time and resources. Therefore, there has always been a demand for businesses and institutions to integrate automatic object identification, data collection, and management technologies into their operations, thereby enhancing their applications and streamlining their business processes. Notably, RFID systems integrated into wireless networks play a pivotal role in fulfilling these innovation-driven demands (Erkan, 2010).

The primary objective of RFID system designs is the real-time retrieval of information without human intervention, thereby enabling the tracking of objects with diverse attributes across expansive geographic areas, free from constraints. This capability extends to the analysis and seamless transmission of object data to the relevant units. The integration of RFID with diverse communication technologies for automatic object identification, object tracking, data management, and analysis systems provides a swifter, more efficient, cost-effective, and high-capacity solution. Therefore, the exploration of RFID's amalgamation with various communication technologies for automatic object identification, object tracking, data management, and analysis systems becomes imperative, as it has the potential to catalyze the emergence of pioneering data communication technologies (Erkan, 2010).

2. RFID (Radio Frequency Identification)

Radio Frequency Identification (RFID) represents an automated technology for object identification, relying on wireless communication

through Radio Frequency (RF). Categorized under the broader Auto-ID (Automatic Identification) technology umbrella, RFID plays a pivotal role in enabling real-time object recognition and tracking, as illustrated in Figure 1. A notable advantage of RFID technology is its capacity to preempt data entry errors (Erkan, 2010; Finkenzeller, 2003).

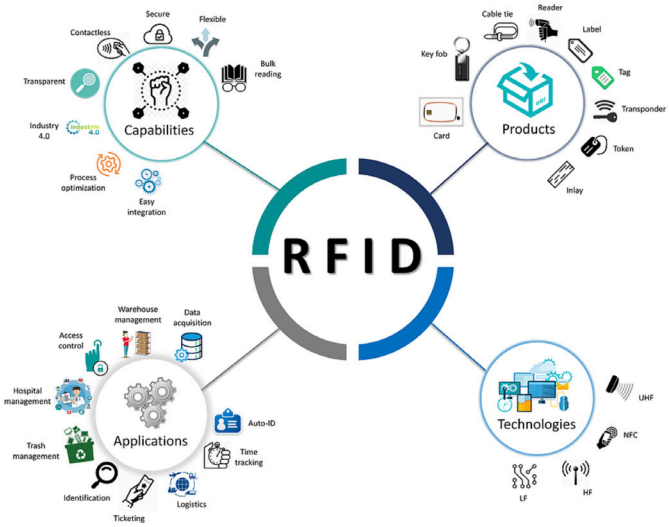

Figure 1. *RFID technology.*

In terms of architectural design, RFID systems closely resemble microchip cards, often referred to as smart cards. Both systems utilize electronic data-carrying devices, commonly known as tags equipped with microprocessors and antennas, analogous to smart card systems. These tags draw power from either an internal battery or signals transmitted by the reader. Importantly, data interchange between tags and readers, as well as among tags themselves transpires without the need for galvanic contact points, instead relying on magnetic/electromagnetic fields and wireless communication via radio frequencies (Erkan, 2010; Finkenzeller, 2003; Ahson & Ilyas, 2008).

RFID systems encompass a range of integral components, including tags available in both active and passive variants, readers that can be either mobile or fixed, controllers often manifested as PCs or servers, and network devices, available in both wired and wireless configurations. The foundation of RFID systems draws from several fields, encompassing electrical electronics (i.e., microprocessor architecture, logic design, and FPGA), communication (i.e., radio, radar, microwave, and antenna technology), and computer engineering. Significantly, RFID systems play a pivotal role in object tracking, data management and analysis, system management, and interface software.

In a basic RFID system, data communication and energy transfer transpire between the reader and the tag, as shown in Figure 2. When the reader emits electromagnetic waves, these waves interact with the tag's antenna, consequently activating the microchip enclosed within the tag. The microchip subsequently modulates the signals it receives and conveys them back to the reader via the tag's antenna (Hunt et al., 2007).

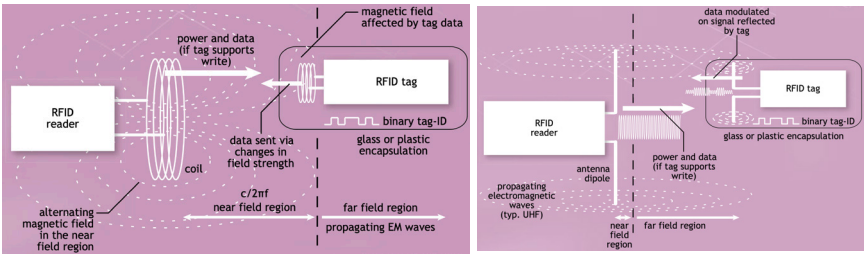

a) *Near field communication* **b)** *Far field communication*

Figure 2. Communication in an RFID system (Want, 2004).

Figure 2 shows the sequence of events involved in the detection of RFID tags within the reader's interrogation area. When a tag necessitating communication enters this designated area, it utilizes RF (Radio Frequency) signals to transmit not only its unique identification code but also any recorded data to the reader. The reader's primary function is to convert these incoming signals into digital data. Subsequently, the data generated on the reader's end is dispatched to the relevant system services via middleware, controllers, queries, servers, and an array of network devices.

RFID systems are effectively categorized into two primary divisions: mobile and fixed applications. Fixed RFID systems encompass a gamut of peripheral components, including RFID antennas, typically requiring two to four antennas per reader. These systems also incorporate a main computer or server, software, lighting, and sensors. They are commonly referred to as RFID portals. Within the context of RFID portals, identity information pertaining to tagged objects passing through the RF field, akin to a door, is captured and subsequently transmitted to the relevant service units, including computers and network systems. In contrast, mobile RFID systems, while constrained in terms of read/write distance and power when juxtaposed with fixed systems, offer substantial advantages in data collection and processing across various locations (Hunt et al., 2007; Glover & Bhatt, 2006).

Through the integration of RFID systems with an array of wireless communication technologies, the capacity for automatic identification and tracking of virtually any object is achieved. Additionally, this integration facilitates the creation, collection, and management of dynamic data associated with these objects. Consequently, it enables the real-time generation of information, thereby resulting in notable enhancements in service quality, distribution, management, data throughput, and security.

2.1. RFID System Components

The establishment and management of RFID systems necessitate a comprehensive array of software and hardware prerequisites. These prerequisites encompass integral components, including active/passive tags, readers, controllers, the selection of suitable frequencies and standards for the RFID system, and the adoption of wired/wireless communication technologies (Figure 3) (Rappaport, 2002). A paramount element in this ecosystem is the middleware, which plays a pivotal role in orchestrating the RFID system.

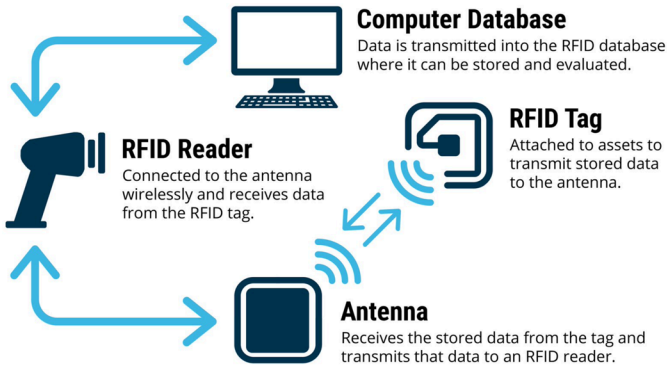

Figure 3. *RFID system components.*

Among the pivotal components within RFID systems, tags stand prominently. These tags represent devices equipped with an antenna and a microchip, classified into two fundamental categories based on their power source—active and passive tags. Additionally, there exist semi-passive tags that amalgamate features from both categories. Complementing the tag, the reader assumes an indispensable role in establishing the connection between the tags and the broader environment. This connection facilitates bidirectional data communication between the reader and the readable/writable tags. All readers incorporate an antenna for signal transmission and reception, with the reader responsible for generating and decoding signals emanating from the tags. Readers are available in two principal vari-

ants: fixed and mobile (portable), both sharing a common set of fundamental components (Glover & Bhatt, 2006; Lahiri, 2005; Kraus & Marhekfa, 2002; Rao et al., 2005).

The efficient operation and management of RFID systems necessitate the employment of specialized middleware. Typically, integrator companies craft middleware tailored to the unique needs of businesses or institutions. To ensure a seamless operation, these software systems must interface seamlessly in real time. This integration facilitates the accessibility of data and reports to company personnel without necessitating the use of distinct software applications for each task. Consequently, the development of robust middleware is imperative to guarantee the secure and expeditious transmission of data to its intended destinations in real-time (Erkan, 2010; Curty et al., 2007; Manish & Shahram, 2005).

3. System Design

The necessity arises to investigate the movements of objects across extensive geographical areas, monitoring object transactions and services, facilitating data management, and sharing detailed object information with other systems. In such contexts, the integration of RFID systems with wireless communication technologies holds promise for developing various alternative systems.

A pivotal aspect of next-generation wireless networks is the quality of wireless communication. The incorporation of RFID into wireless communication systems can enable the automatic collection, monitoring, and management of dynamic data from both stationary and mobile objects, fostering innovations in the wireless industry. This innovation benefits a wide spectrum of stakeholders, including companies, institutions, vendors, customers, service/application/content providers, policymakers, and users (Erkan, 2010).

RFID system designs are centered on achieving real-time information collection, monitoring, and management with minimal human intervention. Consequently, leveraging faster, more efficient, secure, and high-capacity communication technologies is imperative to provide instantaneous access to dynamic object information across vast geographical areas, allowing object tracking and directing object data to relevant units without imposing limitations. This embodies the contemporary requirements. In our study, we seamlessly integrated an RFID system suitable for automatic object identification, tracking, data management, and analysis into Wi-Fi networks. Additionally, we conducted a comprehensive examination of ALOHA-based protocols within this system (Figure 4) (Erkan, 2010).

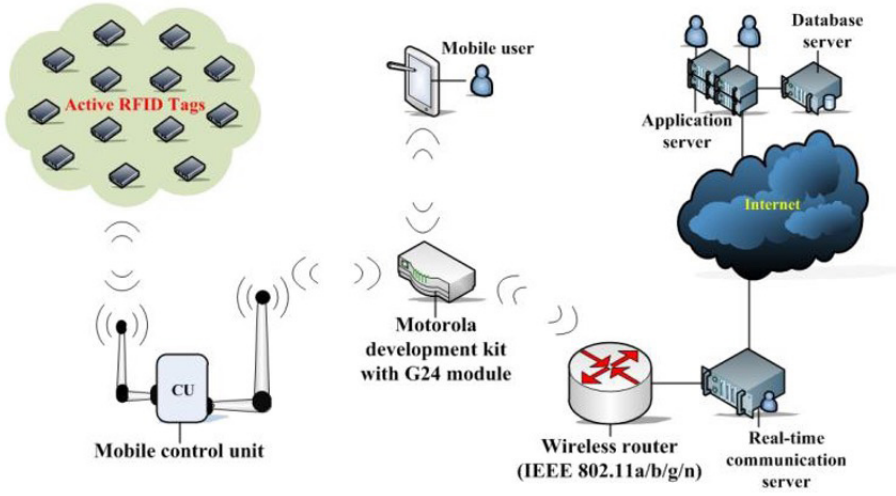

Figure 4. *RFID system architecture.*

An RFID system utilizes multifunctional RFID readers that seamlessly integrate with Wi-Fi standards and encompass mobile communication features (Rappaport, 2002; Gast, 2002; Ross, 2008; Ohrtman & Roeder, 2003). It offers flexibility for configuring diverse network topologies. One approach involves integrating a control unit that complies with Wi-Fi standards and supports mobile applications within Wi-Fi networks. When RFID readers are present, the control unit strategically bridges the gap between the readers and Wi-Fi devices. Conversely, in scenarios without RFID readers, the system exclusively relies on Wi-Fi networks, with control units facilitating communication between RFID tags and Wi-Fi devices. In this setup, control units operate in real-time, ensuring Quality of Service (QoS), and they include RFID reader functionalities while establishing seamless communication with Wi-Fi devices. Significantly, the control unit excels in securely and promptly transmitting tag information obtained from the reader to Wi-Fi networks. The software and hardware requirements for this RFID system can be summarized as follows (Erkan, 2010):

- RFID System components that support Wi-Fi standards
- Wi-Fi Control Units and other Wi-Fi devices (access point, router, etc.)
- Wi-Fi Network Services and services, middleware and software interfaces

3.1. Anti-Collision Protocols in RFID Systems

Wireless communication technologies confront a pervasive challenge: the occurrence of collisions when multiple devices share a common frequency band for data exchange. This predicament is notably conspicuous in RFID systems, a quintessential embodiment of wireless communication. Within the RFID milieu, the cohabitation of readers and tags, both operating within an identical frequency band, begets a dual taxonomy of collisions: reader collisions and tag collisions [40-42]. Reader collisions unfurl their entanglement when proximate readers simultaneously launch inquiries to a tag, leading to the entwining of reader signals and rendering the tag impotent in deciphering any of the incoming signals. In contrast, tag collisions come to pass when multiple tags concurrently transact their "ID" to a reader, culminating in the superposition of tag signals and consequently incapacitating the reader from distinguishing any of the tags (Erkan, 2010; Engels & Sharma, 2002; Waldrop et al., 2003; Zhai, 2005).

The reverberations of these collisions resonate profoundly. In specific scenarios, readers fail to discern the entirety of objects, necessitating the redux of data transmission between the reader and tags to attain successful recognition. Singularly, passive tags with limited functionality are culpable for provoking tag collisions, given their lack of collision detection capabilities and an inability to discern neighboring tags. These tag collisions precipitate the imperative for supplementary communications within the RFID system, precipitating delays in data transmission and hampering overall system efficiency. Consequently, the imperative emerges for the deployment of an efficacious tag collision prevention protocol capable of real-time operation, facilitating the identification of tags amidst the maelstrom of collisions.

The spectrum of tag collision avoidance protocols bifurcates into two cardinal archetypes: probabilistic protocols, rooted in the ALOHA paradigm, and deterministic protocols, premised on the orchestration of random number generation to govern the chronology of data transfer. ALOHA-based protocols attenuate the probability of tag collisions by endowing each tag with the prerogative to endeavor transmission of its ID at randomly selected intervals. However, these protocols remain fallible and engender the conundrum of deferred identification of specific tags over protracted intervals, as encapsulated by the "label clarity problem." In contradistinction, tree-based protocols engender the instantiation of a conceptual binary tree during the labyrinthine journey of tag recognition. These protocols iteratively cleave a set of tags into binary subsets and embark upon the herculean endeavor of recognizing these subsets sequentially. This cyclical process persists until each subset cradles only a solitary tag, thereby enabling the identification of all tags nestled within the reader's

query domain. Although tree-based protocols circumvent tag exposure, they concede to a more prolonged tag recognition latency when juxtaposed with their ALOHA-based counterparts (Erkan, 2010; Cha & Kim, 2006; Zhen et al., 2005).

An effective collision avoidance protocol in an RFID system must possess the following features:

- Swift tag recognition: The RFID reader must promptly and accurately identify all tags within its designated query area, even when tagged objects are in motion. Failure to match the speed of moving objects can lead to a tag clearance problem, resulting in a breakdown of object recognition and tracking. Thus, the collision avoidance protocol's design should prioritize the consistent recognition of all tags.

- Resource-efficient tag recognition: Passive RFID tags operate under strict power constraints, relying on the reader's signal for activation. Additionally, these tags possess limited computational capabilities and minimal memory capacity. Therefore, the collision avoidance protocol should strive for efficient tag recognition, minimizing the demand for additional communication and computational resources.

3.2. ALOHA Protocol

The ALOHA protocol, distinguished by its simplicity, plays a pivotal role as a fundamental multiple access procedure in the domain of radio frequency identification (RFID) systems. At its core, this protocol orchestrates the transmission of data packets from RFID tags to a designated reader. This orchestrated process strictly adheres to the principles of a tag-driven random Time Division Multiple Access (TDMA) procedure. Within the ALOHA paradigm, each RFID tag independently generates a random number, which dictates the duration of its data transmission wait. In the absence of conflicting signals from other tags, the transmitting tag successfully conveys its data. Following this transmission, the tag embarks on the same cycle by generating a fresh random number and diligently adhering to the associated time interval. In instances of collision, precise time intervals are judiciously allocated to facilitate orderly data transfer by the impacted tags. It is imperative to underscore that the deployment of the ALOHA protocol is exclusively reserved for read-only RFID tags, which predominantly handle the transmission of concise data, such as serial numbers. Notably, the duration of data transmission constitutes a minuscule segment of the overall repetition time, allowing for substantial intervals between consecutive transmissions. Furthermore, subtle deviations in repetition times among tags contribute to the mitigation of potential data packet collisions. Data packet collisions can be effectively reduced when two

tags engage in data transmission at distinct time intervals (Erkan, 2010; Zheng & Kaiser, 2016; He & Wang, 2013; Liu & Lai, 2006; Namboodiri et al., 2012).

4. Findings

Figure 5 illustrates the time series of data transmission in an ALOHA-based RFID system. The variable G denotes the number of tags concurrently transmitting at time t. The average presented load is computed as the mean over an observation period. The load (G) of a data packet at transmission time (t) is determined by the following formula:

$$G = \sum_1^n \frac{T_n}{T} . r_n \quad (1)$$

where n is the number of tags in the system and r is the number of data packets transmitted by n tags during the observation period T.

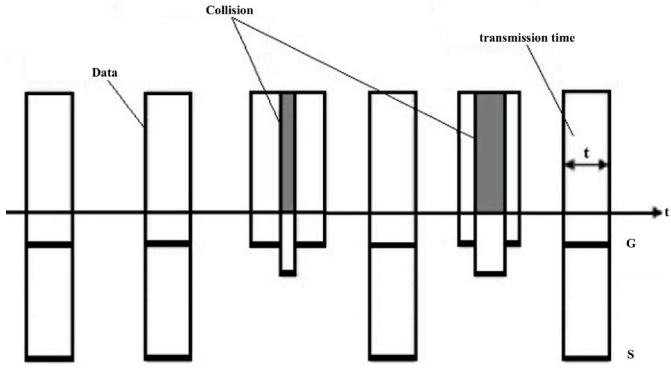

Figure 5. *Work produced (S) and load offered (G) in the ALOHA protocol.*

In the context of error-free data packet transmission, the rate of work executed during the transmission time remains constant at 1. Conversely, in all other scenarios, where data transmission may not have occurred or where data suffered corruption due to collisions, the throughput remains at 0. The average throughput (S) of a transmission channel is calculated in relation to the offered load (G) using the following equation:

$$S = G.e^{(-2G)} \quad (2)$$

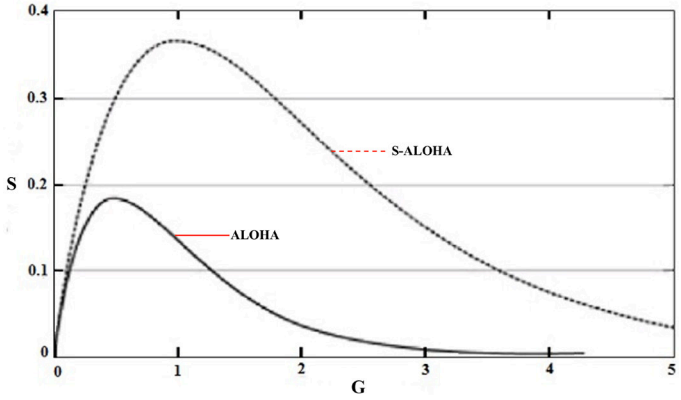

Figure 6. *Comparison of ALOHA and S-ALOHA procedures.*

Figure 6 illustrates the relationship between throughput (S) and the presented load (G). A peak throughput of approximately 18% is observed when G equals 0.5. Lower G values result in a predominantly idle transmission channel, while higher G values lead to a significant increase in tag collisions, leaving over 80% of the channel capacity unused. The ALOHA procedure, despite its simplicity, is well-suited as a collision avoidance technique for read-only tag systems. To calculate the probability of success (q), one can utilize the average offered load (G) and throughput (S):

$$q = \frac{S}{G} \tag{3}$$

Equation 3 provides information on the time required to reliably read all tags in the query area. This time depends on the number of tags in a reader's query area. Figure 7 shows the average time spent reading all tags in the query area in our RFID system using the ALOHA procedure.

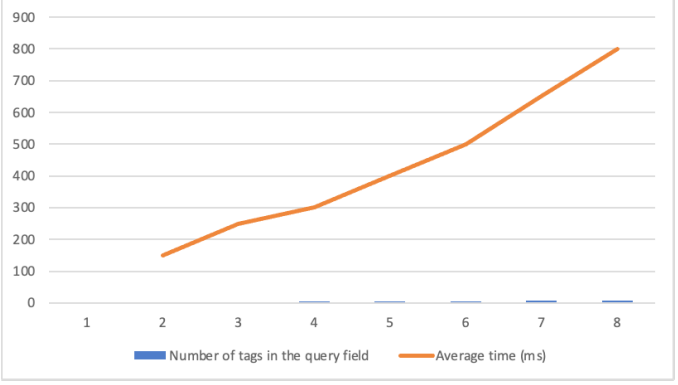

Figure 7. *Tag identification time.*

We can express k error-free data packet transmissions in observation time T with a Poisson distribution with probability $p(k)$. The $p(k)$ value can be calculated from the transmission time of a data packet and the average offered load G as follows:

$$p(k) = \frac{\lambda^{k}}{k!} . e^{k} \tag{4}$$

The average G/t value is found as follows:

$$p(k) = \frac{\left(G\frac{T}{t}\right)^{k}}{k!} . e^{\left(-G\frac{T}{t}\right)} \tag{5}$$

ALOHA protocol can be examined in two different structures: slotted and framed. In Slotted ALOHA, a certain time interval is allocated to each tag and the tag transfers its content within this time interval. In the Framed ALOHA protocol, tags are divided into groups of N tags, and when a group's turn comes, the group elements transfer their contents one by one. How long a tag will wait or how the order or time to be allocated to the tag will be determined determines the success of this method.

- *Slotted ALOHA (S-ALOHA):* It endeavors to alleviate the inherent challenges associated with low throughput and suboptimal performance in the ALOHA protocol. The ALOHA protocol restricts data packet transmission exclusively to synchronized time slots, a process regulated by the reader. In response to these limitations, S-ALOHA was introduced which is a novel TDMA-based collision avoidance protocol. S-ALOHA seamlessly integrates both random and polling routing strategies, offering an enhanced and more reliable approach to data transmission (Erkan, 2010; Liu & Lai, 2006; Namboodiri et al., 2012).

- *Dynamic Slotted ALOHA (DS-ALOHA):* The throughput (S) of the S-ALOHA protocol reaches its maximum efficiency when the offered load (G) is approximately 1. According to this conceptual framework, it is desirable for a reader to possess a number of tags equal to the available slots within its query area. Introducing an excessive number of tags to the system leads to a swift deterioration in throughput. In the most adverse scenario, this renders the reader incapable of detecting any serial numbers, even after numerous attempts, because no tag can exclusively transmit during a single slot. Addressing this issue involves maintaining an adequate number of slots. However, this solution comes at the expense of impairing the performance of the collision avoidance algorithm. The system must continuously maintain a list of potential tags, even in cases where only one

tag resides within the reader's query area. To address these inherent challenges, researchers turn to the dynamic S-ALOHA protocol, which leverages varying slot numbers to optimize system performance(Erkan, 2010; Cha & Kim, 2006).

4.1. Case Study: S-ALOHA

In the S-ALOHA procedure, the collision interval is effectively halved compared to the simple ALOHA procedure. Specifically, in the simple ALOHA procedure, a collision ensues when two tags attempt to transmit data packets within the time interval T < 2t, where 't' denotes the transmission time, assuming uniform data packet sizes. In contrast, the S-ALOHA procedure mandates that data packets commence transmission exclusively at synchronized time points, reducing the collision interval to T = t. This relationship establishes the throughput (S) of the S-ALOHA procedure as follows:

$$S = G.e^{(-G)} \tag{6}$$

The S-ALOHA procedure achieves a maximum work rate (S) of approximately 37%, a fact vividly depicted in Figure 6. It is crucial to emphasize that the incidence of data collisions can be mitigated when multiple data packets are capable of concurrent transmission. Remarkably, tags in closer proximity to the reader have the potential to outperform their counterparts due to the stronger signal strength they emit, a phenomenon commonly referred to as the catch-up effect. This capture effect exerts a significant influence on business behavior, with the pivotal factor being the 'k' threshold, signifying the requisite signal strength differential for a data packet to be reliably detected by the receiver.

$$S = G.e^{(\frac{k.G}{1+k})} \tag{7}$$

To exemplify the practical application of the S-ALOHA procedure, consider our RFID system. In this context, the labels feature unique 8-bit serial numbers, ensuring the distinctiveness of serial numbers among up to 256 tags. To facilitate effective tag control, we have established fundamental commands for synchronization, an indispensable component of RFID systems, in addition to other crucial commands like writing, encryption, and authorization, facilitating seamless interactions between tags and readers. These commands are:

- REQUEST: Synchronizes all tags in the reader's query area. It requests the tags to transmit the tag information to the reader.

- SELECT: The tag serial number is sent as a parameter. The tag with the corresponding serial number is selected to perform read-write

commands. Tags with different serial numbers continue to react to the REQUEST command.

- READ_DATA: The data of the selected tag is read by the reader.

In standby mode, the reader periodically transmits a REQUEST command. Concurrently, the reader introduces five tags into its query area, as depicted in Figure 8. Upon detecting the REQUEST command, each tag employs a random check generator to select one of the three available slots for transmitting its serial number to the reader. In our example, random slot selection leads to collisions between tags in slots 1 and 2, with slot 3 successfully transmitting the serial number of the fifth tag without errors.

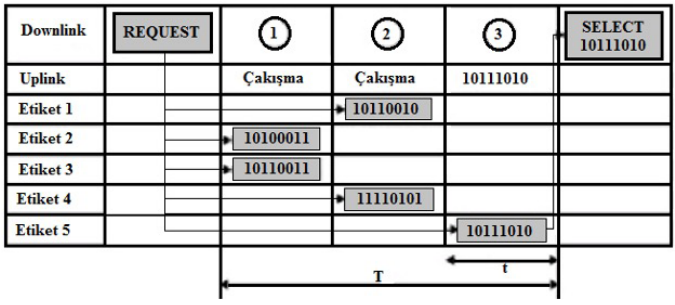

Figure 8. *S-ALOHA procedure for tag identification in our RFID system.*

When a serial number is successfully read without errors, the system proceeds to select the detected tag by transmitting a SELECT command. Subsequently, this enables the tag to be read and written without encountering any further collisions with other tags. In the event that no serial number is detected during the initial attempt, the REQUEST command is cyclically repeated. Following the completion of processing for the previously selected tag, a new REQUEST command is utilized to search for other tags within the reader's query area.

5. Conclusion

This study is focused on assessing the performance of ALOHA-based anti-collision protocols within RFID systems. We configured several network settings within simulation programs to achieve this, considering alternative design schemes. Our examination meticulously scrutinizes the efficacy of anti-collision protocols for both tags and readers, offering illustrative examples to elucidate their appropriateness in specific application scenarios based on results from a variety of simulations. It is crucial to underscore that neither tree-based nor probabilistic protocols provide uni-

versally applicable solutions for all RFID systems. Consequently, rigorous performance testing through simulations or other relevant tools is a prerequisite before practical deployment. This knowledge equips stakeholders with the insights necessary for protocol optimization, modification, or the selection of the most suitable option.

References

Ahson, S., & Ilyas, M. (2008). RFID handbook: Applications, technology, security, and privacy. CRC Press Taylor & Francis Group, Boca Raton, 978-1-4200- 5499-6.

Cha, J., & Kim, J. (2006). Dynamic framed slotted ALOHA algorithm using fast tag estimation method for RFID system. in Proceedings of the IEEE Consumer Communications and Networking Conference (CCNC'06), Las Vegas, USA.

Curty, J.P., Declercq, M., Dehollain, C., & Joehl, N. (2007). Design and optimization of passive UHF RFID systems. Springer Science-FBusiness Media, New York, 978-0-387352749.

Engels, D.W., & Sarma, S.E. (2002). The reader collision problem, in Proceedings of IEEE International Conference on System, Man and Cybernetics, Hammamet, Tunus.

Finkenzeller, K. (2003). RFID handbook: Fundamentals and applications in contactless smart cards and identification. John Wiley & Sons, Chichester, England, 0470844027.

Gast, M. (2002). 802.11 wireless networks: The definitive guide. O'Reilly Media, Inc., Sebastopol, CA, 0-596-00183-5.

Glover, B., & Bhatt, H. (2006). RFID essentials. O'Reilly Media, Inc., Sebastopol, CA, 978-0-59-600944-1.

He, Y., & Wang, X. (2013). An ALOHA-based improved anti-collision algorithm for RFID systems. IEEE Wireless Communications, 20(5), 152-158.

Hunt, V.D., Puglia, A., & Puglia, M. (2007). RFID: A guide to radio frequency identification. John Wiley & Sons Inc., New Jersey, 978-0-470-10764-5.

Kraus, J.D., & Marhefka, R.J. (2002). Antennas: For all applications. McGraw-Hill, New York, 978-0-072321036.

Lahiri, S. (2005). RFID sourcebook. Pearson Education, Inc., New Jersey, 0-13-185137-3.

Liu, L., & Lai, S. (2006). ALOHA-based anti-collision algorithms used in RFID system. In 2006 International Conference on Wireless Communications, Networking and Mobile Computing (pp. 1-4). IEEE.

Manish, B., & Shahram, M. (2005). RFID field guide: Deploying radio frequency identification systems. Prentice Hall PTR, New Jersey, 0-13-185355-4.

Namboodiri, V., DeSilva, M., Deegala, K., & Ramamoorthy, S. (2012). An extensive study of slotted Aloha-based RFID anti-collision protocols. Computer communications, 35(16), 1955-1966.

Ohrtman, F., & Roeder, K. (2003). Wi-Fi handbook-building 802.11b wireless networks. McGraw-Hill Companies, Inc., New York, USA, 0-07-141251-4.

Rao, K.V.S., Nikitin, P.V., & Lam, S.F. (2005). Antenna design for UHF RFID

tags: A review and a practical application. IEEE Transactions on Antennas and Propagation, Vol. 53, no.12, pp. 3870-3876.

Rappaport, T. S. (2002). Wireless communications: Principles and practice. Prentice Hall PTR, Pearson Education Inc., New Jersey, 0-13-042232-0.

Ross, J. (2008). The book of wireless: A painless guide to Wi-Fi and broadband wireless. No Starch Press, Inc., San Francisco, CA, 978-1-59327-169-5.

Waldrop, J., Engels, D.W., & Sarma, S.E. (2003). Colorwave: an anticollision algorithm for the reader collision, in Proceedings of IEEE International Conference on Communications, pp. 1206-1210.

Want, R. (2004). The magic of RFID. ACM Queue 2(7): 41-48.

Zhai, J., & Wang, G. (2005) An anti-collision algorithm using two-functioned estimation for RFID tags, in Proceedings of International Conference on Computational Science and its Applications, pp. 702-711.

Zhen, B., Kobayashi, M., & Shimizu, M. (2005). Framed ALOHA for multiple RFID objects identification, IEICE Transactions on Communications, Vol. 88,Is. 3, pp. 991-999.

Zheng, F., & Kaiser, T. (2016). Adaptive Aloha anti-collision algorithms for RFID systems. EURASIP Journal on Embedded Systems, 2016, 1-14.